2013

Performance and Economic Evaluation of Storage Technologies

Trishna Das

Iowa State University

Performance and economic evaluation of storage technologies

by

Trishna Das

A thesis submitted to the graduate faculty

in partial fulfillment of the requirements for the degree of

DOCTOR OF PHILOSOPHY

Major: Electrical Engineering

Program of Study Committee:

James D. McCalley, Major Professor

Venkataramana Ajjarapu

Dionysios Aliprantis

Steve W. Martin

Umesh Vaidya

Iowa State University

Ames, Iowa

2013

TABLE OF CONTENTS

LIST OF TABLES

LIST OF FIGURES

ACKNOWLEDGEMENTS

I am deeply grateful and whole heartedly indebted to my most dearest and most respected Sir who was the real driving force for this PhD. Only because of His love and prayers, this PhD has come to a good end. This PhD has taught me much more than what one will find in the pages of this dissertation. He taught me the real philosophy of life is to become a servant of the Supreme Lord through one's words, actions and thoughts. Life is not meant to get lost in a rat's race for money, power and bodily amelioration but to serve the Supreme Lord by serving His pure representatives and in service to them helping others to attain their ultimate welfare. By His pure example of living the teachings of Lord and dedication to train today's intelligentsia in these pure teachings, He has created this internal revolution that is saving many lives from the fire of ignorance and nescience. I am extremely indebted to Him for bringing such happiness, wisdom and satisfaction to my heart that is impossible to taste in today's world.

I wish to express my deepest gratitude to dearest Sir's wife for her motherly love and blessings. She has imbibed Sir's training so immaculately and is a living aspiration for me. I pray I can humbly serve Them Both and perfect my life.

Only because of Sir, today I can honestly perceive and feel a deep sense of gratitude to the Supreme Lord Sri Krsna for His mercy upon me. He made many miracles for the completion of this PhD and I am deeply amazed to realize His depth of vigilance and mercy upon us.

I am extremely grateful to my dear husband for his sacrifices and hard work for this PhD. This is his PhD more than mine and I feel deeply fortunate to have him as a partner.

ABSTRACT

In the last decade there has been a drastic increase in the penetration of variable generation (VG) such as wind and solar. VG increases the MW variability that must be met in the regulation and reserve markets. If VG penetration levels are allowed to increase without providing additional flexibility in the form of fast response regulation, reserves, and capacity, then the required capabilities will be provided by the existing conventional generation fleet. This "do-nothing" approach will lead to increased cycling of the existing plants and thus weaken the health of the current grid. The increase VG capacity penetration will also necessitate increased transmission capability in the grid in order to facilitate increased VG energy penetration. All these boils down to endowing the grid with the capability to be flexible by investigating the various options such as transmission expansion, demand control, fast responding generation, VG MW output control, expanding the balancing areas and/or investing in storage technology.

In this dissertation, the primary focus is on storage technologies, which is one of the attractive means to meet VG variability due to their fast response. With sufficient energy storage capability, they also promise many other valuable grid services such as peak shaving, load leveling, relieving congestion, increasing VG energy penetration, and deferring generation and transmission expansion plans. The objective and contribution of the dissertation is hinged on developing tools and assessment methodologies to perform economic assessment of storage.

The work develops a high-fidelity technology adaptive storage dispatch model for production costing study within a co-optimized energy and ancillary market. This tool is

used to investigate the grid benefits and economic viability of different class of storage under various wind penetration scenarios, compare them with other competing solutions, and devise appropriate monetizing schemes for their services. This work also proposes an integrated approach involving production costing and automatic generation control simulation tools to assess short-term storages. Based on the application in IEEE 24 bus system, many conclusions and indicators on storage venture's profitability and risks are drawn.

CHAPTER 1   INTRODUCTION

1.1 INTRODUCTION

Storing is an inherent nature of human psychology and intelligence for ensuring a sustainable future. From time immemorial we see animals and humans hoard food that is consumed during times of the year when there were no crops. Later century's storage was used as a business scheme to earn greater profits from people by storing crops and supplies during surplus times and then selling at very high prices during scarcity. Storing water was a radical idea to meet the human needs of irrigation and consumption by construction of dams and reservoirs. This expanded the human thinking of storing sources of energy that can be used at a later time.

As human race advanced in technology and science there was advent of electrical energy in the later nineteenth century. Electricity became the popular convenient way to transform energy from different sources that included, solar, chemical, and mechanical and so on. Electricity's versatility was adapted in various applications like transportation, heating, lighting, communication, medical science and in recent time's computation. By the latter half of the twentieth century electricity was part of common man's life and not considered as an elusive magical power with men that were called wizards. Today, electricity is the backbone and driving force of the modern industrial civilization.

Power industry over many years has been thriving heavily on fossil fuel based generation technologies. Storing and transporting these fuels such as natural gas, coal, oil has been an integral part of the overall resource management strategy and system

operations. Electricity unlike the other forms of energy cannot be stored, and has to be transmitted and used as it is being generated. It can be converted to another form of energy such as potential, kinetic or chemical. Thus until recently electricity was not stored in a major scale.

Most electricity is generated by burning fossil fuels and using the steam produced to run the steam turbines to generate electricity. Though there is an abundance of fossil fuels available yet it is a finite resource. It is fast depleting with the increase in consumption of electricity and changing lifestyle of people that is heavily dependent on artificial means than natural living. Thus the exhaustion of fossil fuels has a significant consequence upon generation of electricity.

The more grave concern is the emissions of harmful gases such as carbon dioxide from the fossil fuel generation units. Increased emissions have led to rise of global warming that is a serious threat to the human race. The climate change alarm with the rise in prices of fossil-fuels such as oil due to its fast depletion has made nations of the world support renewable sources of energy. Renewable sources such as the sun, wind, rain, tides and geothermal heat are naturally replenished and free from emissions. In the last decade there has been a drastic increase in the penetration of renewables especially in the power generation sector.

1.2 MOTIVATION

Variable generation (VG), i.e., wind and solar, increases the MW variability that must be met in the regulation and reserve markets, and it effectively increases MW requirements in capacity markets since it offers little itself. If VG penetration levels are

allowed to increase without providing additional flexibility in the form of fast response regulation, reserves, and capacity, then the required capabilities will be provided by the existing conventional generation fleet. For example, a "do-nothing" approach, assuming high VG growth, will likely result in cycling existing plants, many of which were built to be base-loaded, particularly nuclear, coal-fired, and combined cycle plants. Cycling these plants result in larger and more frequent thermal variations throughout the plant which in turn increases maintenance and causes more frequent forced outages and shorter lifetimes. Likewise, VG's lack of capacity for peak periods results in operating the power system with an overall level of increased capacity while individual units operate at lower capacity factors.

To provide regulation, reserves, and capacity services that high VG penetration levels will require, the following solutions are proposed:

- Increase conventional generation:

    This is the traditional solution to providing these services. Combustion turbines are often used, since they are fast and their investment costs are relatively low. The advantages of this approach are it is an energy resource and it provides grid stabilization via additional inertia and voltage control. By "conventional generation," we refer to synchronous machines, some of which may be quite fast such as the GE LMS100, a 100 MW combustion turbine which can synchronize and reach full load in 10 minutes at 46% efficiency [1].

- Control VG:

    Controlling VG away from its maximum energy extraction point provides for ramp-down capability if the VG is on-line and generating, and ramp-up capability if the VG is generating below its maximum energy extraction point. The strength of this approach is that

VG-ramping capability can be extremely fast; in addition, this approach requires no significant capital investment in that, given a VG facility is to be built, its implementation requires only control and communication.

- Demand control:

  Demand-side control can also provide these services. Of particular interest are thermal-electric loads (air conditioning, space heating, and water heating) and energy-intensive manufacturing processes such as aluminum smelting [2].

- Expand balancing area (BA) size:

  This approach has two beneficial effects: it increases the amount of conventional generation that can be utilized, and it increases the geographical diversity of the VG which tends to decrease the normalized variability (variability as a percentage of installed capacity). It is possible to increase BA size for purposes of automatic generation control while retaining the grid oversight typically provided by regional BAs.

- Storage Technology:

  Storage technologies typically store electricity in the form of chemical energy (batteries), kinetic energy (flywheel), potential energy (pumped hydro, compressed air) during off-peak demand periods and discharge the stored energy during peak demand periods. Storage technologies are attractive to meet variability by VGs due to their fast responding ability. Furthermore since they absorb electricity at off-peak periods when renewables like wind are in excess they help to curtail spillage of renewables by charging during those times. Thus they help to improve the penetration of VGs.

  Storage technologies though have been around for many decades and promise a wide range of benefits to the nation's power sector such as grid optimization improvement for

bulk power production, smoothing variable renewable energy sources, alleviating investment planning to support peak demands, and providing ancillary services [3], due to the high capital investments there are some impediments in their wide-spread usage in the grid. Therefore tools that capture the impact of storage and its contributions in grid operation have become the necessity for system planners to understand the role of storage in future generation portfolios and adequately value them [4]. In this dissertation, the integration of storage technologies into the grid will be investigated for its economic viability.

1.3 OBJECTIVE

The objective of this work is to develop a modeling and evaluation approach to assess the extent to which storage will play a role in providing grid services to make the grid economical and flexible enough to accommodate the VGs in future generation portfolios. A high-fidelity technology adaptive storage model is developed that emulates the various abilities of every storage technology so that it can be used in studies to value its contributions, and appropriately monetize its benefits. Using this simulation environment we can analyze the various benefits that storage has the potential to offer to the grid such as relieving transmission congestion, transmission deferral, lowering the LMP (locational marginal price) price of electricity, reducing cycling of conventional units and impact on cycling.

Storage technologies majorly can be classified based on their input (charging) and output (discharging) energy forms.

- **Type-1 storage** use electric energy as input but not as output, an example includes producing ice during off-peak periods for use in air conditioning during peak periods. Such storage technologies also provide the functionality to control the demand, and can participate in demand side management programs.

- **Type-2 storage** provides electric energy as an output but does not use it as an input, e.g., concentrated solar thermal generation utilizes solar energy to heat molten salt which is then used as a heat source for a steam-turbine process, hydrogen production through steam-reforming and then conversion to electricity via fuel cells.

- **Type-3 storage** technology is that which utilizes electric energy as input and produces electric energy as output. Pumped hydro (PHS), compressed air energy storage (CAES), batteries ranging from lead acid to latest sodium sulfur, flywheels and so on are the existing storage technologies that have been successfully adapted into grid operations.

- **Type-4 storage** is another type where the energy input is non-electric and the output is also non-electric. Most fossil fuels allow this such as natural gas, petroleum and coal are stored and retrieved in the fossil fuel form.

The use of natural gas to make ammonia which can be stored and then used to produce nitrogen for fertilizer which can be stored and used to produce biofuels which can be stored and finally utilized to fuel our vehicles illustrates how circuitous a 'storage' route may be.

In this work, type-3 storages are investigated because of their capability to offer multiple benefits including load leveling, regulation, reserves, congestion relief, and capacity services (for both generation and transmission), during both the charging and the

discharging cycles. This type includes technologies with both low power to energy ratios (CAES and pumped hydro) called as bulk energy storage and high power to energy ratios (flywheels, batteries, and super-capacitors) called as short-term storages. The dissertation will develop modeling and evaluation approaches addressing both varieties of type-3 storage and draw suitable conclusions on conditions of their economic viability and grid profitability.

1.4 DISSERTATION ORGANIZATION

The dissertation is organized as follows.

Chapter 2 presents literature survey on type-3 storage technologies, storage taxonomies on storage based on their characteristics and services they provide. This chapter also presents the various research challenges in the realm of storage integration in grid, and emphasizes the research focus of this dissertation.

Chapter 3 develops a high-fidelity storage dispatch model for electricity markets. The model developed is endowed with the ability to adapt to different class of storage devices, and also captures these energy limited storage devices' ability to provide multiple market services. The chapter illustrates application of the developed model in production costing studies to assess the avenues where different class of storage participates in grid affairs.

Chapter 4 assesses the role of bulk energy storage in co-optimized energy and ancillary market using the dispatch model developed in chapter 3. Compressed air energy storage is used as the representative bulk energy storage device, and its impact on grid under various wind penetration levels are investigated. The chapter also develops a systematic methodology to incorporate cycling related costs within generation bids, and quantify the

ability of storage to reduce such costs. The chapter sheds light on strategies to monetize storage benefits and how they impact on payback of such projects. Finally the chapter compares bulk energy storage to other solutions including combustion turbine and transmission expansion.

Chapter 5 assess short-term storage devices using an integrated approach developed which involves connecting production costing and automatic generation control (AGC) tools. This chapter presents state space models of CAES and battery, and integrates them into AGC module of IEEE 24 bus system. The chapter investigates the various grid-level and machine-level benefits such fast acting storage promises, and devises ways to monetize them for their improved economics. Batteries and flywheels have been used as representative for this class of storage devices. The chapter also discusses the importance of importing valuable information about such device's grid services from small-time sale studies such as AGC to long-term planning studies in order to render the assessments and the conclusions credible. Finally, the chapter also sheds light on few other applications of state space models of storage, which can help appropriately size them for specific geography.

Chapter 6 presents conclusions, significant contributions of this dissertation and some directions for future work. The chapter also draws market prices from MISO and PJM in order to relate the discussions and conclusions presented in this dissertation about storage to some of the existing markets. The chapter also gives a list of my publications through the course of my PhD.

CHAPTER 2   LITERATURE SURVEY

2.1 INTRODUCTION

With the increasing popularity of storage technology especially to further the integration of renewable energy onto the grid, there is a need of different taxonomy based on its various features. We need to classify the storage technologies based on its ability to serve the grid, the different monetary avenues, performance, investment and maintenance cost and demand response functions. Such taxonomy will be very handy and useful for the energy policy makers and the power system planners to invest appropriately for future portfolios, and investigators to develop appropriate storage models. In this chapter a literature survey on type-3 storages is performed and taxonomies of various storage technologies based on their characteristics and potential grid applications are created. The chapter also sheds focus on some of the major challenges in the realm of storage integration to grid.

In further discussions, storage technologies are broadly classified into two categories based on their energy storage capability: bulk energy storage and short-term storage. Bulk energy storages are those that have the capability to sustain stored energy across several hours, while short-term storages are those that have very high ramp rate with the ability to instantaneously respond to net-load fluctuations and typically have sub-hourly energy sustaining capacity.

2.2 STORAGE TYPES

In this section, an overview of the various existing type-3 storage technologies is presented. The storage options considered are directly controllable within the power

systems. This survey excludes storage schemes such as PHEVs and others which cannot be directly controlled.

2.2.1 Long-term or large-scale storage technologies

2.2.1.1 Pumped Hydro Storage (PHS)

Pumped hydro storage facilities have proved to be reliable technology over the years for applications requiring long-term and large storage capacities, and have proliferated in most parts of the world. Typically, cheap off peak power is used to pump the water into an elevated reservoir, thereby storing energy in the form of potential energy, which is utilized through conventional hydro-turbine technology as electricity demand increases [5]. Presently, siting of new PHS face objections regarding their effect on environment, similar to what transmission lines are facing [6]. Pumped hydro is particularly difficult to use in the Midwest of the United States.

2.2.1.2 Compressed Air Energy Storage (CAES)

CAES technology is similar to PHS, in that the cheap off peak power is used to store energy in the form of compressed air in huge tanks or caverns through compressors [7]. For high wind energy penetration levels, CAES's ability to support large-scale power applications with low capital cost per unit energy makes it attractive. CAES can be used at the wind plant level, as illustrated in Figure 2.1, or at the system level. Some studies also hint at utilizing CAES systems at small-scale power levels in the range of 10 MW or less for the purpose of load shifting up to 3 hours, transmission curtailment, forecast hedging etc [6].

The new generation CAES are the undersea air storage bags. These bags would store the compressed air and would be placed in water bodies such as lakes, oceans that provide naturally a high pressure environment thus saving on expending efforts and funds to build the high pressure containers. Hydrostar from Canada, E.ON from Europe and University of Nottingham are investigating to commercialize this concept [8, 9].
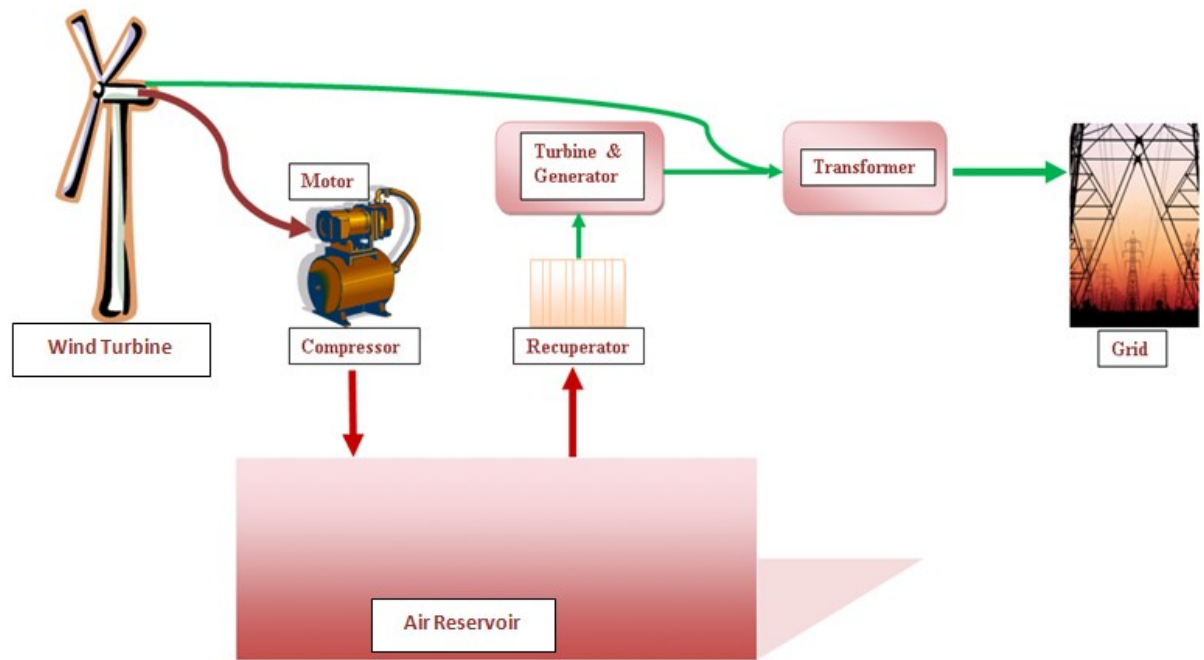
Figure 2.1 CAES system with Wind Source

2.2.2 Short-term or small-scale storage technologies

2.2.2.1 Chemical Storage

Chemical storage devices are typically the electrochemical storage devices that convert chemical energy to electrical energy. These devices are categorized as primary batteries, secondary batteries and fuel cells [10]. Batteries have chemical components such as the electrodes built in them whereas fuel cells have synthetic fuel that supply energy from

outside such as hydrogen, methanol or hydrazine. Secondary batteries are batteries that can be recharged and primary batteries cannot be recharged once the active chemical built in them is used up. Thus "batteries" refer to only secondary batteries. This energy conversion requires comparatively less maintenance, no noise and no harmful emissions.

Fuel cells—Hydrogen energy storage (FC– HES)

Fuel cells use chemical energy to produce electricity by electrolysis of water, and in the presence of an electrolyte triggers reaction between the hydrogen in the anode side and oxygen from air (oxidant) in the cathode side to form water and produce electricity in this process of oxidation-reduction. It produces water and heat as by-products, and hence is environment friendly. According to the electrolyte the electrochemical cell is named as proton exchange membrane fuel cell (PEMFC), solid oxide fuel cell (SOFC), molten carbonate fuel cell (MCFC) etc [11]. Typical fuel cell key processes are electrolysis, oxidation-reduction to generate peak-hour demand, and a hydrogen buffer tank ensuring adequate resources in emergency periods [6].

Battery Energy Storage

Battery storage technology has made rapid advancement from the earlier applications in electronics to transportations for hybrid electric vehicles (HEVs), to recently in electric grid applications such as primary frequency control [12, 13] etc. In following sub-sections various battery technologies have been presented.

i. Sodium Sulfur Battery (NaS)

NaS battery technology, a high-temperature battery system working at around 300°C with an efficiency of 89% [14], has been successfully used in countries like in Japan, USA etc. for large-scale power grid applications such as peak shaving, and wind power stabilization, backup power. On a daily basis, NaS batteries can discharge for about eight hours [15, 16]. NaS batteries consist of molten sulfur as the anode and molten sodium as the cathode separated by a solid electrolyte made of beta alumina ceramic. During discharge, the electrolyte lets only positive sodium ions flow through it, while electrons flow in the external battery circuit to produce electricity. The sodium ions combines with the sulfur to form sodium polysulfide during discharge, which reverses during charging process releasing the positive sodium ions back to form sodium.

ii. Flow Battery Technology

These batteries are between the fuel cell and secondary battery as the electrolyte contained in the electrochemical cell converts chemical energy to electrical energy directly. . They are also known as redox batteries, flow cells and regenerative fuel cells [17]. Their supply of power is dependent on the charged electrolytes.

This battery system can increase in power capacity in terms of storage amount by increasing size of tanks and power output by increasing the size of electrodes. These operate around ambient temperature unlike other batteries that require high temperature ranges. The major drawbacks of this storage scheme are the manufacturing, installation, maintenance and reliability issues.

Vanadium redox batteries and Zinc bromide batteries are the commercially available flow batteries. Vanadium redox battery is a stack of power cells that form the two oppositely charged electrolytes and are separated by a proton exchange membrane. In Zinc bromide batteries the electrolyte is stored in separate tanks and thus called a hybrid flow battery [18].

iii.   *Lead-Acid Batteries*

Lead acid batteries consist of lead and lead dioxide electrodes in sulphuric acid as electrolyte. When discharged the electrodes turn into lead sulphate and sulphuric acid dissolves as water. These batteries are the forerunner in field of battery technology and thus have the lowest cost. These batteries are deployed in various applications such as the UPS, emergency lighting, electric vehicles and grid energy storage devices [19]. Southern California grid in 1988 installed a 40-MWh lead-acid battery for peak shaving application [20].

iv.   *Nickel-Cadmium Batteries*

This is a relatively mature battery technology finding its utility in backup power applications, spinning reserves, power-ramp control and power tools. They have a low energy density, good lifetime, high discharge rate and competitive price [21].   These batteries are toxic due to presence of cadmium.

v.   *Nickel-Metal-Hydride Batteries*

Nickel-metal-hydride (NiMH) batteries have the same electrical behavior as the nickel-cadmium batteries. Some of the benefits of NiMH batteries are high power applications, low maintenance, long life, good energy density and low cost per watt, good thermal design and

configurable design [22]. These batteries have successfully demonstrated its operation in hybrid electric vehicles.

2.2.2.2 Thermal Energy Storage

Thermal energy involves storing energy in a thermal reservoir such as molten salt, pressurized water etc. by either supplying heat from solar energy or extracting heat to maintain the reservoir at colder state.

Typically they are used in applications to offset temperature difference between day and night, such as heating at night, or producing ice during night, supplying chilled water systems etc. to cool the building in hot day time in HVAC/R applications [23]. Themis power station in France that uses molten salt to store heat is designed to store 40,000kWh of thermal energy, equivalent to almost 1 day of average sunlight [6].

2.2.2.3 Super-Capacitors

Super-capacitors are growing in popularity in the storage market as it has attractive claims. Their operation is similar to capacitors with one major difference being the usage of ionic conductor as electrolyte instead of insulating material, for the electrolyte made of conductors with a very large specific surface allows ion movement. Some of the major benefits in deploying these storage devices are improved power quality, enhanced reserve capacity, increase system reliability and stability, effective load management and rapid charge-discharge characteristics [24]. Some of the disadvantages are leakage issues, high maintenance and high capital costs.

2.2.2.4 Flywheel energy storage (FES)

Flywheels work under the principle of mechanical inertia. Energy is stored in the form of rotational kinetic energy by rotating a disc or rotor (flywheel), which can be extracted in the form of electricity by expending the stored rotational energy in opposite direction [25]. The configuration can be thought of as a combined motor-generator module. The larger the flywheel speed, the greater is the storage capacity. However, it requires expensive strong material such as steel or composite materials to withstand the high centrifugal stresses. A flywheel mounted on magnetic bearings placed in vacuum chamber can store 400 Whr/kg for a period of 24 hours when rotated at 15000 rpm [6]. Various applications [26] of flywheel technology includes load leveling on railway power systems, power quality improvement in green energy systems, UPS systems for short duration ride through, and frequency regulation [27].

2.2.2.5 Superconducting magnetic energy storage (SMES)

Superconducting magnetic energy storage (SMES) stores energy in the form of a magnetic field that is created by the flow of direct current in a superconducting coil such as niobiumtitane (NbTi) filaments [6, 28], below its superconducting critical temperature. This energy is released back, by discharging the coil, when needed for various purposes such as meeting peak demand during day, improving power quality, and powering transportation systems [6, 29]. SMES includes a power conditioning system that is basically an inverter/rectifier module. The advantage of SMES over other storage technologies are its very low power loss with a high efficiency of greater than 90% and its very fast

charging/discharging responses [29]. The main limitation is the high cost related to the requirements of refrigeration and superconducting wire.

2.3 STORAGE TAXONOMY

2.3.1 Based on general characteristics

Table 2.1 presents a comprehensive comparisons of various storage options [6, 24, 30, 31, 32, 33, 34, 35, 36, 37, 38] with respect to different performance criteria. For instance, in the wake of drastic promotion of renewable energy, specifically wind farms, there is a growing interest in identifying large capacity and fast responding storage options to smooth out slow and fast wind variations respectively. Therefore such a classification of storage technologies based on their characteristics will help choose the best suited technology for specific applications.

From the table CAES is a highly attractive large scale storage option as it is a matured technology with long life expectancy, large power capacity, low capital and maintenance costs for per unit energy and reasonable efficiency. CAES also finds its applicability in ancillary services provided to the grid, peak-shaving, and VAR support [39]. The CAES [40] is also expected to address the variability of wind energy by performing load leveling, ramping and frequency regulation, reducing or eliminating wind spillage.

NaS batteries are a viable option for fast responding storage with high power ratings and efficiency with moderate capital cost per unit power and per unit energy. The key differentiating characteristics of this battery is its exceptional energy density which is five time higher than other existing batteries [41]. These batteries have one third of the footprint

Table 2.1 Energy Storage Technology Compared

	Batteries		Flywheels	Fuel Cells	Thermal Storage	SMES	Super Capacitors	Pumped Hydro	Compressed Air
	NaS	Lead Acid							
Power Density	Good	Good	Very Good	Very Good	Excellent	Excellent	Very Good	Very Good	Very Good
Energy Density	Excellent 170 kWh/m3	Very Good 40 kWh/m3	Fair	Very Good	Excellent	Fair	Good	Very Good	Very Good
Life time	15 yrs	3-12 yrs	20 yrs	<20 yrs	20 yrs	>20 yrs	8-10 yrs	30 yrs	30 yrs
Recharge Time	Very Good	Good	Excellent	Fair	Very Good	Excellent	Excellent	Fair	Fair
Dynamic Response	ms	ms	ms	1s	Mins	ms	Less than 1 min	Less than 3 min	Less than 10 min
Maintenance Cost	Moderate	High	Moderate	Low	Low	Low	High	High	Low
Environmental	Benign	Toxic	Benign	Benign	Benign	Adverse Health impact	Benign	Adverse effects	Benign
Cost/kW	$1800	$120	$100 -$300	$4000	$600	$975	$120	$1000	$400
Application	Peak-shaving, Gen Reserve, UPS, Voltage support, regulation	Peak-shaving, Gen Reserve, UPS, Voltage support, regulation	Frequency control, Gen Reserve, Long term back up supply, Voltage support, regulation	Transportation, Back-up power,	Peak-shaving, Enhanced cooling systems,	Short duration energy storage, improve power quality	Short term power supply, Voltage support, regulation	Frequency control, Gen Reserve	Peak-shaving, black stat capability, load leveling, frequency voltage control
Round Trip Efficiency %	89-92	75	85-90	59	Depends on Storage medium	90-95	95	70-85	70+

when compared with traditional lead-acid batteries [42] with a very prompt response of 1 ms for full charge to full discharge which makes it best suited to deal with the fast fluctuations of wind plant. Table 2.1 also indicates NaS as environmentally friendly with moderate maintenance costs and wide range of applications.

Flywheel technology which is conceptually built on the potter's wheel principle is a mechanical battery. This latest technology in storage virtually requires no maintenance. Its cyclic life capability makes it very attractive for frequency regulation services. In ISO New

England these flywheels have been installed and proved to be effective for over 150,000 full charge/discharge cycles at a constant full power charge/discharge rate with zero degradation in energy storage over time. This system round trip efficiency is over 85 %. These fast responsive flywheels produce less CO_2 emissions compared to the conventional fuel units. From Table 2.1 flywheel cost/kW is very attractive in comparison to other technologies.

2.3.2 Based on grid services provided

Table 2.2 gives storage technology application in various grid reliability services that are necessary for the balanced operation of the grid. This kind of taxonomy is a step further ahead than the previous commonly used taxonomy, wherein various storage technologies' characteristics are suited to specific grid application requirements for an easy perusal. Inertial response can be emulated with additional technology in power-electronics based storage like flywheel, batteries. Here we find that storage technologies such as CAES are desirable as it can provide all grid reliability services. Apart from these, storage technologies such as CAES, batteries and PHS can also reduce transmission curtailments. Fast acting technologies such as flywheels, SMES, super-capacitors can improve power quality. It is to be noted that most of the battery technologies can serve as both bulk as well short-term energy storages based on their rating.

The various abbreviations are:

IR – Inertial Response, Reg – Regulation, LF – Load Following, SR – Spinning Reserve, NSR – Non-Spinning Reserve, RR – Replacement Reserve, VS – Voltage Support

Table 2.2 Storage Technology Grid Reliability Applications

✔ - Possible   ● - Not possible

Storage Type	Reliability Function									
	IR	Primary Frequency Response	Reg	LF	Energy	SR	NSR	RR	VG Tail Event Reserve	VS
CAES	✔	✔	✔	✔	✔	✔	✔	✔	✔	✔
PHS	✔	✔	✔	✔	✔	✔	✔	✔	✔	✔
Flywheel	✔	✔	✔	●	●	●	●	●	●	✔
Metal Air Batteries	✔	✔	✔	✔	✔	✔	✔	✔	✔	✔
Lead Acid Batteries										
Valve Regulated Lead Acid (VRLA)	✔	✔	✔	✔	✔	✔	✔	✔	✔	✔
Flooded Stationary Lead Acid Battery	✔	✔	✔	✔	✔	✔	✔	✔	✔	✔
Starting Lighting & igniting Batteries	✔	✔	✔	✔	✔	✔	✔	✔	✔	✔
Flow Batteries										
Zinc Bromide	✔	✔	✔	✔	✔	✔	✔	✔	✔	✔
Vanadium Redox	✔	✔	✔	✔	✔	✔	✔	✔	✔	✔
Polysulphide Bromide	✔	✔	✔	✔	✔	✔	✔	✔	✔	✔
Nickel Cadmium	✔	✔	✔	✔	✔	✔	✔	✔	✔	✔
Lithium Ion	✔	✔	✔	✔	✔	✔	✔	✔	✔	✔
Sodium Sulphur Batteries	✔	✔	✔	✔	✔	✔	✔	✔	✔	✔
Super Batteries	✔	✔	✔	✔	✔	✔	✔	✔	✔	✔
Electrochemical Capacitor Energy Storage (ECES)	✔	✔	✔	✔	✔	✔	✔	✔	✔	✔
Superconducting Magnetic Energy Storage (SMES)	✔	✔	✔	✔	●	●	●	●	●	✔
Fuel Cells	✔	✔	✔	✔	✔	✔	✔	✔	✔	✔
Thermal Storage										
Ice Storage	●	●	✔	✔	✔	✔	✔	✔	✔	●
Molten salt	●	●	✔	✔	✔	✔	✔	✔	✔	●
Hot Bricks	●	●	✔	✔	✔	✔	✔	✔	✔	●

2.3.3 Based on available operational modes

Four-quadrant vs. two-quadrant regulation provision: Four quadrant (4Q) regulation provision means the technology can provide regulation up (RU) and regulation down (RD) via both its charging and discharging operations. Two quadrant (2Q) regulation provision means the technology provides RD and RU by only two ways. For example, as seen in Figure 2.2, a FW provides RD by charging and RU by discharging only [43], by virtue of its storing energy in the form of kinetic energy in a unidirectional rotating mass. On the other hand, the bulk storage technologies are capable of supplying RU and RD through charging or discharging alone within an hour. Batteries that have a physical storage medium to retain energy are capable of also operating in 4Q regulation mode, depending on its MWh size.
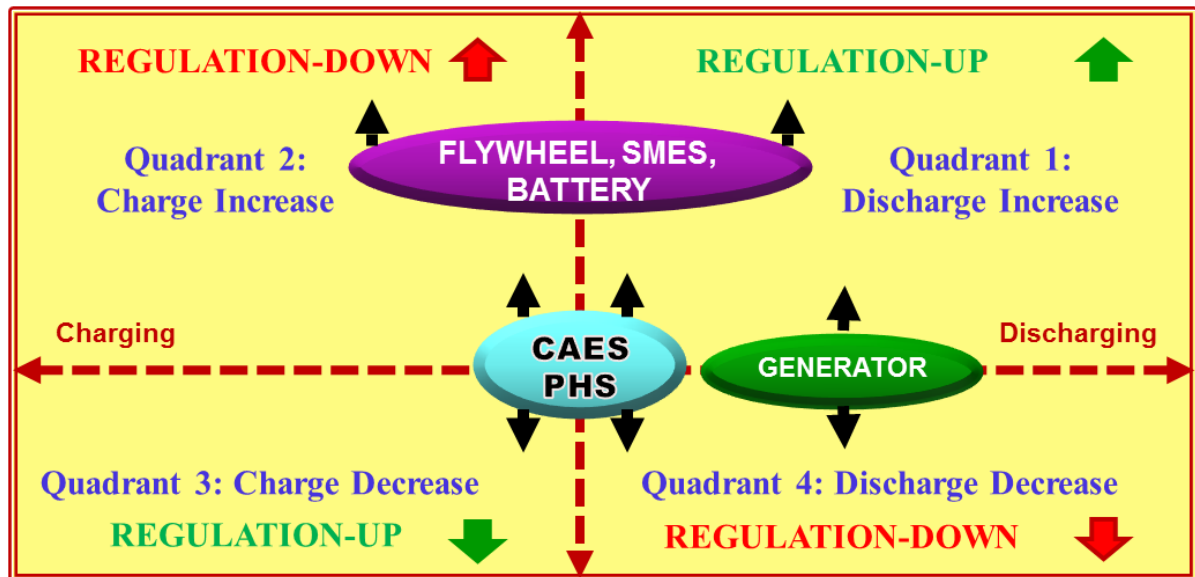
Figure 2.2 Storage modes of regulation provision

2.3.4 Based on opportunities in demand response programs

Considering the charging operation of storage to be load in the system, storage technologies are available for participating in various demand response programs. From Table 2.3 we find the most batteries, CAES, PHS and fuel cells are capable of participating in all the demand response programs. Storage is meant only to aid the grid with its operations; utilizing storage for demand response is more preferred than utilizing the domestic and the commercial loads. One of the major challenges in implementing demand response is the control strategy required to monitor and command distributed resources. Storage technologies can be easily controlled by the utility services. Furthermore, in some cases using commercial and domestic loads for demand response programs may impose discomfort on the customers, which is not the case with storage.

From the survey presented in Tables 2.2 and 2.3 we find storage to have the potential to provide reliability grid services and participate in demand response programs. Yet there are many challenges with storage technologies making its way within national generation portfolio.

Table 2.3 Storage Technology Demand Response Applications

✔ - Possible   ● - Not possible

Storage Type	Demand Response Programs					
	Grid services			Energy Bids		Dynamic Pricing
	Emergency Interruptible Load Service	Capacity	Ancillary Services	Day Ahead	Real Time	Time of the Day Schedule/ Streaming Prices/ Call Options
CAES	✔	✔	✔	✔	✔	✔
PHS	✔	✔	✔	✔	✔	●
Flywheel	●	●	●	●	✔	✔
Metal Air Batteries	✔	●	✔	✔	✔	✔
Lead Acid Batteries						
VRLA	✔	✔	✔	✔	✔	✔
Flooded Stationary Lead Acid Battery	✔	✔	✔	✔	✔	✔
Starting Lighting & igniting Batteries	✔	✔	✔	✔	✔	✔
Flow Batteries						
Zinc Bromide	✔	✔	✔	✔	✔	✔
Vanadium Redox	✔	✔	✔	✔	✔	✔
Polysulphide Bromide	✔	✔	✔	✔	✔	✔
Nickel Cadmium	✔	✔	✔	✔	✔	✔
Lithium Ion	✔	✔	✔	✔	✔	✔
Sodium Sulphur Batteries	✔	✔	✔	✔	✔	✔
Super Batteries	✔	✔	✔	✔	✔	✔
ECES	✔	✔	✔	✔	✔	✔
SMES	✔	●	●	●	✔	✔
Fuel Cells	✔	✔	✔	✔	✔	✔
Thermal Storage						
Ice Storage	✔	●	✔	✔	●	✔
Molten salt	✔	●	✔	✔	●	✔
Hot Bricks	✔	●	✔	✔	●	✔

2.4 RESEARCH CHALLENGES

In this section some challenges with storage technologies gaining wide-spread utilization within grid are summarized:

2.4.1 Technological

2.4.1.1 Materials Research

Storage technologies have suffered from high investment cost that has led to its low investments in the grid portfolios. Of course, because of its low acceptance in the grid their manufacturing cost and production costs have remained high. There have been many research efforts to investigate better materials for storage technologies. In the field of batteries most of the research funds are dedicated to find newer materials with higher efficiency and lower cost. Recent development of the nano-materials has been a promising option for the batteries and electrochemical capacitors [44]. These high-strength materials could benefit storage technologies such as flywheels, SMES and the containment vessels of CAES. Further developments on superconducting materials would impact SMES. Materials with higher thermal strength enabling higher round-trip efficiency are of great interest for upcoming storage technologies.

2.4.1.2 Power Conversion System (PCS)

Every storage technology needs some auxiliary power conversion system to interact with the grid. The PCS contributes 20% of the total cost of the storage technologies as stated in [44]. There is much scope of improving and optimizing the performances of these devices

to help storage technologies improve its efficiency and lower its cost. In particular the semiconductor switches, device cooling system, packaging, and ways to integrate storage to the grid require significant research break through.

2.4.1.3 Improved Fabrication Techniques

Manufacturing processes for small-scale storages such as batteries and capacitors that require mass production needs to be made more efficient, less expensive, with better safety for workers and made environmental friendly.

2.4.2 Workforce Expertise and Training

The US grid is familiar with bulk storages such as PHS which is attractive where geographical conditions support requires attention to mitigate adverse environmental effects. Yet newer technologies such as CAES, flywheels, new generation of flow batteries, fuel cells and others have very little practical implementation in the grid. So there is limited knowledge about operation and maintenance for storage technologies, and there is significant need for special training and detailed manuals to provide guidelines to operators of storage facilities.

2.4.3 Economic Evaluation and Operational Strategies

Storage technologies have been part of the power system for many decades. Recent advancement in storage technologies has changed the traditional paradigm of utilizing these resources. In current times there is great need to develop a systematic methodology to evaluate the economics of the various types of storage technologies available. These

economic assessments are essential to investigate the different operational strategies of storage technologies and how their services can be remunerated. Here some of the critical building blocks for the economic evaluation framework are summarized:

2.4.3.1 Dispatching Framework

Typically storage has been dispatched for grid services and evaluated for economic viability using "price taker" models [45, 46, 47], where historical market prices are used to ascertain energy arbitrage opportunities for storage and the extent of revenues storage can earn. Such price taker methods use storage efficiency and fuel cost to find a bidding strategy such that storage can make overall profits from energy transactions in market [48].

The pitfalls of this approach of dispatching storage technology are as follows:

1. *Grid Interactions:* In assessing storage as a price taker entity in the market, we do not account for storage's interaction with grid and vice-versa. For instance, storage energy and ancillary dispatches will impact market prices, which will not be captured. It also doesn't account for storage's value in the grid under various grid scenarios such as increased variable generation and impact of competitive technologies.

2. *Dispatch in Co-optimized Market:* Studies do acknowledge that [45, 47] bulk energy storage can make higher revenues by dispatching in a co-optimized market than just energy only market. There are opportunities to reserve a portion of energy from being dispatched in energy market for providing regulation services in ancillary market, and carry over the left over energy by virtue of participation in ancillary market to the next day to sell it in energy market.

Depending upon price signals such a dispatch of storage in a co-optimized market will beget higher revenues. However there are no systematic dispatch tools that can identify such opportunities for gaining higher revenues by providing both energy and ancillary services using both charging and discharging operations. A dispatch framework that can ascertain such opportunities in the co-optimized market for storage will help better value its capability to provide various services.

2.4.3.2 Modeling Needs

There is a requirement for high-fidelity storage models that can capture the typical and the special characteristics of each storage technology in the various planning studies.

1. *Multiple Services:* In operational planning studies done to optimally dispatch storage for grid operations, one of the essential characteristic that has not been rightly modeled in the past storage models is the inter-dependency of the storage and its reservoir status. Studies fail to capture the dependency of the charging side and discharging side commitments to its reservoir energy status. Thus this leads to erroneous dispatch of the storage in the grid. The most important areas of improvements that are needed are summarized below.

2. *Technology Adaptability:* In recent times there has been much technological advancement in newer and existing storage technologies, but proper representation of different storage models in the planning software is lacking. Over the years, PHS has been popular, and hence most of the commercial power system planning software has a model of PHS in-built in their software [49, 50]. However due to

differences in the operational characteristics of various storage technologies, poor representation will lead to under-estimating the value of storage. For example, as mentioned in section 2.3.3, different types of storage provide regulation in different ways and need appropriate dispatch schemes. Even within the class of bulk-energy storage, certain storage are adept to perform simultaneous charge-discharge operation within same hour like batteries, while such a quick turnover from charge to discharge and vice-versa is a challenge in PHS. These features have economic implications.

Therefore it is not just enough to create a technology neutral model [51], i.e., representing storage through generic characteristics, but they have to be technology-adaptable with specific characteristics of the various storage technologies' modeled. Such models would also avoid the need for system planners to change their existing programs and platforms, as they can simply upgrade these models into the existing system programs.

2.4.3.3 Monetizing Benefits

Due to lack of the high fidelity storage models with ability to adapt itself to represent the different storage technologies' unique characteristics, many of the benefits and services provided by these technologies are not captured. Hence there arises a need to capture and monetize the benefits offered by the storage technologies to the grid under the renewable integrated future grid generation portfolios. The needs mentioned in this section are a consequence of needs for assessment framework and storage dispatch modeling mentioned in sections 2.4.3.1 and 2.4.3.2.

1. *Revenue opportunities from co-optimized market:* With increasing wind penetration and with the consequent increase in intra-hour ramping and regulation requirements, storage finds newer avenues to participate in grid services due to fast ramping capability apart from the traditional "peak shaving" applications. As a consequence of inadequate storage dispatch models there are no economic assessments that capture entirely the storage technology benefits.

   Modeling details of certain specific aspects of storage such as reservoir capacity will also enable .;;lascribing economic value to its capacity flexibility.

2. *Assessment of Grid Benefits:* With the changing grid portfolio we find newer challenges in grid operations that can be greatly relieved by investing in storage technologies. But there are no tools that evaluate the grid phenomenon of cycling, higher ramping capability, wind spillage, emissions, and the quality of reserves especially regulation reserve quality. Therefore study framework that can quantify these storage benefits to grid are needed in order to effectively monetize them.

   To assess the benefits of certain storage, study framework that integrates tools at various time scales are also required. For instance, tool that can integrate the storage dispatch models and storage transient models will be valuable to study the interaction of storage capacity bids with markets and also the real-time performance of storage respectively, each of which will educate the investigator about benefits to storage and grid at respective time-scales.

3. *Benefit Programs:* There is a need to make newer policies and incentives by the policy makers for storage technologies to get revenue for the various benefits it has to offer to the grid. There have been efforts towards this by Federal Energy

Regulation Committee (FERC) [52]. FERC issued a ruling on October 20, 2011, that would fairly compensate energy storages for providing certain key reliability services on the electric grid. There have been pilot programs in ISO-NE to compensate fast-responding resources for its actual performance. As part of the previous point, tools will be used to study the effectiveness of these benefit programs too.

2.5 CONCLUSION

This chapter presents a survey on various types of type-3 storage technologies, divided into two broad categories as bulk or long-term storage and short-term storage technologies. In this chapter, taxonomies of various storage technologies based on their characteristics and potential grid applications are also created. Such storage taxonomies help to understand the commonalities and variability among the various technologies in terms of their characteristics and functionalities, and render valuable help in choosing the best suited technologies for specific applications. They also help in creating suitable generic models for each category of storage, thereby making it possible to accommodate a broad variety of storage within planning studies.

The chapter also sheds focus on some of the major challenges in the realm of integration of energy storage onto power grid. The main focus of this dissertation will be on the challenges of section 2.4.3 corresponding to developing suitable framework for operational planning and performing comprehensive economic evaluation of storage.

CHAPTER 3   HIGH-FIDELITY DISPATCH MODEL OF STORAGE TECHNOLOGIES FOR PRODUCTION COSTING STUDIES

3.1 INTRODUCTION

With the increase in wind penetration and the consequent increase in intra-hour ramping and regulation requirements, storage finds multiple avenues to participate in grid services. Traditionally storage is dispatched in energy markets as a price taking unit [53]. Storage dispatch within a co-optimized framework for both energy and ancillary services (AS) have been investigated [54, 55, 56, 57, 58, 59]. However, such price-taking approaches that self-schedule storage based on historical market prices cannot account for the impact of storage dispatch on market prices, nor can they assess the value of storage under changing grid scenarios [60, 61]. In this dissertation, storage technologies are dispatched in a co-optimized market by allowing them to submit bids to a central scheduler as an active market participant [62]. Although some studies have developed such storage models [63, 64, 65, 66, 67], none of them have accounted for the interdependencies between reservoir level and all ancillary to which they may contribute.

The objective of this chapter of the dissertation is to create a high-fidelity storage dispatch model for assessing the full economic benefit of different storage technologies within production costing (PC) studies. The storage technologies are classified into two broad classes based on their energy storage capability: bulk energy storage and short-term storage [68]. Bulk energy storage has the capability to sustain stored energy across several hours, as is the case for pumped hydro storage (PHS) and Compressed Air Energy Storage (CAES). While short-term storage are those that have very high ramp rate with the ability to

instantaneously respond to net-load fluctuations, typically with sub-hourly energy sustaining capacity, which is the case for batteries, flywheels, and superconducting magnetic energy storage (SMES). The model has high-fidelity by virtue of its ability to capture the different storage technologies' specific characteristics and realistically dispatch them for energy and AS at hourly and sub-hourly (5-minute) dispatch intervals. This is illustrated by adapting the developed model to three different storage technologies, namely CAES, batteries and flywheels.

Section 3.2 identifies the modeling needs for dispatching storage technologies in a co-optimized market and delineates the various contributions of the proposed model. Section 3.3 presents the PC formulation; Section 3.4 presents the proposed high-fidelity dispatch model for bulk and short-term storage technologies, and Section 3.5 presents simulation results of a PC study for the IEEE 24-bus reliability test system (RTS) integrated with wind and storage. Section 3.6 concludes.

3.2 MODELING NEEDS IN CO-OPTIMIZED MARKET

We have identified two types of modeling needs necessary to adequately represent storage in both hourly and sub-hourly dispatch programs. These modeling needs differ depending on whether the storage is bulk or short-term, as described in what follows.

3.2.1 Grid services and operational modes

3.2.1.1 Bulk energy storage technologies

Bulk storage technologies have the capability to provide multiple services in such as peak shaving, regulation, spinning, and non-spinning reserves.

Their typical modes of hourly commitments are: charging, discharging, and idling. With respect to regulation service, bulk technologies can provide up- and down-regulation services via both their charging and discharging operations. Figure 3.1 shows four-quadrant storage operation, i.e., charge increase/decrease and discharge increase/decrease. A conventional generator can be considered to operate in two quadrants, i.e., discharge increase/decrease to provide up- and down-regulation respectively. A bulk storage technology is capable of operating in this same way, and it is also capable of operating in the other two quadrants, i.e., charge increase/decrease to provide down- and up-regulation respectively.
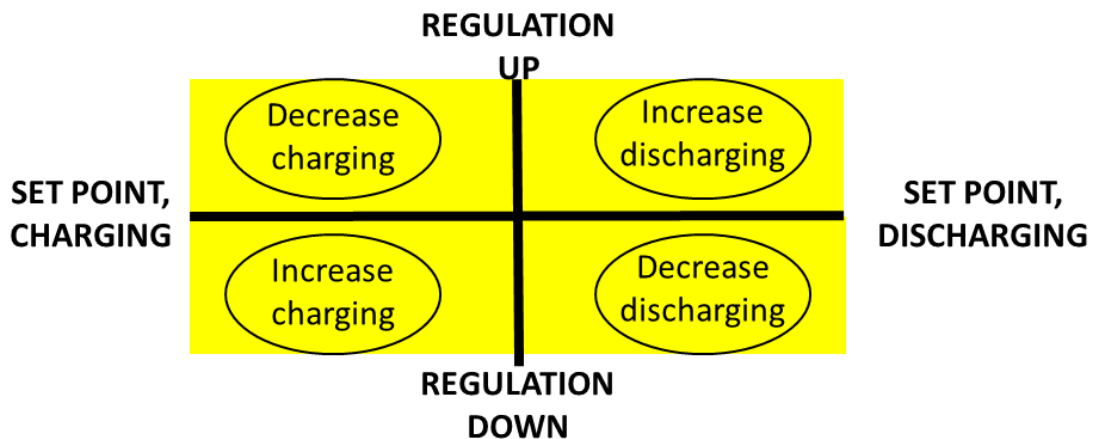
Figure 3.1 Four-quadrant storage operation and regulation provision

3.2.1.2 Short-term storage technologies

Short-term storage technologies are typically employed in balancing market to provide regulation services [68]. As seen from Fig. 1, flywheel, SMES and batteries operate in two quadrants, i.e., up-regulation by discharging and down-regulation by charging. This implies the model must be able to dispatch them for charging and discharging in same period, be it an hourly and sub-hourly dispatch program.

Though technically, bulk technologies like CAES can also charge and discharge within the same hour, when dispatched at sub-hourly intervals. However, due to the losses involved in frequent round-trip operations, combined with the fact that they can operate in four-quadrants may obviate the necessity to have a same hour charge/discharge. Instead, their hourly charging and discharging can be regulated in a co-optimized market to take advantage of sub-hourly price volatility.

As the MWh size of short-term storage devices increase, they can also provide other services, though their operation will still be in two quadrants due to unidirectional rotation of flywheel and current flow in superconducting coil. On the other hand, larger batteries can operate in four quadrants due to bi-directional current flow, a feature not captured in recent literature [55, 57, 58].

3.2.2   Capacities

3.2.2.1 Bulk energy storage technologies – Energy capacity

When emulating bulk technology's ability to provide multiple services, it is essential to observe the energy limitation of the storage reservoir. The energy capacity of bulk storage introduces inter-period dependency in storage dispatch, and therefore the model must

capture the relationship between reservoir energy status and energy and AS commitments through both charge and discharge operations, for realistic dispatch decisions. There are published studies that have modeled bulk energy storage providing multiple services within a hourly unit commitment (UC) program [54, 59, 63, 64, 65, 66]; however, all lack this essential component of capturing the interdependency between dispatch decisions in a co-optimized market and the reservoir energy status.

3.2.2.2 Short-term storage technologies – Power capacity

The charge/discharge capacities for storage are expressed in terms of their MW capacity as is done in standard dispatch programs. This convention is satisfactory for short-term storage technologies with sub-hourly continuous charging and discharging capabilities, when dispatched at sub-hourly (say, 5-min) intervals [68]. However when such technologies are assessed using hourly dispatch programs, their hourly charging and discharging capacity should be expressed in terms of energy capacity subject to the number of charge-discharge cycles in an hour; doing otherwise will lead to lower estimation of their commitments and revenues [59].

3.3 PRODUCTION COSTING FORMULATION

The PC formulation is a multi-period linear programming model with DC power flow constraints. This problem has network structure. The energy flows for the set G of generation and set T of transmission arcs are optimized to supply the set D of demand nodes over dispatch horizon T_h, where the primary characteristics of each arc are cost of energy flow, efficiency, minimum and maximum capacity. All arc flows are in per-unit energy.

However, we choose a power base of 1MVA and a time base of 1 hour, so that, for PC simulations of 1-hr time steps, arc flows are numerically equal to the power flows. Operating reserves provide MW capacity service over an hour, which is expressed in terms of hourly energy (MW-hr).

3.3.1   Hourly Unit Commitment Formulation

The objective function of hourly UC problem in equation (3.1), a mixed integer linear program, minimizes the total production cost. Generator offer bids are modeled as a piecewise non-decreasing cost function [69], as shown in Figure 3.2.
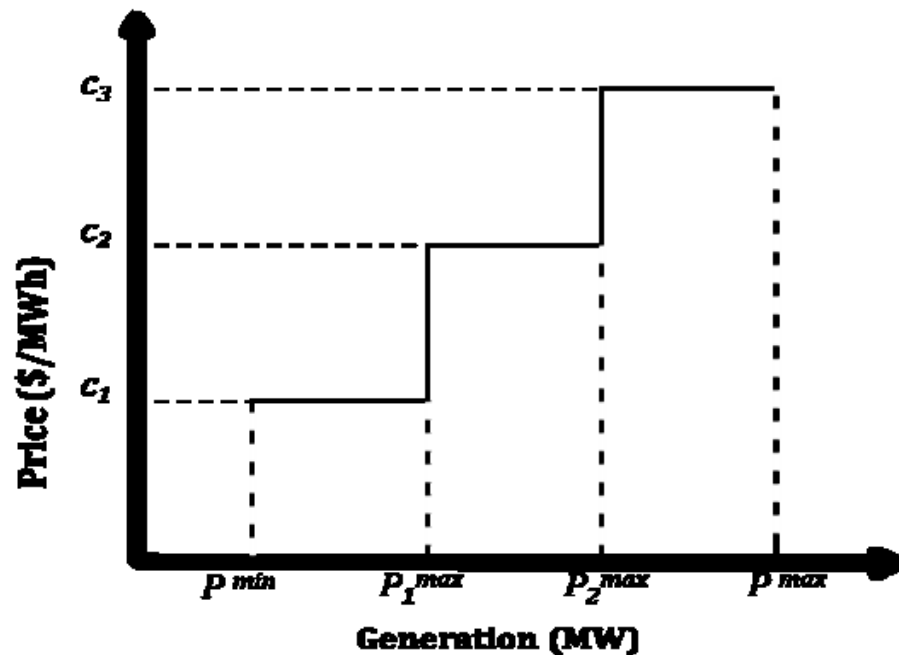
Figure 3.2 Generator bid function

In the network flow based optimization model, this is modeled as three parallel flow segments with different cost and flow limit characteristics as shown in Figure 3.3.
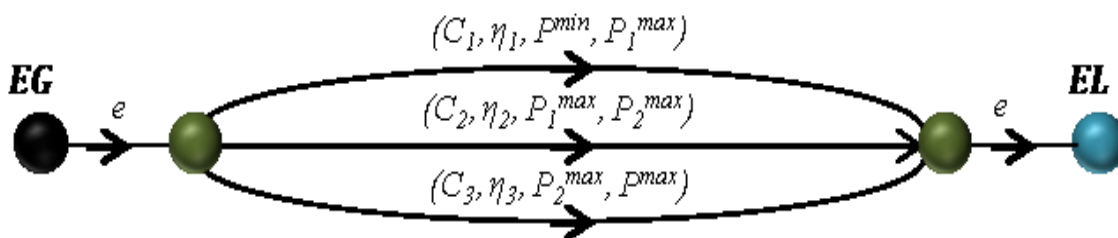
Figure 3.3 Generation arc characteristics with piecewise bid function

Minimize

$$
\sum_{t \in T_h} \sum_{(i,j) \in G, T} C_{(i,j)}(t).e_{(i,j)}(t) + \sum_{t \in T_h} \sum_{(i,j) \in G} C^{sr}{}_{(i,j)}(t).e^{sr}{}_{(i,j)}(t) +
$$

$$
\sum_{t \in T_h} \sum_{(i,j) \in G} C^{nsr}{}_{(i,j)}(t).e^{nsr}{}_{(i,j)}(t) + \sum_{t \in T_h} \sum_{(i,j) \in G} C^{reg+}{}_{(i,j)}(t).e^{reg+}{}_{(i,j)}(t) +
$$

$$
\sum_{t \in T_h} \sum_{(i,j) \in G} C^{reg-}{}_{(i,j)}(t).e^{reg-}{}_{(i,j)}(t) + \sum_{t \in T_h} \sum_{(i,j) \in G} S^x{}_{(i,j)}(t).\left(X_{(i,j)}(t) + X^0{}_{(i,j)}(t)\right) + \quad (3.1)
$$

$$
\sum_{t \in T_h} \sum_{(i,j) \in G} S^y{}_{(i,j)}(t).\left(Y_{(i,j)}(t) + Y^0{}_{(i,j)}(t)\right) + \sum_{t \in T_h} \sum_{j \in D} Pen_j(t).L_j(t)
$$

- $e_{(i,j)}(t)$ is p.u. energy flow and $C_{(i,j)}(t)$ its cost at hour t across all system arcs (i,j)

- $e^{sr}{}_{(i,j)}(t)$ is p.u. spinning reserve capacity and $C^{sr}{}_{(i,j)}(t)$ its cost at hour t, where $(i,j) \in G$;

- $e^{nsr}{}_{(i,j)}(t)$ is p.u. non-spinning reserve capacity and $C^{nsr}{}_{(i,j)}(t)$ its cost at hour t, where $(i,j) \in G$;

- $e^{reg+}{}_{(i,j)}(t)$ is p.u. up-regulation capacity and $C^{reg+}{}_{(i,j)}(t)$ its cost at hour t, where $(i,j) \in G$;

- $e^{reg-}{}_{(i,j)}(t)$ is p.u. down-regulation capacity and $C^{reg-}{}_{(i,j)}(t)$ its cost at hour t, where $(i,j) \in G$;

- $S^x{}_{(i,j)}(t)$ is start-up and $S^y{}_{(i,j)}(t)$ is shut-down costs, $(i,j) \in G$;

- $X_{(i,j)}(t)$ is start-up and $Y_{(i,j)}(t)$ is shut-down indicators;

- $X^0{}_{(i,j)}(t)$ is start-up and $Y^0{}_{(i,j)}(t)$ is shut-down indicators for non-spinning reserves, where $(i,j) \in G$;

- $L_j(t)$ is p.u. energy demand not served at hour t, where $j \in D$;

- $Pen_j(t)$ is the cost penalty for $L_j(t)$

The optimization is subject to the following constraints [65, 70, 71]. Equation (3.2) ensures nodal energy balance at every node j. Equation (3.3) constrains the arc energy within limits.

$$\sum_i \eta_{(i,j)}(t).e_{(i,j)}(t) - \sum_k e_{(j,k)}(t) + L_j(t) = d_j(t) \tag{3.2}$$

$$E^{min}{}_{(i,j)} \leq e_{(i,j)}(t) \leq E^{max}{}_{(i,j)} \tag{3.3}$$

- $\eta_{(i,j)}(t)$ is the efficiency of the arc (i,j)

- $d_j(t)$ is the p.u. demand at hour t at node j

Transmission arcs are modeled by DC power flow relations.

$$e_{(i,j)}(t) = b_{(i,j)}(t)\left(\theta_i(t) - \theta_j(t)\right), \; \forall (i,j) \in T \tag{3.4}$$

$$-\pi \leq \theta_i(t) \leq +\pi \tag{3.5}$$

- $b_{(i,j)}(t)$ is the p.u. susceptance of line (i,j)

- $\theta_i(t)$ is the angle at node i at hour t, bounded by (5)

Wind is modeled as negative load, limited by hourly forecast $W(t)$ based on historical data, as shown by (3.6).

$$e_{(i,j)}(t) \leq W_{(i,j)}(t), \; \forall (i,j) \in \text{wind generator} \tag{3.6}$$

Each generator is limited within bounds, as shown in (3.7).

$$U_{(i,j)} \, E^{\min}{}_{(i,j)} \le e_{(i,j)}(t) \le U_{(i,j)} \, E^{\max}{}_{(i,j)} \,, \; \forall (i,j) \in G$$

(3.7)

- $U_{(i,j)}(t)$ is the UC decision (binary variable) at hour t; where it is 1 if ON and 0 if OFF.

- $E^{min}{}_{(i,j)}$ and $E^{max}{}_{(i,j)}$ are the hourly minimum and maximum possible p.u. energy production.

Generation units are subject to hourly ramp-up and ramp-down constraints, as shown in (3.8) and (3.9) respectively.

$$e_{(i,j)}(t) - e_{(i,j)}(t-1) \le rr_{(i,j)}(t)\,60 \,, \; \forall (i,j) \in G$$

(3.8)

$$e_{(i,j)}(t-1) - e_{(i,j)}(t) \le rr_{(i,j)}(t)\,60 \,, \; \forall (i,j) \in G$$

(3.9)

- $rr_{(i,j)}(t)$ is the per minute ramp rate

The required up-regulation ($R^+(t)$) and down-regulation ($R^-(t)$) for the system at hour $t,$ as given in (3.10)-(3.11), is provided by the committed generators that are ON; wherein generator's regulation bid is constrained by its 5-min ramp rate, as given in (3.12)-(3.13). The required capacity for hourly up- and down-regulation services are estimated as a function of system net-load variability [72].

$$\sum_{(i,j)} e^{reg+}{}_{(i,j)}(t) \ge R^+(t) \,, \; \forall (i,j) \in G$$

(3.10)

$$\sum_{(i,j)} e^{reg-}{}_{(i,j)}(t) \ge R^-(t) \,, \; \forall (i,j) \in G$$

(3.11)

$$0 \le e^{reg+}{}_{(i,j)}(t) \le U_{(i,j)}(t)\, rr_{(i,j)}(t)\, 5 \;,\; \forall (i,j) \in G \tag{3.12}$$

$$0 \le e^{reg-}{}_{(i,j)}(t) \le U_{(i,j)}(t)\, rr_{(i,j)}(t)\, 5 \;,\; \forall (i,j) \in G \tag{3.13}$$

The required contingency reserves (a 10-min service) at every hour are provided by spinning ($RSR(t)$) and non-spinning reserves ($RNSR(t)$), as shown by (3.14)-(3.15); wherein each generator's spinning and non-spinning reserve bids are constrained by its 10-min ramp rate as shown by (3.16) and (3.17). The required contingency reserve must be at least greater than the maximum generation, with $RSR(t)$ contributing at least 50% of it. Due to (18), a generator can choose to commit for non-spinning reserve only when OFF.

$$\sum_{(i,j)} e^{reg+}{}_{(i,j)}(t) + \sum_{(i,j)} e^{sr}{}_{(i,j)}(t) \ge R^+(t) + RSR(t) \;,\; \forall (i,j) \in G \tag{3.14}$$

$$\sum_{(i,j)} e^{reg+}{}_{(i,j)}(t) + \sum_{(i,j)} e^{sr}{}_{(i,j)}(t). + \sum_{(i,j)} e^{nsr}{}_{(i,j)}(t)$$
$$\ge R^+(t) + RSR(t) + RNSR(t) \;,\; \forall (i,j) \in G \tag{3.15}$$

$$0 \le e^{reg+}{}_{(i,j)}(t) + e^{sr}{}_{(i,j)}(t) \le U_{(i,j)}(t)\, rr_{(i,j)}(t)\, 10 \tag{3.16}$$

$$0 \le e^{nsr}{}_{(i,j)}(t) \le U^0{}_{(i,j)}(t)\, rr_{(i,j)}(t)\, 10 \;,\; \forall (i,j) \in G \tag{3.17}$$

$$U_{(i,j)}(t) + U^0{}_{(i,j)}(t) \le 1 \;,\; \forall (i,j) \in G \tag{3.18}$$

- $U^0{}_{(i,j)}(t)$ is the non-spinning reserve commitment decision (binary) at hour t when it is

  OFF; 1 indicates quick start.

Every generator is constrained by its upper and lower limits for offering both energy

and AS, as given by (3.19-3.21).

$$e_{(i,j)}(t) + e^{reg+}{}_{(i,j)}(t) + e^{sr}{}_{(i,j)}(t) + e^{nsr}{}_{(i,j)}(t) \leq E^{\max}{}_{(i,j)}, \ \forall (i,j) \in G \tag{3.19}$$

$$e_{(i,j)}(t) + e^{reg+}{}_{(i,j)}(t) + e^{sr}{}_{(i,j)}(t) \leq U_{(i,j)}(t)\, E^{\max}{}_{(i,j)}, \ \forall (i,j) \in G \tag{3.20}$$

$$e_{(i,j)}(t) - e^{reg-}{}_{(i,j)}(t) \geq U_{(i,j)}(t)\, E^{\min}{}_{(i,j)}, \ \forall (i,j) \in G \tag{3.21}$$

Equation (3.22 and 3.23) defines the relationship between UC decision variables and

start-up and shut down indicators, which are part of the objective function in (3.1).

$$U_{(i,j)}(t) - U_{(i,j)}(t-1) = X_{(i,j)}(t) - Y_{(i,j)}(t) \quad , \ \forall (i,j) \in G \tag{3.22}$$

$$U^0{}_{(i,j)}(t) - U^0{}_{(i,j)}(t-1) = X^0{}_{(i,j)}(t) - Y^0{}_{(i,j)}(t), \ \forall (i,j) \in G \tag{3.23}$$

The generating units are also subject to minimum up and down time constraints [73].

3.3.2 Economic Dispatch Formulation

3.3.2.1 Hourly Dispatch

The economic dispatch (ED) formulation is a linear program, given by equations

(3.1-3.21), where the UC binary variables are known parameters. It will not have start-

up/shut-down components in the objective function, nor minimum up/down time constraints.

3.3.2.2 5-minute Dispatch

The 5-minute ED has the same formulation as the hourly ED, with the following modifications:

a. *Ramping Constraint: G*enerator participation in energy market is constrained by 5-min up/down ramp rates, imposed using (3.8) and (3.9) modified accordingly.

b. *Energy Capacity:* The unit of energy is defined as MW-5min, with base power being 1 MVA and time being 5 minutes.

c. *UC-ED relationship:* A T_h-hour ED will be formulated as *T_h*12* 5-min ED, while maintaining the hourly UC decisions across every 12 5-min successions. The 5-min wind and load data is the source of net-load variability within the 5-min ED.

3.3.3 Regulation Requirement Estimation

Regulation is a capacity service dedicated to compensate for the unscheduled minute-to-minute fluctuations in the system net load (load minus wind) and generation [74]. Typically many studies assume the regulation and ancillary service requirements as some percentage of peak-load in the system. ISOs compute the required regulation based on historical cleared regulation or net load deviations [74, 75, 76]. In this chapter, the regulation requirements are made an increasing function of 1-minute net load variability [77, 78], as given by (3.24) for RU and (3.25) for RD.

$$R^+(t) = \alpha^+ \, max(\sigma_{5\,min.}) \tag{3.24}$$

$$R^-(t) = \alpha^- \; max(\sigma_{5min.})$$
<div align="right">(3.25)</div>

where

- $max(\sigma_{5min.})$ is the maximum of standard deviations of 1-minute net load deviations over every 5 minutes interval, i.e., the market clearing interval, in an hour. This is obtained from the 1-minute load and wind data for the scheduling hour t.

- The constant multipliers α^+ and α^- are estimated from historical net load deviations data, such that 99 percentile of all 1-minute variations within every 5-minute intervals are accounted, which is enough to comply with CPS-2 standards of allowing only 2% net load violations [77].

3.4 STORAGE MODELING

Figure 3.4 shows a generic storage node i connected to a grid node j. for two consecutive time periods. In Figure 3.4, and in all notation used in this section, subscripts *(j,i)* denote charging, subscripts *(i,j)* denote discharging, and subscripts *(i,i)* denote reservoir energy level. The figure also shows the various AS storage can provide through charging and discharging operations. This section elaborates how these arcs are used to devise a dispatch model for the two classes of storage technologies, respecting their operational features as delineated in section 3.2.
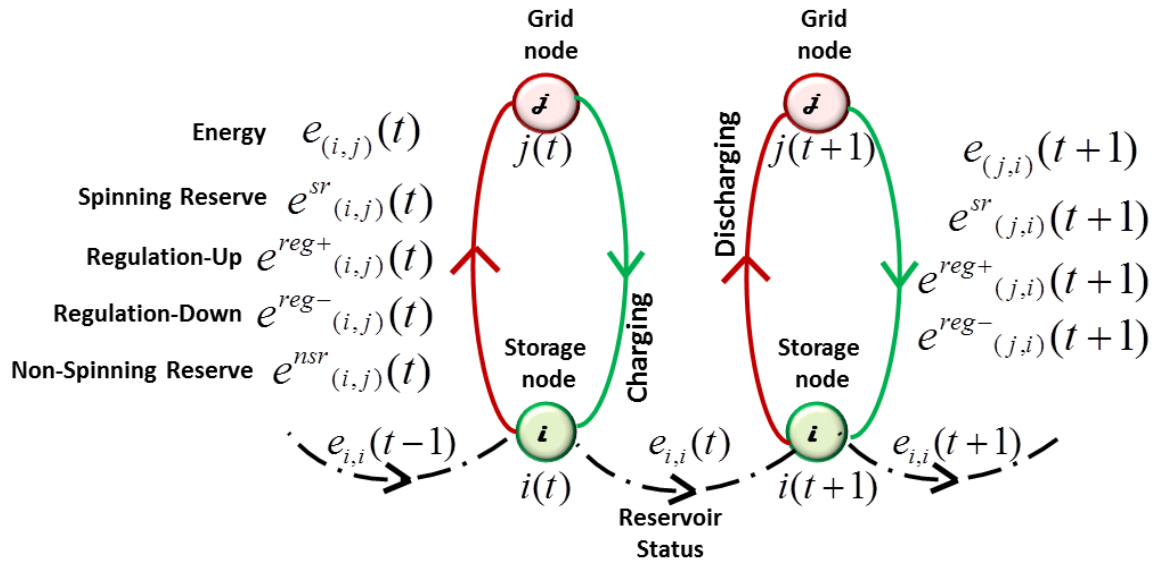
Figure 3.4 Storage model

3.4.1 Bulk energy storage technologies

3.4.1.1 Modeling hourly discharging and charging operation

The modeling for discharging arc *(i,j)*, is identical to the modeling of generation per (3.7)-(3.23). The modeling for charging arc *(j,i)* is similar to discharging arcs, with the difference being in the manner in which charging operation provides ancillary services (i.e., like the difference in load and generation entities providing ancillary services. E.g., increase in generation provides up-regulation, while load entity achieves that by decrease in demand).

The energy charged $e_{(j,i)}(t)$ from the grid at period *t* is included within (3.2), and is subject to the charging limits ($E^{min}_{(j,i)}$ and $E^{max}_{(j,i)}$) modeled by (3.3). The ramp rates ($rr_{(j,i)}$) are modeled using (3.8-3.9). The AS provided through charging operation, namely up-regulation ($e^{reg+}_{(j,i)}(t)$), down-regulation ($e^{reg-}_{(j,i)}(t)$) and spinning reserves

$(e^{sr}_{(j,i)}(t))$ are included within (3.10-3.11) and (3.14-3.15). The up- and down-regulation capacity bids are limited by 5-min ramping capability as in (3.12-3.13) and spinning reserve capacity bids are limited by 10-min ramping capability of the charging operation as in (3.16).

Equations (3.26-3.28) ensure that the charging operation respects its charging limit, while also ensuring the hourly bulk storage charging and discharging operations are disjoint, i.e., within a single hour storage either charges, discharges or stays idle. This is accomplished using (3.28). This variable $U^C_{(j,i)}(t)$ is also used in (3.12), (3.13) and (3.16) accordingly (i.e., in the place of $U_{(j,i)}(t)$) for charging arc.

$$e_{(j,i)}(t) - e^{sr}_{(j,i)}(t) - e^{reg+}_{(j,i)}(t) \geq E^{\min}_{(j,i)} U^C_{(j,i)}(t) \tag{3.26}$$

$$e_{(j,i)}(t) + e^{reg-}_{(j,i)}(t) \leq E^{\max}_{(j,i)} U^C_{(j,i)}(t) \tag{3.27}$$

$$U^C_{(j,i)}(t) + U_{(i,j)}(t) + U^0_{(i,j)}(t) \leq 1 \tag{3.28}$$

Equation (3.26) models the charging operation's ability to provide up-regulation and spinning reserve services by reducing its charge at period t. So accordingly, (3.26) ensures that the storage charges additional energy above its minimum rating ($E^{min}_{(j,i)}$) to provide these services. Equation (3.27) models the charging operation's ability to provide down-regulation by increasing the charge in period t. Thus (3.27) ensures availability of enough charging space from its maximum rating ($E^{max}_{(j,i)}$) to provide this service.

3.4.1.2 Modeling hourly storage reservoir operation

Existing models [63, 64, 65, 66] capture the dependency between charge/discharge operations and reservoir status using equation (3.29), i.e., the stored energy at period t modeled by the reservoir status arc *(i,i)* is comprised of energy stored up until period *t-1* less any leakage, plus (less) the energy to be charged (discharged) at period t.

$$e_{(i,i)}(t) = \eta_{(i,i)} e_{(i,i)}(t-1) + \eta_{(j,i)} e_{(j,i)}(t) - e_{(i,j)}(t)$$

(3.29)

But equation (3.28) doesn't account for all the AS that the storage is capable of providing. For instance, if the storage is committing to supply down-regulation through its charging operation, then it needs to ensure that the reservoir has sufficient capacity to store that anticipated volume of energy.

In our high-fidelity model, the storage reservoir dynamics accounts for both the energy and AS provisions. The stored energy at period t is comprised of energy stored up until period *t-1* less any leakage, plus (less) the energy to be charged (discharged) at period t, and the anticipated services to ancillary market (3.30).

$$e_{(i,i)}(t) = \eta_{(i,i)} e_{(i,i)}(t-1) + \eta_{(j,i)} e_{(j,i)}(t) - e_{(i,j)}(t)$$

$$+ \eta_{(j,i)} e^{reg-}_{(j,i)}(t) - \eta_{(j,i)} e^{reg+}_{(j,i)}(t) - \eta_{(j,i)} e^{sr}_{(j,i)}(t)$$

$$+ e^{reg-}_{(i,j)}(t) - e^{reg+}_{(i,j)}(t) - e^{sr}_{(i,j)}(t) - e^{nsr}_{(i,j)}(t)$$

(3.30)

Also, in the existing models the reservoir capacity is typically limited within a minimum and maximum ($E^{min}_{(i,i)}$ and $E^{max}_{(i,i)}$), without accounting for its participation in ancillary market [63, 64, 65]. Studies that just model two-quadrant regulation operation of bulk

storage also do not model these equations (3.31) and (3.32), which are a consequence of these technologies' four-quadrant operation [54, 55, 58, 59].

$$e_{(i,i)}(t) + \eta_{(j,i)}(t)\, e^{reg+}{}_{(j,i)}(t) + \eta_{(j,i)}(t)\, e^{sr}{}_{(j,i)}(t) \le E^{\max}{}_{(i,i)} \tag{3.31}$$

$$e_{(i,i)}(t) - e^{reg-}{}_{(i,j)}(t) \ge E^{\min}{}_{(i,i)} \tag{3.32}$$

If storage is scheduled to provide up-regulation and spinning reserve via its charging operation at period t, then (3.31) ensures enough volume within the reservoir at that period to inject the additional charge and reduce it when required. If due to some uncertainty, the anticipated reduction in charging to provide up-regulation or spinning reserve does not happen, still the free volume ensured within the reservoir by (3.31) will accommodate the excess energy charged. Similarly, if the storage is scheduled to supply down-regulation via its discharging operation at period t, then (3.32) ensures that it has enough stored energy in its reservoir, either amassed at the same period or *apriori*, to provide this. For the provision of AS these constraints that account for anticipated energy flow in and out of the reservoir must be modeled. Otherwise the reservoir does not operate within realistic bounds and consequently the commitment decisions will be infeasible.

3.4.2   Modeling bulk storage in 5-min. dispatch program

Typically storage technologies are more effective and reap higher benefits from real-time balancing markets with shorter dispatch intervals. The developed storage dispatch model is equally applicable in real-time ED programs.

All the characteristics of 5-min. ED mentioned in section 3.3.2.2 holds true for storage modeling too. Storage participation in electricity market is constrained by 5-min

up/down ramp rates. The basic energy unit being MW-5min., a 100MW CAES with 4 hour storage capacity is modeled in a 5-minute dispatch program with 4800MW-5min energy capacity, i.e., it could sustain energy across 48 5-min. dispatch intervals.

3.4.3   Short-term storage technologies

The proposed charging, discharging and reservoir operation models for bulk technologies can be adapted to short-term technologies by introducing certain operation specific equations and appropriately changing arc parameters such as efficiency, bids, ramp rate, and capacity bounds to represent these technologies with high fidelity.

3.4.3.1 Operational mode

The short-term storage technologies are directly dispatched using ED without needing to decide their commitments, due to their zero transition cost and time. Therefore constraint (3.28) is not imposed for those storage technologies, thereby capturing their ability to perform charge and discharge operations in the same period.

3.4.3.2 Dispatch interval

a.   5-minute Economic Dispatch
Similar to what is mentioned in section 3.4.2 the following modeling aspects apply to short-term storage dispatch within 5-minute ED:

1. *Energy Capacity:* A flywheel of 20 MW with 15-min charging or discharging time typically has 5MWh energy storage capacity. In 5-minute dispatch program, it is modeled to have 60MW-5min reservoir energy capacity, i.e., could sustain energy across 3 dispatch intervals.

2. *Same period charge/discharge:* Though such devices can perform both charging and discharging in a given period, still at any instant they can either only charge or discharge. Equation (3.33) ensures the two-quadrant regulation commitments of such devices are bound by the maximum energy that can be charged or discharged in a 5-min interval, assuming $E^{max} = E^{max}_{(j,i)} = E^{max}_{(i,j)}$.

$$e^{reg+}_{(i,j)}(t) + e^{reg-}_{(j,i)}(t) \leq E^{max}(t)$$

(3.33)

b. Hourly Economic Dispatch

When short-term technologies such as flywheel and batteries are dispatched using hourly ED, the maximum possible hourly charge and discharge ($E^{max} = E^{max}_{(i,j)} = E^{max}_{(j,i)}$) commitments is estimated using (3.34).

$$E^{max} = P^{max} \ x \ T^{C/D} \ x \ C\text{-}D_{cycles}$$

(3.34)

where, we define $C\text{-}D_{cycles}$ as the maximum number of full charge and discharge cycles within an hour, and $T^{C/D}$ as the time in hour taken for one full charge or discharge. For instance, a 20MW (P^{max}) flywheel with $T^{C/D}$ of 0.25 hour can perform an equivalent of 2 full charge and discharge cycles, and hence it can commit to the up- and down- regulation market a maximum energy capacity of 10MW-hr each.

3.5 NUMERICAL ILLUSTRATION

A 48-hour PC study was performed using the IEEE 24-bus RTS system as shown in Figure 3.5. The results assess the ability of high-fidelity storage dispatch model to simulate each storage class' unique operation. The generation bid data are given in Tables A1-A3 of the appendix. The CAES's energy bid is 1/3rd of a typical gas unit. Storage was co-located with wind at bus 21, which is in the upper part of the system with cheaper generation.
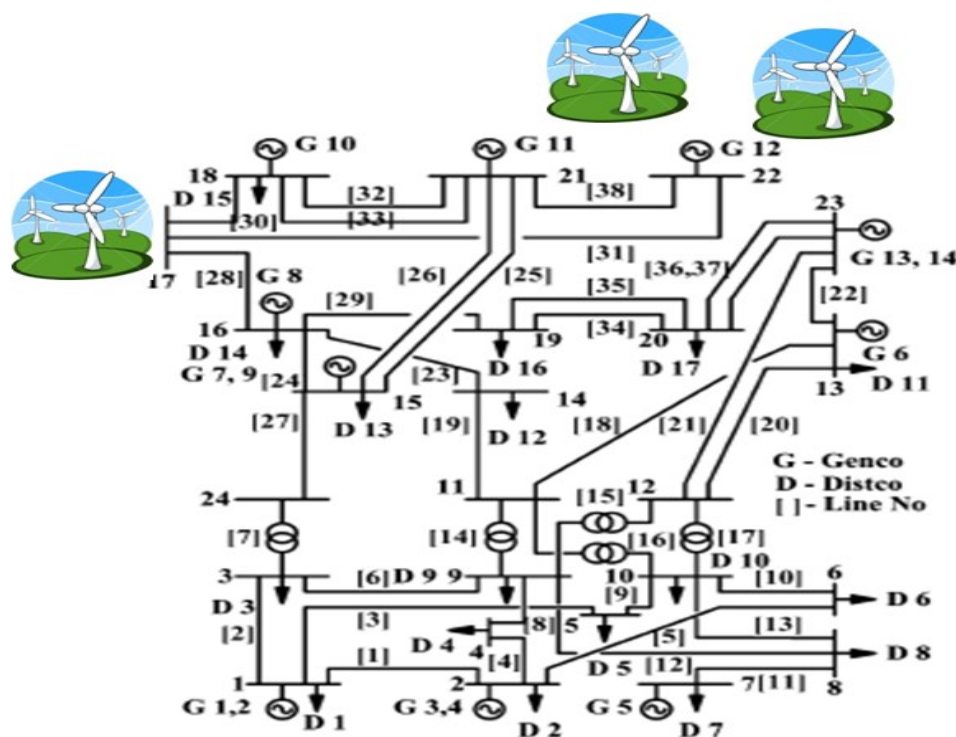
Figure 3.5 IEEE 24-bus RTS system

The data for load and wind generation, as shown in Figure 3.6 at 1-min. resolution, is taken from CAISO for two typical winter days [79]. From the 1-min. net load deviations, standard deviations (σ) for every 5-minute intervals were calculated, from which hourly regulation requirements were estimated as mentioned in section 3.3.3.
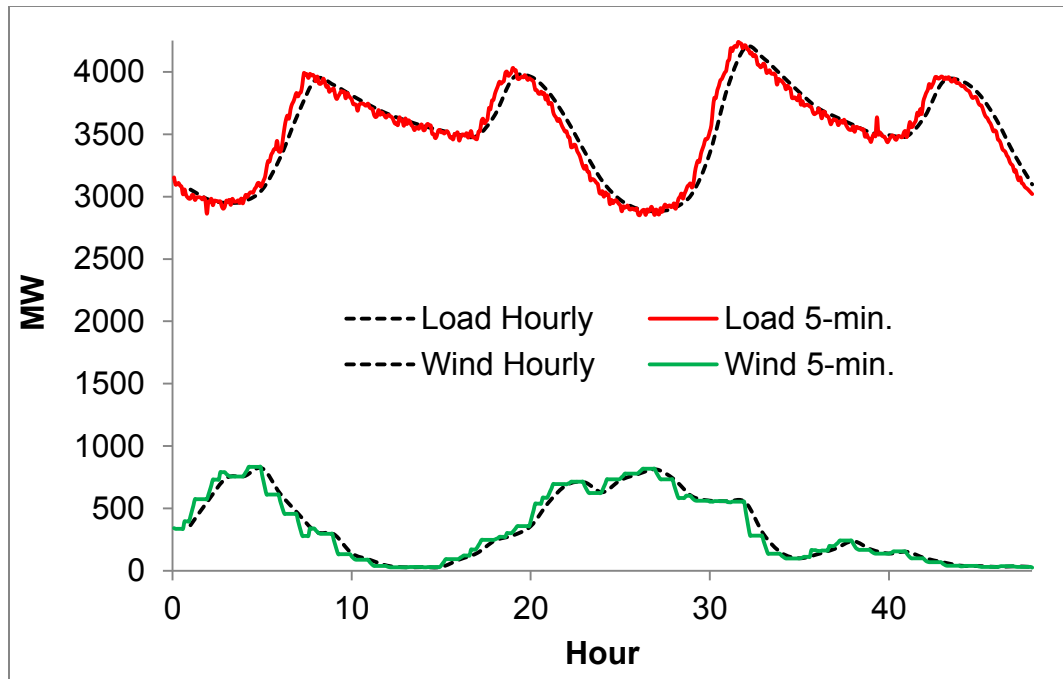
Figure 3.6 48-hour Wind and Load Data

3.5.1 Bulk Energy Storage Technologies

The model's ability to emulate typical operation of bulk energy storage is discussed first, followed by a discussion on the specific aspect of the proposed model, i.e., its ability to account for the relationship between various grid services and bulk technology's reservoir status. Any CAES used in this study is assumed to have ratios of charge to discharge and reservoir energy capacity to discharge as 1MW:1MW and 4MWh:1MW respectively. The round trip efficiency is 80%.

3.5.1.1 Energy Arbitrage

The CAES is comprised of a 50 MW turbine, a 50 MW compressor and a 200 MWh reservoir. The wind capacity penetration is 22%. Figure 3.7 shows CAES operation in

relation to the locational marginal price (LMP) at bus 21. The discharge operation is shown in the negative scale.
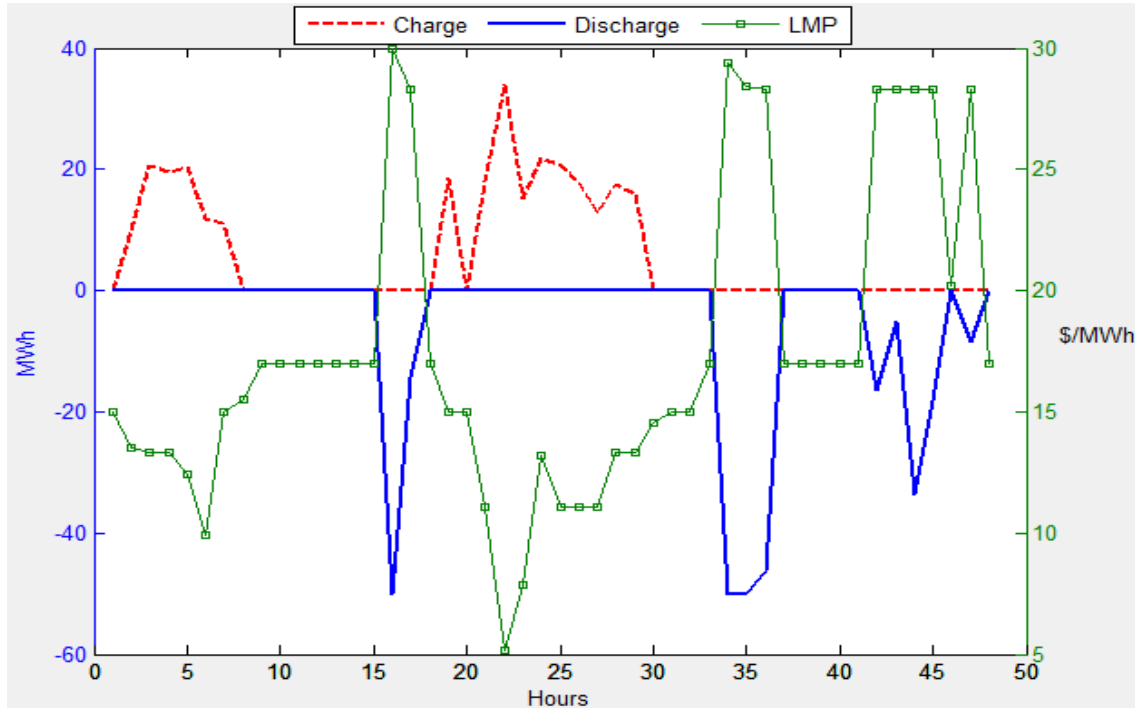
Figure 3.7 Hourly CAES commitments in relation to LMP

Figure 3.8 shows the data in Figure 3.7 with respect to sorted LMPs, and it is observed that CAES is charged during low LMPs (≤15$/MWh ($l_c$)) and discharged during high LMPs (≥28.03$/MWh ($l_d$)). This demonstrates the ability of the model to ensure strategic bulk storage dispatch such that it takes advantage of energy arbitrage opportunities. Price taker models [56] devise strategic storage bidding such that the marginal price of discharge is at least 1.25 (80%[-1]) times marginal price of charge, in order to ensure overall revenue. In this case as seen in Figure 3.8, the market dispatches CAES in such a way that l_d is at least 1.89 times l_c.
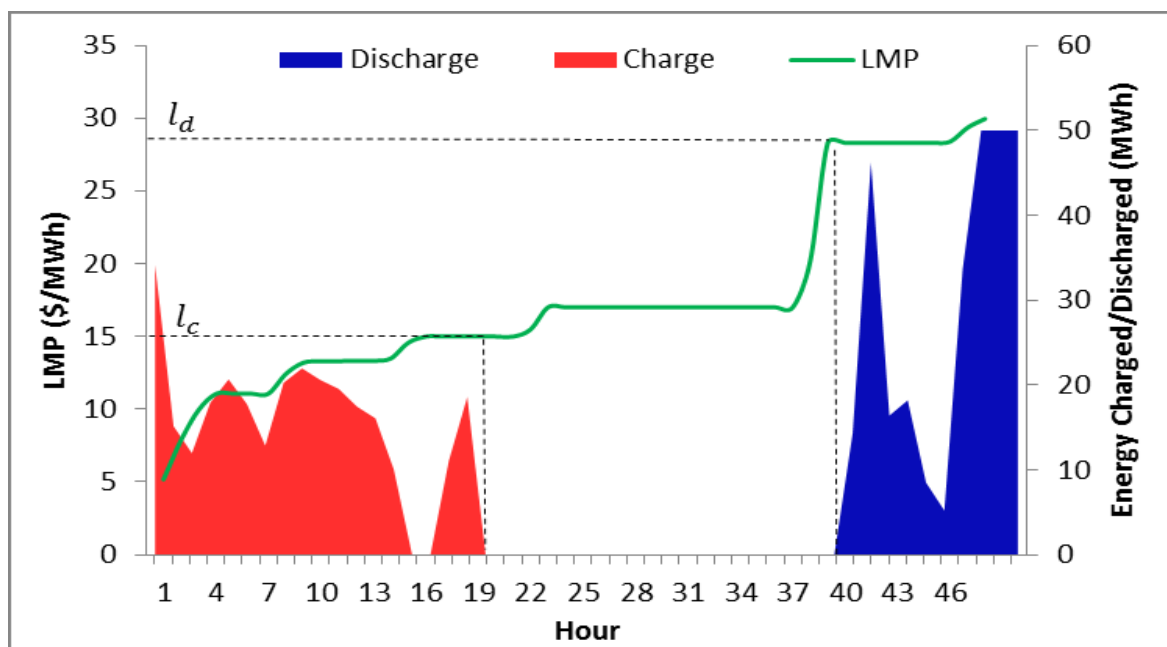
Figure 3.8 CAES operation with respect to sorted LMPs

3.5.1.2 Load shifting

Figure 3.9 shows the hourly system load and bus 21 LMPs with and without CAES of size 50 MW. It can be observed that by dint of their participation through arbitrage opportunities, as seen in Figure 3.7, CAES increases LMP during low-LMP periods, and decrease LMP during some high-LMP periods. This is also reflected in the hourly load plot, wherein the load at some high LMP period (not necessarily peak load) is shifted to low load periods (valleys).

The overall impact of reduction in high LMPs is the reduction in system production costs. With increasing CAES size at bus 21 from 25 MW to 50MW to 100 MW, there is decrease in 2-day production costs from 2.655 M$ to 2.645 M$ to 2.635 M$ respectively, compared to 2.697 M$ when there is no CAES in the system. This reflects the fact that CAES energy bids are relatively low.
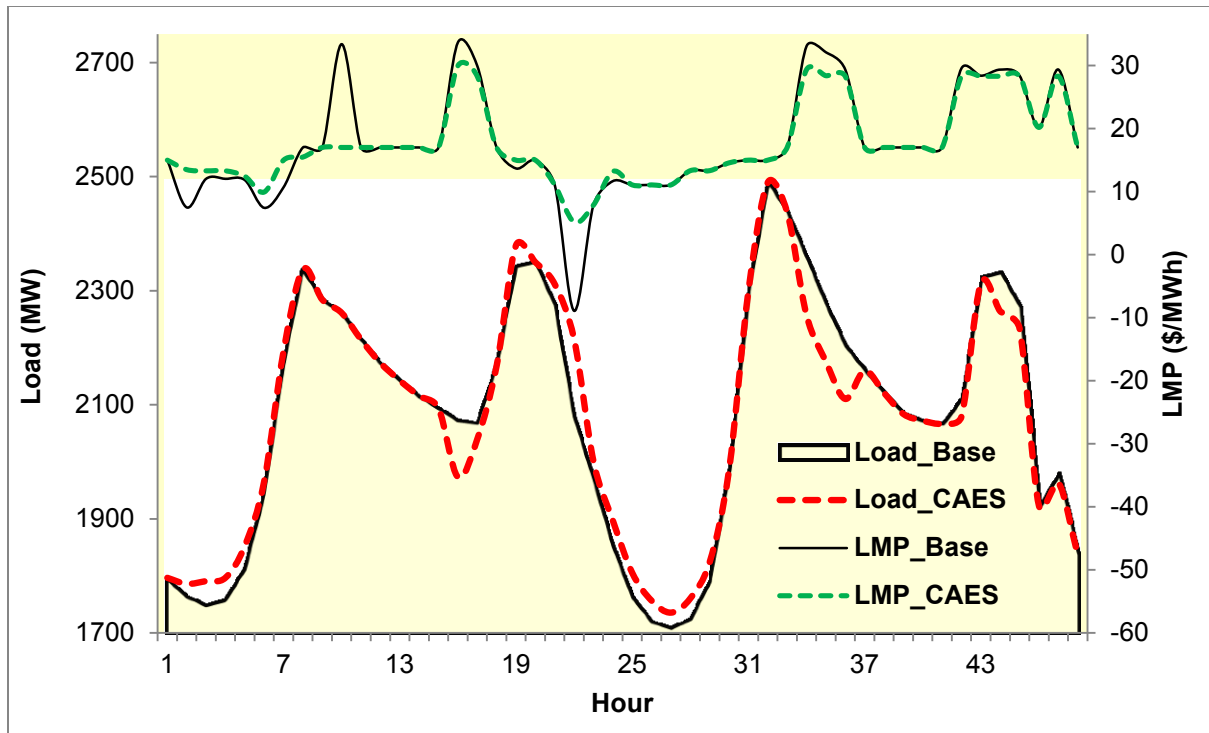
Figure 3.9 Hourly load and bus 21 LMPs

Here the model's ability to emulate general characteristics of typical bulk storage's participation in market is emulated. The following section sheds light on a specific aspect of the proposed model, i.e., in accounting the relationship between various services provided by the bulk storage and its reservoir status, that impact its dispatch commitments.

3.5.1.3 Multiple Services

a. Energy capacity

Figure 3.10 shows AS dispatch of 100MW CAES at 22% wind penetration obtained using the developed high-fidelity model. Figure 3.11 shows AS dispatch obtained using the model of (3.28). In Figure 3.11, it is observed that the ancillary commitments are independent of reservoir level, i.e., the provision of up-regulation

in certain hours and spinning reserves in most of the hours, both through discharge operation, is not supported by the energy level in the reservoir as indicated by the arrows, which means the modeled operation is actually infeasible. The high-fidelity model ensures CAES commitments for regulation and spinning reserves are always supported by the reservoir energy level, and therefore are feasible.
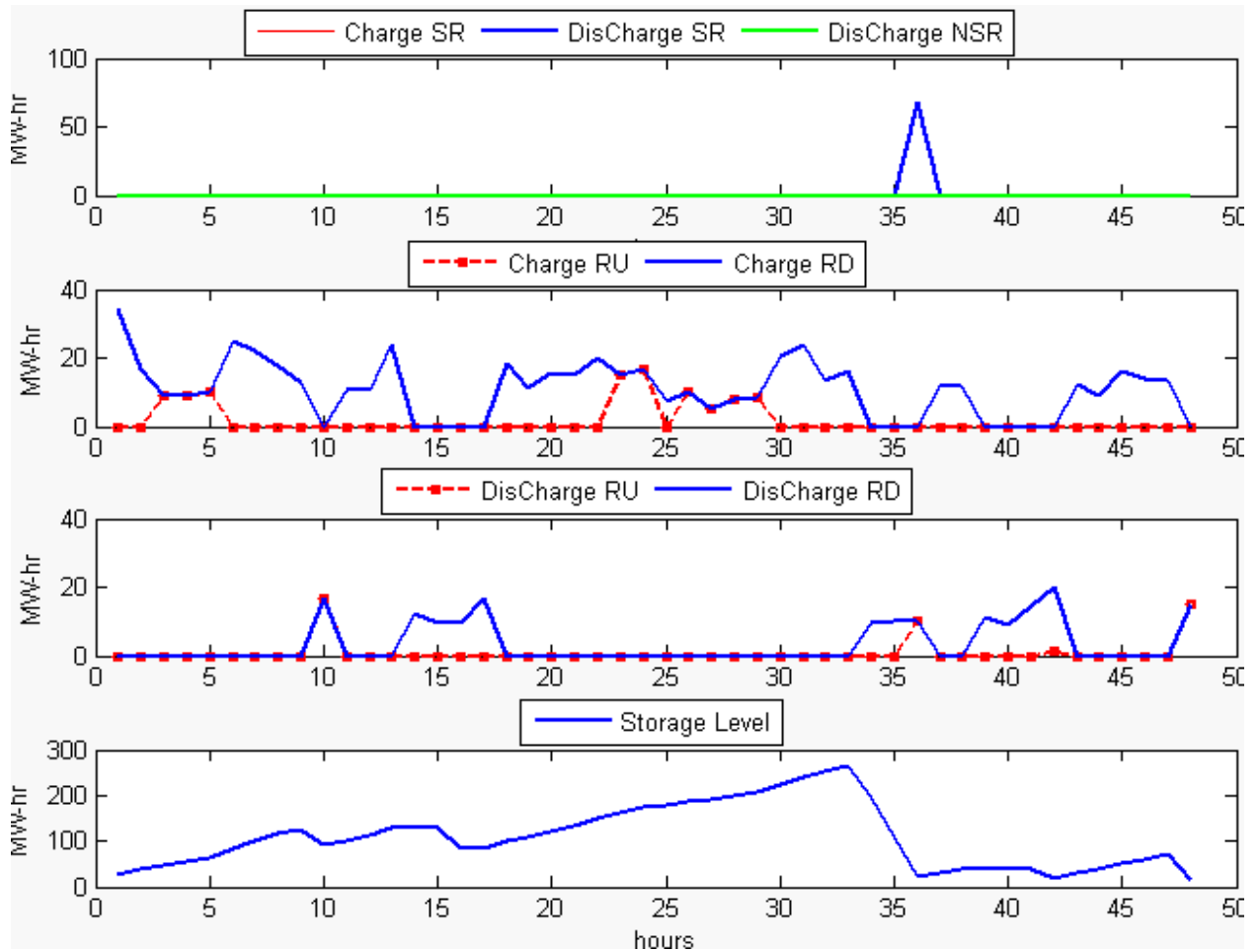
Figure 3.10 CAES participation in ancillary services
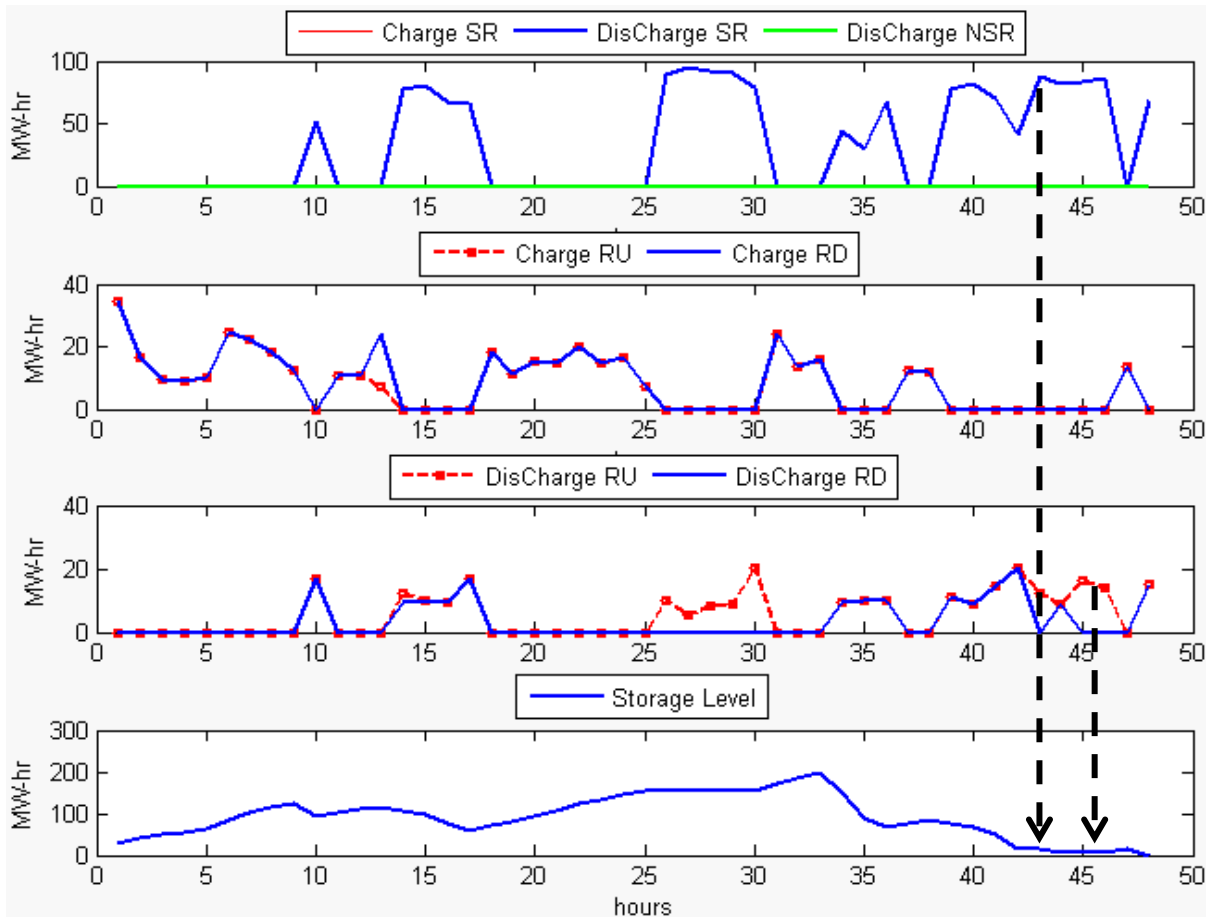
Figure 3.11 CAES participation in ancillary services unrelated with reservoir

The reservoir modeling influences how CAES is dispatched and consequently the production costs and storage revenue as well. The 100 MW CAES makes 2-day revenue of $11.8K from the ancillary market when dispatched using the high-fidelity model compared to $40.5K revenue earned with the exiting model of (3.28), as more AS are dispatched by the existing model than what CAES can actually commit for.

b. Cross arbitrage

When energy and ancillary provisions are co-optimized, it introduces the opportunity for *"cross arbitrage"*, i.e., arbitrage across both markets, especially applicable to bulk energy storage technologies. For instance, by virtue of providing RD through

charging mode, some energy is stored within the reservoir that can be sold in the energy market and earned a profit. Due to modeling of reservoir's interactions between energy and ancillary market, this possibility of cross-arbitrage across the markets is captured. The revenue that 100 MW CAES makes from energy market based on the high-fidelity model is $0.01128M compared to $0.00354M (~69% decrease) as per the existing model as this model does not facilitate cross-arbitrage.

Table 3.1 presents the revenues ($C_{revenue}$) CAES get from energy and ancillary markets, the operational cost ($C_{op.\ cost}$) computed from the energy discharge and bid price, and the payback period for both the models for 50MW and 100MW CAES. The payback period is defined as the number of years required to breakeven the investment (C_{inv} [80]) on CAES, and is computed by solving the cost balance equation (3.34).

$$\left(C_{revenue} - C_{op.\ cost} \right) \sum_{t=0}^{N} \frac{1}{(1+r)^t} = C_{inv} \tag{3.35}$$

where t is the payback period, r is the rate of interest. The existing model promises higher revenue from ancillary market, than what it actually can serve. While the high-fidelity model developed promises higher revenue from energy market due to the opportunity for cross arbitrage. Their implications on the economic evaluation are seen from their payback periods.

Table 3.1 CAES revenues and payback

Case CAES 50 MW	Energy (M$)	Ancillary (M$)	Op. Cost (M$)	Payback (yrs)
Existing model	0.459	3.81	0.992	7.79
High-fidelity model	1.47	3.09	1.42	8.13
CAES 100 MW				
Existing model	0.644	7.37	1.16	7.44
High-fidelity model	2.05	2.15	1.66	20.04

The existing model identifies higher revenues from the AS market, however with infeasible AS commitments. On the other hand, the high-fidelity model identifies higher revenue from the energy market due to the opportunity for cross arbitrage. The influence on the economic evaluation is seen in their respective payback periods. The economic evaluation based on the high-fidelity model suggests against investing in a larger sized CAES at this wind penetration level, whereas that based on the existing model encourages such an investment.

3.5.2 Short-term Storage Technologies

The battery and flywheel market participation using 2-day hourly and 5-min ED are studied by appropriately changing the high-fidelity model parameters and equations to adapt to these technologies. For the 5-min PC study, the load, wind and regulation requirement data at 5-min intervals are used. The round trip efficiency is assumed to be 85% and 90% for flywheel and battery technologies respectively.

3.5.2.1 Two-Quadrant operation and dispatch intervals

Figure 3.12 shows the flywheel dispatch, with P^{max} of 20 MW and $T^{C/D}$ of 15 minutes. We observe that flywheel provides down-regulation by charging (accelerating) and up-regulation by discharging (decelerating), both within every hour. It also shows the stored energy status at 5-min dispatch intervals.
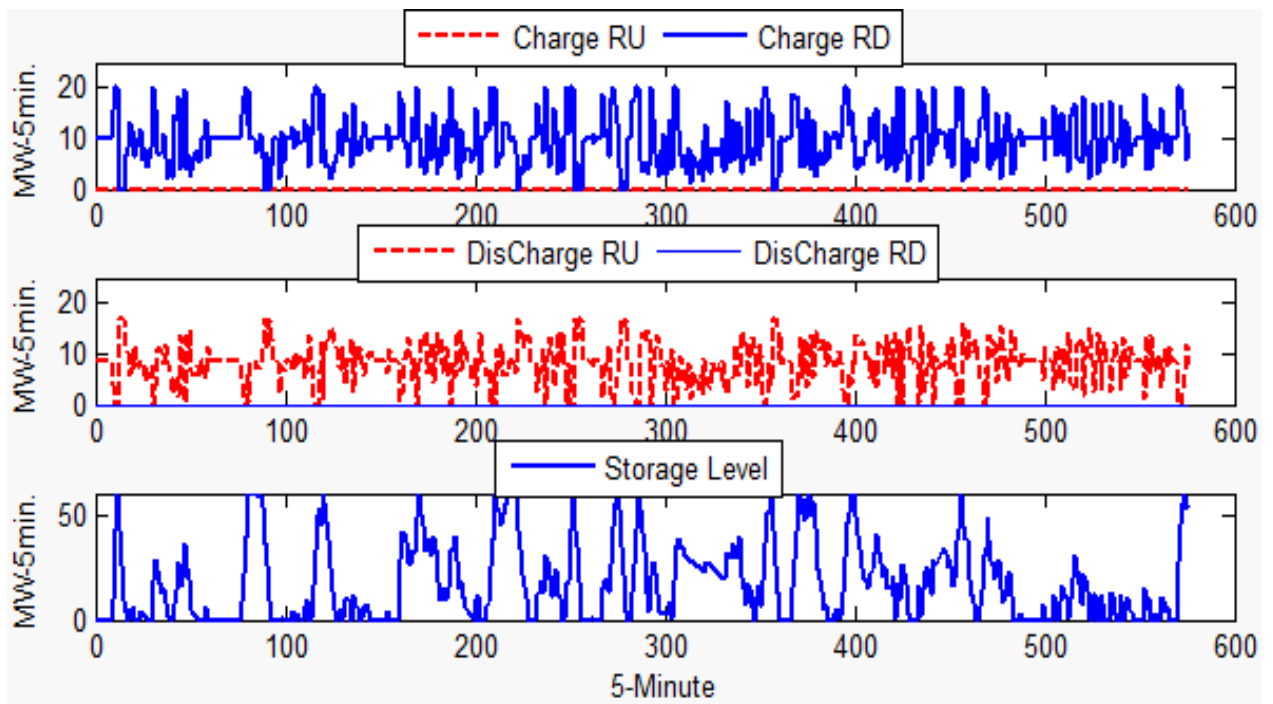
Figure 3.12 Flywheel participation in ancillary services – 5-min dispatch

Figure 3.13 shows the hourly commitments using hourly and 5-min ED. The influence of intra-hour net-load variability captured in 5-min ED is seen in terms of flywheel's highly changing hourly commitments, while the commitments from hourly ED is relatively stable. Table 3.2 presents the 2-day regulation capacity commitments based on both 5-min. and hourly ED, which shows the ability of proposed model to dispatch such short-term storage technologies in hourly programs with high fidelity. This aids in modeling

such resources in long-term planning programs in order to account them in future energy system portfolios.
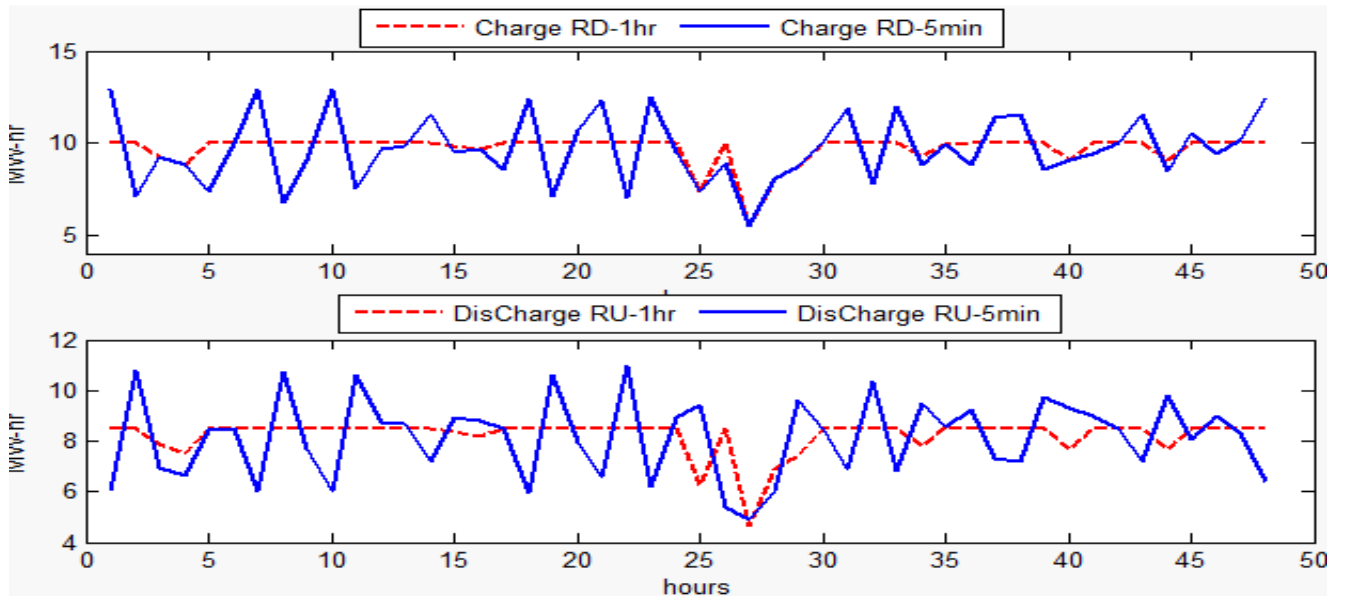
Figure 3.13 Flywheel participation in ancillary services- hourly dispatch

Table 3.2 shows the estimated yearly revenue from the AS market, and the payback period for a 20MW flywheel with an investment cost of $1630/kW. We observe that the economic implication of dispatching flywheel in 5-min ED is better than in hourly ED.

Table 3.2 Flywheel profits and payback

Case	RU/RD (MW-hr)	Ancillary (M$)	Payback (Years)
Hourly dispatch	395.00/464.71	3.59	9.09
5-min dispatch	391.13/465.52	3.91	8.33

Figure 3.14 shows the hourly market clearing prices (MCPs) for up-regulation for three cases: base case (without flywheel) using 1 hour ED, base case using 5-min ED, and the case with 20 MW flywheel using 5-min ED. Two observations are made by comparing:

1. *Hourly and 5-min base case:* The higher hourly MCPs from 5-min dispatch due to intra-hour net-load variability benefits flywheel economics (Table 3.3).

2. *5-min base case and 20MW flywheel:* participation of storage in regulation provision reduces the MCPs, and consequently the system production cost. (Figure 3.14)
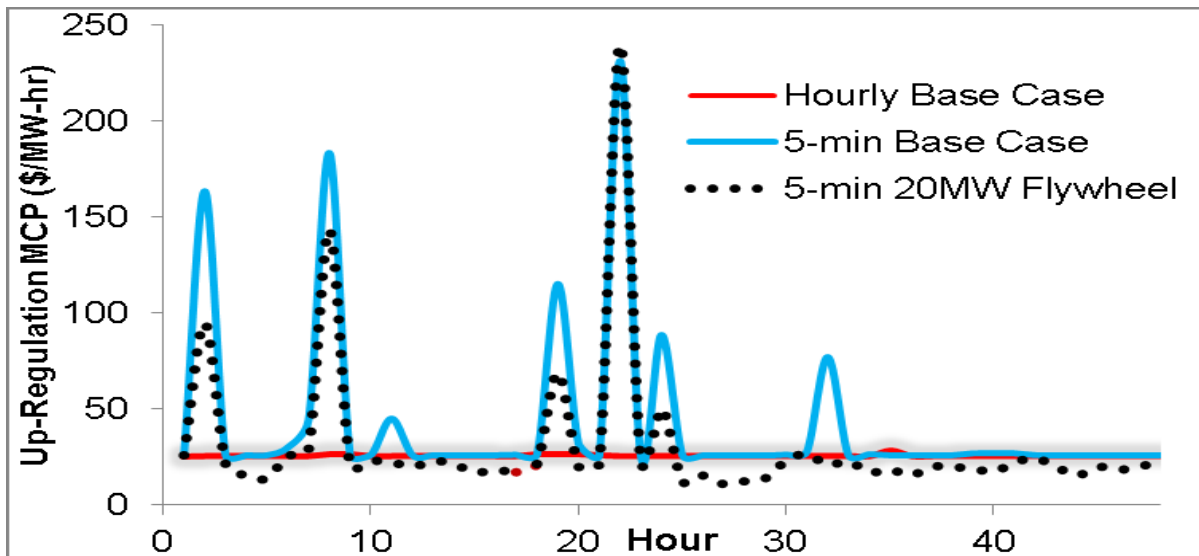
Figure 3.14 Hourly MCPs for up regulation

3.5.2.2 Battery configuration: Bulk or short-term?

Battery technologies can also be similarly modeled as a short-term storage and dispatched for two-quadrant regulation services using the ED. However, an interesting aspect of battery compared to a flywheel is its ability to operate in four-quadrants depending

upon its size, i.e., a battery with appreciable energy storage capacity can be dispatched like a bulk-storage. Thus for a given size of battery, there is an interesting problem of deciding the best battery configuration that yields maximum benefit. This kind of investigation further demonstrates the need and ability of such high-fidelity technology adaptive storage dispatch model.

For instance, a 15 MWh battery can be designed using many different combinations of cells in series and parallel, resulting in a battery with:

1. Power rating of 60MW and storage capability of 15 mins.

2. Power rating of 30MW and storage capability of 30 mins.

3. Power rating of 5MW and storage capability of 3 hours

4. Power rating of 7.5MW and storage capability of 2 hours

Table 3.3 presents the economic assessment using 2-day PC study, by adapting the storage model to the above described battery configurations. We assume battery investment cost to be $1000/kWh. From the payback period we see that, for this MWh rating, a configuration with high power density gets higher benefits from the ancillary market.

Table 3.3 Battery profits and payback

Case	Energy (M$)	Ancillary (M$)	Payback (yrs)
60 MW, 15 mins.	-	10.3	1.45
30 MW, 30 mins.	-	7.32	2.05
7.5MW, 2hr	1.03	2.28	4.54
5MW, 3hr	0.699	1.54	6.71

This demonstrates the need of such studies that capture the ability of the proposed model to adapt to different characteristics of storage technologies that enable their economic assessment using PC studies.

3.6 CONCLUSION

In this paper a high-fidelity storage dispatch model was developed for PC studies that captured the relationship between storage's provision of energy and AS with its reservoir status, while also accounting for specific features of bulk and short-term storage technologies. This model was adapted to represent three storage technologies, namely CAES, flywheel and battery in IEEE 24-bus RTS system, and dispatch them in a co-optimized energy and ancillary market.

For bulk energy storage, the simulations corroborated the need for modeling the inter-dependencies between reservoir status and all possible energy and ancillary dispatches for fidelity of commitments and economic assessment. The model is seen to capitalize on cross-arbitrage opportunities while beneficially dispatching bulk storage technology in a co-optimized market environment. The results also showed the adeptness of the developed storage model to dispatch short-term technologies such as flywheel and battery with high-fidelity in hourly and 5-minute dispatch programs.

In future investigations, the high-fidelity model will be used to perform detailed economic evaluations of different class of storage technologies under high renewable scenarios, evaluate appropriate schemes to monetize storage benefits, and compare against other competing solutions.

CHAPTER 4   ASSESSING THE ROLE OF BULK ENERGY STORAGE IN THE GRID

4.1 INTRODUCTION

Bulk energy storages have the capability to sustain stored energy across several hours. This type of storage technology is one of the most promising ventures for the renewables integrated grid the future is heading towards. Energy Storage Council reports that it believes bulk energy storage to be the "sixth dimension" of the electricity value chain following fuels/energy sources, generation, transmission, delivery and customer energy services [81]. This long-term storage adds flexibility to the grid that alleviates the grid security and reliability [82]. The missing part of today's grid economic framework is its ability to monetize and value the benefits from bulk storages such as CAES and batteries.

In this chapter, we have six main objectives that are accomplished via five different studies:

Study 1: Illustrate typical operation and associated benefits of bulk storage within a power system;

Study 2: Provide a method of quantifying the effect of storage on cycling;

Study 3: Economically assess the long-term value of storage in terms of pay-back period;

Study 4: Compare storage benefits to use of a gas turbine;

Study 5: Compare storage benefits to transmission expansion; and

Study 6: Develop a method to identify storage siting potential.

Overall, bulk storage technologies are evaluated using 48-hour production cost simulation under different case studies to bring out its impact on the grid and the ways storage can earn its benefits. The high-fidelity storage model in PC developed and presented in chapter 3 is used to study bulk storage technologies in this chapter. The IEEE RTS 24-bus system was integrated with CAES, chosen as a representative of bulk storage in the grid.

We present a sequence of case studies that show the role of bulk storage in future scenarios. Section 4.2 investigates CAES under different wind penetration levels, and section 4.3 performs a cycling assessment and quantifies the impact of storage integration on conventional unit cycling under increasing wind penetrations. Section 4.4 provides economic indicators on such storage projects in terms of payback assessments. The section also devises ways to monetize storage benefits to grid and quantifies its impact on payback. Section 4.5 compares CAES investments to other solutions such as CT and transmission expansion. A storage optimal allocation methodology has been developed in order to compare storage expansion benefits to transmission expansion. Section 4.6 uses the optimal storage allocation tool to find indicators that help in identifying candidate locations for a possible economical storage investment in any system. Finally section 4.7 presents the conclusions.

4.2 STUDY 1: CAES UNDER DIFFERENT WIND PENETRATION LEVELS

4.2.1 Impact on System Production Cost

In these studies the optimization program objective function value is referred to as the system production cost. Later sections compute the total production cost that would include the cost expended for the generation unit cycling. The ancillary service (AS)

revenue includes the revenues earned by the unit for its commitment in the regulation-up market, regulation-down market, spinning reserve and non-spinning reserve market.

In the system a storage unit – CAES of 50MW, 100MW and 200MW was included at bus 21 co-located with a wind farm. The system wind penetration level was increased and the production cost was observed. The wind penetration is the nameplate capacity penetration.

We observe from Figure 4.1 that the production cost decreases as the level of wind penetration increases as seen from the green bars representing the base case without any storage unit. When we include CAES unit the production cost is reduced under increasing wind penetration level and it further reduces with increasing sizes of CAES unit. This is because CAES participates in the energy market and replaces more expensive generation at the top of generation stack during periods of high load.
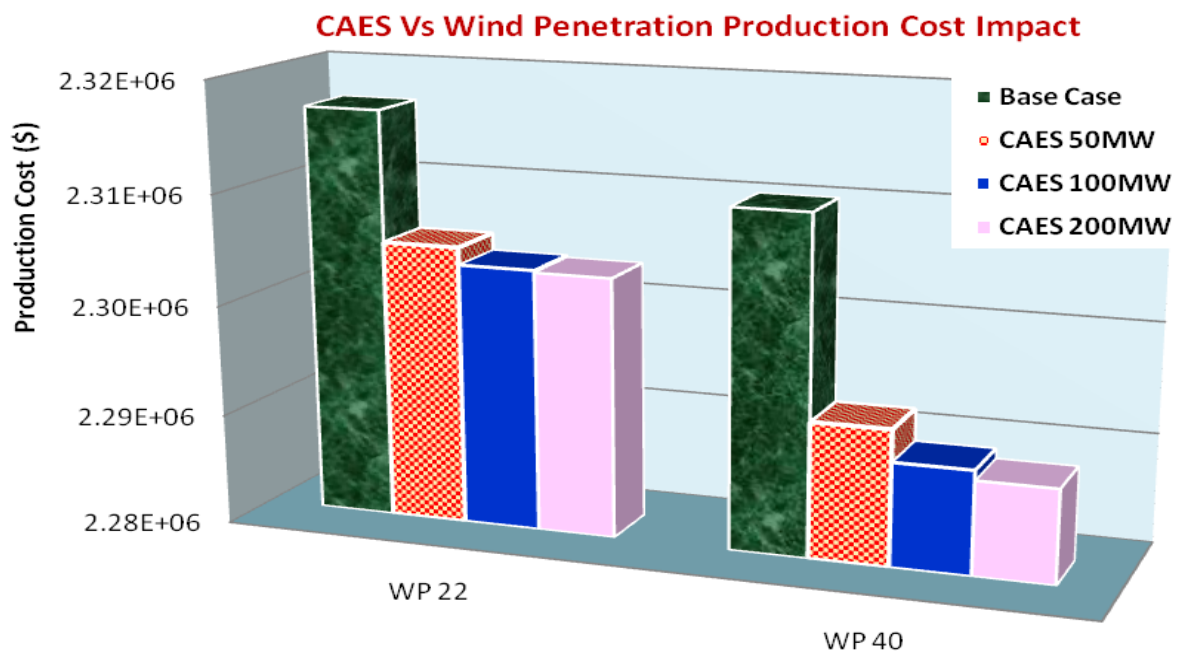
Figure 4.1 Production Cost with CAES under different wind penetration levels

4.2.2   Impact on Fossil Generation Units Starts

As a consequence of CAES participation in the energy and AS market, it reduces the number of starts of coal and natural gas units. As seen from Figure 4.2 50MW CAES participation in the grid relieves coal and natural gas units start-ups.
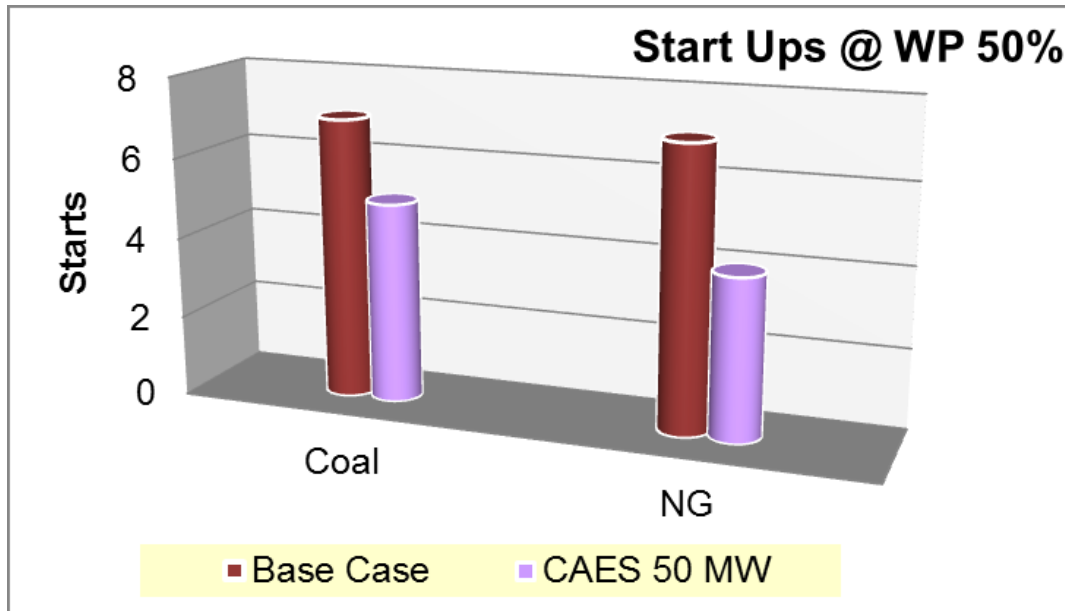
Figure 4.2 Start-ups of Coal And Natural gas units with and without CAES

Figure 4.3 shows the total starts of 50MW CAES unit under 50% wind penetration in green bars plotted against the system load curve. In the same plot, the blue and orange bars in negative direction shows the coal and natural gas unit starts in the base case that were averted in the case with 50MW CAES. From this plot we can conclude that CAES participation in grid reduces fossil fuel unit shut down/start up cycles that are beneficial for these units as it reduces the unit stress.

CAES is three times as efficient as a typical combustion turbine. Hence they are designed for cyclic operation. CAES consumes $1/3^{rd}$ of the fuel compared to the combustion

turbine and thus emits $1/3^{rd}$ of its emissions. Consequently start-up cost for CAES is lesser compared to other fossil fuel generations such as coal and natural gas. From the grid perspective it is better to cycle and frequently start the CAES and other bulk storage technologies compared to slow responding conventional fossil fuel generating units.
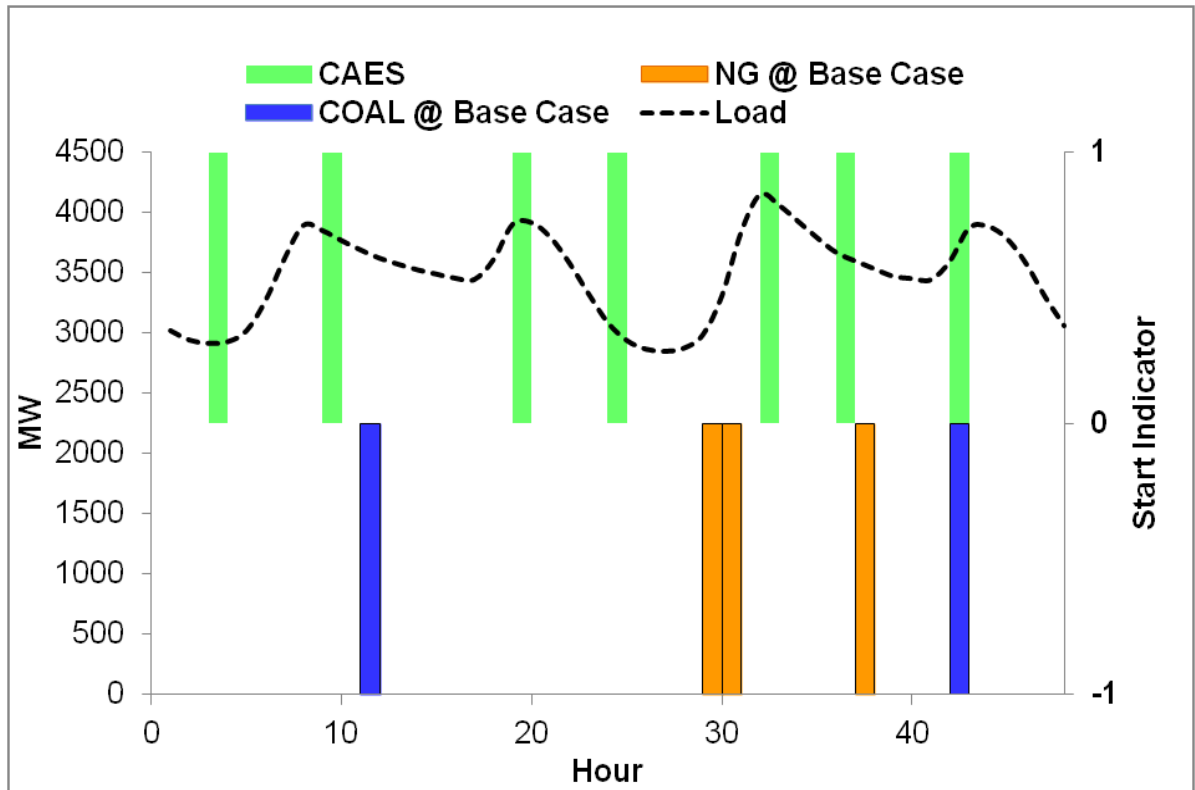
Figure 4.3 CAES reducing fossil fuel start-ups for simulation with and without CAES

4.2.3   CAES Energy and Ancillary Revenue

The AS and energy revenues earned by the 100MW CAES unit under different wind penetrations is shown in Figure 4.4. With higher levels of wind penetration the CAES unit earns higher revenues, especially from AS markets. The CAES unit energy revenue $C_{revenue}$ is calculated as:

$$C_{revenue} = \sum (P_{turbine} * LMP_i(t) - P_{compressor} * LMP_i(t)) \tag{4.1}$$

$P_{turbine}$: amount of power discharged through the turbine side (MW)

$P_{compressor}$: amount of power charged through the compressor side (MW)

LMP: Locational Marginal Price ($)

i: Bus number

t: Hour of charge/discharge

Under 60% wind penetration CAES has negative energy revenue implying the charging expenditure is more than the amount earned through its discharging operation as seen from Figure 4.4. By virtue of cross-arbitrage, the charging capability of CAES from energy market is utilized to supply regulation services. Thus we can understand that under higher wind penetrations, the bulk storages such as CAES would benefit more from its AS than from its energy transactions with the grid. The reason is that with increasing wind penetration, if the system regulation requirement increases (which will occur unless wind is controlled to provide AS), then CAES earns more revenue from the AS markets; since it is the low cost regulation provider, it is naturally scheduled to provide the majority of the system regulation for better grid economics.

Figure 4.5 shows that as the CAES size increases, the total revenues earned by the bulk storage increases under every wind penetration level. The profitability of increasing storage size is higher under higher wind penetrations than at lower wind penetrations, as higher wind penetrations offer greater opportunities for storage contribution to grid services.

**CAES 100MW Vs Wind Penetration
Energy and Ancillary Profits**
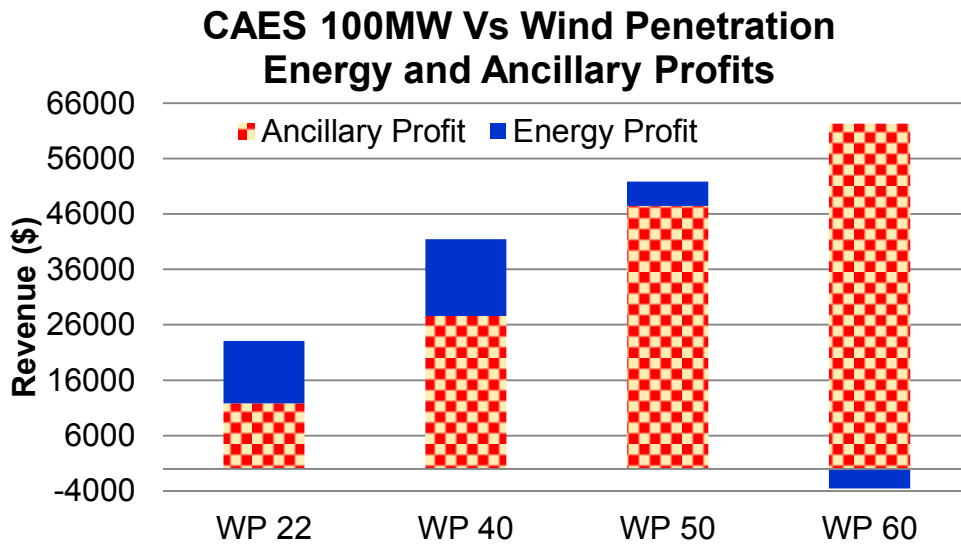
Figure 4.4 Revenues for 100MW CAES under different wind penetration levels
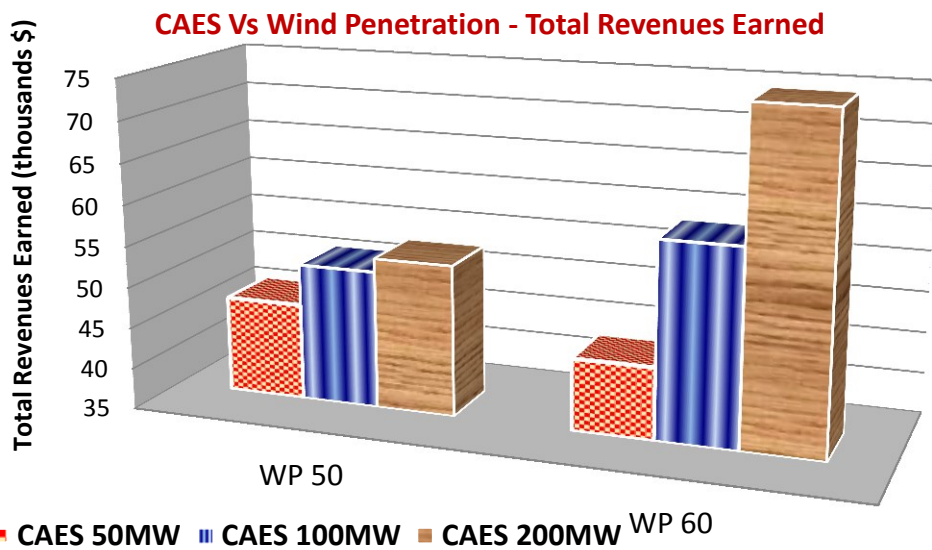
Figure 4.5 Total revenues under increasing wind penetration levels and storage sizes

4.2.4 Impact on System Regulation Service

Both the charging and discharging operation of the storage units is engaged is

supplying services such as regulation up and down. As shown in Figure 4.6 as storage unit

size increases its participation in regulation commensurately increases. Bulk storage, though has the capability to provide spinning and non-spinning reserves, is generally not seen to be committed for those services given the fact that other resources supply them at a price competitive to the offer of CAES unit. Thus the grid benefits from committing the bulk storage for energy and regulation services are higher in terms of lower LMPs, lower MCPs thus lower production cost and higher quality of regulation reserves than committing other generation units. This in return benefits storage too.
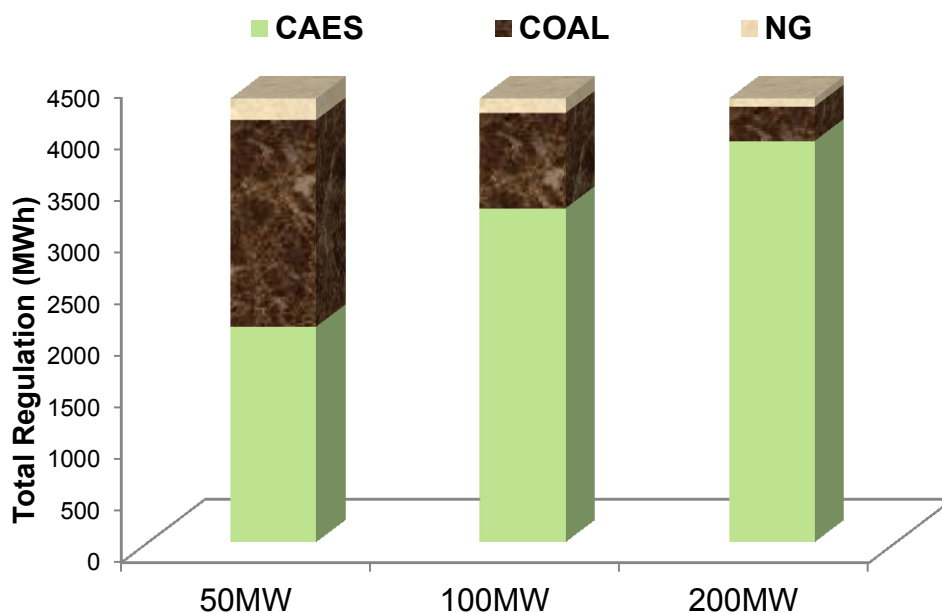
Figure 4.6 Regulation provided with increasing CAES unit sizes under 60% WP

As seen from the bar-chart in Figure 4.7, as wind penetration increases the regulation requirement increases. In this chart we see that a 100MW CAES unit is the primary regulation provider and its participation increases with higher levels of wind penetration.
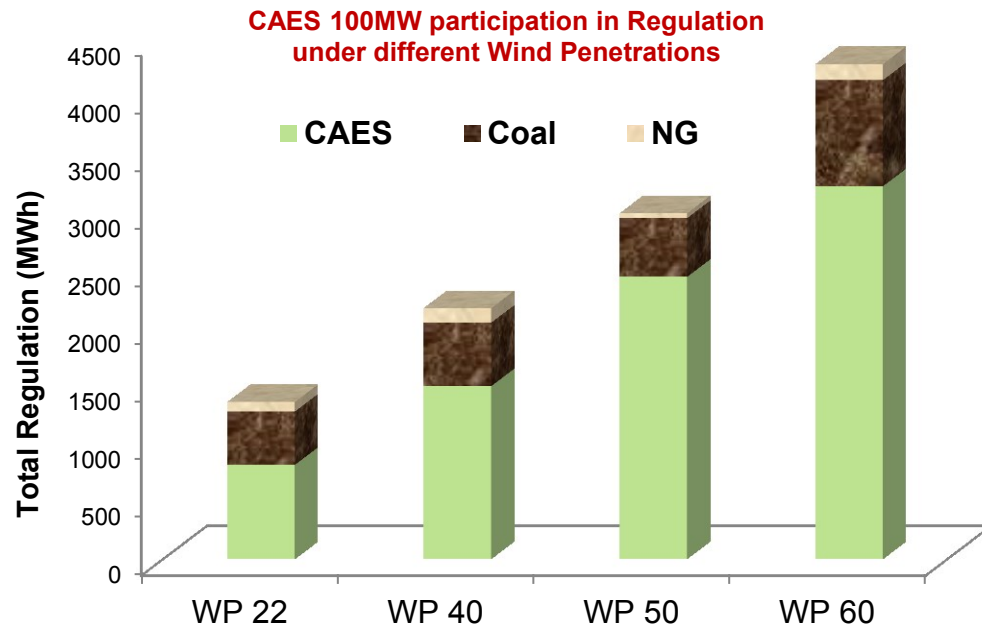
Figure 4.7 CAES participation in Regulation under different wind penetration levels

Figure 4.8 bolsters the conclusion about the increasing AS revenue earned by CAES under increasing wind penetrations. Within the same level of wind penetration, with increasing CAES sizes, its AS revenue increases. At lower wind penetrations, the potential for a larger sized CAES to make revenues is lesser, which will have serious economic implications on such investments.
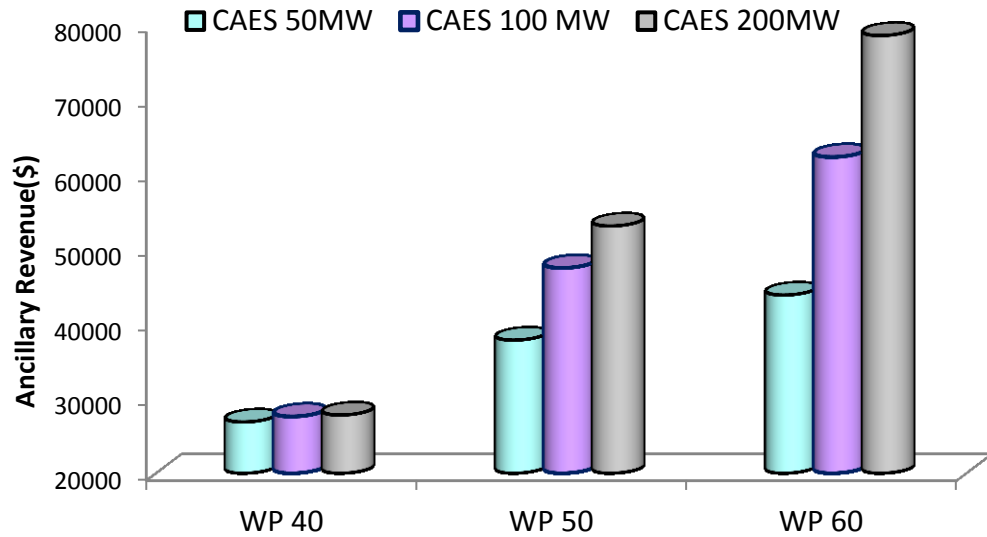
Figure 4.8 Ancillary revenue earned by CAES under increasing wind penetration levels

4.2.5 Impact on System Emissions

The system emissions decrease with increasing wind penetration as there is more emission free generation onto the grid as observed from Figure 4.9. With the inclusion of CAES unit, it is observed that the system emissions are further reduced. Within a given wind penetration level, increasing CAES size reduces the level of emissions. This is because CAES replaces a part of the fossil fuel generation in the grid and aids in wind penetration.
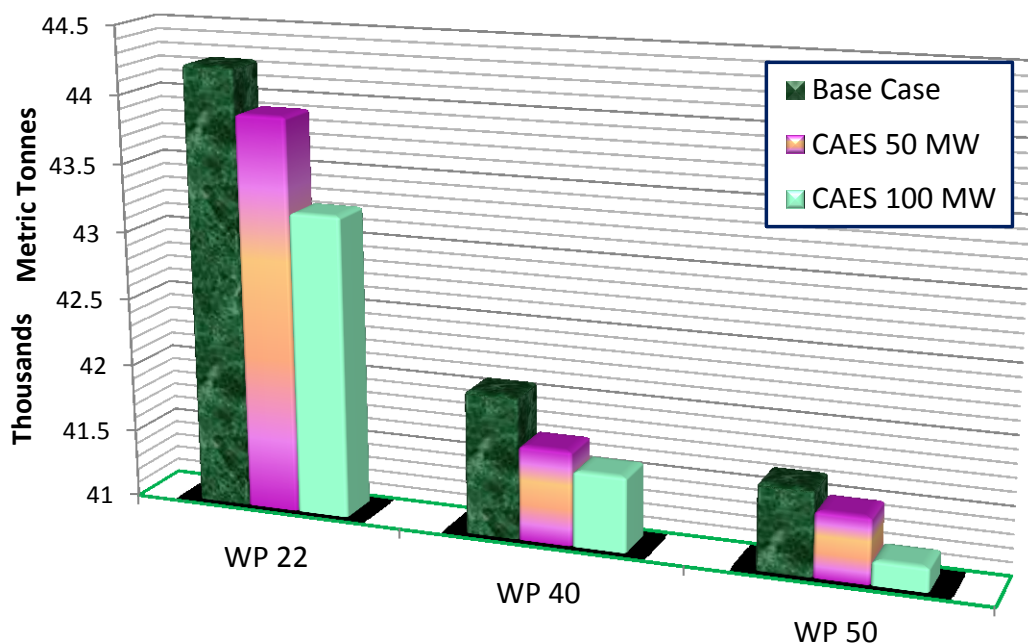
Figure 4.9 Total system emissions under different wind penetration and CAES sizing

Figure 4.10 shows the charge and discharge operations of a 50MW CAES, and also plots the changes in wind and coal generation without and with CAES. It illustrates how CAES aids wind penetration primarily by charging (thereby greening the grid), and relieves emissions from coal generation through its discharge operation. It is the case for this particular system where CAES is strategically co-located with the wind such that it can easily charge from the excess wind generation at times of low-demand. But as the figure also shows an instance around hour 30, when CAES charges from a low-cost coal unit indicating that without much renewable support, bulk storage penetration may increase low-cost fossil unit generation and the associated grid issues. Thus in such a case CAES may lead to *double-counting* in terms of emissions, i.e. an emitting generation resource is used to

charge it and since CAES has some emissions while discharging, it would contribute more towards the systems emissions than just utilizing the fossil units by itself.

In Figure 4.10 we see from the red and black labels the starts and shut-down of coal units with and without CAES in the system. Between hour 9 to 18 we observe that with CAES the coal units generation time were reduced by postponing their starts and pre-poning their shut-downs. The same effect can be observed between hours 36 and 43. Though CAES charges from coal at around hour 30 we see that CAES participation reduces the overall coal generation. Furthermore its can be observed that the CAES does not cause coal units to start for its charging but rather postpones of pre-pones its starts in a way it can reduce coal generation.
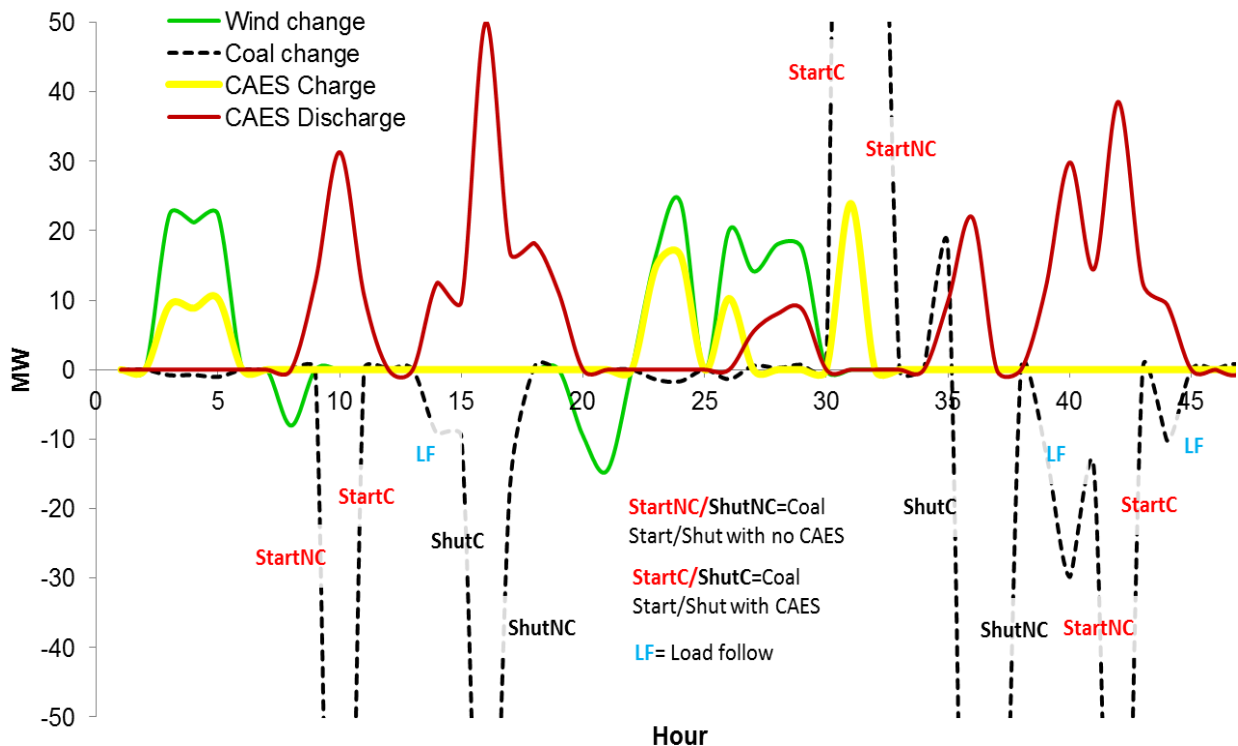
Figure 4.10 CAES charging aid wind penetration and discharging reduces coal generation

4.2.6   Conclusions

The following conclusions are drawn from this assessment:

a. CAES reduces the production cost of the system. As size of CAES is increased and with higher wind penetration levels there is significant reduction on the production cost.

b. Inclusion of CAES in the grid reduces the total number of starts of fossil fuel units such as coal and natural gas.

c. Under higher wind penetrations, bulk storages would benefit primarily by providing AS. As the storage unit size increases its participation in regulation market commensurately increases. The economics of a larger storage under lower wind penetration may not look good.

d. Inclusion of CAES and other non-emitting bulk storages reduce the total system CO_2 emissions.

4.3 STUDY 2: CYCLING ASSESSMENT

Cycling phenomena is defined as the unit stop/start sequence, load reversal (full load to minimum load and back), load following, and high frequency MW changes as seen by the automatic generation control (AGC). Since the base load units such as the coal units are not designed for such frequent cycles between different operating points, it causes stress and fatigue in these generating units. This causes increased wear and tear in the components of the generators such as the boiler that degrade the life cycle of the plant. Typically costs associated with heat rate degradation due to unsteady operation are incorporated within regulation offers. However Aptech based on their long-term assessments of conventional

plants quotes a higher cost impact of cycling phenomena, which are seen to be exacerbated under high renewables. So in this section:

1. Systematic methodology is devised to incorporate the realistic cycling costs reported by various studies in open literature within all the generator's AS offers

2. The impact of storage integration on these cycling costs are quantified

4.3.1 Cycling Metrics

We can measure the impact of cycling in terms of:

a) Type of start-up – hot, warm or cold

b) The quantity of fuel consumed at start-up

c) Auxiliary power usage

d) Degradation of the operating efficiencies (heat rate degradation)

e) Decrease in unit response rate

f) Increase in maintenance

g) Forced outage rate (FOR)

h) Increase in annual maintenance cost

i) Impacts on environment – emission

j) Very low load operation

k) Increase in upgrades

Aptech [83] defines the cost of cycling as:

Total Cost of Cycling = Δ Maintenance and Capital Spending + Δ Replacement Power Cost Due to Forced Outages + Δ Long-Term Heat Rate Impacts + Δ **Operational Heat Rate Impacts** + Δ Startup Auxiliary Power and Chemicals + Δ Startup Fuel and Manpower + Δ Capital Cost Impacts Due to Unit Life Shortening   (4.2)

Here, Δ refers only to those costs attributed to cycling

Based on the 48-hour PC simulation results the total cycling cost ($Cy\$$) is estimated as given in equation (4.3). In this study we are considering the operational heat rate impacts as it is a 48-hour simulation. In this short-period simulation the long-term heat rate impacts are not captured and hence not included in the generator cycling components of their offers.

$$Cy\$ = \sum_t \sum_i Starts_i(t) \, \Delta HS_i + (RU_i(t) \\ + RD_i(t))(2.\Delta HRD_i + \Delta VOM_i + \Delta MA_i) + SR_i(t).\Delta HRD_i$$

(4.3)

HS: Hot Start

RU: Regulation-Up served (MWh)

RD: Regulation-Down served (MWh)

HRD: Heat Rate Degradation

VOM: Variable Operational and Maintenance

MA: Margin Adder

SR: Spinning Reserve served (MWh)

4.3.2   Incorporating Cycling Cost in Generator Offers

To capture the effect of cycling, additional cost related to cycling can be added to the offers of the generators. The cycling cost values estimated and reported by APTECH [84,

85, 86] are appropriately used to determine the cycling cost component for the regulation, start-up, shut-down and spinning reserve costs. A minimum and maximum cycling component was obtained for each service. The next few sub-sections assess the cost structures of energy and AS offers provided by generators, and presents means to integrate cycling component in them.

4.3.2.1 Regulation Offers

The regulation offer construct is given in the PJM manual [87], which is a function of heat rate degradation due to non-steady and low load operations, variable operational and maintenance cost and a margin adder for enabling the utilities to recover any miscellaneous long-term costs. Equation (4.4) referred from the PJM Manual, indicates that the cycling related costs are broken down into these three categories appropriately, and added as cycling components to the original regulation offer.

Though in the PJM Manual their offer construct includes the cycling components, they have not incorporated the true cost of cycling as reported by APTECH after their long-standing studies on cycling of coal units. Hence here these components added to the generation offer as per equation 4.3 reflect the cost values reported by APTECH studies and made the required manipulation to appropriately incorporate in the given cycling components.

The regulation offer with cycling components is given by equation 4.4

$$\textit{Cycling components} = \textit{Original offer} + \Delta\, \textit{HRD} + \Delta\, \textit{VOM} + \Delta\, \textit{MA} \qquad (4.4)$$

1. *Δ Heat rate degradation (HRD):* APTECH quotes minimum and maximum values of costs related to load following functionalities for different generators [84] as

given in table A5 of the Appendix, as a function of their ramp characteristics. Considering the typical ramp rate for regulation services to be twice that of load following ramp rate, the costs for 2 times the base ramp rate were extracted from the report.

2. *Δ Variable and Operation Maintenance (VOM) increase:* The Table A4 is the data reproduced from APTECH report [85] quotes the cycling costs of a conventional coal plant related to its load following operation. Among all the cycling components mentioned, the lower and higher estimates for costs related to operation (E1) and maintenance (E2) gives the minimum and maximum VOM components. These costs are normalized to respective coal generation ratings in the IEEE 24 bus system. The cycling induced VOM component for other generators are estimated based on the ratios of typical VOM components of all generators assumed for original regulation offer construction, as quoted in [87].

3. *Δ Margin Adder (MA) increase:* From the same table the lower and higher estimates of cycling cost related to capital maintenance are used to estimate the additional margin adder (MA) component of the regulation offer.

4.3.2.2 Spinning Reserve (SR)

To the SR offer construct [87], a cycling component related to heat rate degradation at low load operation is added based on APTECH quotes. The minimum and maximum values of this HRD related cost are obtained for the base ramp rate of each generator [84].

4.3.2.3 Start-up (SU) and Shut-down (SD)

Frequent SU and SD are more detrimental to the life cycle of the unit than the load following [83]. Thus it is essential to categorize the SU offer based on the type of SU. The SUs are categorized as cold, warm and hot, with cold being the more severe for the unit. APTECH [85, 86] quotes the comprehensive cycling costs for different kinds of starts. In the 48-hour simulation studies, we assume all starts as hot starts and take the corresponding minimum and maximum cycling costs for hot starts. The equivalent yearly hot starts for this typical coal generator in APTECH report is estimated using the GADS report, and the cost per hot start (HS) is estimated for generators in IEEE 24 bus system. This incremental component for start-up cost is estimated for other generators too by maintaining the same ratio as the original start-up cost ratios.

The total cycling cost related to unit starts (shut-start cycle) are spilt between the cost of start-up and shut-down operations in the same proportion as the original assumed start-up and shut-down costs are.

All these cycling induced additional offer components of respective operations are listed in the Table 4.1. The *ΔHRD* component for regulation offer is 2 times the *ΔHRD* component for SR offer shown in Table 4.1.

Table 4.1 Cycling components for generation offers

Gen (Bus)	Δ HS Cost ($/Start cycle) Min/Max	Δ HRD - SR offer ($/MW-hr) Min/Max	Δ MA - Reg offer ($/MW-hr) Min/Max	Δ VOM - Reg offer ($/MW-hr) Min/Max
Oil (1)	79/286	1.91/3.84	0.0028/0.0256	0.0057/0.0473
Coal (1)	79/286	1.91/3.84	0.0028/0.0256	0.0057/0.0473
Oil (2)	79/286	1.91/3.84	0.0028/0.0256	0.0057/0.0473
Coal (2)	79/286	1.91/3.84	0.0028/0.0256	0.0057/0.0473
NG (7)	25/89	1.92/2.32	0.00168/0.01536	0.00342/0.02838
NG (13)	25/89	1.92/2.32	0.00168/0.01536	0.00342/0.02838
NG (15)	25/89	1.92/2.32	0.00168/0.01536	0.00342/0.02838
Coal (15)	79/286	1.91/3.84	0.0028/0.0256	0.0057/0.0473
Coal (16)	79/286	1.91/3.84	0.0028/0.0256	0.0057/0.0473
Coal (22)	39/124	1.4/3.1	0.0028/0.0256	0.0057/0.0473
Coal (23)	39/124	1.4/3.1	0.0028/0.0256	0.0057/0.0473
Coal (23)	39/124	1.4/3.1	0.0028/0.0256	0.0057/0.0473
CT	22/118	0.94/2.8	0	0
CAES (21)	12/ 61	0.42/1.7	0	0

4.3.3   Case Studies

In this section four different scenarios under 60% wind penetration level are compared. The scenario specifications are mentioned below:

- *Scenario 1:Base Case*

    o   The offers do not have any cycling cost added.

    o   There is no storage unit in the system.

- *Scenario 2: CAES 100MW*

    o   The offers do not have any cycling cost added.

    o   There is a CAES unit of 100MW at bus 21.

- *Scenario 3: Minimum Cycling Cost Case*

    o   The offers are having the minimum cycling cost components.

    o   The storage unit of 100 MW CAES is at bus 21.

- *Scenario 4: Maximum Cycling Cost Case*

    o   The offers are having the maximum cycling cost components.

    o   The storage unit of 100 MW CAES is at bus 21.

4.3.3.1 System Cycling Cost

Figure 4.11 shows the cycling cost incurred under all the scenarios. It is seen that the total cycling and the costs decrease with adding the cost of cycling to the generation offers. Table 4.2 compares the yearly cycling cost incurred under each scenario, which are approximated based on 48-hour simulation.
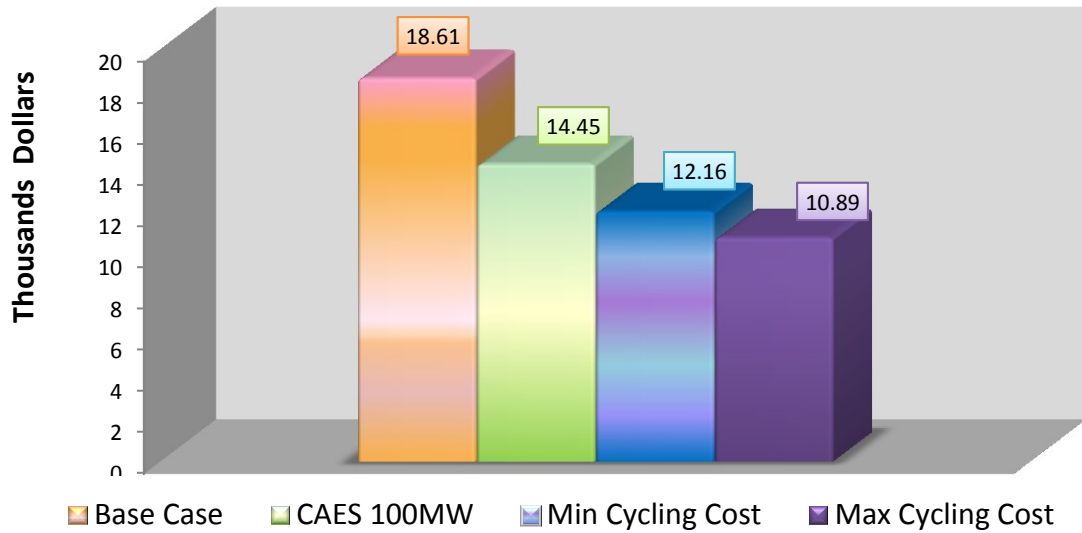
Figure 4.11 Cycling cost for the system under different scenarios

Table 4.2 Cycling Case Study Comparison

Scenarios	Yearly Cycling Cost (M$)	Savings (M$)
Base case	3.39	-
100MW CAES	2.63	0.76
Min Cycling Cost + 100 MW CAES	2.21	1.18
Max Cycling Cost + 100 MW CAES	1.98	1.4

With storage of 100MW CAES unit the cycling cost is reduced to $2.63M over a year which is a saving of $ 0.76M compared to the base case. The storage unit relieves the traditional units from serving the regulation demand and also reduces the starts and shut downs as discussed in section 4.2, which saves on the cycling cost of the system. These base-load units benefit by addition of storage unit as the storage reduces the thermal stress of the units and thus prevents it from performance and economic degradation.

With increase in regulation offers by addition of cycling component, the system cycling cost further decreases as it further increases the contribution from storage in regulation services replacing the conventional units.

4.3.3.2 Conventional Unit Starts

In Figure 4.12, we assess the number of starts that coal and natural gas undergo under the different scenarios. We observe that under base case over two days coal units have a total of 8 starts and natural gas units have a total of 6 starts. With inclusion of 100MW CAES, we find the number of starts for coal is reduced to 6 and for natural gas it is reduced to 4. Under scenario 4 with addition of cycling cost into offers, we find that it further reduces the coal starts to 5 and natural gas still has 4 starts.
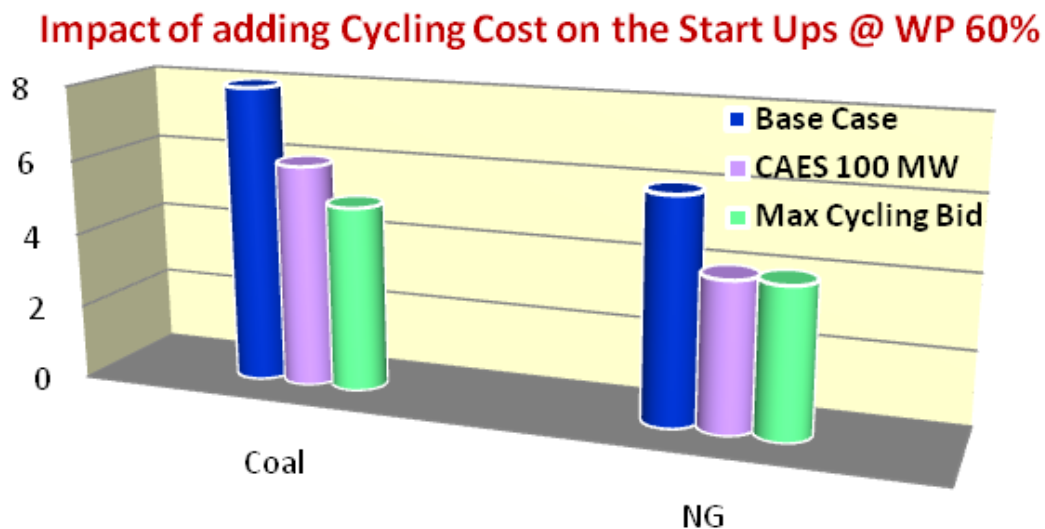
Figure 4.12 Starts of Coal and Natural gas units under the different scenarios

4.3.3.3 Regulation Service

Figure 4.13 shows the regulation provision under different scenarios. In base case we observe coal units supplying almost the entire regulation. This is because the coal acting as the base-load provider with cheap regulation offers than the other faster better quality generation units. For instance to commit the natural gas units to provide regulation would further incur the start-up cost apart from its higher regulation offer. Hence the optimization program chooses coal to provide the regulation. With the cycling component added to the regulation bid of coal units we find that coal participation is reduced and natural gas participation encouraged.

When we include a 100MW unit of CAES we find that CAES primarily supplies the regulation of the system. By adding the cycling cost to the offer of the generators, we see that CAES participation in regulation increased almost to the full requirement. Both the results in sections 4.3.3.2 and this section corroborate the decreasing cycling costs in Figure 4.11.
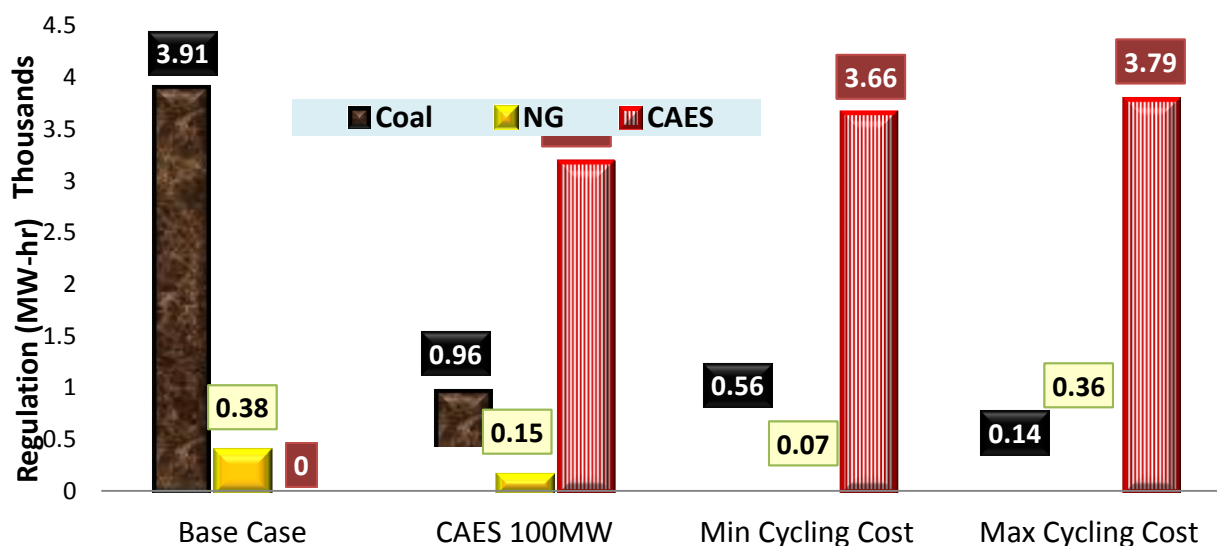
Figure 4.13 CAES participation in regulation under the different scenarios

Without Coal Participation in the Regulation Market

To investigate the scenario without coal participation in the regulation market two scenarios were investigated. First scenario is the base case without CAES unit in the system and second case is with CAES 100 MW unit in the system.

When coal generation does not participate in regulation we find from Figure 4.14 the natural gas units act as the regulation provider. With CAES 100 MW under this scenario we find CAES unit heavily participates in the regulation market though natural gas supplies more regulation than CAES under this scenario.
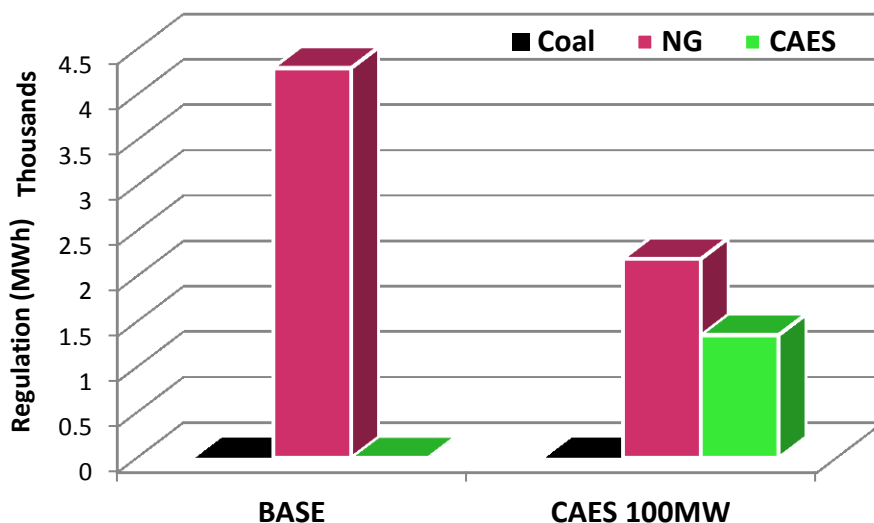
Figure 4.14 Regulation market without Coal participation

With coal participation in the regulation market the production cost is lesser compared to the base case without coal in regulation market. Without coal in regulation market it is seen from Figure 4.14 that natural gas units participate in the regulation market which has a higher regulation offer than coal which is one of the reason resulting in slight increase of $ 5.3K in the production cost compared to the base case with coal in regulation market. On the other hand, we observe coal participation in regulation market under base

case incurs a heavy cycling cost of $ 34.5K much higher than $ 20.2K in the base case without coal participation in the regulation market. This is because the cost of cycling natural gas units is less compared to cycling coal units.

Under CAES 100MW scenario, with coal participating in regulation, we find the cycling cost is reduced to $ 14.1K which is lesser compared to without coal participation in the regulation market. This implies that CAES relieves coal unit cycling by participating as the primary regulation provider as observed from its AS profit from the Table 4.3. In conclusion if there are units with higher ramping capability that participate in regulation market in the system, then we do not observe an appreciable reduction due to CAES in the cycling cost (as the original cycling cost itself is less).

Table 4.3 Comparison of Scenarios With and Without Coal in Regulation Market

	BASE CASE		CAES 100 MW	
	With Coal in Regulation	Without Coal in Regulation	With Coal in Regulation	Without Coal in Regulation
Production Cost (M$)	2.3423	2.3476	2.3089	2.195
Cycling Cost (K$)	34.5	20.2	14.1 (-20.4)	16.5 (-3.7)
CAES AS Profit (K$)	-	-	62.3	43.9
CAES Energy Profit (K$)	-	-	-3.5	58.8
CAES Total Revenue (K$)			58.80	43.87

While without coal in regulation market we find that production cost ($ 2.19M) with CAES 100MW is lesser compared to with coal in regulation market. Without coal participation in regulation market, CAES is participates in the energy market as seen from

the energy profits of $ 58.8K and thus reduces the production cost. As seen from Figure 4.14 natural gas unit provides most of the regulation. The production cost is primarily influenced by the energy prices and thus the optimization program chooses CAES to participate more in energy market than in AS market as it is beneficial for the grid.

4.3.3.4 CAES Revenues

Storage is providing economic benefits to the system by relieving cycling and providing the bulk of regulation services. However, without including cycling costs within the generation offers, storage cannot benefit from the provision of this service. With inclusions of cycling cost within the offers, we observe in Figure 4.15 that CAES earns greater revenues, as it effectively increases system MCPs at times when storage is not marginal.
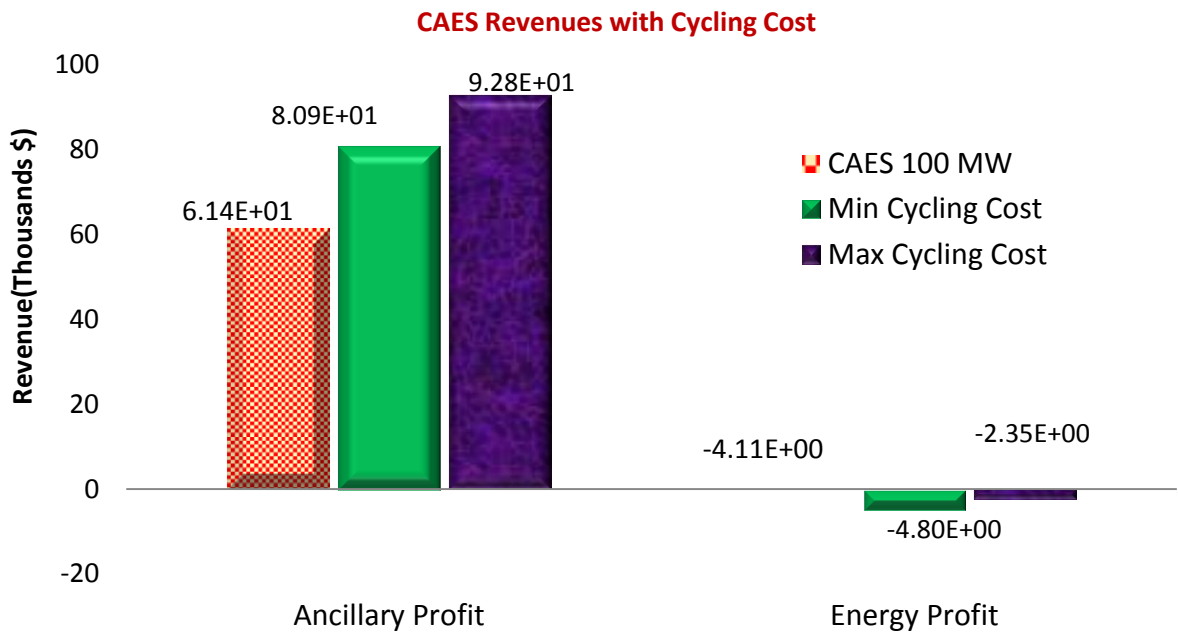
Figure 4.15 CAES Energy and AS Revenue under the different scenarios

4.3.3.5 System Production Cost

Figure 4.16 shows the market clearing prices (MCP) for both regulation down and regulation up. Under base case we see that the MCP for regulation down is a constant horizontal line as coal is the marginal unit that sets the price. Under the CAES 100MW scenario we find that CAES becomes the marginal unit for regulation many times and thus lowers the MCP. Similarly in the regulation up scenario we find that under the base case, coal sets the MCP during most of the periods and if coal is not available natural gas becomes the marginal unit. With CAES we find that it relieves these traditional units from supplying regulation up requirement, and hence lowers the MCPs.
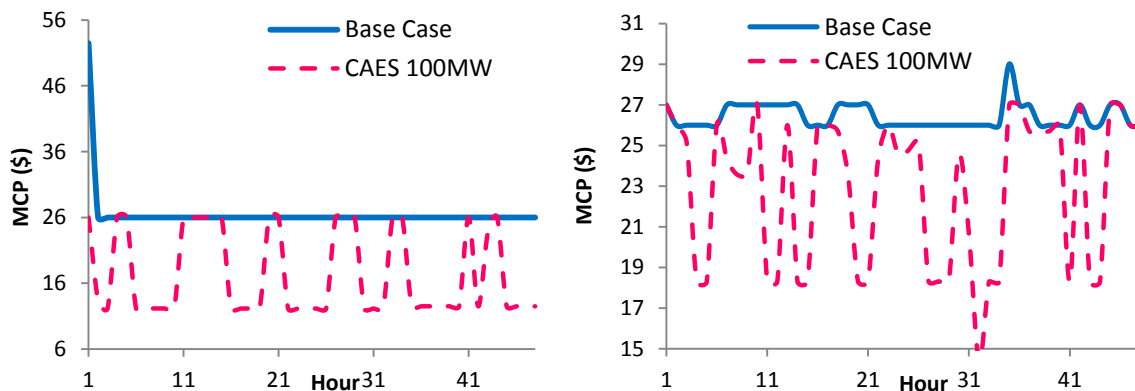
Figure 4.16 Regulation MCPs (a) Down regulation (b) Up regulation

In Figure 4.17, we observe the production cost under the four scenarios. We find the production cost at base case is highest, and 100MW CAES in the system decreases the production cost a good deal as it reduces MCPs (as a result of its lower energy bids) and because it reduces conventional unit starts (as a result of its effect on load leveling). Production cost with cycling cost included in the bids is higher than the storage only case.

The cycling cost and production cost under the different scenarios stacked together in this plot brings out the actual total production cost under the different scenarios. In the base case and with CAES 100MW case, the cycling cost incurred is not included in the offers and estimated post-facto. While for the other two scenarios (3 and 4), the cycling costs are accounted within the offers and the program generated optimized production cost. We realize that the cost of production is much higher in the base case with the addition of the cycling cost incurred. When the cycling cost is stacked on to the production cost of scenario 2 with 100MW CAES, we find the total production cost is appreciable to the scenarios 3 and 4 where the cycling cost in included in the offers.
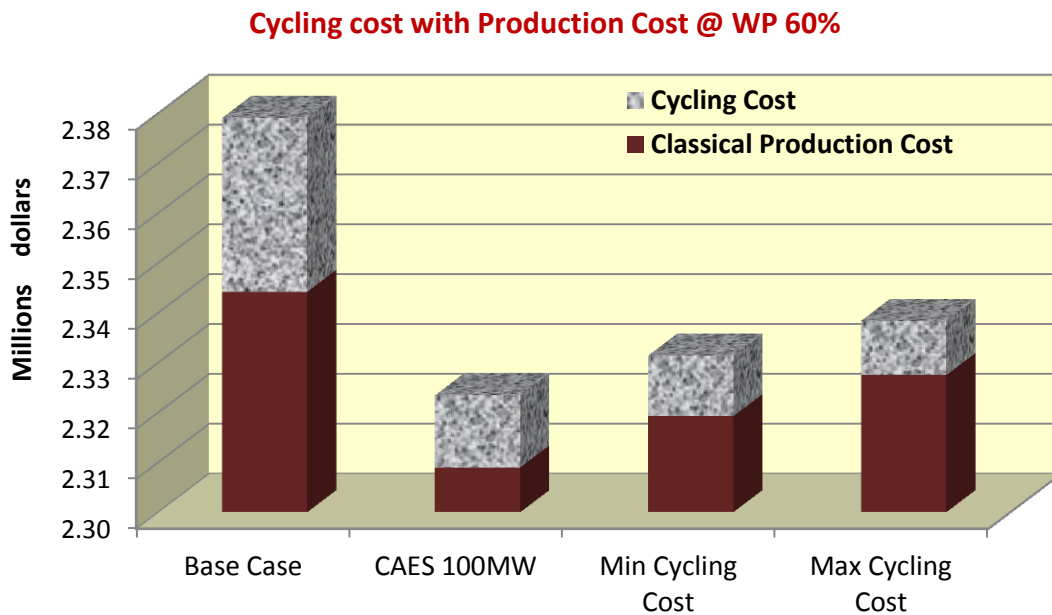
Figure 4.17 cycling Cost added to System production cost under different scenarios

Thus by including the cost of cycling in the offers, we not only reduce more cycling related costs but also benefit the storage to earn more profits from the grid as was observed in Figure 4.15, and still can keep the production cost at lower levels than the base case. The

higher production cost is primarily due to increase in start-up and shut-down cost, which does not seem to provide much incremental benefit to reduce starts than just including a storage, as observed in Figure 4.12. Therefore, just by incorporating cycling components in the regulation offers alone will benefit storage and grid, without increasing the production cost by too much. However, such a situation may come about, only if conventional generators do in fact increase their AS offers. Otherwise, we need to devise some special incentives for storage technologies just as production tax credit is awarded to wind generators without penalizing the other generators for CO_2 emissions.

4.3.4 Conclusions

From the cycling assessment study the following conclusions are drawn:

a. The section discussed a methodology to include cycling related cost components to the AS offers and start-up/shut-down costs, and also to estimate these cycling related costs from co-optimized dispatch decisions.

b. With CAES storage unit the system cycling cost is significantly reduced as it relieves the base load units from serving the regulation demand, and also reduces the conventional unit starts. Participation of CAES in regulation service also lowers the MCPs and the system production costs.

c. Offers with increased cycling cost component encourage higher CAES participation in regulation, and higher revenues for storage.

d. In this study the impact of cycling on emissions has not been assessed. It is observed that due to degraded heat rate and operational efficiency while providing regulation services and starts, a conventional unit emits more than its

usual emission under normal operation [88]. The benefits of storage will be more pronounced if such emissions are taken into account.

4.4 STUDY 3: PAYBACK ASSESSMENT

4.4.1 Different CAES Sizes with increasing Wind Penetration

Table 4.4 presents an economic assessment to estimate the payback of each storage project based on 48-hour production costing simulation. We observe that for CAES units of 50 MW and 100 MW size, the payback period improves under increasing wind penetration levels. This is because, as the wind penetration increases the system regulation requirement increases, and as seen from the table CAES is dispatched more for regulation services than any other.

- Comparing the paybacks of the two CAES sizes within the lower penetration level (22%), we find that the smaller capacity CAES has a better payback. Though the revenue from energy market is higher for the bigger CAES, still its ability to benefit from AS market is lower due to lesser opportunities at lower wind penetration. Combined with higher investment cost and operational cost, the economics for a bigger storage project at lower wind penetration will not make justice to its potential. For practical purposes, to generalize to other systems, the required regulation service in the grid may be considered as a proxy for the wind penetration levels.

Table 4.4 Simple Payback for different wind penetration levels and CAES sizes

Attributes	CAES 50MW			CAES 100MW		
Wind Penetration	WP 22	WP 40	WP 60	WP 22	WP 40	WP 60
Energy Discharge (MWh)	386.45	395.13	132.57	452.06	650.23	368.22
Up-Reg/Down-Reg (MW-hr)	288/682	513/933	883/1206	138/682	474/1025	1503/1728
Spin/Non-Spin (MW-hr)	0/0	49.4/0	18/0	67/0	58/100	245/0
Yearly Fuel Cost (M$)	1.23	1.46	2.37	1.35	1.71	2.73
Yearly Fixed O&M Cost (M$)	1.63	1.63	1.63	3.26	3.26	3.26
Investment Cost (M$)	25.5	25.5	25.5	51	51	51
AS Revenue (K$)	16.97	26.85	43.85	11.81	27.58	70.07
Energy Revenue (K$)	8.06	8.44	-0.033	11.28	13.88	-5.61
Total Yearly Revenue (M$)	4.55	6.42	7.97	4.20	7.55	11.73
Yearly Profit (M$)	1.70	3.34	3.97	-0.413	2.57	5.74
Simple Payback (years)	15.02	7.64	6.42	-	19.81	8.88

- At higher wind penetration levels of 40% and 60%, 50MW CAES earns yearly revenue of about $6.42M and $7.97M respectively, making about 24% more. While the 100MW unit earns $7.55M and $11.73M respectively, a leap of about 55%. Thus the ability to exploit the high wind penetration levels is more in bigger storage units than a comparatively smaller unit that gets saturated with its capacity. At very high penetrations, the payback periods are comparable.

4.4.2 Payback Sensitivity

In the previous sections 4.4.1, single 2-day simulation was used to assess the payback terms for CAES under different wind penetration levels for various CAES sizing. In reality the load and wind data varies. To find its impact on the payback period in this section we simulate thirty randomly sampled 2-day load and wind data and then average them to calculate the payback terms. The wind and load data are correlated as it is taken from the yearly data. The Figure 4.18 illustrates the flowchart for this process.
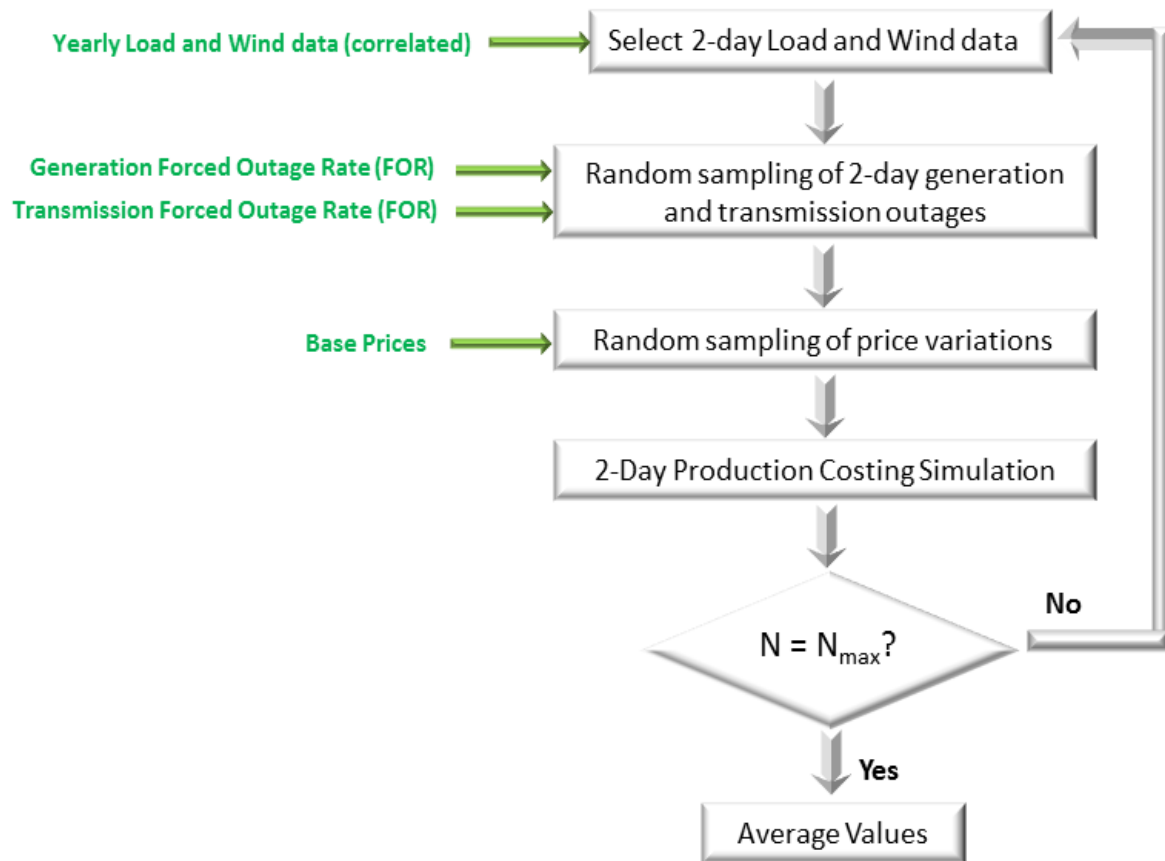
Figure 4.18 Monte Carlo Simulation for estimating Payback

In Figure 4.19 the ancillary and energy profit obtained under each of the 30 two-day simulation is plotted. The simulations with high AS profit and low energy were identified to

be 4, 9 and 16 as shown in orange shaded boxes in the plot. The wind and load profile corresponding to these simulation were plotted given in the lavender filled plots below. We observe that the winds under these days were high and at times of low demand wind exceeded the demand. Hence we find CAES earns higher profits from AS market and low energy profit. This corroborates with the earlier findings that reported as wind penetration increases in the system, CAES unit earns from AS market.

Next we identify the two-day simulation periods with high energy profit and low AS profit. They were identified to be 1, 5 and 16 as shown in green shaded boxes on the plot. The yellow shaded plots show the wind and load profile corresponding to these simulation periods. We observe that the wind is low during these days. Hence CAES participates more in the energy markets.

From the profits plotted we find that CAES earns the highest amount of about $ 70K profit amongst the 30 simulations for two-day from AS market at 18. While the highest amount earned by the CAES unit from the energy market is $ 40K from the 30 two-day simulations. This indicates that storage unit such as CAES would benefit more from its participation in the AS market than in the energy market.

The table 4.5 gives the payback periods with the thirty 2-day simulations. From the payback terms and comparing with the 2-day simulation we find that the trend is same as seen from the previous payback assessment with the smaller size of CAES having a better payback term than a larger size of CAES.

The table 4.6 gives the total starts for the different types of generations. With CAES 100 MW the number of starts in fossil fuel generation units such as coal, oil, natural gas and nuclear are seen to be reduced.
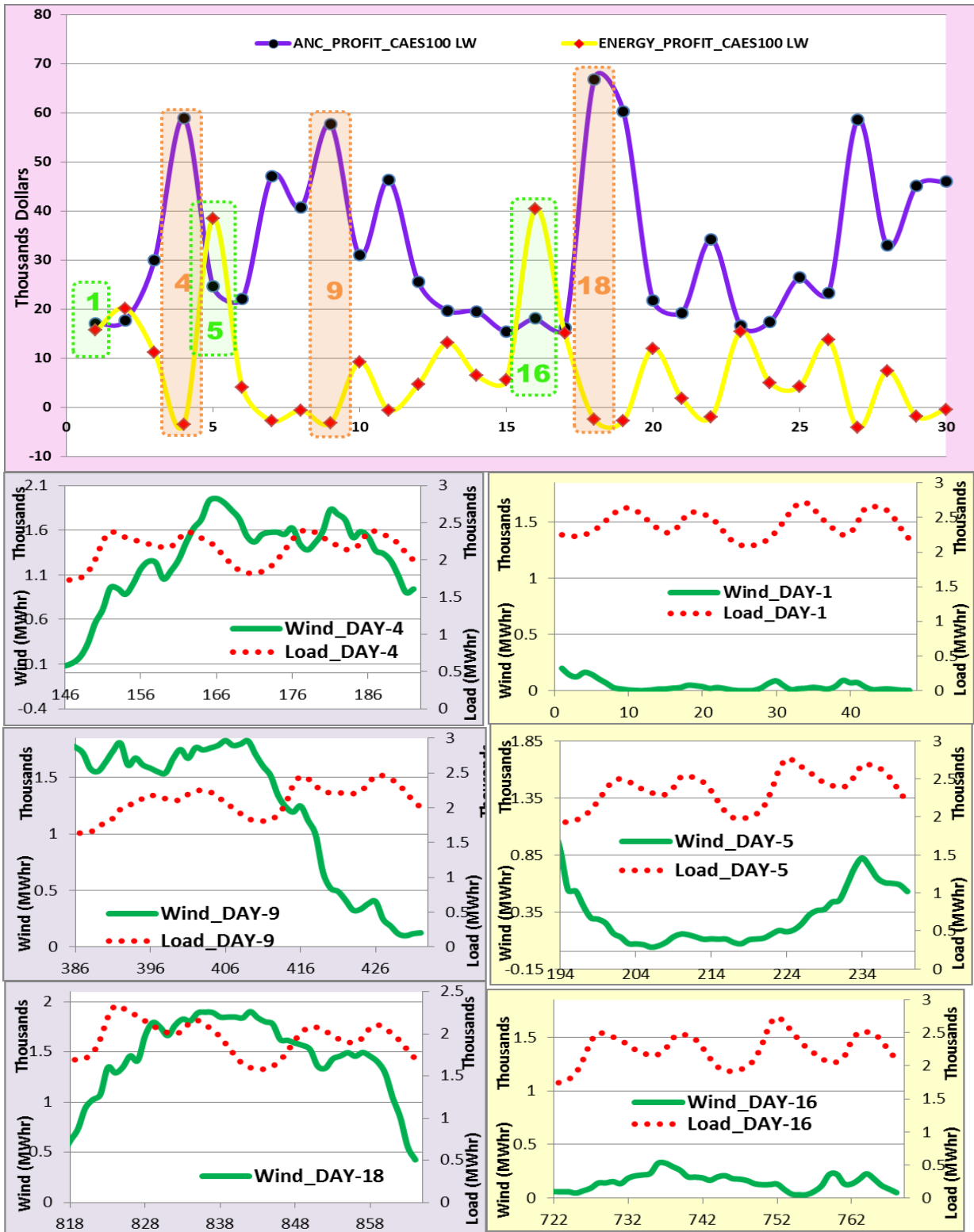
Figure 4.19 Ancillary Profit vs Energy Profit compared with 2-day 30 Wind Load Profile

Table 4.5 Simple Payback from thirty 2-day simulation

WP 40%	CAES 50 MW	CAES 100 MW
Energy Discharge (MWh)	38134.84	47724.16
Up-Reg/Down-Reg (MW-hr)	8992.96/25250.29	9038.82/23808.69
Spin/Non-Spin (MW-hr)	64231.36/30401.93	78996.38/38988.19
Yearly Fuel Cost (M$)	1.08	1.45
Yearly Fixed O&M Cost (M$)	1.63	3.26
Investment Cost (M$)	25.5	51
AS Revenue (M$)	5.97	7.57
Energy Revenue (M$)	1.17	0.778
Total Yearly Revenue (M$)	7.14	8.35
Yearly Profit (M$)	4.43	3.64
Simple Payback using Monte Carlo for 30 2-day simulations (years)	5.76	14
Simple Payback (years) using single 2-day simulation	7.64	19.81

Table 4.6 Starts of different generation types from thirty 2-day simulation

STARTS	Base	CAES50	CAES100	Base-CAES50	Base-CAES100
Coal	446	428	434	18	12
Oil	128	111	101	17	27
Natural Gas	244	243	222	1	22
Nuclear	135	134	120	1	15
CAES	0	168	143	-168	-143

These results corroborate the results from the previous studies comparing starts of fossil units with and without CAES in the system over two days (Figure 4.12). Thus bulk storage in the grid reduces the total conventional generation unit's starts.

4.4.3 Impact of Market Clearing Prices on Payback Period

In this section the impact of market clearing prices (MCPs) on the system payback period is assessed under the scenarios with generation units' offer prices raised by their cycling cost component.

4.4.3.1 Market Clearing Prices - Cycling Cost

The payback period is computed using equation 3.34 from chapter 3:

$$\left(C_{revenue} - C_{op.\,cost}\right)\sum_{t=0}^{N}\frac{1}{(1+r)^t} = C_{inv}$$

Table 4.4 compares the payback periods for 100MW CAES at 60% wind penetration. In these simulations, the minimum up and down time imposed in the production costing simulation were removed. This provides that fossil plants may transition more quickly than they are able to in reality, even instantaneously. This essentially allows them to cycle even more, if the economics benefit from them doing so. Although all fossil plants do have some transition time, studying this situation amplifies the influence of incorporating cycling cost on start-ups and shut-downs over 48 hours and enables identification of the trend that increased cycling would have on regulation market clearing prices (MCPs). The only other way to achieve this end is by changing cost or offer data which would introduce a direct influence on the MCPs. We find that the trend in payback period supports the

conclusions of the earlier cycling assessment study. Cycling cost components effectively increases the MCPs and reduces the payback period from about 11.45 years to 5 years.

Just as system MCPs naturally decrease from the presence of storage, the final column in Table 4.7 shows a scenario with lower MCPs to evaluate the risk involved in such a storage investment. All the generator's regulation bids were reduced by $12.5 by removing the margin adder component, and dispatch simulation was performed. It is seen that when MCPs are less, storage's AS revenues is reduced greatly and in turn energy revenues increase. The energy dispatched from CAES within the energy market in this case is about 1940 MWh over 48 hours, compared to 335 MWh generated otherwise.

Table 4.7 Payback with Cycling Cost for 100MW CAES at 60% Wind

Attributes	CAES	Min Cy$	Max Cy$	MCP_less
Yearly Fuel Cost (M$)	2.71	2.98	3.03	5.52
Yearly Fixed O&M Cost (M$)	3.26	3.26	3.26	3.26
Investment Cost (M$)	51	51	51	51.0
AS Revenue (K$)	61.4	80.9	92.8	3.09
Energy Revenue (K$)	-4.11	-4.8	-2.35	25.5
Total Yearly Revenue (M$)	10.42	13.85	16.46	5.21
Yearly Profit (M$)	4.45	7.61	10.2	-3.57
Simple Payback (years)	11.45	6.70	5.01	-

However, it is observed that the yearly profits (revenue less operational (fuel) cost) are negative, and hence with such a deficit it is unlikely to break even on its investment. The risk is much less for a smaller storage project. For instance, a 50MW CAES project at

reduced system MCPs, still is estimated to incur a yearly deficit, but a smaller one by 1.73M$.

4.4.3.2 Locational Marginal Prices – CO$_2$ tax

In this study carbon dioxide emission tax of \$30/tons is imposed on the energy generated by CO_2 emitting generators. The CO_2 emission rate for each type generation unit is given in Table A6 in the Appendix. By imposing the carbon tax, it is expected that the base-load emitting generations such as coal would generate less, and CAES would benefit more by higher participation in energy services. The imposition of CO_2 tax will also increase the system LMPs, which also improves the arbitrage opportunities for storage.
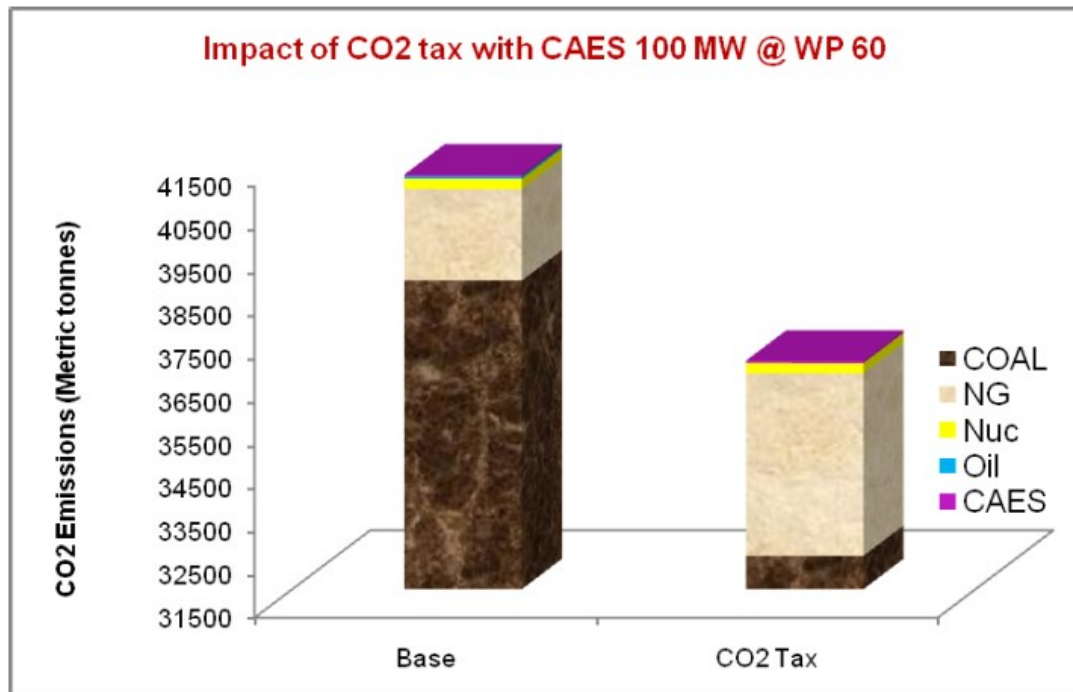
Figure 4.20 Impact of CO_2 Tax on system emissions with CAES

Figure 4.20 shows emissions results for scenarios with and without CO_2 tax at 60% wind penetration. Studying the emissions from the various generations, we observe that the

carbon tax causes the coal plants to produce less, and the overall system emissions are greatly reduced. CAES is receives increased revenues from the energy market and as a result is more profitable.

Table 4.8 Payback with CO_2 Tax at wind penetration 40%

Attributes	Without CO_2 Tax	With CO_2 Tax
Energy Discharge (MWh)	647.09	975.84
Up-Reg/Down-Reg (MW-hr)	388/1017	277/1010
Spin/Non-Spin (MW-hr)	0/200	82/40
Yearly Fuel Cost (M$)	1.71	2.86
Yearly Fixed O&M Cost (M$)	3.26	3.26
Investment Cost (M$)	51	51
AS Revenue (K$)	27.6	19.06
Energy Revenue (K$)	13.9	42.11
Total Yearly Revenue (M$)	7.55	11.13
Yearly Profit (M$)	2.57	5.01
Simple Payback (years)	19.81	10.18

From Table 4.8, we observe that with CO_2 tax CAES is estimated to break even with its investment at half the time it will take if CO_2 tax is not imposed. CAES, with ability to provide load leveling, and due to its low cost and to its low CO_2 emission rates, supplies more energy with the CO_2 tax than without. This results in lowered overall production cost As observed in Table 4.8, most of the discharge commitments in the AS market (for up

regulation and non-spinning reserves) are reduced, and in turn about 300MWh more energy is generated in the energy market. The higher arbitrage opportunities enable CAES to obtain higher revenues within the energy market.

4.5 BULK STORAGE VS OTHER PROBABLE SOLUTIONS

To compare the effectiveness of storage technology we need to compare it against other viable solutions that can help integrate variable generation. In this section, we compare the benefits of the bulk storage, CAES, with the benefits from Combustion Turbine (CT) and transmission expansion.

4.5.1 Study 4: CAES Vs CT

The CAES is assumed to be non-adiabatic, and hence both CAES and CT use natural gas for its operation. The CT energy bid is assumed to be about $60.45, about 3 times larger than the CAES energy bid. This is because CAES is 3 times more efficient than the CT, i.e., its heat rate is a third of the CT's heat rate, as result of its independent compressor and gas turbine operations. The ancillary offers of CT are assumed to be the same as that of a typical natural gas unit. The cycling cost of CT is given in Table 4.1, computed based on data indicated in [84]. Both their ramp rates on the generation side are the same (about 20% of its rating per minute); of course however, CAES can also provide services even through its charging operation.

Here we run the two sets of simulations with CAES and CT of same capacity. As shown in Figure 4.21, CAES 200 MW in the system under 40% and 50% wind penetrations lowers the system production cost compared to a CT of equal capacity.

CAES Vs CT Production Cost Impact
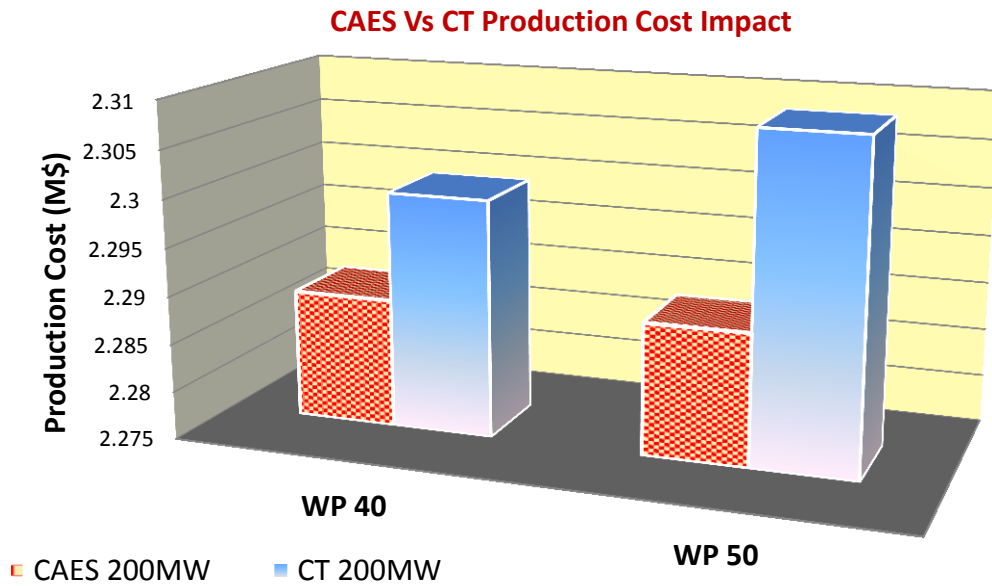
Figure 4.21 CAES vs CT Production Cost under different wind production

A 200MW CAES co-located at bus 21 with wind is able to increase wind energy penetration by about 2% at 40% wind penetration. Storage technologies absorb wind generation that is otherwise spilled due to lack of demand or transmission access. Storage helps to improve the energy penetration of wind and thus improves the overall wind capacity factor for a given penetration level [80].
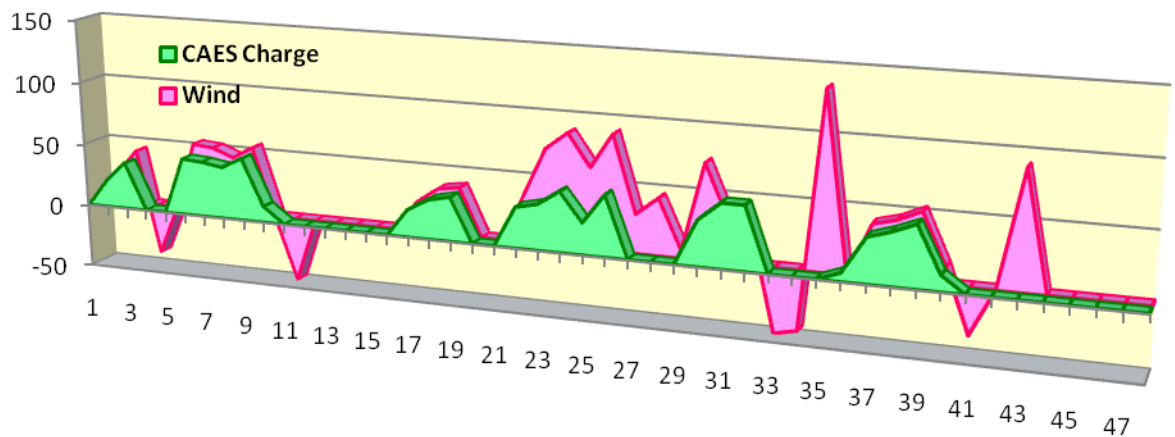
Figure 4.22 CAES charging vs Wind generation changes at 60% wind penetration

Figure 4.22 shows the change in wind generation with and without the 100 MW CAES in pink. CAES charging for the case with the 100 MW CAES is shown in green. We can observe from this figure that the CAES unit charges from wind generation and thus improves wind energy capacity penetration onto the grid.

It is observed that the number of coal unit starts is lower with CAES than with CT by a factor of 3. The main reason for this effect is that the energy price of CAES is closer to coal units' energy offers and hence when the CAES is charged it is preferred to be committed in the energy market and thus reduces coal starts.

CAES participation in the regulation market decreases coal units' regulation provisions significantly than under the case with CT on the grid. As the CT regulation offers are higher and with the added start-up cost it is more expensive than committing an online coal unit to provide the regulation service.

In the case study with 50% wind penetration, CAES reduces the production cost by about $3.64M yearly compared to CT solution. The main reason for this effect, i.e., that the electricity market with the CAES outperforms the market with the CT is that the overall expense of charging the CAES during low LMP periods and discharging during peak periods subject to its round trip efficiency is proving to be cost effective to the grid than using a high priced conventional peaking unit. Apart from this, the fact that CAES is a low-cost high-quality regulation provider makes CAES more preferred than a CT within a renewable-integrated grid scenario.

In studying the impact on emissions with CAES and CT on the system using Figure 4.23, we find that with CAES the system CO_2 emissions is reduced. Generation from coal and natural gas units are reduced with CAES in the grid, which also encourages more wind.

On a yearly basis, approximately 0.441 million metric tons of CO_2 is reduced with CAES compared to CT of equal capacity in the system.

CAES Vs CT - Emissions under WP 22%
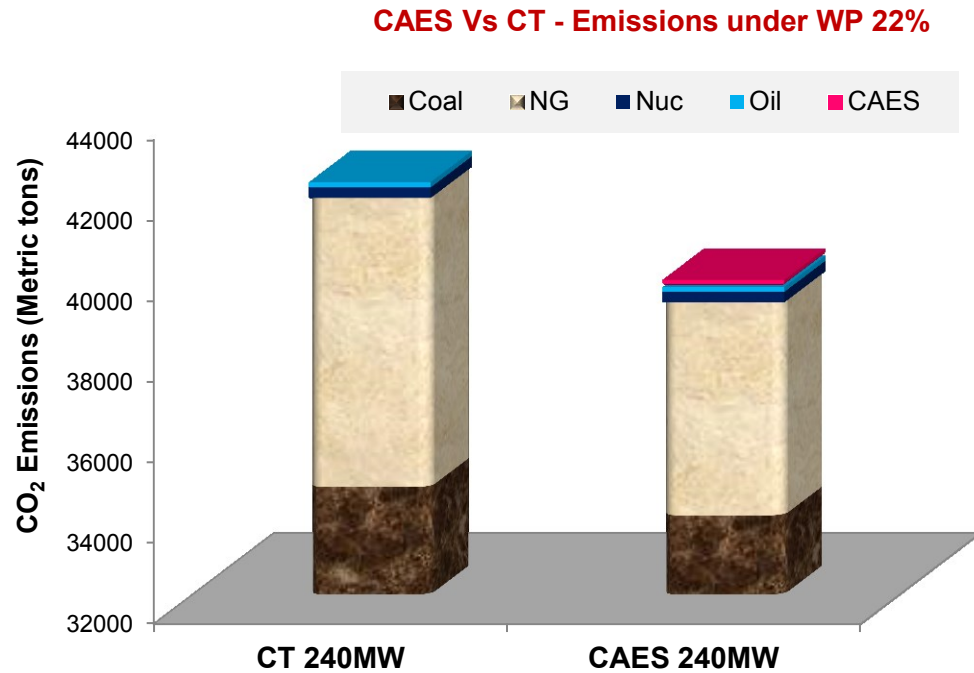
Figure 4.23 CAES Vs CT – Impact on System Emissions

Table 4.9 compares the benefits offered by 200MW CAES and CT each with investment cost of \$500/KW and \$510/KW, respectively. As discussed in the previous paragraphs, CAES is able to provide higher benefits for the same rating under this scenario. CAES being able to provide AS via charging side too, its ability to decrease the cycling related costs are better than a CT. Three different total cost benefits are computed, i.e., one using the savings from production cost, another including the cycling related savings, and the last one also including CO_2 emissions related cost savings. A \$30/metric ton CO_2 tax is imposed. The Cost/Benefit ratio of CAES is about 3.5 times CT's in the first case, and it

increase to 3.75 times with the addition of savings in cycling. It increased to about 6.5 times when savings related to CO_2 emissions are considered.

Table 4.9 Comparison of CAES and CT at 40% Wind Penetration

Attributes	Base	CAES200	CT200
Investment Cost (IC) (M$)		100	110
Production Cost (PC) (M$)	2.31	2.28	2.30
CO_2 Emissions (Metric tons)	42054	41563.7	42138
Coal Cycling Cost (M$)	0.0183	0.0047	0.0155
Total 1 (PC) (M$)	2.31	2.28	2.30
Total 2 (PC + Cycling Cost) (M$)	2.33	2.28	2.32
Total 3 (PC + Cycling Cost + CO_2) (M$)	3.59	3.53	3.58
Yearly Total Cost 1 (M$)	420.42	414.96	418.6
Yearly Total Cost 2 (M$)	423.75	415.82	421.42
Yearly Total Cost 3 (M$)	653.25	642.77	651.47
Yearly Benefit B1 (M$)		5.46	1.82
Yearly Benefit B2 (M$)		7.93	2.33
Yearly Benefit B3 (M$)		10.48	1.78
Yearly Cost/Benefit ratio 1 (IC/B1)		18.32	60.44
Yearly Cost/Benefit ratio 2 (IC/B2)		12.61	47.21
Yearly Cost/Benefit ratio 3 (IC/B3)		9.54	61.80

CONCLUSIONS

CAES proves to be beneficial compared to CT in the overall analysis due to its lower energy and AS offers and higher utilization within grid affairs. The savings in system production cost, emissions and cycling is higher for a CAES than a CT of same capacity.

4.5.2 Study 5: Optimal Allocation of CAES vs Transmission Expansion

The high-fidelity storage and production cost model was used to develop a framework to allocate storage in a system, identifying at effective locations, storage capacities, and investment times, and determining how much storage earns at the identified locations. . The resulting "storage expansion solution" is compared with a transmission expansion solution in terms of the benefits provided by each one.

Neither the transmission nor the storage expansion studies consider variation in investment cost by location. Here only a "copper sheet" transmission expansion is performed to identify the candidate locations where additional capacities could be invested.

Copper sheet analysis is a preliminary transmission plan obtained by allowing the optimization program to decide the areas lacking in transmission facilities by running a power flow with no limits on transmission capacity) [89].

4.5.2.1 Transmission Expansion

Figure 4.24 shows the transmission loading of IEEE 24 bus system at 50% wind penetration in terms of percentage of its MW rating. It is observed that the transmission path from the northern section of the IEEE 24 bus system with most of the generation to the

southern section of the system with high load centers are highly congested, especially the western paths. The stress was such that about 2 MW load at bus 8 had to be curtailed.

A copper sheet transmission expansion was performed to identify the candidate transmission expansion paths, with maximum system transmission increased by 150% of original. Table 4.10 shows most of the transmission in the western section of the system (indicated by the arrow in Figure 4.24) needed additional capacity.

Table 4.10 Transmission Expansion Candidates

Transmission Lines No.	3_9	3_24	8_9	15_21	15_24	16_17	21_22
Capacity (MW)	105	240	105	600	300	300	300
Increase (MW)	50	120	46	112	60	112	20

Figure 4.24 Transmission loading in IEEE 24 bus system

A similar study was performed to identify the candidate storage locations. A storage model with 100 MW charging and discharging capacity and 400 MWh reservoir capacity was installed in all the 24 locations of the system and production costing simulation for 50% wind penetration was performed with storage installed in all buses. CAES energy/AS offers and round-trip efficiency (80%) were used for storage offer and efficiency parameters.

Following identification of the most effective storage locations, two storage expansion (SE) case studies were performed,

> (i)   SE1- Storage participating only in energy market, and
>
> (ii)   SE2- Storage participating in energy and AS co-optimization market.

Storage's rating is estimated by extracting the maximum of charge and discharge commitments over 48 hours.

4.5.2.2 Storage Expansion in Energy Market

SE1 study utilizes storage in 4 locations as shown in Table 4.11, namely buses 3, 8, 9 and 24, which are exactly along the transmission paths in the western section of the system chosen as transmission candidates. It is seen that bulk energy storage can effectively expand transmission, i.e., displace the need for actual transmission expansion, by locating on the load side of the congested transmission and operating to charge during low congestion periods and to discharge during high congestion periods. All the candidate storage locations are in the l oad side of the congested transmission so that the system benefits in reducing total production costs and also so that storage can utilize the available arbitrage opportunity between congested and uncongested time periods due to the associated large difference in prices. The storage in bus 9 and 24 make higher profits from energy

arbitrage. The rating of each storage facility is estimated as the maximum of charge and discharge commitments over 48 hours.

<div align="center">Table 4.11 Storage in Energy Market</div>

Bus	Rating (MW)	Energy Profit ($)
3	56	1404.16
8	31	497.66
9	100	5110.99
24	60	4547.30

4.5.2.3 Storage Expansion in Co-optimization Market

SE2 study utilizes storage in 9 locations as shown in Table 4.12, which are again in the western section of the system along the candidate transmission paths. Apart from acting as a virtual transmission access and benefitting from energy arbitrage, storage also provides AS. It is observed that the storage candidates in the southern section of the system near load centers are deriving benefits mainly from energy sales and candidate storage in the northern generation rich section of the system benefits mainly from AS provisions (even if it requires purchasing cheap energy from energy market for AS provisions). Therefore, storage in co-optimized market is seen to make a higher profit, by an order of magnitude, than if it participates in energy arbitrage alone. The reason for this is due not only to the presence of an additional revenue stream but also to the ability to make use of cross-arbitrage between energy and AS markets. The production cost for SE1 is 2.3M$ while the production cost of SE2 decreases to 2.22M$, compared to the original (without storage or transmission)

production cost of about 2.4M$. The production cost with the transmission expansion solution is 2.16M$, indicating that in this case, storage is capable of providing some of the benefits of transmission, but not all.

Storage used primarily for AS provisions may also be short-term technologies, while storage near the load centers benefitting from high price differences and alleviating transmission congestion need to be bulk storage technologies. Of course, different storage technologies will result in different profits due to their different bids and efficiency parameters.

Table 4.12 Storage in Co-optimization Market

Bus	Rating (MW)	Energy Profit ($)	AS Profit ($)	Total ($)
3	87	33693.77	4.02	33697.79
7	100	48177.25	1.01	48178.26
8	100	55139.91	61.09	55201.00
9	100	49594.89	34.05	49628.95
15	60	-1860.78	3667.66	1806.88
17	26	-394.17	722.68	328.51
18	25	-943.71	1730.20	786.49
21	16	-251.22	460.59	209.37
24	60	-27075.86	52819.69	25743.83

4.5.2.4 Comparison of System Benefits

Figure 4.25 shows Bus 9 LMP in order to compare SE2 storage expansion with transmission expansion scenarios. It is seen that transmission expansion of up to 200% of original capacity gives access to cheaper generation, and thereby reduces higher LMPs and effectively flattens the LMP curve. Storage of 100 MW at Bus 9 also flattens the LMP at that bus, i.e., increases lower LMPs by charging and decreases higher LMPs by discharging.

In this figure 4.25 we observe that the LMPs have negative value implying that the generators pay to generate power. Such a situation arises when generators such as nuclear or wind prefer to continue its generation of power than reduce it momentarily due to lack of demand. These situations are primarily observed in a transmission congested system such as this IEEE RTS system.

Hence the storage units benefit from negative LMPs by getting paid to charge than paying the grid for its charging. Thus only by charging operation it can make profit.

Figure 4.26 shows the highest and lowest LMPs over 48 hours at each bus under different scenarios. It is seen that both storage and transmission expansion mitigates the 2 MW load shed at bus 8, and thereby reduces the peak LMP at buses 7 and 8. Under Base case, buses 7, 8, 9, 10, 3 and 4 seem to have appreciable price differences, and thereby provide arbitrage opportunity for storage. The SE1 and SE2 study both model candidate storage locations among these buses in order to take advantage of energy arbitrage opportunities, and in effect reduce the price difference across all the buses as seen in Figure 25. Both transmission expansion and storage expansion increases wind energy penetration.
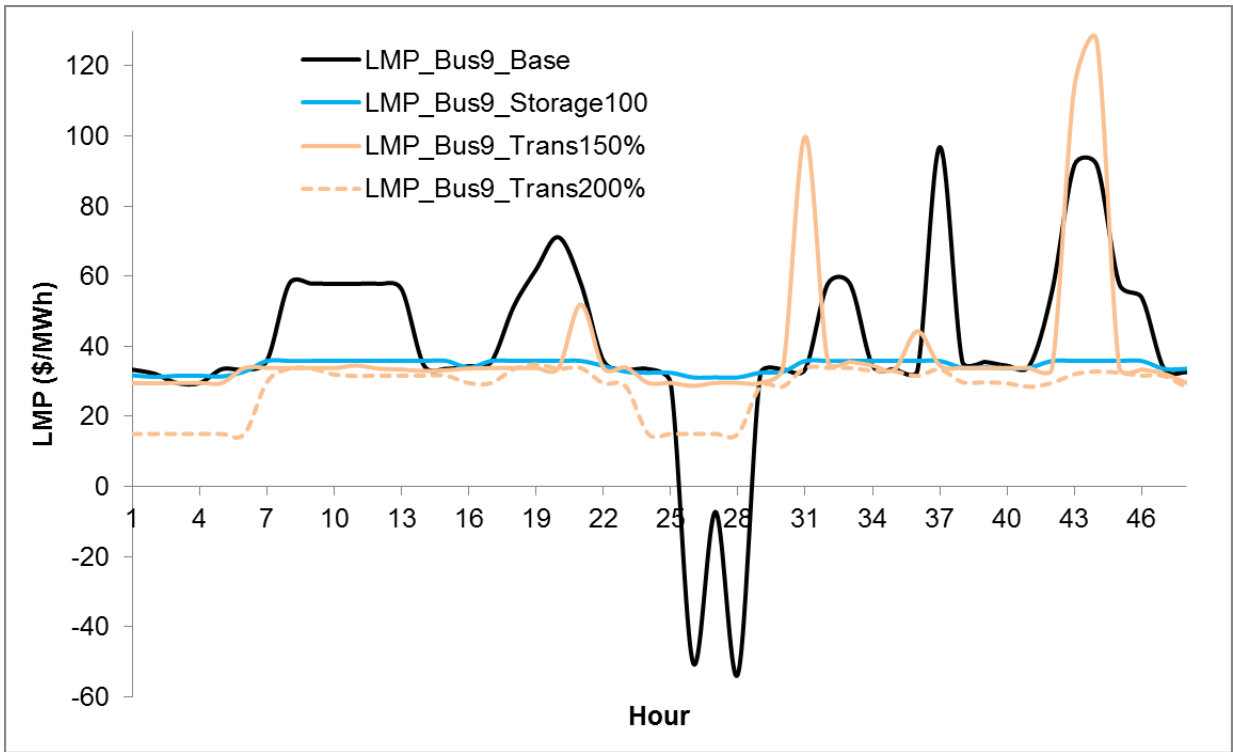
Figure 4.25 Bus 9 LMP under storage and transmission expansion scenarios
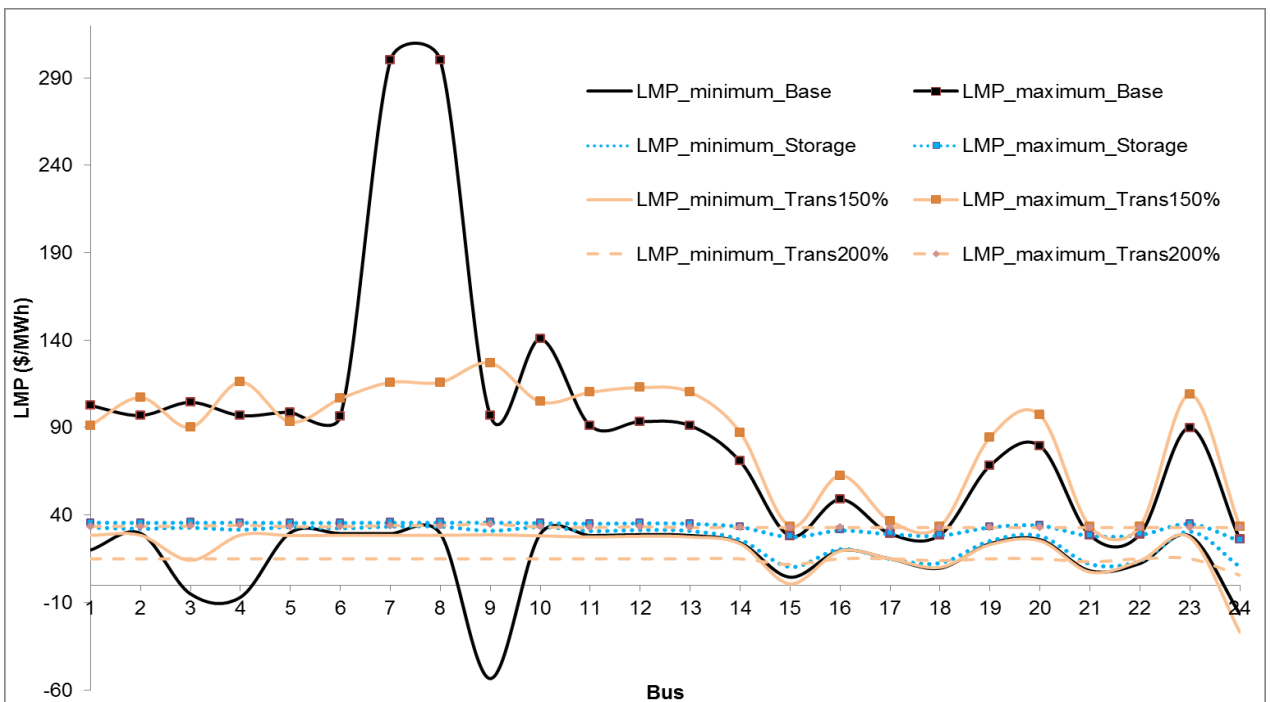
Figure 4.26 Highest and Lowest LMPs under storage and transmission expansion

The Trans150% case increases it by about 13%, while SE2 increases it by about 6%, and hence the lower LMPs at most buses are lesser for Trans150% than the SE2 case. However higher LMPs at most buses are lesser for SE2 case than Trans150%, and it requires Trans200% case to come on par with SE2 on higher side of bus LMPs.

Table 4.13 shows four system attributes, namely production cost, wind spillage, CO_2 emission (CO_2 tax of \$30 /ton) and coal plant cycling cost under storage (SE2) and transmission expansion (150%) scenarios in comparison with the base case. The total investment cost of \$287.07M for storage expansion was computed for additional capacity mentioned in Table 4.10, assuming \$500K/MW investment cost for typical bulk storage. Cost sensitivity is accounted by assuming a lower investment cost of \$200K/MW, typically attributed to short-term storage technologies, thereby obtaining a total investment cost of \$114.83M. Transmission expansion cost is computed to be \$826.30M for the total additional capacities mentioned in Table 4.8, assuming a transmission investment cost of \$3K/MW/Mile [90, 345KV AC]. The transmission length was estimated from the susceptance data, assuming 0.001 ohm/mile. Transmission expansion cost sensitivity was computed assuming shorter transmission lengths, by assuming 0.01 ohm/mile and thereby obtaining \$82.63M as the total cost.

From Table 4.13, it is observed that both storage and transmission expansion reduces total system production costs and reduces CO_2 emission related to coal unit energy production. In this case, for the assumed AS offers, transmission expansion increases coal cycling by increasing their participation in AS, while storage decreases coal unit cycling by providing AS. The impact on cycling cost can be expected to be less pronounced for a system with more natural gas units as marginal AS providers. However such a scenario with

more natural gas units than coal units will come with higher energy production costs and increased need for gas pipelines. A decrease in natural gas price should also benefit bulk storages like CAES (with heat rate $1/3^{rd}$ of natural gas based gas turbine's).

Table 4.13 System Benefits under Storage and Transmission Expansion

Attributes	Base	Storage	Trans150%
Investment Cost (IC) (M$)		287.07 (114.83)	826.30 (82.63)
Production Cost (M$)	2.40	2.22	2.16
CO$_2$ Emission (Metric tons)	41273.21	39334.57	36553.46
CO$_2$ Tax (M$)	1.24	1.18	1.10
Coal Cycling Cost (M$)	0.041	0.007	0.046
Total 1 (PC) (M$)	2.40	2.22	2.16
Total 2 (PC + Cycling Cost) (M$)	2.44	2.23	2.21
Total 3 (PC + CO$_2$ + Cycling Cost) (M$)	3.68	3.41	3.30
Yearly Total Cost 1 (M$)	437.43	404.90	393.04
Yearly Total Cost 2 (M$)	444.82	406.13	401.35
Yearly Total Cost 3 (M$)	670.17	620.89	600.94
Benefit B1 (M$)		-32.53	-44.39
Benefit B2 (M$)		-38.69	-43.46
Benefit B3 (M$)		-49.28	-69.23
Cost/Benefit ratio 1 (IC/B1)		-8.82 (-3.53)	-18.61 (-1.86)
Cost/Benefit ratio 2 (IC/B2)		-7.42 (-2.97)	-19.01 (-1.90)
Cost/Benefit ratio 3 (IC/B3)		-5.83 (-2.33)	-11.93 (-1.19)

Similar to the CAES vs. CT assessment, three total costs are computed; one comprising of system production costs only, another production cost with the coal cycling cost, and the last one includes CO_2 tax with the production cost and cycling cost. The benefits under each case are estimated with respect to base case costs. Three cost-to-benefit ratios are estimated for storage and transmission expansion scenarios.

It is seen that storage is able to provide system benefits in much more cost effective manner compared to transmission expansion projects, assuming lengthier lines. The competition for investment cost per unit benefits (or vice versa) is much tighter for short distance transmission projects in the system and storage projects with low capital storage technologies. Storage's cost to benefit ratio improves with inclusion of coal cycling cost in the picture, which does not help transmission case. Per unit of transmission expansion provides higher CO_2 emission reduction (due to higher wind spillage reduction) than storage expansion.

4.5.2.5 Storage Expansion under Transmission Expanded Situation

Transmission expansion of up to 200% of original capacity has the effect of reducing system costs by giving access to cheaper generation, and thereby decreasing the arbitrage opportunities as observed in Figure 4.25. Under 150% transmission expansion study, the system still provided some arbitrage opportunities for storage, however much reduced than the base case. Storage expansion simulation with 150% transmission capacity places storage at bus 9, making about $12762.85 in total profit, which is about 4 times lower than what the storage at bus 9 earns under base transmission case. However storage at bus 24 makes about $23383.04 in profit, very close to what it made in base case, as the storage profit in those

buses does not depend on LMP differences but on AS provisions and cross-arbitrage between AS and energy market (i.e., charging at cheaper energy price for AS provisions). So even at increased transmission, storage can make its way into grid under higher wind penetration for providing cheaper and effective AS.

4.5.2.6 Conclusion

While it is seen that bulk storage alone can provide most of the benefits that transmission could provide and transmission alone cannot solve system ancillary or ramping related issues; however the value that transmission brings to the grid in terms of competitiveness, relieving system congestion and opportunities are higher. However these come with the usual social and political issues that a transmission project faces. Therefore bulk storage can be a good way to defer a transmission project, and in some cases it would also be cost-effective to do so. In best cases transmission projects together with a fast ramping unit such as storage in today's scenario of increasing variable generation penetration can address system's most of the energy and AS related issues.

4.6 INDICATORS FOR CANDIDATE STORAGE LOCATIONS IN MARKETS

Traditionally opportunities for storage projects in markets are identified using LMP patterns, i.e., observing the differences between peak and low LMPs at a particular system location. This provides a first-hand screening for identifying any possible storage projects in a market, before performing a storage dispatch study within a market optimization framework. In this section, we investigate to find such indicators using the SE studies done in previous section, which can be used as indicators to find candidate locations in existing

markets such as MISO and PJM. Such opportunities are identified in these markets and summarized in chapter 6 under dissertation conclusions.

Based on the LMPs, we can construct "arbitrage value" curves at various locations for 1 MWh transactions, taking into account round trip efficiency (η). For instance, for a 1MWh charge, if 0.8MWh is discharged (considering 80% efficiency), the arbitrage value can be defined in terms of equation (4.5),

$$\text{Arbitrage Value} = \text{LMP}_{discharge}(j)*\eta - \text{LMP}_{charge}(k) \tag{4.5}$$

where j is the time of maximum LMP and k is the time of minimum LMP.

Arranging the LMP over 2 day cycle period in ascending order, arbitrage values in descending order for 24 possible 1MWh transactions can be identified (i.e., pairing the highest LMP with the lowest, and pairing the second highest with the second lowest, and so on). Figure 4.27 shows the arbitrage values for various locations, where the discharge offer of a typical CAES unit is also plotted. Figure 4.27 indicates there are a number of buses where transactions can be profitable for storage. Top 5 buses include buses 7, 8, 9, 3, and 10.
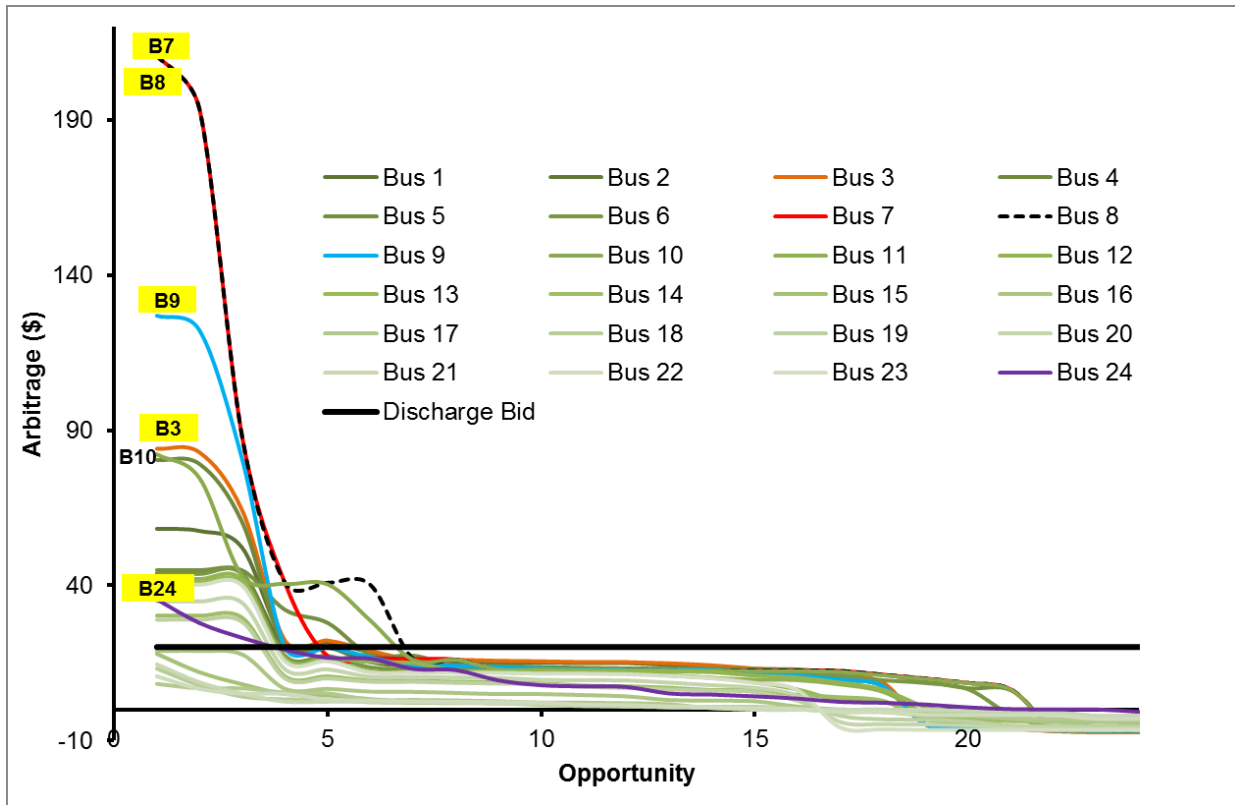
Figure 4.27 Arbitrage opportunities over 48 hours

Figure 4.28 shows the money that storage makes by just charging 1MWh at various locations. The LMPs are negative at some buses such as buses 9, 24 and 3 that charging by itself is profitable. Combined with the fact that these buses get higher value for discharging energy as seen from Figure 4.27, they are well suited for energy arbitrage. This was corroborated by SE1 study results in Table 4.11, where storage was offer only in energy market.
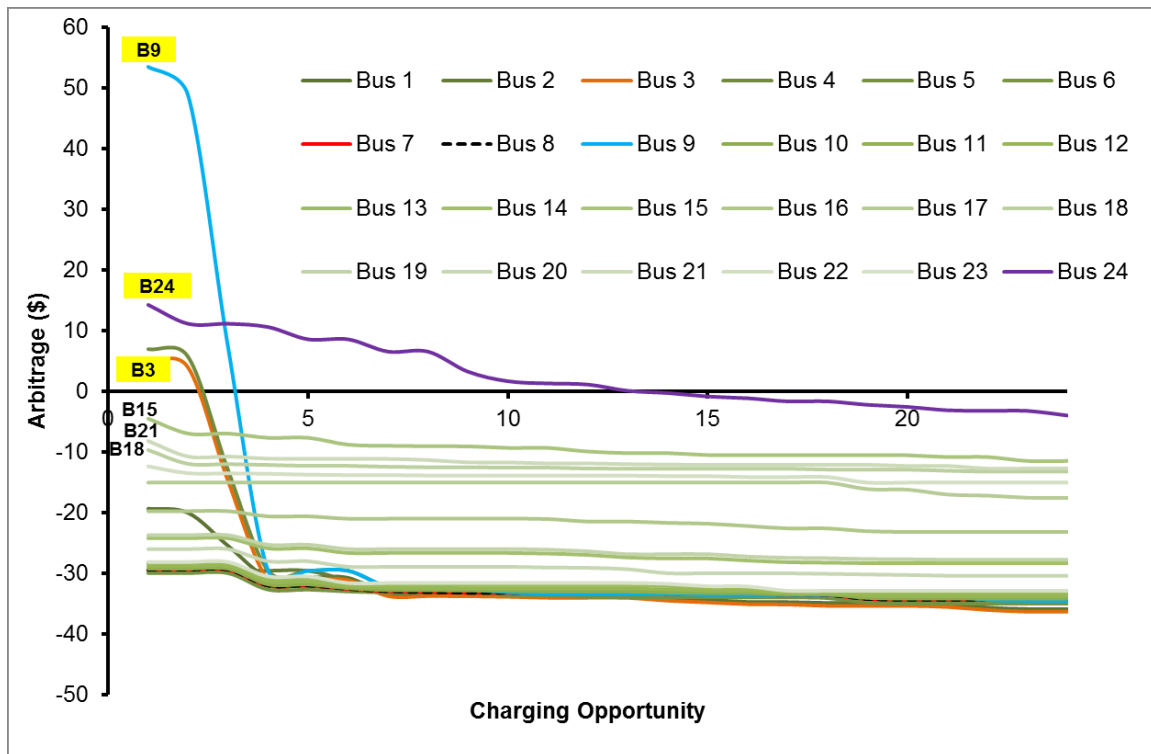
Figure 4.28 Opportunities by charging

This can be also inferred from Figure 4.29 showing sorted LMPs for all the buses. It is seen that buses 9 and 3 have LMPs both well above and below the marginal discharge price, thereby well-suited for energy arbitrage. However, though the storage at buses 7, 8 and 10 are conducive to make high revenue from arbitrage, the lower LMPs in those buses are quite high than the marginal discharge offer. However in a co-optimized market these buses benefit as seen from Table 4.12, by taking advantage of cross-arbitrage opportunities and utilizing AS provisions as cheaper means of charging.

Therefore, the profitability for all the candidate buses increases in a co-optimized market with opportunities for cross arbitrage between energy and AS markets. As seen from SE2 study results in Table 4.12, at buses with high energy selling price such as buses 3, 7, 8 and 9 (seen from sorted LMPs in Figure 4.29), AS provisions (down regulation) were

utilized to charge the reservoir and sell into energy market. On the other hand, at low LMP buses including buses 24, 15, 18, and 21 as seen from Figure 4.27 (LMPs lower than discharge offer), cheaper energy purchases were done to enhance AS provisions.
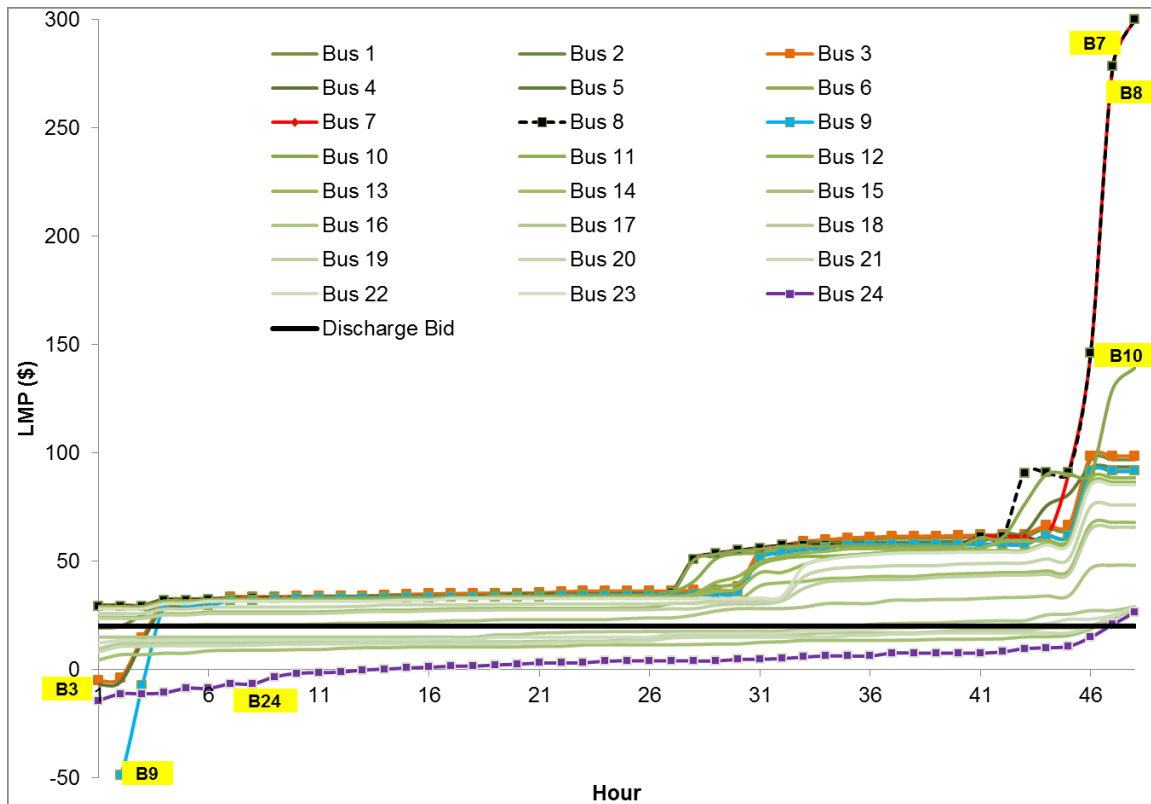
Figure 4.29 Sorted LMPs in base case

This conclusion on bulk storage's market interactions at various locations is quantitatively corroborated using Figure 4.30, where 24 separate simulations were performed with 100MW storage placed at each bus. It is seen that storage at buses 7, 8, and 9 derives major benefit from energy market, while storage at low LMP buses such as 24, 15, 18 and 21 benefit majorly from AS provisions exploiting the opportunities for cross arbitrage.

It is also observed that the buses thriving on energy market benefit the grid by reducing the system production cost the most, with bus 9 reducing it by maximum. The buses that thrive on AS market too reduce system production costs (by virtue of lower MCPs); nevertheless their main benefit is in reducing the cycling cost incurred by conventional generation while providing regulation services. Incidentally, SE2 study chose the union of both these set of buses as the candidate buses for storage allocation.
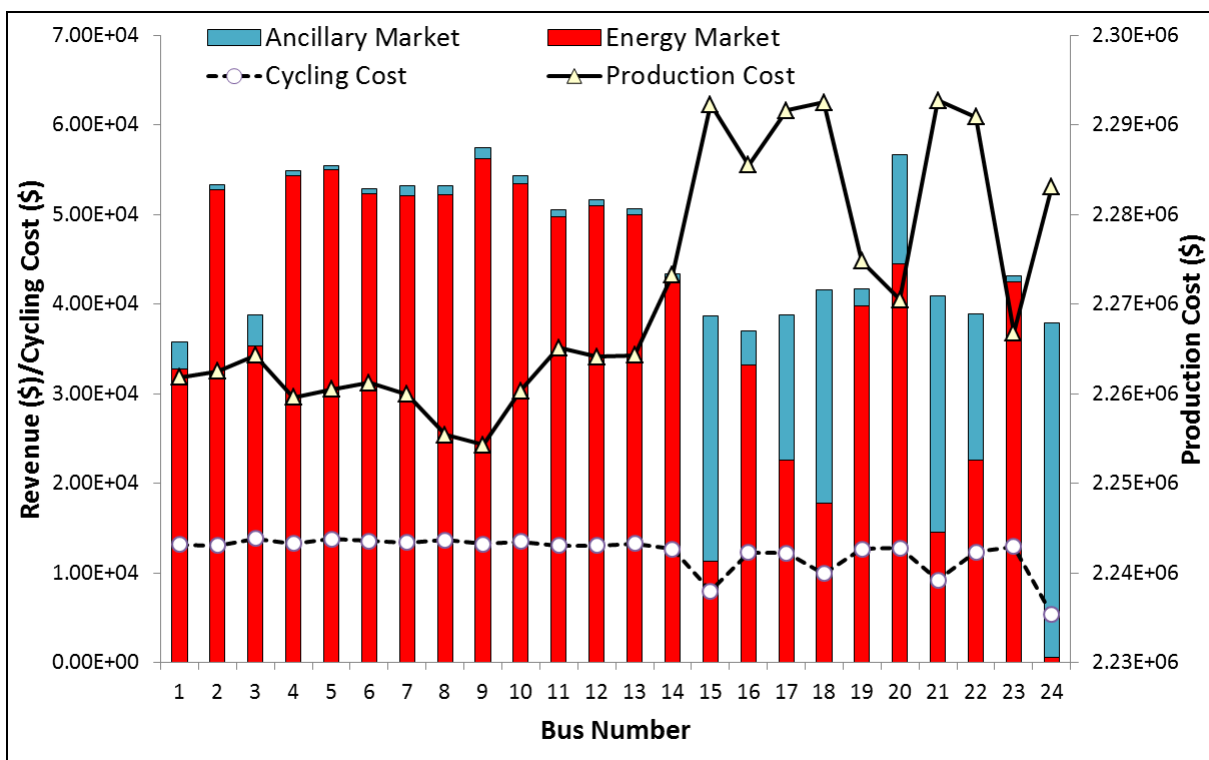
Figure 4.30 Storage at various buses: Profit, production and cycling costs

However it is to be noted that these storage allocation decisions are needed for bulk storage which can provide a range of grid services. Short term storage technologies that provide only up and down regulation may be allocated at any location, though to site them closer to cheaper variable generation is beneficial to arrest the fluctuations instantaneously. Storage expansion simulations performed for 20MW storage with arc characteristics of

short-term technologies showed all candidate locations to be equally beneficial, as seen from Figure 4.31. The estimated AS profits are less at around $1000-$1200 because with higher penetration of storage the AS provisions from storage will be much more than the required regulation services, which consequently reduce the MCPs in the system. When short-term storage is placed separately at each of 24 buses and 24 different simulations are performed, it earns more (about $9248 at all buses) because regulation MCPs are high with some other conventional generator being marginal.
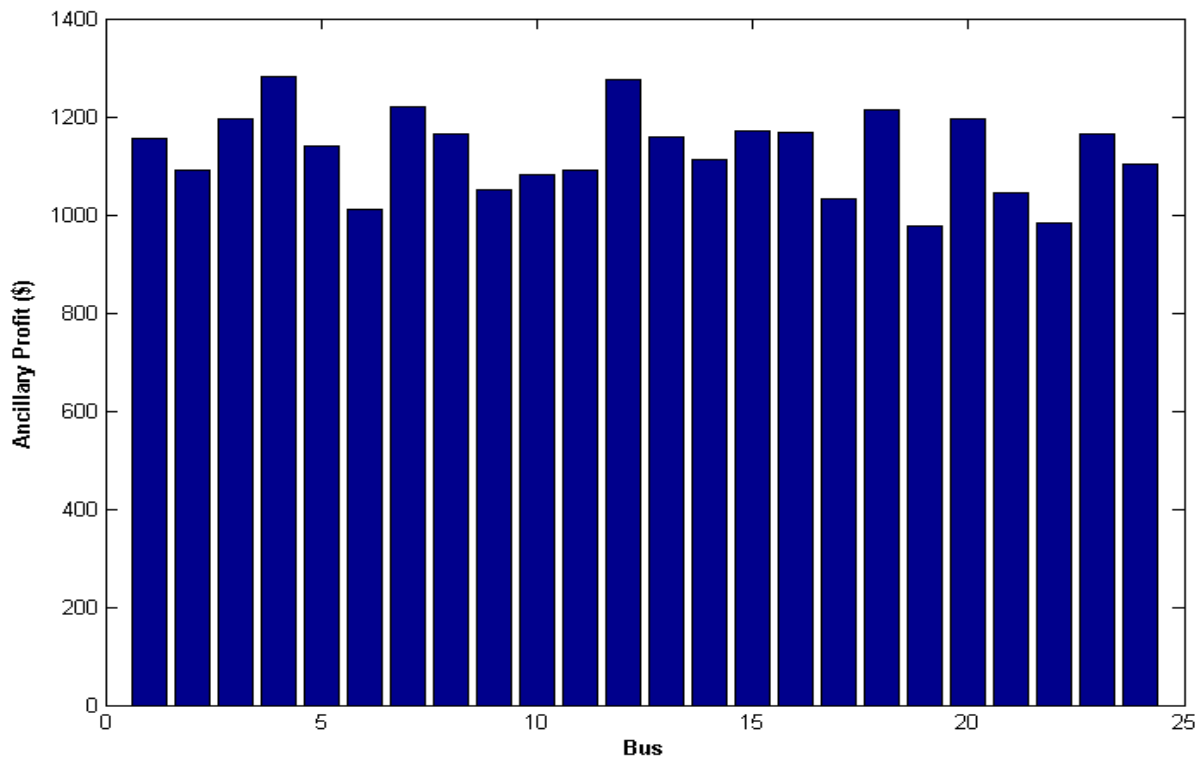
Figure 4.31 Short-term Storage Allocation Study

CONCLUSION

Finally, the indicators for candidate locations for bulk storage allocation can be summarized as follows:

- **In energy market:** Intersection of buses with arbitrage opportunities from energy transactions and charging alone

- **In co-optimization market:** Union of buses with arbitrage opportunities from energy transactions and charging alone

This study also shows that in the grid, depending on the topology of the power system, at different locations different kinds of avenues to earn revenues and aid the grid services are naturally created. Concentrated storage investments are not as beneficial as compared to investing in a mix of storage technologies that are distributed strategically, both from the grid point of view and also in terms of various storage technologies' active role and profitability.

4.7 CONCLUSIONS

The high-fidelity storage dispatch model developed for the production costing study was used to investigate the impacts of bulk storage under various scenarios. Many case studies were performed to draw conclusions on the conditions in which bulk storage prove profitable to the grid in terms of system emissions, cycling and economics; and can make significant energy and AS revenues.

The chapter developed a methodology to incorporate cycling cost into generation start-up/shut-down cost and AS offers. The chapter developed ways to monetize bulk storage's benefits to the grid in terms of its ability to reduce cycling cost and increase wind energy penetration, and quantify their significance to such project's payback periods.

The chapter devised an optimal allocation framework for storage technologies, which can be used to optimally decide on the mix, location and rating of storage investments

in the grid and could also be used in long-term investment planning studies. Such a study was used to assess bulk storage's competitiveness with transmission expansion, and also infer system indicators that could help identify promising candidate locations in any grid for a profitable storage venture.

Some significant conclusions drawn are:

1. Higher wind penetration profit storage ventures, especially of larger capacities. The ability to make revenues is also higher in larger capacities under such high wind penetrations.

2. Bulk storage benefits the grid immensely by relieving conventional unit cycling in terms of starts and regulation provisions, lowers regulation MCPs and reduces system production cost. Increase in generation AS offers with inclusion of cycling components, increases contribution of regulation from bulk storage and its revenues. The reduction in system cycling related costs compensates for increase in system production cost.

3. Risks in storage project's economics are there when the regulation requirements are low (low wind penetration or competing technologies such as demand response) and when MCPs are low. The risk is lower for smaller sized projects, which can still earn from cross arbitrage opportunities in energy and AS market.

4. Giving non-CO_2 emitting storage incentive for wind spillage savings, improves its economics. Sharing production tax credit with variable generation is a viable approach.

5. Bulk storage technology CAES looks better than CT due to its lower energy and AS offers, and higher ability to provide regulation through both charging and

discharging operations, provided system has high wind penetration for cheaper charging of CAES.

6. Bulk storage providing most of the benefits that transmission provides can be a good way to defer transmission projects, and in best cases together with transmission projects can address system's most of the energy and AS related issues under high wind penetrations.

7. Bulk storages earn more revenues from a co-optimization market due to opportunities for cross arbitrage. Due to nature of grid topologies and the distributed opportunities, investing in a mix of storage technologies that are distributed strategically will prove beneficial to both the grid and to the storage technologies.

CHAPTER 5   STORAGE IN AUTOMATIC GENERATION CONTROL AND SHORT-TERM STORAGE ECONOMIC ASSESSMENT

5.1 INTRODUCTION

One of the significant impacts of renewable integration into the traditional and inflexible power system is upon the frequency response of the system [91]. Since these renewables especially wind are intermittent, thus variable and unpredictable, the system is facing frequent and large ramps [92]. It has led to significant rise in regulation reserves (to compensate the minute-to-minute mismatch between generation and load) and contingencies reserves (10-minute spinning and non-spinning) procurement.

The slow responding conventional generation units are counterproductive in facilitating these renewable related services as they add to the net area control error (ACE) and thus impose higher regulation requirements [93]. Furthermore by committing to these fast responding services they undergo fatigue and reduction of unit life time due to the heavy cycling [94]. This eventually contributes to increase in contingency reserves, operational & maintenance costs and overall production costs. Thus the conventional generation units' reserve and ramping capabilities have proven to be insufficient to tackle the renewable integration challenge [77]. Overall, the need is not only for higher ramping capability requirements, but also for higher quality reserves, i.e. fast response (almost instantaneous) and precise control in providing regulation.

Fast ramp providers such as gas turbines, demand side resources and storage technologies are touted as some of the technologies capable of supplying the required amount of regulation at the precisely scheduled moment [95]. Such technologies are capable

of quickly responding to system regulation needs and increasing reliability of the system both in terms of decreasing their generation level and cycling, and improving the frequency response to comply with the North American Electric Reliability Corporation (NERC) Control Performance Standards (CPS) [96].

In this chapter, the effort is to study the impact of fast-responding short-term storage technologies in providing frequency regulation services to the grid and stabilizing the frequency response. The impact of these storage technologies on frequency performance is studied using a slow dynamics Automatic Generation Control (AGC) model; quantified in terms of CPS measures. The chapter presents the following:

1. Slow dynamics model of IEEE 24 bus RTS system in Section 5.2: A single area multi-machine AGC model of RTS system is presented in a state space form. This section also discusses integration of AGC with SCUC and SCED programs, and the manners in which impacts of increasing wind penetration can be accounted within AGC simulation.

2. Slow dynamics model of storage technologies in Section 5.3- CAES and battery, and integrate them within RTS system AGC model.

3. Benefits of fast-responding storage to the grid observed from AGC study, and comparison with few other strategies in Section 5.4.

4. A comprehensive framework to assess the economics of short-term storage technologies in Section 5.5, which involves integration of modeling and simulation methodologies at different time-scales. The short-term storage is modeled within production costing programs using the technology adaptive model developed in chapter 3 to dispatch them for regulation services in 5-

minute RTED market in the IEEE 24 bus RTS system. The production costing tool is used to assess the economic impact of these storage technologies within the markets for various wind penetration levels, while also taking into account information relevant from AGC study that impacts economic assessment.

5. Other applications of the state space models of storage in Section 5.6, such as studying the ability of CAES and batteries to render a wind farm dispatchable, and appropriately size these storage for such an application.

Finally the chapter ends with a conclusion section.

5.2 AUTOMATIC GENERATION CONTROL

5.2.1 Introduction

In the power system the load and generation are constantly changing and hence there is a need to balance out these fluctuations. When the load and generation is balanced the power system is said to be in equilibrium. The reactive power balance is carried out by the Automatic Voltage Regulator (AVR) that maintains the terminal voltage of each generator in the system to a constant value using its excitation system. The real power balance is achieved using two levels of control. The primary control loop is called the Automatic Load Frequency Control (ALFC) or the speed governor that adjusts the turbine output to match the change in the load. All the generators in the system contribute to change in generation to balance the load change. Apart from the power change, the load fluctuation causes a steady state frequency deviation which is balanced using the integral controller. This is called the secondary or supplementary control loop. Both the ALFC and the integral controller loop are together called as the Automatic Generation Control (AGC).

The automatic generation control (AGC) is like a remote control to the generator as it replaces some of the manual controls to change its generation level based on the input signal received at the system control center, i.e., raise, lower or no pulse indicating increase, decrease or maintain the current generation levels respectively. If frequency deviation is positive, the area generation has to be decreased and vice-versa. The main objectives of the AGC are:

  i) Maintain the steady frequency

  ii) Maintain the scheduled tie-line flows

  iii) To distribute the required change in generation among the online generators economically

In a multi-area system, the AGC therefore corrects the frequency deviations and the tie-line deviations in a way that each control area compensates for its own load change. All the generators within a single area are typically replaced by an equivalent generator for that area ALFC. The measurement of the steady-state frequency deviation and the net tie-line deviation (actual-scheduled) is combined into a signal called Area Control Error (ACE). Using the ACE signal, the AGC for each area corrects its own load deviations.

$$ACE = -10\,B\,\Delta f + \left(T_A - T_S\right) \tag{5.1}$$

where B is frequency bias in terms of MW/0.1Hz, usually a function of natural frequency response of the area. In the single area system the AGC has the function of regulating the system frequency in an economic fashion using the available generators. In this case, the ACE signal comprises of only steady-state frequency deviations. The dynamics of a system

with different types of generations such as thermal, hydro, gas, oil, etc. depends on the contributions from various generations towards offsetting the ACE.

5.2.2 Frequency Response- Control Performance Standards

CPS1: It is a short term measure of the ACE i.e. the error between the load and the generation. It is an index to gauge the performance of the ACE in conjunction with the frequency error, and is computed as per equation (5.2). This control parameter reflects the extent to which the generators in the area are contributing towards correcting or hindering system frequency error correction.

$$CPS1 = (2 - CF) * 100\% \tag{5.2}$$

$$CF\ (Compliance\ Factor) = \frac{ACE_{1-min}\ \Delta f_{1-min}}{-10B\ \varepsilon^2} \tag{5.3}$$

where, $\Box f_{1\text{-}min}$ and $\Box C\Box_{1\text{-}min}$ are the 1-minute averages of the frequency deviations and ACE over a year, and $\Box\Box$ is the maximum acceptable steady-state frequency deviation, which is constant for a system. Presently, based on historical frequency deviations, ϵ is 0.018 for eastern interconnection, 0.0228 for western interconnection and 0.030 for ERCOT [97]. A CPS1 score of 200% implies that the actual measured frequency and the scheduled frequency are equal. It is recorded every minute but reported and evaluated annually. NERC has set the minimum long-term score to be 100% for a 12-month rolling average [96].

CPS2: It is the ten-minute average value of the ACE signal. This is a monthly performance standard and limits the ten-minute average of the ACE signal for each control area. The primary objective of CPS2 is to limit unscheduled power exchanges between

balancing areas, and appropriately penalize if one area is found to over- or under-generate to get a very good CPS1 score, while impacting the neighbor area with excessive flows. CPS2 score is generally kept above 90%. However, since in this chapter single area AGC simulation is investigated, CPS2 is not considered.

5.2.3 Single-Area IEEE 24 bus System

In the single area 24-bus IEEE RTS-AGC model consists of the 7 coal generation units, 2 oil generation units and 3 natural gas generation units. The nuclear generation does not participate in the AGC loop due to its slow responding nature. In this section the mathematical model of the two types of generation plant namely thermal and gas is presented. Figure 5.1 shows the AGC block diagram with thermal and gas unit. An integral controller is used as the secondary controller (AGC) and the speed governor of the power plants acts as the primary controller.

The coal and oil generation units are represented using the thermal plant model with corresponding governor, turbine and re-heater modules, and with different ramp rates (3%/min. and 5%/min. of its rating respectively). Natural gas unit is modeled using a gas turbine module with a re-heater (with a ramp rate of 10%/min. of its rating) [98]. The thermal plant consists of a turbine with the re-heater. This turbine is the prime mover for the generator that generates power and feeds it into the power system. The speed governor controls the steam input into the turbine.

Rowen developed this mathematical model for the gas turbine [99]. This model consists of the single shaft gas turbine, its control system and its fuel system. The fuel system consists of two time constants. One time constant is associated with the gas valve

positioning system and the second time constant is of volumetric type associated with the downstream piping and the fuel gas distribution manifold. The error between the reference speed and the rotor speed is fed into the speed governor.
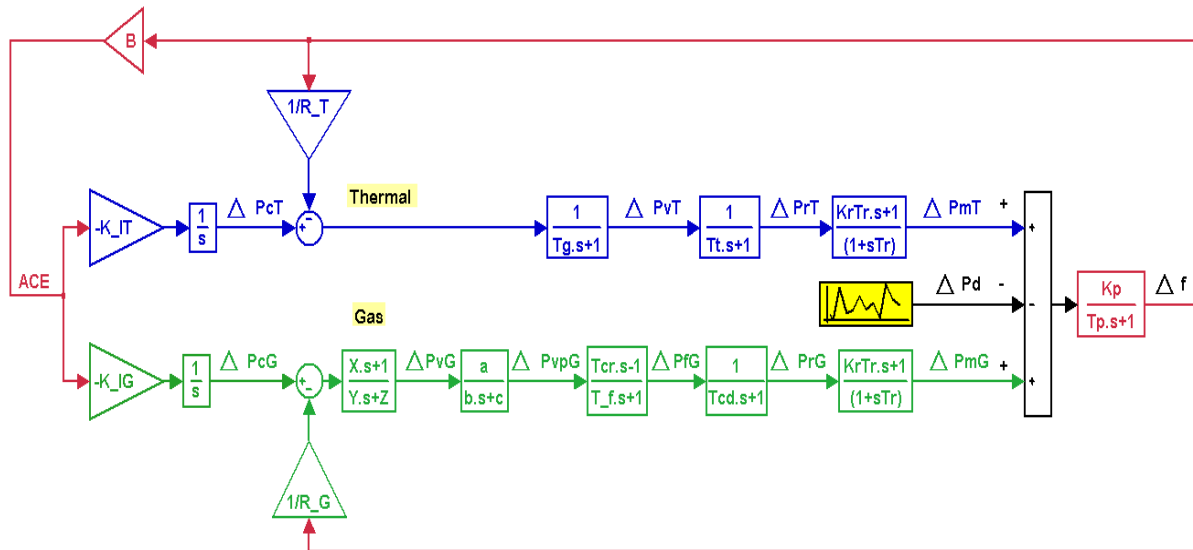
Figure 5.1 Single area AGC block diagram – Thermal and gas

The model parameters are given in Table 5.1. Each generator's governor responds to the frequency deviation based on its respective droop characteristics defined by R. The following sub-section 5.2.3.1 describes the state space representation of slow dynamics of a system with thermal and gas units. The sub-section 5.2.3.2 provides the state space representation of IEEE 24 bus single area system with multi-machines, integrated with economic dispatch program.

Table 5.1 AGC Model Parameters

Description	Parameter	Value
Speed governor lead time constant (sec)	X	0.6
Speed governor lag time constant (sec)	Y	1
Governor Mode	Z	1
Valve positioner constant	a	1
Valve positioner constant	b	0.05
Valve positioner constant	c	1
Fuel time constant (sec)	$T_{\_f}$	0.23
Combustion reaction time delay (sec)	T_{cr}	0.3
Compressor discharge volume time constant (sec)	T_{cd}	0.2
Speed governor regulation parameter for gas unit (Hz/pu MW)	R_G	2.4
Power System Gain Constant (Hz/pu MW)	K_p	20
Power System Time Constant (sec)	T_p	2
Frequency bias constant (puMW/Hz)	B	0.425
Speed Governor time constant (sec)	T_g	0.08
Turbine time constant (sec)	T_t	0.3
Re-heater time constant (sec)	T_r	10
Coefficient of re-heat steam turbine	K_r	0.5
Speed governor regulation parameter for thermal (Hz/pu MW)	R_T	2.4
Coal & Oil Gen integral controller gain (Hz/pu MW)	K_{IT}	0.2
Gas generators integral controller gain (Hz/pu MW)	K_{IG}	0.2

5.2.3.1 State space representation of AGC with thermal and natural gas units

The state space representation is expressed as shown in (5.4) in terms of system states, input signal and disturbances [100]. Without explicit control inputs, it looks like (5.5).

$$\Delta \dot{X} = A \Delta X + B u + \Gamma \Delta P_d$$
$$\Delta Y = C \Delta X \tag{5.4}$$

$$\Delta \dot{X} = A \Delta X + \Gamma \Delta P_d \tag{5.5}$$

The relations between various states of the system are converted into state space form in time domain. The various system states (11 of them) are given in (5.6), where the states can be divided into 3 categories as shown in (5.7): system related state X_p (state 1), thermal unit related states X_T (states 2-5), and gas unit related states X_G (states 6-11).

$$\Delta X = \left| \Delta f \mid \Delta P_{mT} \quad \Delta P_{rT} \quad \Delta P_{vT} \quad \Delta P_{cT} \mid \Delta P_{mG} \quad \Delta P_{rG} \quad \Delta P_{fG} \quad \Delta P_{vpG} \quad \Delta P_{vG} \quad \Delta P_{cG} \right|^T \tag{5.6}$$

$$\Delta X = \Delta X_{sys} = \left| \begin{array}{ccc} \Delta X_p & \Delta X_T & \Delta X_G \end{array} \right|^T \tag{5.7}$$

Components of state matrix A and disturbance matrix Γ:

To find the components of matrices in (5.5), the various slow dynamics relations are expanded and expressed in time domain in the same form as (5.5).

System states:

$$\Delta f = \left(\frac{K_p}{1 + s T_p} \right) \left(\Delta P_{mT} + \Delta P_{mG} - \Delta P_d \right) \tag{5.8}$$

$$\Delta \dot{f} = -\frac{1}{T_p} \Delta f + \frac{K_p}{T_p} \left(\Delta P_{mT} + \Delta P_{mG} - \Delta P_d \right) \tag{5.9}$$

Thermal generation states:

$$\Delta P_{mT} = \left(\frac{1 + s K_r T_r}{1 + s T_r} \right) \left(\Delta P_{rT} \right) \tag{5.10}$$

$$\Delta \dot{P}_{mT} = -\frac{1}{T_r} \Delta P_{mT} + \frac{1}{T_r} \Delta P_{rT} + K_r \Delta \dot{P}_{rT} \tag{5.11}$$

$$\Delta P_{rT} = \left(\frac{1}{1+sT_t}\right)\left(\Delta P_{vT}\right) \tag{5.12}$$

$$\Delta \dot{P}_{rT} = -\frac{1}{T_t} \Delta P_{rT} + \frac{1}{T_t} \Delta P_{vT} \tag{5.13}$$

$$\Delta \dot{P}_{mT} = -\frac{1}{T_r} \Delta P_{mT} + \left(\frac{1}{T_r} - \frac{K_r}{T_t}\right)\Delta P_{rT} + \frac{K_r}{T_t} \Delta P_{vT} \tag{5.14}$$

$$\Delta P_{vT} = \left(\frac{1}{1+sT_g}\right)\left(\Delta P_{cT} - \frac{1}{R_T} \Delta f\right) \tag{5.15}$$

$$\Delta \dot{P}_{vT} = -\frac{1}{T_g} \Delta P_{vT} + \frac{1}{T_g} \Delta P_{cT} - \frac{1}{T_g R_T} \Delta f \tag{5.16}$$

$$\Delta P_{cT} = \left(\frac{-K_{IT}}{s}\right)\left(B\ \Delta f\right) \tag{5.17}$$

$$\Delta \dot{P}_{cT} = -K_{IT} B \Delta f \tag{5.18}$$

<u>Natural Gas generation states:</u>

$$\Delta P_{mG} = \left(\frac{1+sK_r T_r}{1+sT_r}\right)\left(\Delta P_{rG}\right) \tag{5.19}$$

$$\Delta \dot{P}_{mG} = -\frac{1}{T_r} \Delta P_{mG} + \frac{1}{T_r} \Delta P_{rG} + K_r \Delta \dot{P}_{rG} \tag{5.20}$$

$$\Delta P_{rG} = \left(\frac{1}{1+sT_{CD}}\right)\left(\Delta P_{fG}\right) \tag{5.21}$$

$$\Delta \dot{P}_{rG} = -\frac{1}{T_{CD}} \Delta P_{rG} + \frac{1}{T_{CD}} \Delta P_{fG} \tag{5.22}$$

$$\Delta \dot{P}_{mG} = -\frac{1}{T_r} \Delta P_{mG} + \left(\frac{1}{T_r} - \frac{K_r}{T_{CD}} \right) \Delta P_{rG} + \frac{K_r}{T_{CD}} \Delta P_{fG} \tag{5.23}$$

$$\Delta P_{fG} = \left(\frac{1 - sT_{CR}}{1 + sT_f} \right) \left(\Delta P_{vpG} \right) \tag{5.24}$$

$$\Delta \dot{P}_{fG} = -\frac{1}{T_f} \Delta P_{fG} + \frac{1}{T_f} \Delta P_{vpG} - \frac{T_{CR}}{T_f} \Delta \dot{P}_{vpG} \tag{5.25}$$

$$\Delta P_{vpG} = \left(\frac{a}{c + sb} \right) \Delta P_{vG} \tag{5.26}$$

$$\Delta \dot{P}_{vpG} = -\frac{c}{b} \Delta P_{vpG} + \frac{a}{b} \Delta P_{vG} \tag{5.27}$$

$$\Delta \dot{P}_{fG} = -\frac{1}{T_f} \Delta P_{fG} + \left(\frac{1}{T_f} + \frac{cT_{CR}}{bT_f} \right) \Delta P_{vpG} - \frac{aT_{CR}}{bT_f} \Delta P_{vG} \tag{5.28}$$

$$\Delta P_{vG} = \left(\frac{1 + sX}{Z + sY} \right) \left(\Delta P_{cG} - \frac{1}{R_G} \Delta f \right) \tag{5.29}$$

$$\Delta \dot{P}_{vG} = -\frac{Z}{Y} \Delta P_{vG} + \frac{1}{Y} \Delta P_{cG} + \frac{X}{Y} \Delta \dot{P}_{cG} - \frac{1}{YR_G} \Delta f - \frac{X}{YR_G} \Delta \dot{f} \tag{5.30}$$

$$\Delta P_{cG} = \left(\frac{-K_{IG}}{s} \right) \left(B \, \Delta f \right) \tag{5.31}$$

$$\Delta \dot{P}_{cG} = -K_{IG} B \Delta f \tag{5.32}$$

$$\Delta \dot{P}_{vG} = -\frac{Z}{Y} \Delta P_{vG} + \frac{1}{Y} \Delta P_{cG} + \left(-\frac{X}{Y} K_{IG} B - \frac{1}{YR_G} + \frac{X}{YR_G T_p} \right) \Delta f - \frac{XK_p}{YR_G T_p} \left(\Delta P_{mT} + \Delta P_{mG} - \Delta P_d \right) \tag{5.33}$$

The matrices A and Γ for (5.5) is shown in (5.34) and (5.35) respectively.

$$
A = \begin{bmatrix}
-\dfrac{1}{T_p} & \dfrac{K_p}{T_p} & 0 & 0 & 0 & \dfrac{K_p}{T_p} & 0 & 0 & 0 & 0 & 0 \\[2mm]
0 & -\dfrac{1}{T_r} & \left(\dfrac{1}{T_r}-\dfrac{K_r}{T_t}\right) & \dfrac{K_r}{T_t} & 0 & 0 & 0 & 0 & 0 & 0 & 0 \\[2mm]
0 & 0 & -\dfrac{1}{T_t} & \dfrac{1}{T_t} & 0 & 0 & 0 & 0 & 0 & 0 & 0 \\[2mm]
-\dfrac{1}{T_g R_T} & 0 & 0 & -\dfrac{1}{T_g} & \dfrac{1}{T_g} & 0 & 0 & 0 & 0 & 0 & 0 \\[2mm]
-K_{IT}B & 0 & 0 & 0 & 0 & 0 & 0 & 0 & 0 & 0 & 0 \\[2mm]
0 & 0 & 0 & 0 & 0 & -\dfrac{1}{T_r} & \left(\dfrac{1}{T_r}-\dfrac{K_r}{T_{CD}}\right) & \dfrac{K_r}{T_{CD}} & 0 & 0 & 0 \\[2mm]
0 & 0 & 0 & 0 & 0 & 0 & -\dfrac{1}{T_{CD}} & \dfrac{1}{T_{CD}} & 0 & 0 & 0 \\[2mm]
0 & 0 & 0 & 0 & 0 & 0 & 0 & -\dfrac{1}{T_f} & \left(\dfrac{1}{T_f}+\dfrac{cT_{CR}}{bT_f}\right) & -\dfrac{aT_{CR}}{bT_f} & 0 \\[2mm]
0 & 0 & 0 & 0 & 0 & 0 & 0 & 0 & -\dfrac{c}{b} & \dfrac{a}{b} & 0 \\[2mm]
\left(\dfrac{-X}{Y}K_{IG}B-\dfrac{1}{YR_G}+\dfrac{X}{YR_G T_p}\right) & -\dfrac{XK_p}{YR_G T_p} & 0 & 0 & 0 & -\dfrac{XK_p}{YR_G T_p} & 0 & 0 & 0 & -\dfrac{Z}{Y} & \dfrac{1}{Y} \\[2mm]
-K_{IG}B & 0 & 0 & 0 & 0 & 0 & 0 & 0 & 0 & 0 & 0
\end{bmatrix}
\tag{5.34}
$$

$$
\Gamma = \begin{vmatrix}
-\dfrac{K_p}{T_p} & 0 & 0 & 0 & 0 & 0 & 0 & 0 & 0 & \dfrac{XK_p}{YR_G T_p} & 0
\end{vmatrix}^{T}
\tag{5.35}
$$

State Space Representation in Compact Form:

The full-fledged state space representation is reduced to a compact form notation, so that it will be easy to show the integration of storage state space representation into it. Equation (5.5) is rewritten as (5.36), using the state categories shown in (5.7). All the sub-matrices are also defined. Some of the sub-matrices of matrix A_{sys} are null, indicating absence of influence of one state category of state over another. For instance, $A_{TG}=0$ means the states of natural gas unit does not directly impact states of thermal unit, but indirectly impact through the system frequency. On the other hand, $A_{GT}\neq0$ means the states of natural gas unit does get influenced by states of thermal unit as captured in (5.33).

$$\Delta \dot{X}_{sys} = A_{sys}\,\Delta X_{sys} + \Gamma_{sys}\,\Delta P_d \tag{5.36}$$

$$\begin{vmatrix} \Delta \dot{X}_p \\ \Delta \dot{X}_T \\ \Delta \dot{X}_G \end{vmatrix} = \begin{vmatrix} A_{pp} & A_{pT} & A_{pG} \\ A_{Tp} & A_{TT} & A_{TG}=0 \\ A_{Gp} & A_{GT} & A_{GG} \end{vmatrix} \begin{vmatrix} \Delta X_p \\ \Delta X_T \\ \Delta X_G \end{vmatrix} + \begin{vmatrix} \Gamma_{pp} \\ \Gamma_{Tp}=0 \\ \Gamma_{Gp} \end{vmatrix} \Delta P_d \tag{5.37}$$

where,

$$\Delta X_p = \Delta f \tag{5.38}$$

$$\Delta X_T = \begin{vmatrix} \Delta P_{mT} & \Delta P_{rT} & \Delta P_{vT} & \Delta P_{cT} \end{vmatrix}^{T} \tag{5.39}$$

$$\Delta X_G = \begin{vmatrix} \Delta P_{mG} & \Delta P_{rG} & \Delta P_{fG} & \Delta P_{vpG} & \Delta P_{vG} & \Delta P_{cG} \end{vmatrix}^{T} \tag{5.40}$$

$$A_{pp} = -\frac{1}{T_p} \tag{5.41}$$

$$A_{pT} = \begin{vmatrix} \dfrac{K_p}{T_p} & 0 & 0 & 0 \end{vmatrix} \tag{5.42}$$

$$A_{pG} = \begin{vmatrix} \dfrac{K_p}{T_p} & 0 & 0 & 0 & 0 & 0 \end{vmatrix} \tag{5.43}$$

$$A_{Tp} = \begin{vmatrix} 0 & 0 & -\dfrac{1}{T_g R_T} & -K_{IT}B \end{vmatrix}^{T} \tag{5.44}$$

$$A_{Gp} = \begin{vmatrix} 0 & 0 & 0 & 0 & \left(\dfrac{-X}{Y}K_{IG}B - \dfrac{1}{YR_G} + \dfrac{X}{YR_G T_p}\right) & -K_{IG}B \end{vmatrix}^{T} \tag{5.45}$$

$$A_{TT} = \begin{vmatrix} -\dfrac{1}{T_r} & \left(\dfrac{1}{T_r} - \dfrac{K_r}{T_t}\right) & \dfrac{K_r}{T_t} & 0 \\ 0 & -\dfrac{1}{T_t} & \dfrac{1}{T_t} & 0 \\ 0 & 0 & -\dfrac{1}{T_g} & \dfrac{1}{T_g} \\ 0 & 0 & 0 & 0 \end{vmatrix} \tag{5.46}$$

$$A_{GG} = \begin{vmatrix} -\dfrac{1}{T_r} & \left(\dfrac{1}{T_r} - \dfrac{K_r}{T_{CD}}\right) & \dfrac{K_r}{T_{CD}} & 0 & 0 & 0 \\ 0 & -\dfrac{1}{T_{CD}} & \dfrac{1}{T_{CD}} & 0 & 0 & 0 \\ 0 & 0 & -\dfrac{1}{T_f} & \left(\dfrac{1}{T_f} + \dfrac{cT_{CR}}{bT_f}\right) & -\dfrac{aT_{CR}}{bT_f} & 0 \\ 0 & 0 & 0 & -\dfrac{c}{b} & \dfrac{a}{b} & 0 \\ -\dfrac{XK_p}{YR_G T_p} & 0 & 0 & 0 & -\dfrac{Z}{Y} & \dfrac{1}{Y} \\ 0 & 0 & 0 & 0 & 0 & 0 \end{vmatrix} \tag{5.47}$$

$$A_{GT} = \begin{vmatrix} 0 & 0 & 0 & 0 \\ 0 & 0 & 0 & 0 \\ 0 & 0 & 0 & 0 \\ 0 & 0 & 0 & 0 \\ -\dfrac{XK_p}{YR_G T_p} & 0 & 0 & 0 \\ 0 & 0 & 0 & 0 \end{vmatrix} \tag{5.48}$$

$$\Gamma_{pp} = \dfrac{-K_p}{T_p} \tag{5.49}$$

$$\Gamma_{Gp} = \begin{vmatrix} 0 & 0 & 0 & 0 & \dfrac{XK_p}{YR_GT_p} & 0 \end{vmatrix}^T \qquad (5.50)$$

5.2.3.2 IEEE system with multi-machines- State space representation and integration of AGC with dispatch module in Simulink

The IEEE 24 bus system has 7 coal generators, 2 oil generators, and 3 natural gas generators. Equations (5.51) and (5.52) show the ΔX_{sys} and A_{sys} for this system with each individual generator modeled into the AGC.

$$\Delta X_{sys} = \begin{vmatrix} \Delta X_p & \Delta X_{T_1} & \Delta X_{T_2} & \Delta X_{T_3} & \Delta X_{T_4} & \Delta X_{T_5} & \Delta X_{T_6} & \Delta X_{T_7} & \Delta X_{O_1} & \Delta X_{O_2} & \Delta X_{G_1} & \Delta X_{G_2} & \Delta X_{G_3} \end{vmatrix}^T$$

$$(5.51)$$

$$\begin{vmatrix}
A_{pp} & A_{pT_1} & A_{pT_2} & A_{pT_3} & A_{pT_4} & A_{pT_5} & A_{pT_6} & A_{pT_7} & A_{pO_1} & A_{pO_2} & A_{pG_1} & A_{pG_2} & A_{pG_3} \\
A_{T_1 p} & A_{T_1 T_1} & 0 & 0 & 0 & 0 & 0 & 0 & 0 & 0 & 0 & 0 & 0 \\
A_{T_2 p} & 0 & A_{T_2 T_2} & 0 & 0 & 0 & 0 & 0 & 0 & 0 & 0 & 0 & 0 \\
A_{T_3 p} & 0 & 0 & A_{T_3 T_3} & 0 & 0 & 0 & 0 & 0 & 0 & 0 & 0 & 0 \\
A_{T_4 p} & 0 & 0 & 0 & A_{T_4 T_4} & 0 & 0 & 0 & 0 & 0 & 0 & 0 & 0 \\
A_{T_5 p} & 0 & 0 & 0 & 0 & A_{T_5 T_5} & 0 & 0 & 0 & 0 & 0 & 0 & 0 \\
A_{T_6 p} & 0 & 0 & 0 & 0 & 0 & A_{T_6 T_6} & 0 & 0 & 0 & 0 & 0 & 0 \\
A_{T_7 p} & 0 & 0 & 0 & 0 & 0 & 0 & A_{T_7 T_7} & 0 & 0 & 0 & 0 & 0 \\
A_{O_1 p} & 0 & 0 & 0 & 0 & 0 & 0 & 0 & A_{O_1 O_1} & 0 & 0 & 0 & 0 \\
A_{O_2 p} & 0 & 0 & 0 & 0 & 0 & 0 & 0 & 0 & A_{O_2 O_2} & 0 & 0 & 0 \\
A_{G_1 p} & A_{G_1 T_1} & A_{G_1 T_2} & A_{G_1 T_3} & A_{G_1 T_4} & A_{G_1 T_5} & A_{G_1 T_6} & A_{G_1 T_7} & A_{G_1 O_1} & A_{G_1 O_2} & A_{G_1 G_1} & A_{G_1 G_2} & A_{G_1 G_3} \\
A_{G_2 p} & A_{G_2 T_1} & A_{G_2 T_2} & A_{G_2 T_3} & A_{G_2 T_4} & A_{G_2 T_5} & A_{G_2 T_6} & A_{G_2 T_7} & A_{G_2 O_1} & A_{G_2 O_2} & A_{G_2 G_1} & A_{G_2 G_2} & A_{G_2 G_3}
\end{vmatrix}$$

$$\left| \begin{array}{ccccccccccc} A_{G_3p} & A_{G_3T_1} & A_{G_3T_2} & A_{G_3T_3} & A_{G_3T_4} & A_{G_3T_5} & A_{G_3T_6} & A_{G_3T_7} & A_{G_3O_1} & A_{G_3O_2} & A_{G_3G_1} & A_{G_3G_2} & A_{G_3G_3} \end{array} \right|$$

$$(5.52)$$

Generally in AGC simulations, a group of generating units of same class (e.g., thermal generators) is represented using 1 representative model as shown in Figure 5.1. However here each generator's participation in the AGC is individually modeled using MATLAB Simulink, in order to capture the following:

1. **Connection with SCUC and SCED:** Each generator's participation is dictated by the economic dispatch program's output, which decides economic regulation service allocations based on offers, system conditions, physical conditions of the generators, and past dispatch states of the generators.

2. **Ramp rates:** Each generating unit (even if all belongs to thermal group) has different per second ramping capabilities to AGC signals depending upon their capacities.

Implementation of AGC connection with SCUC and SCED:

Figure 5.2 shows the overall operational scheme of power system market within which AGC fits in the real-time operational environment [101]. Typically a day-ahead (DA) 24-hour forecasts of load, wind together with generating unit offers are used by independent system operators (ISOs) to execute security constrained unit commitment (SCUC) and economic dispatch (SCED) respectively to make unit commitment decisions for the next day 24 hours. Then real-time economic dispatch (RTED) market is run at 5-minute intervals considering the real-time load and wind data, and accordingly dispatches are adjusted to meet the uncertainties (In each ISOs, there are intermediate unit-commitment routines

executed on the operating day for reliability purposes). Each generator based on its regulation offers is allocated regulation service in the real time market every 5-min (300s). Based on the real-time market dispatch set points, AGC module gets appropriate signals to ensure that appropriate generators participate in AGC in each period to maintain reasonable frequency response against fluctuating net-load (load(L) - wind(W)).
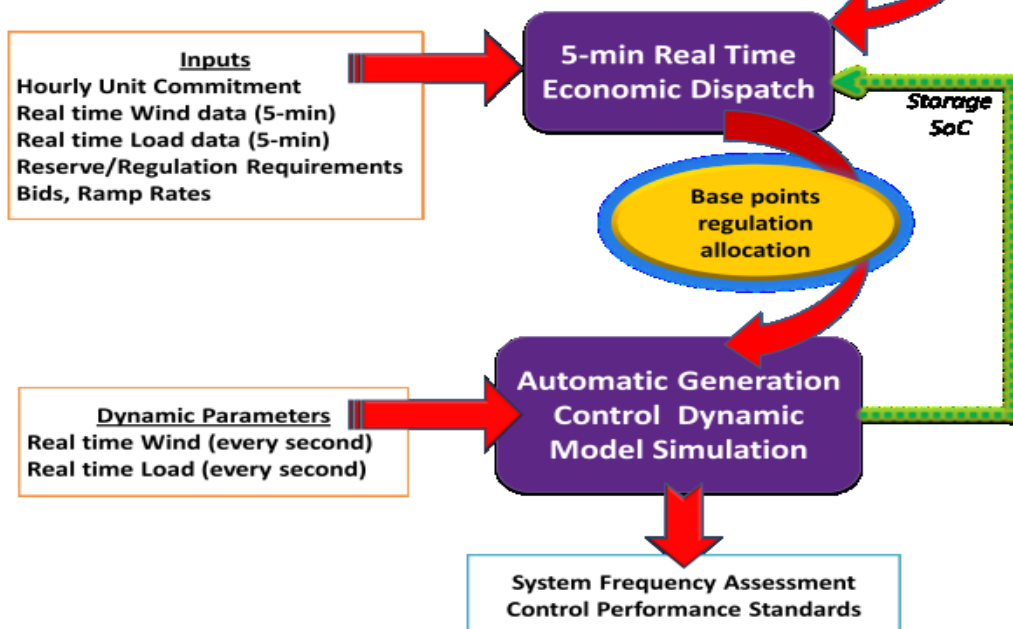
Figure 5.2 Integration of dispatch and AGC for frequency assessment

This feature is implemented in Simulink using the "dynamic saturation blocks" in Figures 5.3 and 5.4, which ensures the unit participates in AGC according to ED decisions. A particular unit may have governor response scheme, but it may not participate in it if the ED doesn't allocate a unit to provide regulation service. This is accounted within the simulation by multiplying the droop parameter of respective unit with sign block of its regulation commitment during each period. The simplification done in the implementation compared to what is shown in Figure 5.2 is: RTED module is not simulated after every 300s of AGC simulation in order to circumvent the computational requirements. Instead, the hourly unit commitments and the regulation allocations obtained from hourly DA-SCUC and SCED are used, and the unit participations in AGC are updated every hour (3600s) of the AGC simulation.
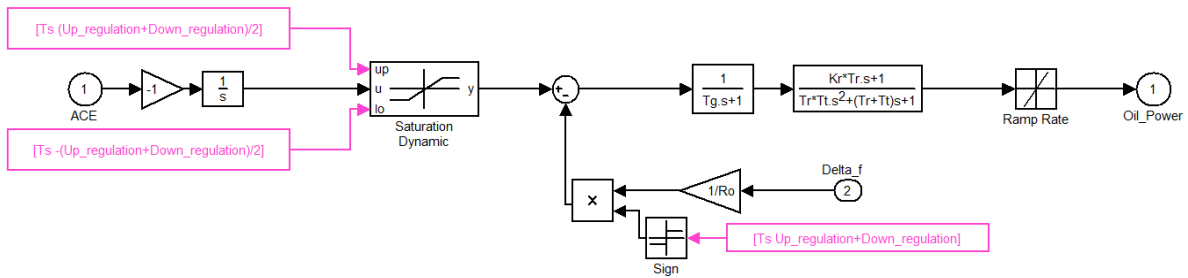
Figure 5.3 Thermal unit in AGC subject to SCUC and SCED decisions- 7 coal and 2 oil

units
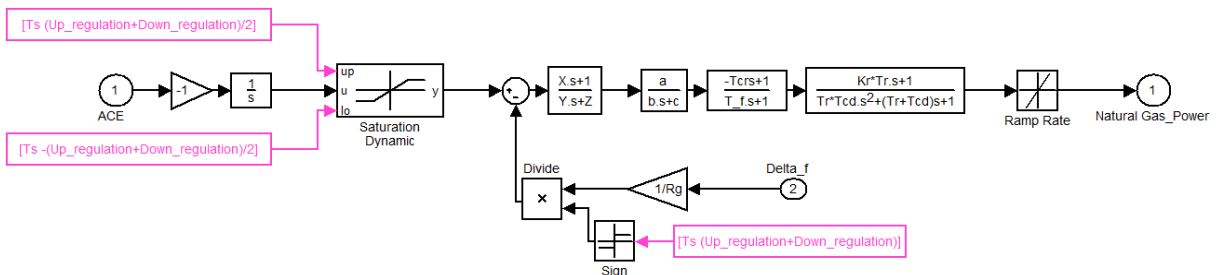
Figure 5.4 Natural gas unit in AGC subject to SCUC and SCED decisions- 3 gas units

5.2.4 Impact of Wind Penetration on AGC

The total wind generation in the system is split into buses 17, 21 and 22 respectively in the ratio 3:4:3. The data for load and wind generation, as shown in Figure 5.5 at 1-min. resolution, is taken from CAISO for two typical winter days [79]. The net-load (NL) data at 1-second resolution is obtained by interpolating the data at 1-minute intervals, and the net-load deviations (ΔP_d) computed at 1-second resolution is input as the disturbance to the AGC model as shown in Figure 5.1. Since typically the generation base points are decided by 5-minute RTED based on the average net-load in that period, the deviations are computed as shown in (5.53).

$$\Delta P_d(t) = (L_{RT}(t) - W_{RT}(t)) - avg_{5-min}(L_{RT}(t) - W_{RT}(t)) \tag{5.53}$$
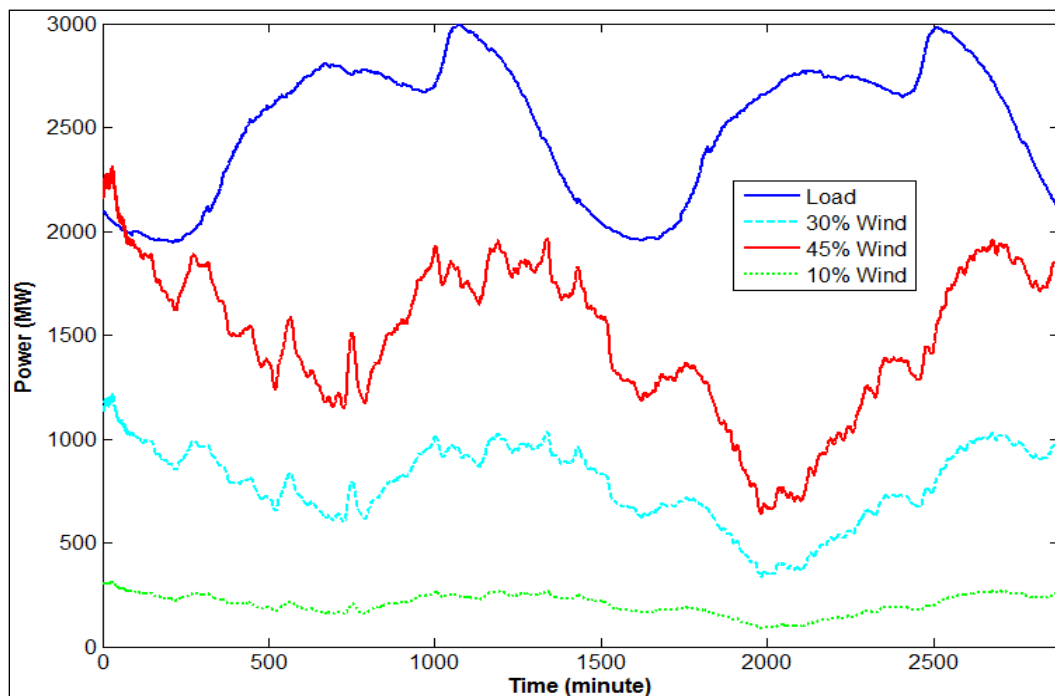
Figure 5.5 System load and wind data over 2 days at 1-minute resolution

As wind penetration increases, three kinds of impact on AGC model is captured within the simulations:

   i)   *Increase in net-load deviations*

   ii) *Higher allocation of regulation service by SCED*

   iii) *Decrease in system inertia*

Figure 5.6 shows the net-load deviations for the two days (172800 s) at different wind penetrations. It can be observed that the deviation increases as the wind penetration increases, with the peak deviation at 60% wind penetration about 5-6 times the peak deviation at 10% wind penetration.
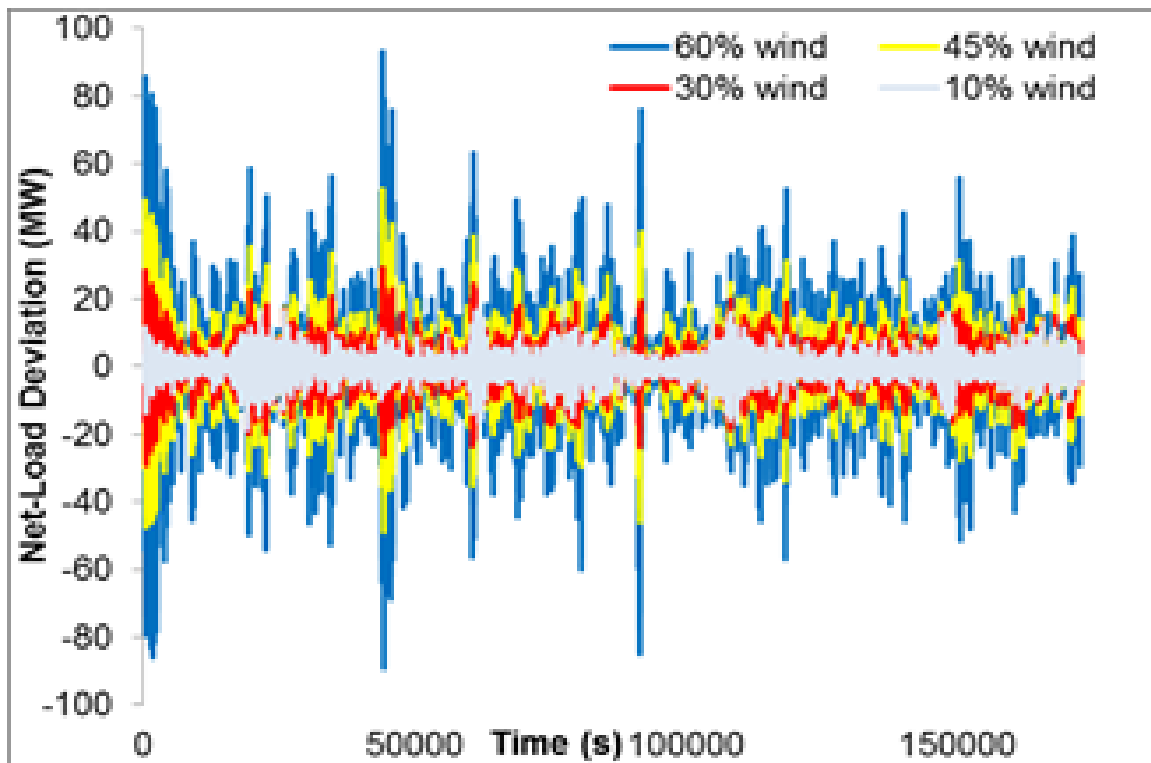
Figure 5.6 Net-load deviations at various wind penetration at 1-s resolution

The increase in net-load deviations with increasing wind penetration imposes higher ramping and regulation requirements on the generators in AGC. Figure 5.7 shows the total

hourly (3600s) regulation allocations by the DA-SCED at various wind penetrations, since the estimation of hourly regulation requirements within the DA-SCED algorithm is made a function of net-load variability within every hour [72]. At each hour, the regulation requirements are allocated amongst coal (regulation offer = $36), natural gas ($27) and oil ($62) units, with coal and gas units taking the bulk of the regulation services due to their offers.
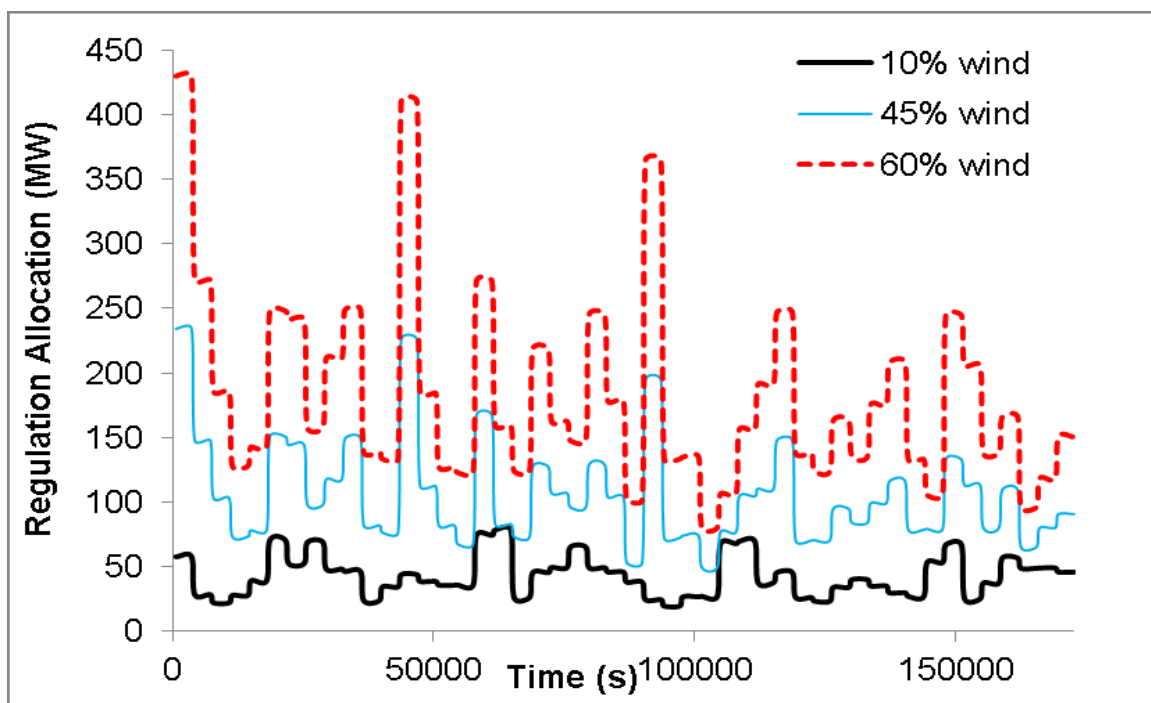
Figure 5.7 Hourly regulation allocations at various wind penetrations

As the wind generation increases, the system usually experiences reduction in inertia (H) mainly due to the displacement in conventional units [102]. In this study, this phenomenon is quantitatively captured using the hourly schedules from SCUC module. The system inertia for AGC simulation is computed as a function of the generators committed during every hour, as decided by the SCUC. Figure 5.8 shows the impact of increasing wind penetration on system inertia every hour (in terms of percentage of the total system H

(MWs/MVA)). This is accomplished by updating Tp (power system time constant) in Figure 5.1, which is a function of H (directly proportional).
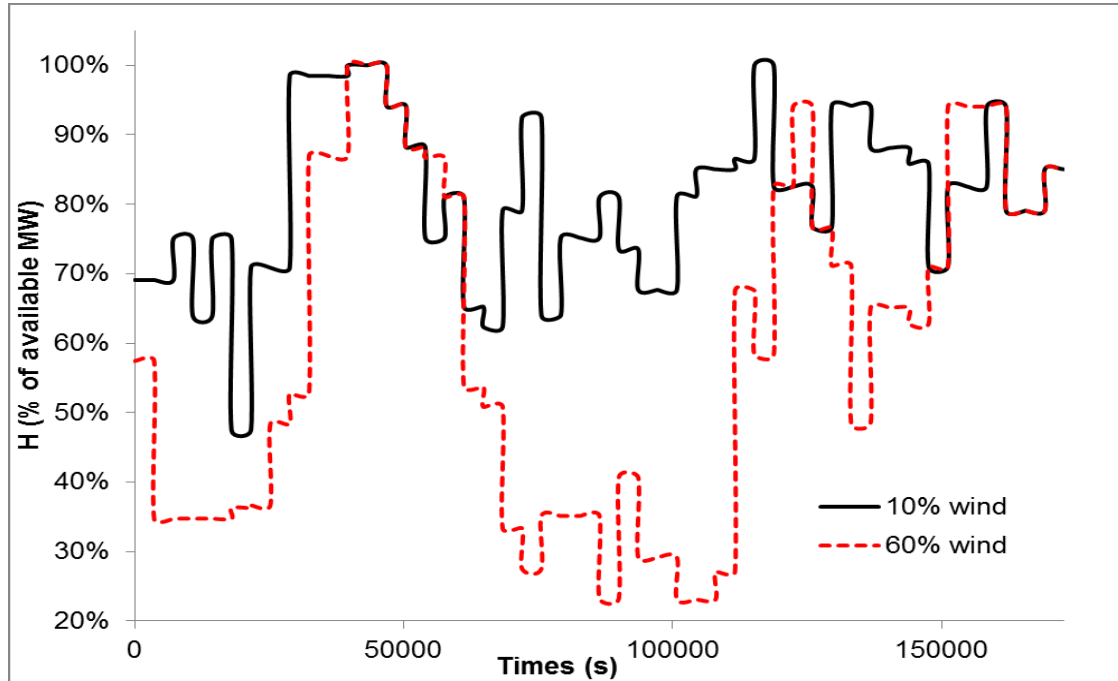
Figure 5.8 Impact of increasing wind penetration on system inertia

There is decrease in the inertia during many hours due to displacement of conventional units by wind generation. The degree of conventional unit displacement also depends on many other factors such as forced outage of generators (captured within the SCUC using a random sampling process based on unit forced outage rates (FOR)), load level, and wind spillage due to transmission flow limits.

5.3 INTEGRATION OF STORAGE IN AGC

Typically storage technologies such as battery, flywheel and Superconducting Magnetic Energy Storage (SMES) [103, 104] that have short-term energy capacity and respond faster are utilized to compensate the ACE instantaneously, and offset the frequency

deviation. Figure 5.9 shows the operational logic behind short-term storage participation in AGC, wherein if ACE is negative due to net-load increase and frequency dips, then storage discharges short burst of power to offset it, and if ACE is positive due to net-load decrease causing frequency increase, then storage quickly absorbs power. The ability to absorb and discharge at any instance also depends on the reservoir (storage medium) energy status. As shown in Figure 2.2, the modes of operation for short-term storage can be termed as "two-quadrant" operation, i.e., quick bursts of charge increase and discharge increase as required.
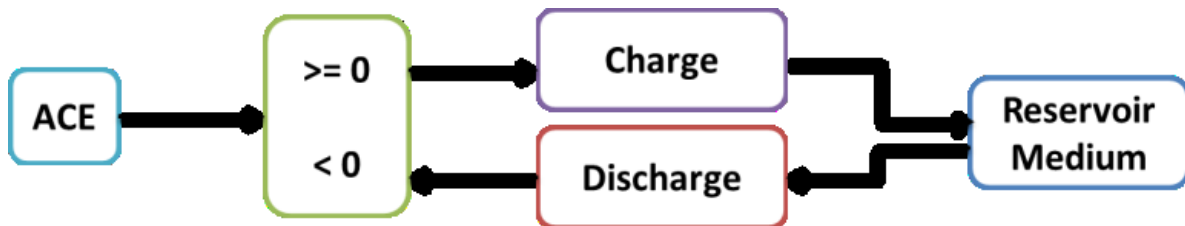
Figure 5.9 Short-term storage participation logic in AGC

Bulk energy storages stores energy for hours, e.g. CAES and PHS. Thus these storage technologies have the ability to offer both in energy and AS markets. For instance, a generator operates in two-quadrant as shown in Figure 2.2, it provides regulation through its discharge operation only, i.e., by moving up and down from a discharge set point committed in energy market. Similarly, in a given hour, depending upon whether the bulk storage is charging or discharging from the energy market, it can also provide regulation by moving up or down about its charge and discharge commitments. This makes such bulk storage operate in all the "four-quadrants". In this section, we present the state space model of CAES and battery for integrating them within AGC module, and specifically focus on investigating the impact of fast-responding battery storage on system frequency response.

5.3.1   State Space Model of Compressed Air Energy Storage

CAES operation is similar to that of the conventional gas turbine (or combustion turbine (CT)), with the difference being that the expansion and compression stages are made independent. A conceptual design of CAES is shown in Figure 5.10.
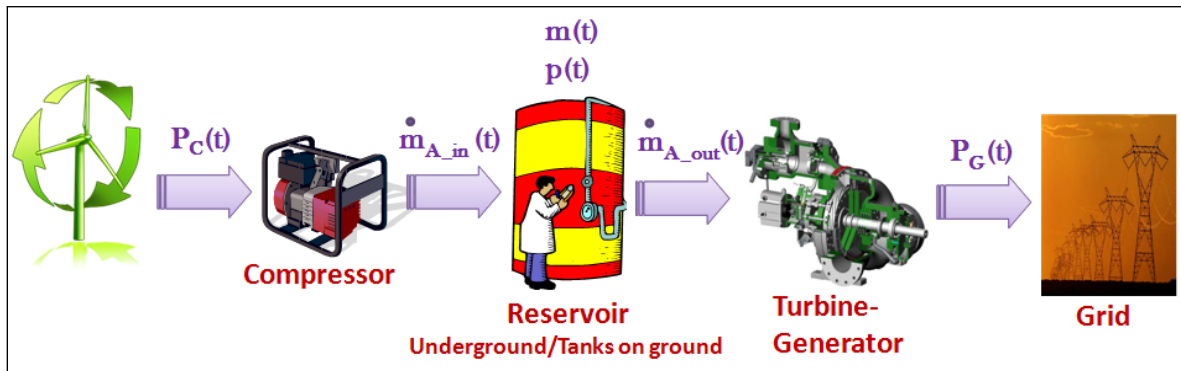
Figure 5.10 Conceptual representation of a basic CAES system

This section presents the integration of slow dynamics model of CAES into AGC module as shown in Figure 5.11. The turbine model is similar to that of the natural gas unit model presented in section 5.2.3, with the only difference being the absence of the re-heater. The compressor system's pressure rising process is modeled as first order inertia system with large time constant T_{1C}, and the speed control system is approximately represented as another first order inertia system with time constant T_{2C}, with $T_{1C} > T_{2C}$.
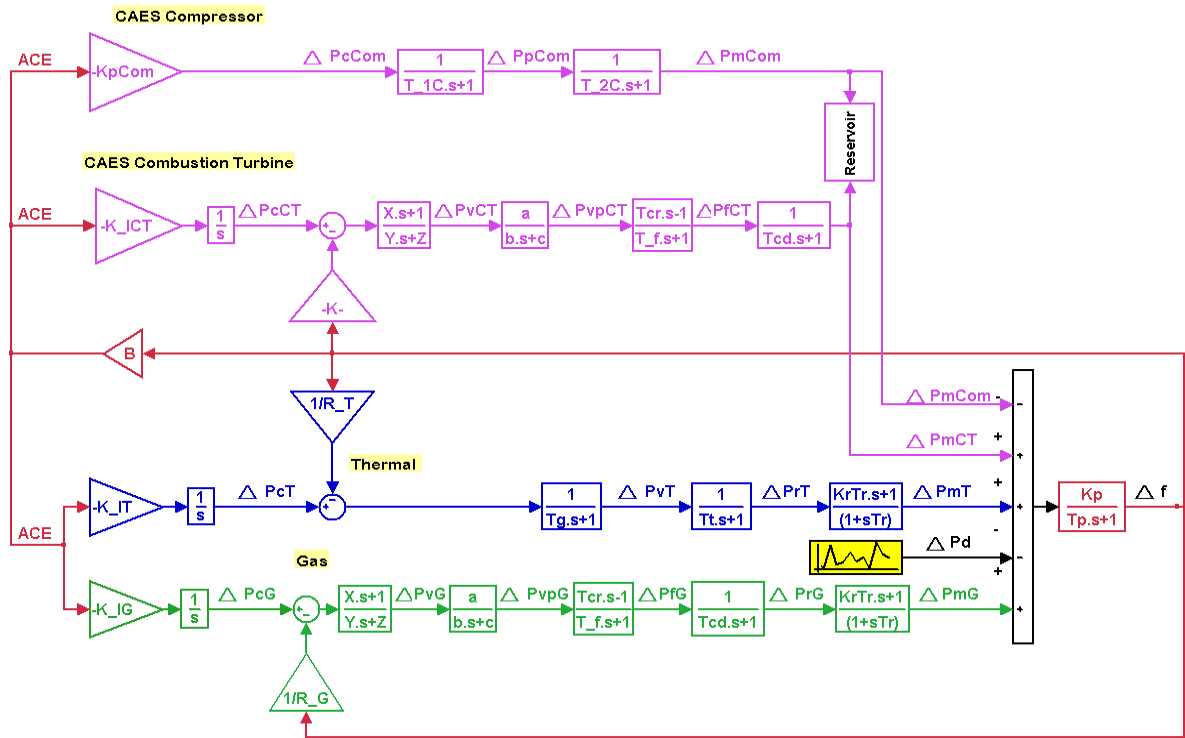
Figure 5.11 Slow dynamics model of CAES integrated into AGC

The following equations show the development of state space representation of CAES's slow dynamics. Equation (5.54) shows states related to compressor operation, (5.55) shows states related to turbine operation, and (5.56) shows states related to reservoir operation (i.e., reservoir energy, mass and pressure).

$$\Delta X_{Com} = \left| \begin{array}{cc} \Delta P_{mCom} & \Delta P_{pCom} \end{array} \right|^{T} \tag{5.54}$$

$$\Delta X_{CT} = \left| \begin{array}{ccccc} \Delta P_{mCT} & \Delta P_{fCT} & \Delta P_{vpCT} & \Delta P_{vCT} & \Delta P_{cCT} \end{array} \right|^{T} \tag{5.55}$$

$$\Delta X_{Res} = \left| \begin{array}{ccc} E_{Res} & m_{Res} & p_{Res} \end{array} \right|^{T} \tag{5.56}$$

System state:

Both turbine and compressor power generation and withdrawal will impact the system frequency, depending upon which one of the components is available online in a particular hour (based on CAES commitments by SCUC indicated by U and U^C parameters). The turbine impacts the frequency in a manner similar to any conventional generation, and the compressor impacts in a manner similar to a load disturbance.

$$\Delta \dot{f} = -\frac{1}{T_p}\Delta f + \frac{K_p}{T_p}\left(\Delta P_{mT} + \Delta P_{mG} + \left(U\,\Delta P_{mCT} - U^c\,\Delta P_{mCom}\right) - \Delta P_L\right) \tag{5.57}$$

Combustion Turbine states:

$$\Delta P_{mCT} = \left(\frac{1}{1+sT_{CD}}\right)\left(\Delta P_{fCT}\right) \tag{5.58}$$

$$\Delta \dot{P}_{mCT} = -\frac{1}{T_{CD}}\Delta P_{mCT} + \frac{1}{T_{CD}}\Delta P_{fCT} \tag{5.59}$$

$$\Delta P_{fCT} = \left(\frac{1-sT_{CR}}{1+sT_f}\right)\left(\Delta P_{vpCT}\right) \tag{5.60}$$

$$\Delta \dot{P}_{fCT} = -\frac{1}{T_f}\Delta P_{fCT} + \frac{1}{T_f}\Delta P_{vpCT} - \frac{T_{CR}}{T_f}\Delta \dot{P}_{vpCT} \tag{5.61}$$

$$\Delta P_{vpCT} = \left(\frac{a}{c+sb}\right)\Delta P_{vCT} \tag{5.62}$$

$$\Delta \dot{P}_{vpCT} = -\frac{c}{b}\Delta P_{vpCT} + \frac{a}{b}\Delta P_{vCT} \tag{5.63}$$

$$\Delta \dot{P}_{fCT} = -\frac{1}{T_f}\Delta P_{fCT} + \left(\frac{1}{T_f} + \frac{cT_{CR}}{bT_f}\right)\Delta P_{vpCT} - \frac{aT_{CR}}{bT_f}\Delta P_{vCT} \tag{5.64}$$

$$\Delta P_{vCT} = \left(\frac{1+sX}{Z+sY}\right)\left(\Delta P_{cCT} - \frac{1}{R_{CT}}\Delta f\right) \tag{5.65}$$

$$\Delta \dot{P}_{vCT} = -\frac{Z}{Y}\Delta P_{vCT} + \frac{1}{Y}\Delta P_{cCT} + \frac{X}{Y}\Delta \dot{P}_{cCT} - \frac{1}{YR_{CT}}\Delta f - \frac{X}{YR_{CT}}\Delta \dot{f} \tag{5.66}$$

$$\Delta P_{cCT} = \left(\frac{-K_{ICT}}{s}\right)\left(B\,\Delta f\right) \tag{5.67}$$

$$\Delta \dot{P}_{cCT} = -K_{ICT}B\Delta f \tag{5.68}$$

$$\Delta \dot{P}_{vCT} = -\frac{Z}{Y}\Delta P_{vCT} + \frac{1}{Y}\Delta P_{cCT} + \left(\frac{-X}{Y}K_{ICT}B - \frac{1}{YR_{CT}} + \frac{X}{YR_{CT}T_p}\right)\Delta f - \frac{XK_p}{YR_{CT}T_p}\left(\Delta P_{mT} + \Delta P_{mG} + \left(UP_{mCT} - U^C P_{mCom}\right) - \Delta P_L\right) \tag{5.69}$$

Compressor states:

$$\Delta P_{mCom} = \left(\frac{1}{1+sT_{2C}}\right)\left(\Delta P_{pCom}\right) \tag{5.70}$$

$$\Delta \dot{P}_{mCom} = -\frac{1}{T_{2C}}\Delta P_{mCom} + \frac{1}{T_{2C}}\Delta P_{pCom} \tag{5.71}$$

$$\Delta P_{pCom} = \left(\frac{1}{1+sT_{1C}}\right)\left(\Delta P_{cCom}\right) \tag{5.72}$$

$$\Delta \dot{P}_{pCom} = -\frac{1}{T_{1C}}\Delta P_{pCom} + \frac{1}{T_{1C}}\Delta P_{cCom} \tag{5.73}$$

$$\Delta P_{cCom} = -K_{PCom}B\Delta f \tag{5.74}$$

$$\Delta \dot{P}_{pCom} = -\frac{1}{T_{1C}}\Delta P_{pCom} - \frac{BK_{PCom}}{T_{1C}}\Delta f \tag{5.75}$$

Reservoir states:

Equation (5.76) shows the reservoir energy status which depends on the overall energy compressed and generated over a period.

$$E_{Res} = \frac{1}{s}\left(\Delta P_{mCom} - \Delta P_{mCT}\right) \tag{5.76}$$

$$\dot{E}_{Res} = \left(\Delta P_{mCom} - \Delta P_{mCT}\right) \tag{5.77}$$

The following modeling assumptions are made for capturing other subtle states of the CAES reservoir such as mass and pressure:

- Isentropic process, i.e., no heat is added to the flow, and so the temperatures remain constant.

- Ideal gas with a constant specific heat.

- The ratio of fuel to air inside turbine is constant.

The compressor train compresses the air at atmospheric pressure to the reservoir pressure. The rate of flow of air mass into the reservoir is [105] given by (5.78).

$$\Delta m_{Com} = \frac{\Delta P_{mCom}}{c_{p1}T_{in}\left[\left(\frac{P_2}{P_1}\right)^{\frac{\gamma-1}{\gamma}} - 1\right]} = K_{m_{Com}}\Delta P_{mCom} \tag{5.78}$$

$$\gamma = \frac{C_{p1}}{C_{v1}} \tag{5.79}$$

where C_{p1} is the specific heat at constant pressure, P_2 and P_1 are the compressor output pressure and input pressure, respectively (in bar), T_{in} is ambient temperature at input of Compressor (K), and C_{v1} is specific heat at constant volume.

The air withdrawn from the reservoir by turbine is compressed in a high pressure stage, and subsequently combusted with fuel in a low pressure stage. The mass of air discharged from the reservoir is calculated using the turbine equation [106]. The rate of flow of air discharged from the reservoir is given by (5.80).

$$\Delta m_{CT} = \frac{\Delta P_{mCT}}{\eta_M \eta_G c_{p2} T_2 \left(1 + \frac{\dot{m}_{CT}}{\dot{m}_{fuel}}\right) \left(\frac{C_{p1} T_1}{C_{p2} T_2}\left[1 - \left(\frac{P_2}{P_1}\right)^{\frac{k_1-1}{k_1}}\right] + 1 - \left(\frac{P_b}{P_2}\right)^{\frac{k_1-1}{k_1}}\right)} = K_{m_{CT}} \Delta P_{mCT} \quad (5.80)$$

where, T_1 is the HP turbine inlet temperature (K), T_2 is the LP turbine inlet temperature (K), P_1 and P_2 are the pressures in LP and HP turbines (in bar). P_b is the atmospheric pressure, $\dot{m}_{CT}/\dot{m}_{fuel}$ is the ratio of the air discharge rate from the reservoir to the rate of flow of fuel that combines in the combustion chamber to generate electricity, and is the CAES round trip efficiency [107].

Inside the reservoir as the compressor pumps in air, the mass of air increases and simultaneously, the pressure of the reservoir increases. Typically, the reservoir operates within the pressure range of 15 to 70 bar. The CAES reservoir can be an underground storage, depleted natural gas/oil fields, piping systems or compressed air tanks with different ratings. The mass and pressure inside the reservoir is computed by [108],

$$m_{Res} = \frac{1}{s}\left(\Delta m_{Com} - \Delta m_{CT}\right) \quad (5.81)$$

$$\dot{m}_{Res} = \left(\Delta m_{Com} - \Delta m_{CT}\right) = K_{m_{Com}} \Delta P_{mCom} - K_{m_{CT}} \Delta P_{mCT} \quad (5.82)$$

$$p_{Res} = \frac{R}{V}\left(\frac{1}{s}\left(\Delta m_{Com} T_{in} - \Delta m_{CT} T_s\right)\right) \quad (5.83)$$

$$\dot{p}_{Res} = \frac{R}{V}\left(\left(\Delta m_{Com}T_{in} - \Delta m_{CT}T_s\right)\right) = \frac{R}{V}\left(K_{m_{Com}} T_{in}\Delta P_{mCom} - K_{m_{CT}} T_s\Delta P_{mCT}\right) \qquad (5.84)$$

where Km_{Com} and K_{mCT} are the reciprocal of denominators of the equations (5.78) and (5.80) respectively, R is the gas constant (J kg^{-1} K^{-1}), V is the volume of the storage(m^3), T_{in} is temperature at input of storage and T_s is the temperature at which the compressed air is stored in the storage (K). This design where the pressure changes with the mass of air is referred to as sliding pressure [108].

The energy that the reservoir can store is determined by the pressure and mass values of the reservoir. In real time, the reservoir cannot be discharged below a minimum pressure and charged beyond a maximum pressure limit. This model facilitates enforcing this operational constraint during the simulation by conducting the charging and discharging of CAES reservoir within the operational pressure ranges. The gradual pressure leakage from the reservoir of 15bar/hour [109] is also accounted in this model.

5.3.1.1 CAES Reservoir model validation with Huntorf operational data

The CAES reservoir model was validated with the output curves from the Huntorf model [109]. The input power P$_{mcom}$ and output power P$_{mCT}$ used to validate the state space model are shown in Figure 5.12. These curves are the real-time input/output power to the Huntorf CAES. The pressure from the state space model was compared to the Huntorf CAES and verified its operation. As can be see from Figure 5.13 that the Huntorf CAES pressure ranges between 48-62 bars while the state space model pressure ranges from 30-62 bars. The pressure for the state space model starts from 30 bar as the CAES reservoir was charged from empty to full. On the otherhand the Huntorf model real time data is a snapshot

from its real time operation and had previously charged its reservoir with corresponding pressure of 48bar.
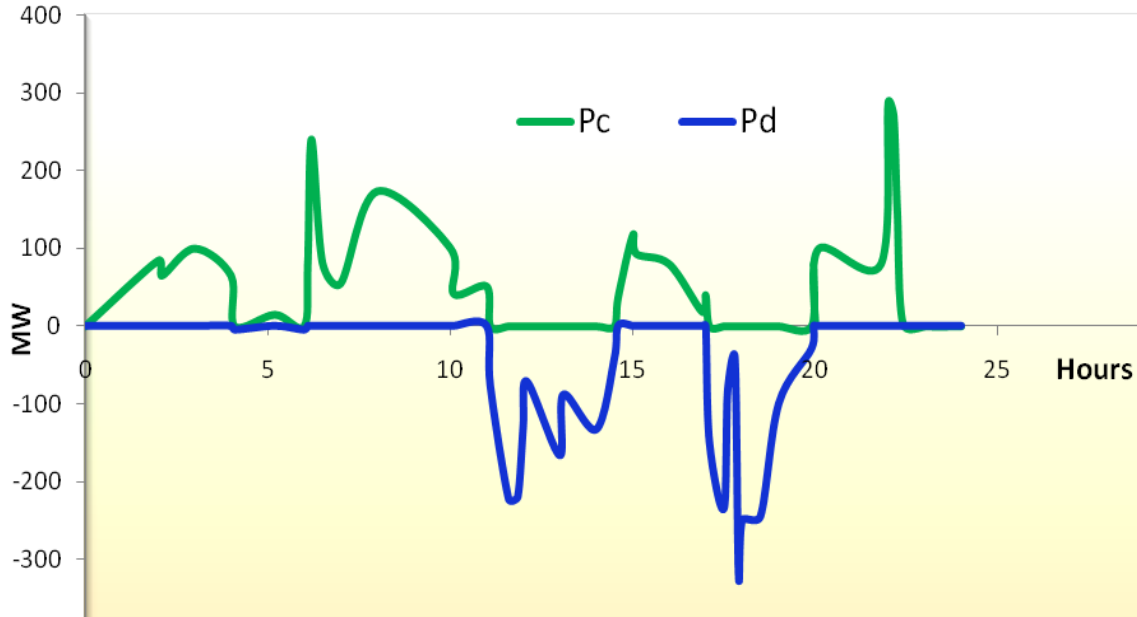
Figure 5.12 Input/output curves from real-time data of Huntorf CAES
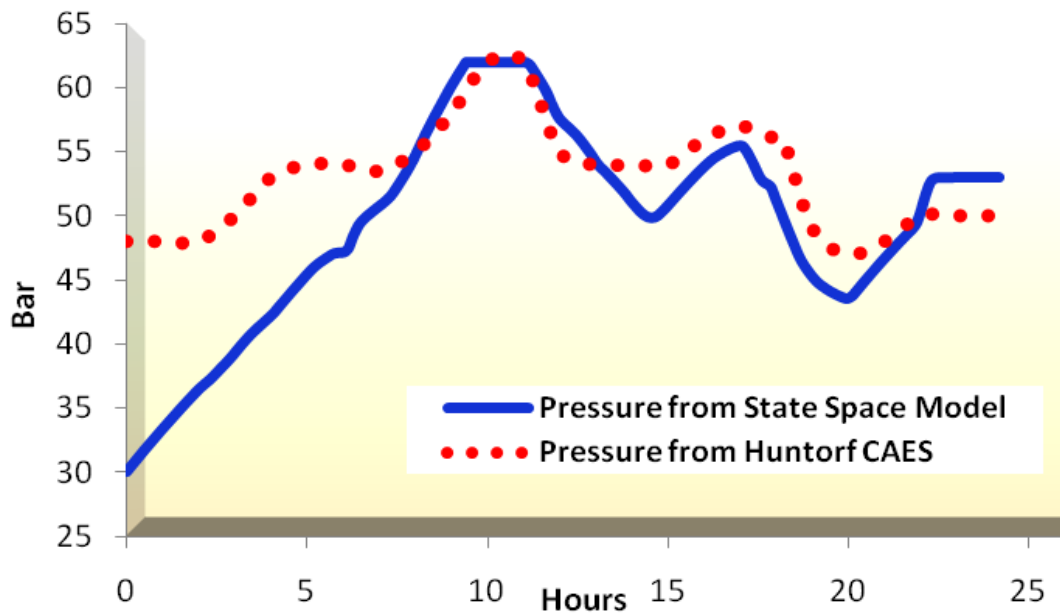
Figure 5.13 Pressure curves compared from State Space model and Huntorf CAES

5.3.1.2 Integration of CAES state space into AGC

The various system states are divided into 6 categories: system related state X_p (1 state), thermal unit related states X_T (4 states), gas unit related states X_G (6 states), CAES compressor related states (2 states), CAES turbine related states (5 states), and CAES reservoir related states (3 states). Equation (5.85) shows the standard state space representation of IEEE 24 bus RTS system integrated with CAES. The state matrices that are non-empty and capture the interactions between various components are defined subsequently.

$$
\begin{vmatrix} \Delta\dot{X}_p \\ \Delta\dot{X}_T \\ \Delta\dot{X}_G \\ \Delta\dot{X}_{Com} \\ \Delta\dot{X}_{CT} \\ \Delta\dot{X}_{Res} \end{vmatrix} = \begin{vmatrix} A_{pp} & A_{pT} & A_{pG} & A_{p,Com} & A_{p,CT} & A_{p,Res}=0 \\ A_{Tp} & A_{TT} & A_{TG}=0 & A_{T,Com}=0 & A_{T,CT}=0 & A_{T,Res}=0 \\ A_{Gp} & A_{GT} & A_{GG} & A_{G,Com} & A_{G,CT} & A_{G,Res}=0 \\ A_{Com,p} & A_{Com,T}=0 & A_{Com,G}=0 & A_{Com,Com} & A_{Com,CT}=0 & A_{Com,Res}=0 \\ A_{CT,p} & A_{CT,T} & A_{CT,G} & A_{CT,Com} & A_{CT,CT} & A_{CT,Res}=0 \\ A_{Res,p}=0 & A_{Res,T}=0 & A_{Res,G}=0 & A_{Res,Com} & A_{Res,CT} & A_{Res,Res}=0 \end{vmatrix} \begin{vmatrix} \Delta X_p \\ \Delta X_T \\ \Delta X_G \\ \Delta X_{Com} \\ \Delta X_{CT} \\ \Delta X_{Res} \end{vmatrix} + \begin{vmatrix} \Gamma_{pp} \\ \Gamma_{Tp}=0 \\ \Gamma_{Gp} \\ \Gamma_{Com,p}=0 \\ \Gamma_{CT,p} \\ \Gamma_{Res,p}=0 \end{vmatrix} \Delta P_d
$$

(5.85)

where,

$$
A_{Com,Com} = \begin{vmatrix} -\dfrac{1}{T_{2C}} & \dfrac{1}{T_{2C}} \\ 0 & -\dfrac{1}{T_{1C}} \end{vmatrix}
$$

(5.86)

$$
A_{p,Com} = \begin{vmatrix} \dfrac{-U^C K_p}{T_p} & 0 \\ & \end{vmatrix}
$$

(5.87)

$$A_{Com,p} = \left| \begin{array}{cc} 0 & \dfrac{-BK_{PCom}}{T_1} \end{array} \right|^{T} \tag{5.88}$$

$$A_{p,CT} = \left| \begin{array}{ccccc} \dfrac{UK_p}{T_p} & 0 & 0 & 0 & 0 \end{array} \right| \tag{5.89}$$

$$A_{CT,p} = \left| \begin{array}{ccccc} 0 & 0 & 0 & \left(\dfrac{X}{Y}K_{ICT}B - \dfrac{1}{YR_{CT}} + \dfrac{X}{YR_{CT}T_p} \right) & K_{ICT}B \end{array} \right|^{T} \tag{5.90}$$

$$A_{CT,CT} = \left| \begin{array}{ccccc} -\dfrac{1}{T_{CD}} & \dfrac{1}{T_{CD}} & 0 & 0 & 0 \\ 0 & -\dfrac{1}{T_f} & \left(\dfrac{1}{T_f} + \dfrac{cT_{CR}}{bT_f} \right) & -\dfrac{aT_{CR}}{bT_f} & 0 \\ 0 & 0 & -\dfrac{c}{b} & \dfrac{a}{b} & 0 \\ -\dfrac{UXK_p}{YR_{CT}T_p} & 0 & 0 & -\dfrac{Z}{Y} & \dfrac{1}{Y} \\ 0 & 0 & 0 & 0 & 0 \end{array} \right| \tag{5.91}$$

$$A_{CT,T}(4,1) = A_{CT,G}(4,1) = \dfrac{-XK_p}{YR_{CT}T_p} \tag{5.92}$$

$$A_{CT,Com}(4,1) = A_{G,Com}(5,1) = \dfrac{U^C XK_p}{YR_{CT}T_p} \tag{5.93}$$

$$A_{G,CT}(5,1) = \dfrac{-UXK_p}{YR_G T_p} \tag{5.94}$$

where. $A_{CT,T}$, $A_{CT,G}$, $A_{CT,Com}$, $A_{G,Com}$, and $A_{G,CT}$ are (5X4), (5X6), 5X2), (6X2), and (6X5) matrices respectively, with all the other elements being zero.

$$\Gamma_{CT,p} = \left| \begin{array}{ccccc} 0 & 0 & 0 & \dfrac{XK_p}{YR_{CT}T_p} & 0 \end{array} \right|^{T} \tag{5.95}$$

$$A_{Res,Com} = \left| \begin{array}{cc} 1 & 0 \\ K_{m_{Com}} & 0 \end{array} \right|$$

$$\left| \begin{array}{cc} \dfrac{RK_{m_{Com}} T_{in}}{V} & 0 \end{array} \right| \tag{5.96}$$

$$A_{Res,CT} = \left| \begin{array}{ccccc} -1 & 0 & 0 & 0 & 0 \\ -K_{m_{CT}} & 0 & 0 & 0 & 0 \\ \dfrac{-RK_{m_{CT}} T_s}{V} & 0 & 0 & 0 & 0 \end{array} \right| \tag{5.97}$$

5.3.2 Battery integration into AGC

The battery model available in Matlab Simulink has been used in this work [110, 111], a simplistic version of which is shown in Figure 5.14. The model captures three typical characteristics of batteries: exponential voltage drop of a typical battery when it is charged, the linear relationship between charge and voltage up until a nominal value, and finally the non-linear discharge beyond the nominal voltage value. The various parameters of the model are estimated based on the charge-discharge characteristics of various batteries, i.e., lead acid, lithium ion, Ni-Cd, and Ni-MH. In this work, the Ni-MH battery model of Simulink is used with suitable parameters to realize a 1 MW 1200V 1000A (66.67Ah) battery with a response time of 100ms.

The operational logic in integrating battery into AGC is depicted in Figure 5.15. The parameter *series_cells* is used in the model (within and outside the battery) to increase the battery power rating by emulating the series connection of many cells that adds up all the voltage to make up a high-power battery bank with similar A-h rating. The battery voltage is always positive and the current is bidirectional. The internal voltage E of the battery is a function of its state of charge (SoC), as shown in Figure. 5.14. At full-charge the battery

voltage is at its maximum rated voltage of about 1200V and decreases as the state of charge

decreases to a low of 1020V. The SoC is given by (5.98)

$$SoC = 100\left(1 - \frac{1}{Q}\int_0^t i\,dt\right) = 100\left(\frac{Q - it}{Q}\right) \tag{5.98}$$

$$\Delta SoC = 100\left(\frac{1}{Q}\int_o^t i\,dt\right) = 100\left(\frac{1}{Q}\frac{\Delta I_{batt}}{s}\right) \tag{5.99}$$

$$\Delta \dot{SoC} = 100\left(\frac{\Delta I_{batt}}{Q}\right) \tag{5.100}$$
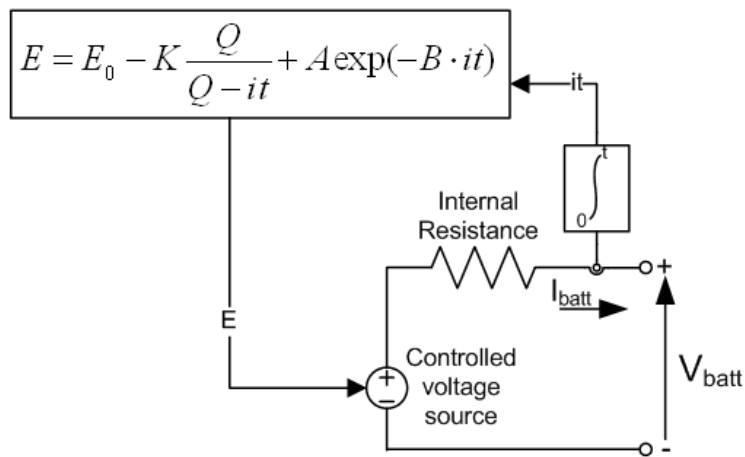
Figure 5.14 Simplistic representation of battery model in Matlab Simulink
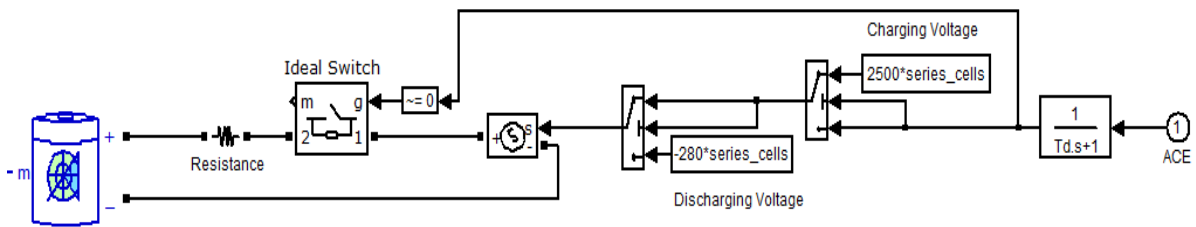
Figure 5.15 Battery integration into AGC

The battery is connected to the grid through ac/dc converter. The voltage across the converter is a function of the system ACE. The change in the voltage is proportional to the deviation in the ACE and consequently the system frequency, as given by (5.101).

$$\Delta V_{conv} = \left(\frac{K_0}{1 + sT_d} \right) (B \Delta f) \tag{5.101}$$

$$\Delta \dot{V}_{conv} = -\frac{1}{T_d} \Delta V_{conv} + \frac{K_0 B}{T_d} \Delta f \tag{5.102}$$

As shown in Figure 5.15, a positive voltage V_{batt} across the first convertor (i.e., positive ACE) triggers a convertor leg to apply 2500V across the battery terminals, whereby the battery is charged. A negative voltage (negative ACE) across the first convertor triggers a convertor leg such that -280 V is applied across the battery terminals, thereby discharging the battery. When the deviation is 0, the battery terminal is open-circuited thereby not charging or discharging.

$$V_{batt} = \begin{cases} 2500, & if \ V_{conv} > 0 \\ -280, & if \ V_{conv} < 0 \\ \infty, & if \ V_{conv} = 0 \end{cases} \tag{5.103}$$

The battery current is given by (5.104),

$$\Delta I_{batt} = \frac{1}{(R_{int} + R_{batt})} (\Delta E - \Delta V_{batt}) \tag{5.104}$$

where, R_{batt} is battery external resistance of 1.48ohm. As the current flows out or into the battery the state of charge of the battery changes, as shown in (5.100). The converter voltage varies from -280 V to 2500 V, such that the maximum current is restricted to 1000A. The charging and discharging power output from the battery is given by (5.105),

$$P_{batt} = E I_{batt} \tag{5.105}$$

5.4 AGC SIMULATION RESULTS

In this section AGC simulation with battery is presented. Three cases were investigated. Case 1 is the base case with the existing generators providing regulation through AGC according to the dispatch set points obtained from SCUC-SCED. Case 2 and case 3 are case 1 with the addition of 1MW and 2 MW batteries respectively.

5.4.1 Frequency Response Assessment

Figure 5.16 shows the 12-hour frequency response at 10% wind penetration, for all the three cases respectively. It is seen that the frequency response is progressively better with increasing battery contribution in the system.
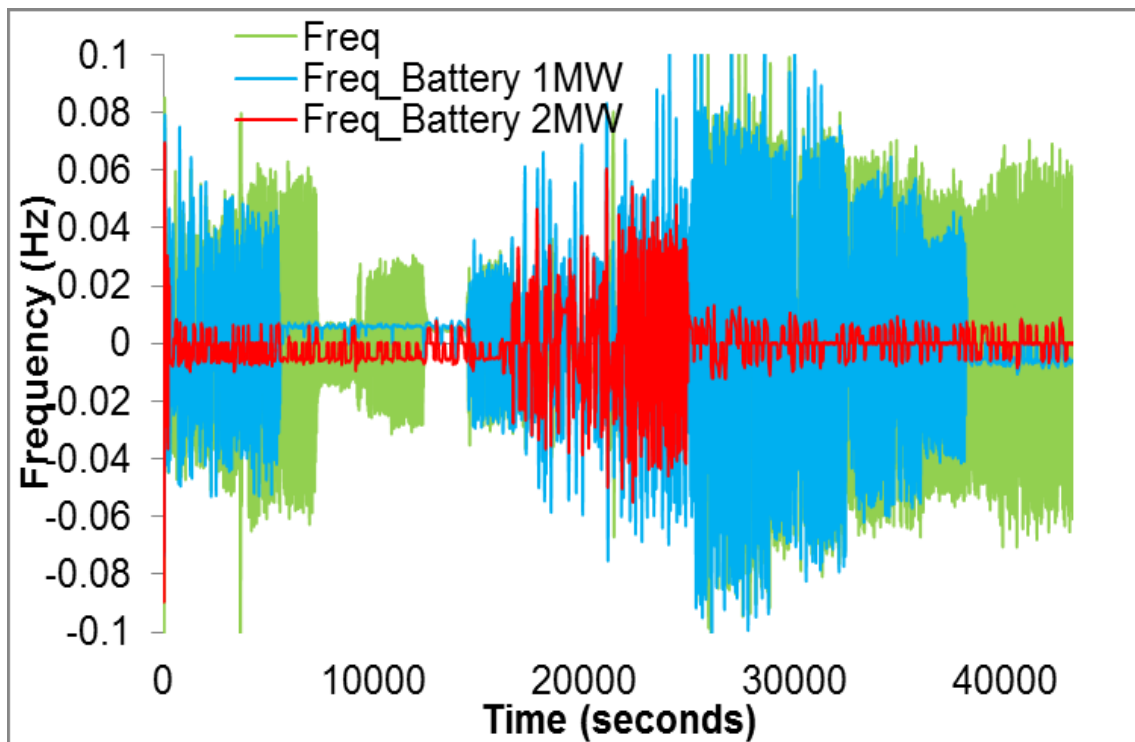
Figure 5.16 Frequency response at 10% wind penetration

Figure 5.17 and Figure 5.18 show the ACE movement vs. generation movement over a period of 10 minutes for case 1 and case 3 respectively. According to the SCUC-SCED decisions, in this period only coal units are dispatched to supply regulation, and hence respond to the AGC signals.
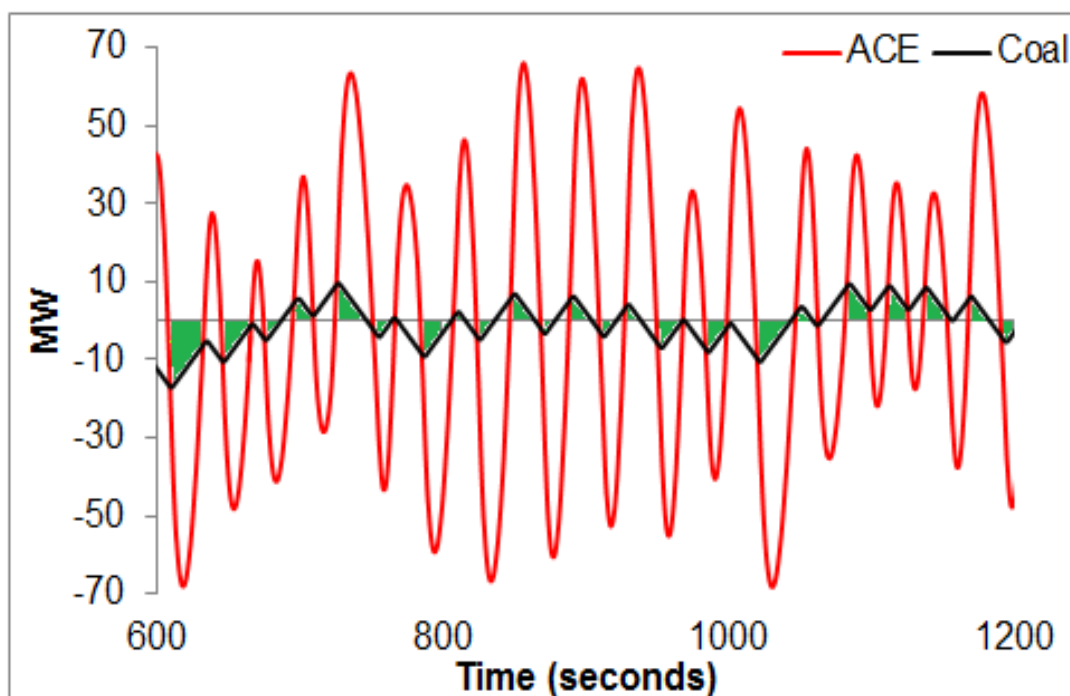
Figure 5.17 ACE vs. Resource Response – without storage

The following can be observed from the two figures:

1. *ACE Reduction*: When battery contributes to frequency regulation in Figure 5.18, the ACE is highly reduced due to its very fast movement, compared to coal alone trying to supply regulation as seen in Figure 5.17. Just comparing the peak ACE, an improvement of about 7-times is observed.
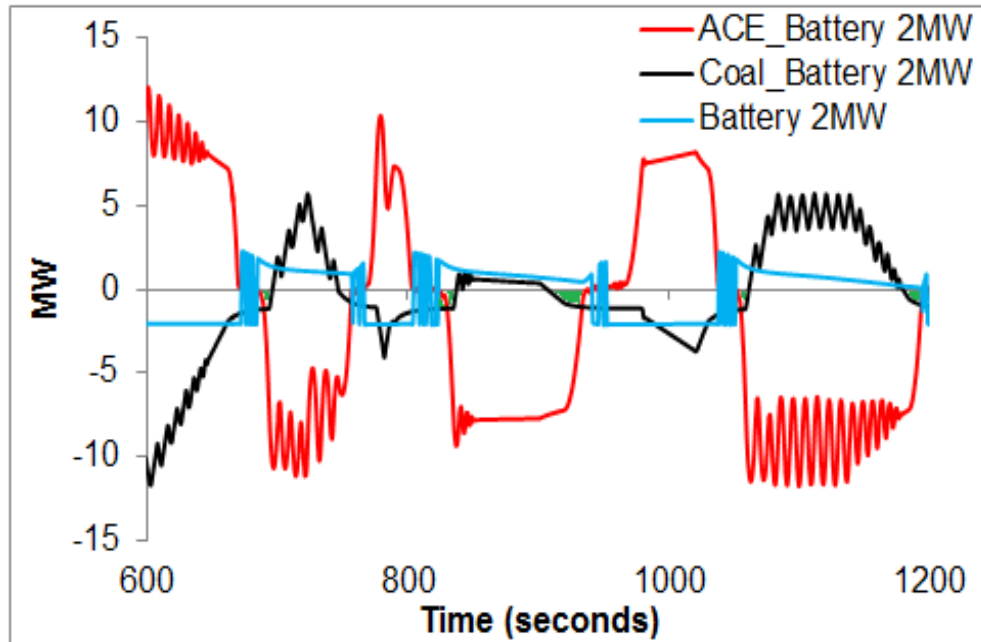
Figure 5.18 ACE vs. Resource Response – with storage

2. *Impact of slow responding units on ACE:* As seen in Figure 5.17, many times coal units, due to their slow movement, are unable to respond to the steep ramps of ACE caused by net-load fluctuations. Because of that even though coal unit move to offset the ACE, still it contributes to the total system ACE as seen by the shaded regions. The performance of conventional units will be much poorer with increasing wind penetration. On the other hand, as seen in Figure 5.18, due to battery's very quick response, the ACE is offset instantaneously. Due to efficient frequency response, and highly reduced ACE movement, the coal movements are also less and do not contribute to system net ACE.

5.4.2 CPS1 Measure

Figure 5.19 shows CPS1 curves with ϵ=0.0228 Hz at various wind penetration levels. It is seen that without fast responding storage, for case 1 the CPS1 values decrease

with increasing wind penetration. The available generating units are unable to offset the steep ramps of net-load deviation that occurs with increasing wind penetration. For the present case, beyond 15% wind penetration, the CPS1 values decrease less than 100%, and beyond 17.5% it is even worse.

The CPS may be improved by many ways, such as increasing fast acting regulation providers, aggregating control areas to reduce net-load variation, wind output control and inertia emulation, and increasing regulation requirement in SCUC/SCED algorithm. An ideal solution may be a combination of all these strategies, and fast responding devices may form a vital piece of that strategy. Fast responding regulation can be provided from combustion turbine, demand response and storage devices. In this study, the impacts of batteries are assessed. As seen in Figure 5.19, with increasing penetration of fast responding storage, the CPS values are improving, thereby enabling higher penetrations of wind in the system without violating the NERC CPS criteria for frequency response. In this case study, an addition of 10 MW battery to the existing AGC fleet helps facilitate about 10-15% more wind integration without causing frequency issues. Figure 5.20 shows the CPS-1 curves with a slightly relaxed frequency bounds, with $\epsilon=0.0342$ Hz. Consequetly the CPS-1 values are better in all the cases, again the addition of fast responding storage facilitating higher wind penetration.
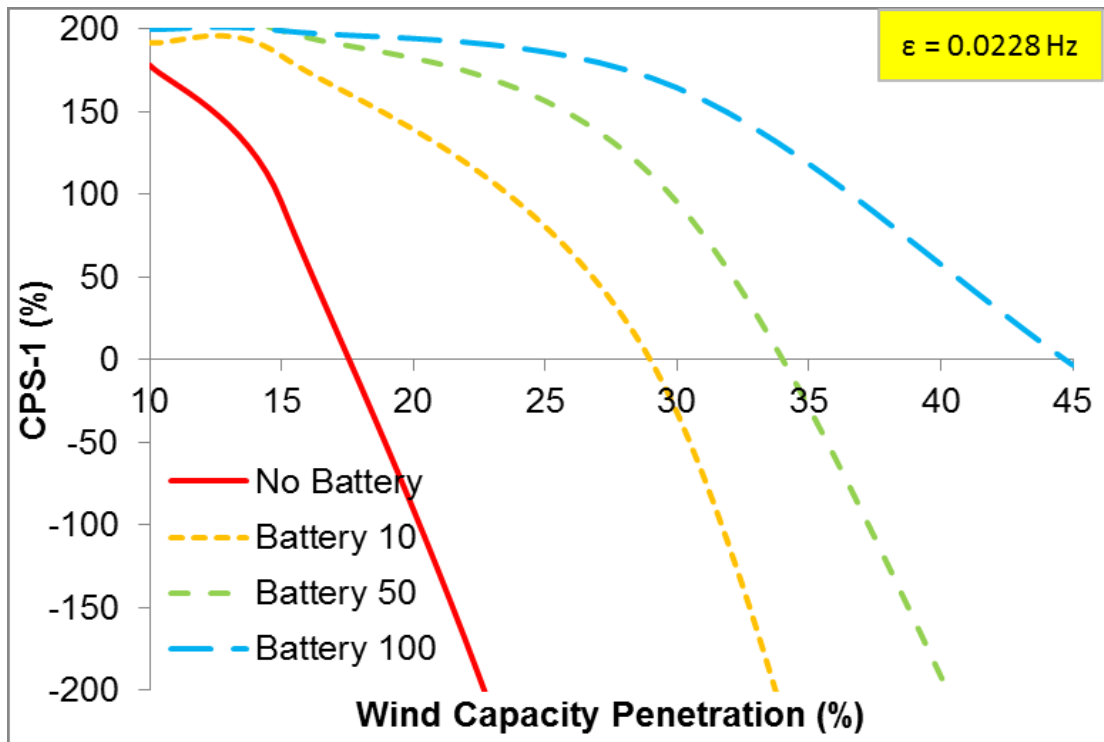
Figure 5.19 CPS-1 at various wind penetration – ϵ=0.0228 Hz
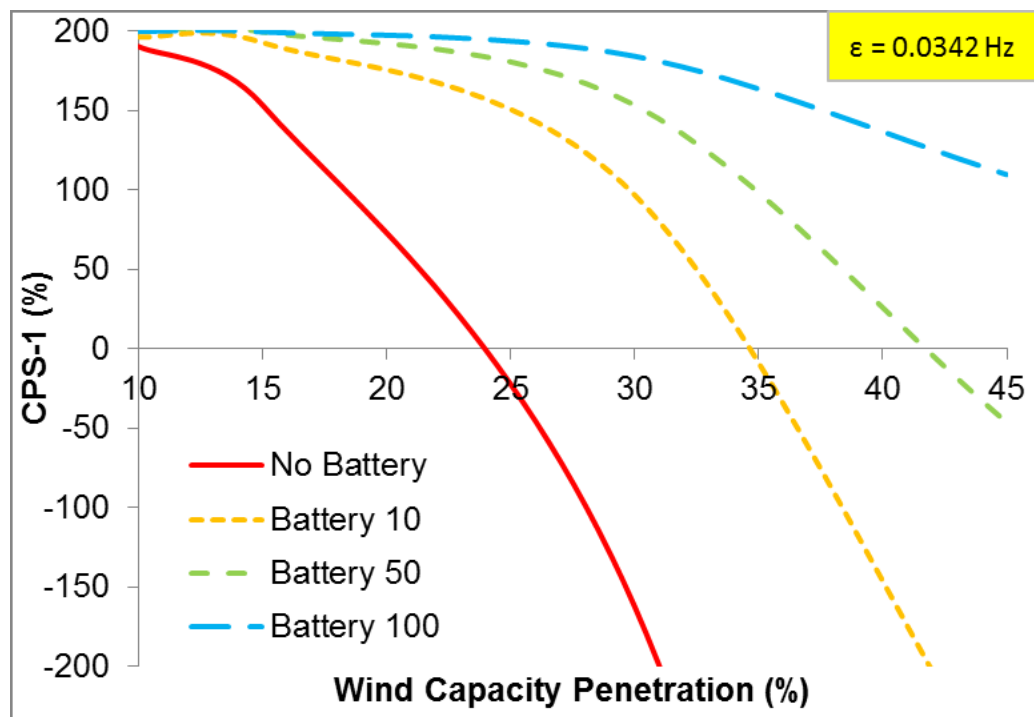
Figure 5.20 CPS-1 at various wind penetration – ϵ=0.0342 Hz

5.4.3   Generation Miles & Regulation Deployment

Figures 5.21 and 5.22 show the coal and natural gas units' movements for the first 12 hours of the AGC simulation. The movements are termed as "mileage" [93] that denotes the net absolute MW movements in both the directions (up and down) made by a generator in response to AGC signals to offset ACE. The results are summarized in Table 5.2, where from it is clear that with fast responding storage in the system, not only the total ACE-miles decreases, but additionally the movements by conventional units, especially coal also decreases. Just an addition of a 2 MW battery to the AGC fleet in this case study reduces about 60% and 77% of contribution from coal and natural gas units respectively.
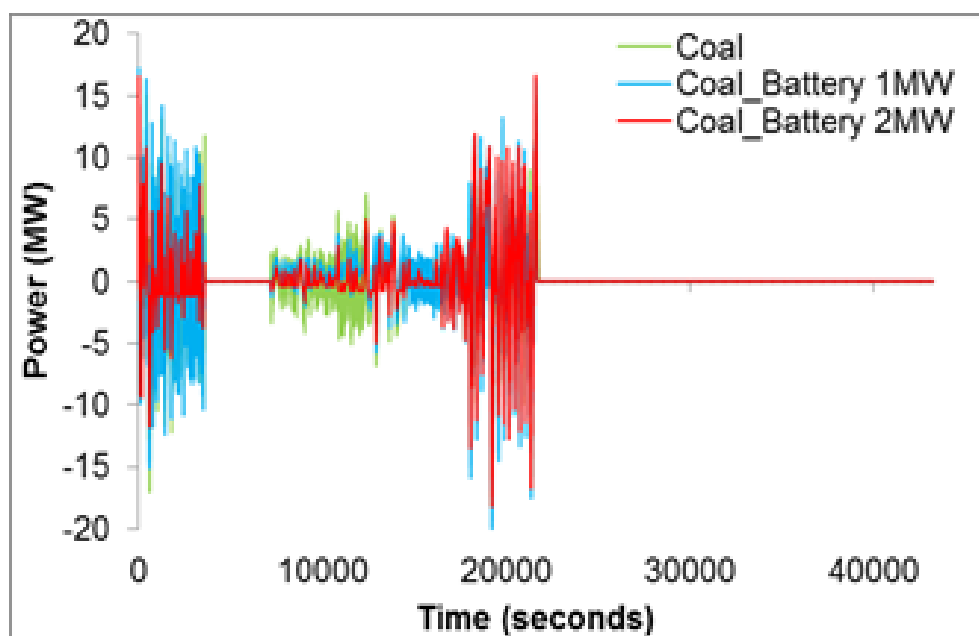
Figure 5.21 Coal unit movement for various cases
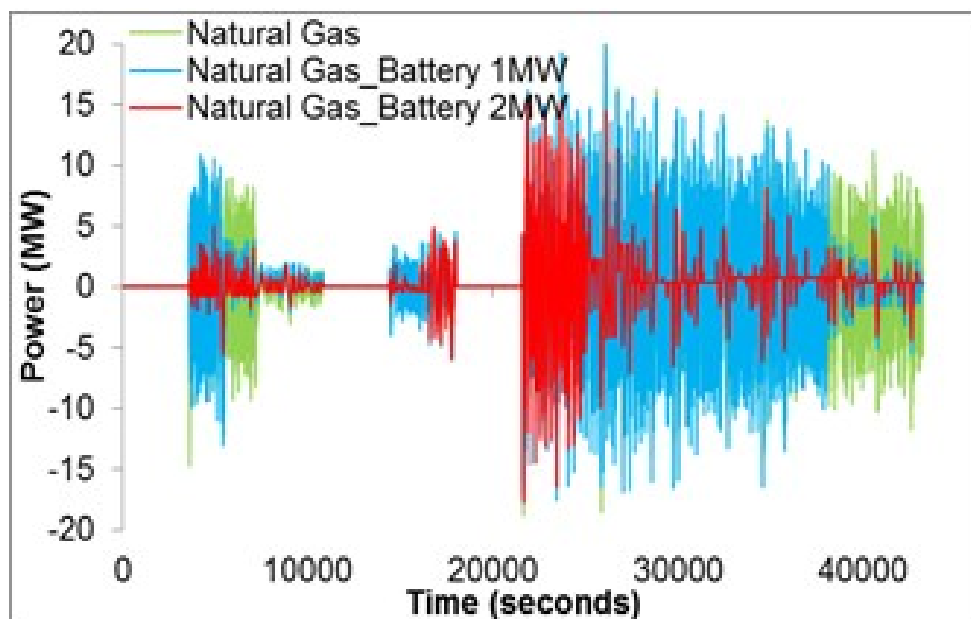
Figure 5.22 Natural gas unit movement for various cases

Table 5.3 shows the regulation in MW-hr expended from various units during the first 4 hours under case 1 and case 3. With the inclusion of 2MW battery, the total regulation supplied over the 4 hours decreases in case 3 by about 24.3 % compared to case 1. In case 3, the battery supplies about 37% of the total regulation required, while regulation from coal and natural gas units reduced by about 45% and 65% respectively. The reduction in coal and natural gas unit participation and hence the reduction in their cycling also has an impact on the overall system operating cost, CO_2, SO_2 and NO_x emissions, and also on the forced outage rates (FOR) and life of these conventional units that are not designed to cycle. The results shown are at 10% wind penetration. At higher wind penetration, the benefits from battery for frequency response and also for improving the health of the conventional units are highly pronounced and economically very valuable.

Table 5.2 Impact of Battery on Generation Miles-Wind Pen. 10%

Case	ACE miles (MW)	Coal Miles (MW)	Natural Gas Miles (MW)	Storage Miles (MW)
1	1533481.99	4022.91	13004.07	0
2	1299097.69 (-15.28)	3058.43 (-23.97)	10738.32 (-17.42)	2677.51
3	351546.9 (-77.08)	1633.36 (-59.40)	2933.50 (-77.44)	18089.44

Table 5.3 Impact on Hourly Regulation Deployments (MW-hr)-Wind Pen. 10%

Hour	Coal	Natural Gas	Total	Coal_Batt2MW	Natural Gas_Batt2MW	Battery 2MW	Total
1	3.89	0	3.89	2.35	0	1.04	3.38
2	0.08	3.44	3.52	0.002	1.00	0.68	1.68
3	1.04	0.72	1.76	0.45	0.44	0.72	1.61
4	2.02	0	2.02	1.07	0	0.72	1.79
Total	7.03	4.16	11.19	3.872 (-44.9%)	1.45 (-65.2%)	3.15	8.47 (-24.3%)

Decrease in regulation deployment also means there can be a decrease in regulation capacity allocation by AS market. As discussed in section 5.4.2, the hourly regulation requirements specified in SCUC-SCED is a function of net-load variability and additional capacity allocations (δ_{CPS}) to improve CPS standards as shown in (5.106). ERCOT allocates additional regulation by monitoring the CPS scores [75].

$$Reg(t) = fn(\Delta NL(t)) \pm \delta_{CPS} \tag{5.106}$$

Since these short-term storage devices improve the CPS even with lesser deployment of regulation service as observed in Table 5.3, this could lead to reduction in the total hourly regulation allocations and consequently the production cost. This is illustrated in Table 5.4 for higher wind penetration of 30%. Case 1 and Case 2 are two 48-hour generation dispatch scenarios, with Case 2 allocating 40% higher regulation over Case 1 and consequently resulting in increased production cost of about $10000 over 2 days. Table 5.4 also shows the 12-hour regulation deployment based on the regulation allocation decisions of production cost. We can observe that increased regulation allocation is useful in deploying more regulation (about 16.86 MW-hr, i.e., ~17.5%) to ensure increase in CPS1 measure, though still lesser than 0. While with a 1MW battery added to the SCED of Case 1 enables maintaining a good CPS-1 score even with same regulation deployment, thereby saving the requirement for additional 40% allocation of regulation services by production costing for betterment of CPS. This reduces regulation market MCPs and system production cost.

Table 5.4 Regulation and Generation Miles for 12 hours – Wind Pen. 30%

Case (48-hr Prod. cost M$)	Regulation (MW-hr)	ACE miles (MW)	Coal Miles (MW)	Natural Gas Miles (MW)	Storage Miles (MW)	CPS-I
1 (2.32)	96.09	1121483	14474	81934.11	0	-205.2
2 (2.33)	112.95	1312925	21643.15	90821.47	0	-107.4
1+Battery1MW	97.73	553531.3	12143.19	57112.54	8307.18	32.56

5.4.4   Comparison with Technologies

Table 5.5 shows the 12-hour AGC simulation results for various different technologies under 40% wind penetration. For $\epsilon=0.0342$ Hz, the CPS-1 measure is shown

for all the cases. While the 150% transmission expansion case reduces system production cost from about 2.37M$ in base case to about 2.16M$, it requires the support of faster ramping unit to enhance the CPS-1 score. In this case, transmission expansion alone increases coal cycling due to the exposure of cheap coal to more regulation services. The table also shows a 1MW battery to be performing almost 16 times the MW miles possible to be performed by a 1MW CT, and hence offers CPS-1 score on par with a 20MW CT which is about 44 times its investment cost. The CT operation in AGC is tantamount to CAES operation in generation mode. The total regulation deployment obtained from the 12 hour AGC simulation with 1MW battery is about 100.65 MW-hr, compared to about 125.98 MW-hr with 20MW CT to get a similar CPS-1 score. CAES with ramping characteristics similar to CT at the discharge side and with additional capability to provide regulation through charging operation at a higher rate (compressor) can be expected to provide slightly better performance in terms of improving CPS-1 score, however far short of short-term storage's ability.

Table 5.5 Technology Comparison - Wind Pen. 40%

Case	Investment (M$)	Coal Miles (MW)	NG Miles (MW)	CT/Batt Miles (MW)	CPS-I
Base	-	47265.50	36378.34	-	-651.87
CT 2MW	1.1	47467.98	36370.41	1046.54	-646.06
Trans.150%	82.6	58308.28	16137.38	-	-574.83
Batt-1MW	0.25	46043.61	33677.20	8684.21	-532.02
CT 20MW	11	47385.79	36214.21	10729.78	-507.33

5.5 SHORT-TERM STORAGE ECONOMIC ASSESSMENT

The technology adaptable model for short-term technologies with 5-minute SCED described in chapter 3 is used to investigate the participation, grid impacts and economic viability of short-term storages such as flywheel and battery under various wind penetration scenarios. It should be noted that the revenue estimation for short-term storages from production costing studies are based on the MCPs for regulation capacity. All the grid benefits discussed are also by virtue of capacity commitments of short-term storages in the AS market. However in order to evaluate the economics of short-term storage credibly, the integrated approach of production costing with AGC has to be taken as shown in Figure 5.2.

5.5.1   Integrated approach

From the discussions in previous section 5.4.3 that used the integrated approach, the economic implications of using short-term storage could be in terms of:

1. Reduction in regulation deployment

2. Reduction in conventional unit cycling

Table 5.6 shows the MCPs, the revenue that battery earns by supplying regulation and the savings due to decrease in regulation deployment in the first four hours. The table also estimates the reduction in cycling related costs in these hours, as a consequence of reduction in coal and NG unit deployments. According to the cycling studies done by APTECH [84, 85], the estimation of cycling costs related to load following (which include components such as heat-rate degradation, operation and maintenance costs, FOR and

upgrades) on an average for a coal and NG unit is about \$3.34/MW-hr and \$1.92/MW-hr respectively as shown in Table 4.1. According to Table 5.6, battery in this case promises a minimum of about \$97.5 (Reg + Cyc savings) savings in these first four hours by virtue of its performance, i.e., instantaneous response and frequent cycling. Aptech studies also quote higher values of these cycling costs, depending upon the specific characteristics of each unit studies and the ramp rates they are subjected to. These savings may further increase when the savings in emissions related to unsteady cycling operations are considered along with a suitable emission tax.

Table 5.6 Economic Implications of Battery in AGC

Hr	MCP (\$/MW-hr)	Batt2MW (\$)	Reg. Saving (\$)	Coal Cyc (\$)	NG Cyc (\$)
1	36	37.44	18.36	5.14	0
2	27	18.36	49.68	0.26	4.68
3	36	25.92	5.4	1.97	0.54
4	36	25.92	8.28	3.17	0
		107.64	81.72	10.55	5.22

NE-ISO proposes to pay for these short-term storages based on performance, i.e., the actual mileage a device provide [93]. *Pay by performance* values the quality of rapidly providing regulation by these short-term fast responding storages.

$$Mileage \text{ } \$ = (MW \text{ } miles)(CS)(MCP) \qquad (5.107)$$

where, the capacity-service ratio (CS) is the ratio of the MW capacity to the MW-miles a conventional regulation provider may perform within an hour.

In this chapter, we propose the following economic incentive for mileage performance of storage as expressed in (5.108), which will be credited to the hourly storage revenue.

$$Mileage\ \$ = \frac{(Storage\ MW\ miles)}{(Total\ Gen.\ MW\ miles)}(\$\ Saving) \tag{5.108}$$

The 2 MW battery, with an average of about 1507.45 MW-miles per hour (from Table 5.2), contributes about 79.8% of the total generation miles. Therefore, the additional revenue associated with the mileage-service over the first 4 hours will be about $77.8, i.e., 79.8% of the $97.5 estimated savings, thereby totaling the revenue in these hours to be $187.44. This impacts the payback period of the battery investment, and hence encourages penetration of such storage devices. For instance, based on economic evaluation a 2MW battery makes about $46.86/hr with payment for its performance, compared to about $26.91/hr normally. Estimating yearly revenues from this, a 2MW battery can breakeven its $500k investment in about 1.22 years with payment for performance compared to about 2.12 years otherwise.

5.5.2   Production costing study and estimated AGC information

In this section, short-term storages of various sizes are dispatched using high-fidelity dispatch model in grid at 5-minute intervals under various wind penetration, and for all the cases AGC study is not performed. Instead, information about such storage's services gained from previous AGC studies are used to add credibility to the production cost study results. This discussion will help learn what is important from these small time-scale studies that need to be imported into long-term studies; so that such technologies' economic

assessment can be done in a reasonable manner (if a full-fledged integrated approach is not possible).

The actual payment or storage revenues is subject to the duration for which the device is able to supply regulation service in each hour and the payment it receives for its performance (mileage payment), as discussed in section 5.5.1. As shown in Table 5.2, the 2MW battery performing almost 79.8% of MW miles earned additional revenue of about 72% of its revenue from deployed regulation. The 1 MW battery in Table 5.2 performing only about 16% of the MW miles is expected to earn lesser percentage of revenue for its mileage performance. PJM MCP data in early January 2013 shows the additional payment for performance ranges from about 5% to 120% of the payment made for regulation capacity. As far as the actual deployment of regulation service from short-term storage is concerned, it depends on:

i. ***Actual regulation deployed by AGC*** - The AGC simulations do indicate that typically about 15-20% of the regulation service allocated by SCED gets deployed.

ii. ***Fade time/Utilization Factor*** - Short-term storage will face fade time i.e., time when it cannot take any more charge due to hitting the maximum and minimum state of energy (when it hits the 100% or 0% energy capacity within every hour). Therefore the utilization factor (UF), which is defined as the ratio of average hourly energy delivered to its rated energy will be less than 100%. Studies do indicate a *UF* for flywheel of about 30% to 58% [43, 112]. From the AGC studies, we can estimate UF to be about 39% (2MW battery in Table 5.3)-64% (1MW battery in Table 5.4).

Assuming that the factor (i), i.e., the required regulation deployment in reality is high enough to be more than the short-term storage's capacity, UF factor (30-65%) and the additional mileage payment (16%-72%) must be taken into account appropriately in the forthcoming revenue/profit results reported based on 48-hour 5-min. SCED.

5.5.2.1 Wind penetration levels

In the system a flywheel storage of size 20MW and 50MW was included at bus 21 co-located with a wind farm. The system wind penetration level was increased and the production cost was observed. The wind penetration is the nameplate capacity penetration.

From Figure 5.23 we observe that when we include flywheel unit the production cost is reduced under all wind penetration levels for which regulation requirements increase. The production cost further reduces with increasing sizes of flywheel unit. For instance, at 60% wind penetration, 20MW flywheel reduces the yearly production cost by about $5.14M compared to its base case. However at lower wind penetration, beyond a storage size there is not much scope for grid to benefit.
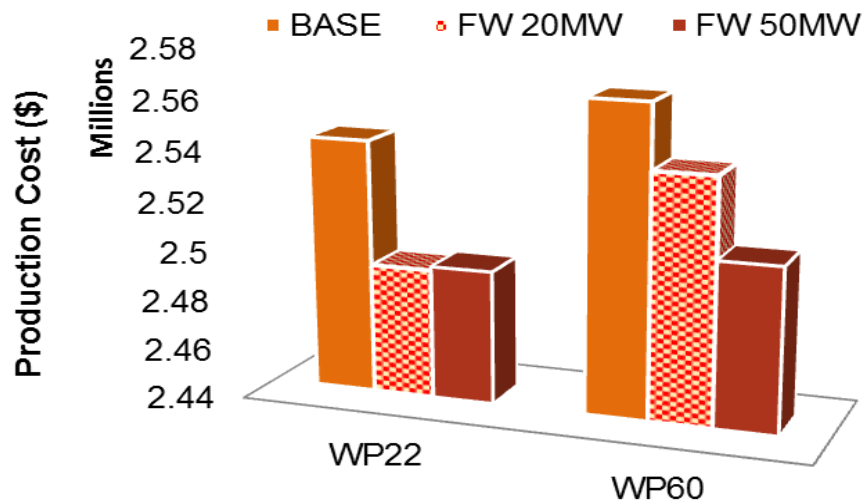
Figure 5.23 System production cost with flywheel in SCED

Flywheel storage has no fuel cost and is cheaper than all other generating technology with a regulation offer price of $ 2 /MW-hr. Thus when flywheel is added to the grid it replaces the expensive generating units to supply the regulation which is a pricey grid service. At times flywheel also is the marginal unit in the regulation market and sets a lower Market Clearing Price (MCP). These reasons justify the lowering of system production cost with flywheel.

Also, as discussed in section 5.4.3 with the help of Table 5.4, short-term storages do reduce system production cost by reducing the amount of regulation capacity procured by the market. A similar AGC study for these bigger sized short-term storages considered in Figure 5.23 will help us estimate the system frequency response and the CPS scores. Based on equation (5.8), the hourly regulation requirement (δ_{CPS}) can be reduced if the CPS is satisfactory and very high, and the system can afford to operate with a lower CPS with the support of short-term storage. This will help lower production costs, market prices and relieve some generation capacity from regulation market. *Implementation of this idea can be thought of as a feedback from AGC studies to the economic dispatch program in Figure 5.2, based on continued monitoring of the impact of short-term storage's services on CPS scores.* In this case, the CPS scores may be computed more frequently than usual intervals.

From Figure 5.24 we observe that under same wind penetration, the AS revenue earned by flywheel is more with higher size. However, how much more depends on the regulation requirement at a given wind penetration. For instance, at 22% the scope for a bigger flywheel of 50MW to earn from AS is less. A 20 MW flywheel is committed to deliver about 856.65MW-hr of regulation over 48 hours, while a 50MW flywheel is dispatched to deliver 1243.21MW-hr of regulation service. However when the wind

penetration is increased to 60%, we find that the 50MW flywheel is estimated to earn twice as much revenue compared to the 20 MW flywheel, since the required regulation amount is higher at 60 % wind penetration and a larger unit will benefit more. While the 20 MW flywheel is dispatched to deliver 887.77MW-hr of regulation, the 50 MW flywheel is dispatched to deliver 2202.48MW-hr.
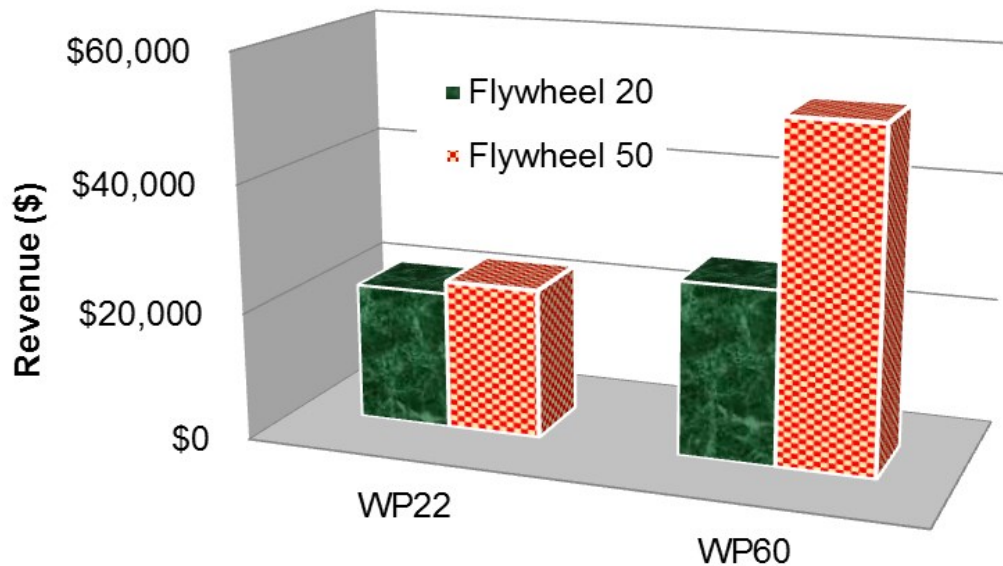
Figure 5.24 Flywheel AS revenue vs. wind penetration

These simulations indicated that wind spillage is not affected to any significant degree by the flywheel installments in the grid. This is because flywheel is a fast responding short-term storage aiding the grid to relieve minute-to-minute power deviations by supplying and absorbing short bursts of power, acting as a net-zero energy resource. They do not necessarily absorb spilled wind energy and retain it over time to deliver during peak periods like any bulk storage. A bigger size battery with sufficient storage capacity could perform such functionalities like reducing wind spillage similar to bulk energy storage.

In previous section the impact of battery operation on conventional unit cycling was studied, and the hourly benefits of cycling reduction were appropriately estimated and included within storage performance monetization. Here the potential to reduce cycling related costs of conventional units by virtue of short-term storage's capacity commitments in AS market are studied and quantified. Figure 5.25 shows that the cycling costs are significant under high wind penetration with higher regulation requirements. The inclusion of flywheels that are designed for cycling operation is able to relieve the conventional units from cycling stress incurred by providing regulation service. Thus greater the size of flywheel lesser the cycling cost at higher wind penetrations.
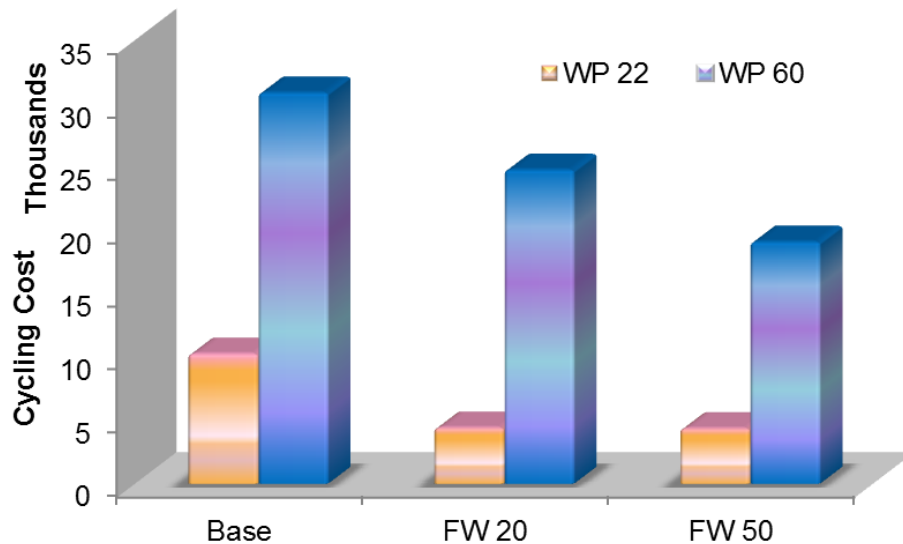
Figure 5.25 Impact on Conventional Unit Cycling Costs

5.5.3 Payback Assessment

In Table 5.7 the simple payback for flywheel unit of 20MW and 50MW at 22%, 40% and 60% wind penetration is given. The regulation offer times its regulation

commitment is considered as the operational cost of storage unit. The investment cost of $1630/KWh [113] ($407.5/kW) is assumed for the flywheel with 15-minute charging and discharging time ($T^{C/D}$). The AS revenue of the unit is estimated using the hourly MCPs obtained from the 5-minute production costing study over 48-hours. In estimating AS revenues from capacity commitments, UF of 50% was assumed and hence 50% of AS profit estimated from production costing study is used in payback calculation. Two payback periods were computed, one without mileage compensation and another with assumed mileage compensation worth 50% of original revenue subjected to UF (Note: AGC simulations are required to estimate actual mileage compensation).

From Table 5.7, as wind penetration increases the payback period reduces for short term storage. Flywheel of 50MW had a longer payback term compared to 20MW unit at lower wind penetration of 22%. However at 60% wind penetration the payback periods of 20MW and 50MW units are comparable. It is to be noted that beyond a certain wind penetration, the scope for a smaller flywheel to earn is limited by its size, however it continues to improve on its payback due to higher MCPs at higher wind penetration. With inclusion of payment for performance, the economics is sure to improve depending on the percentage of additional mileage based revenue the storage earns. In this case, with the assumption being 50%, the payback also improves by about 35%.

The table also shows results for a generic battery, where it has better economics than a flywheel of same size. The short-term battery's characteristics are same as flywheel except for a higher efficiency of about 90% compared to flywheel's 85% and lower investment cost of about $1000/KWh ($250/KW). Ofcourse, there are battery types at various investment cost levels and efficiencies, and accordingly the payback period will change. However, the

assumed cost of $250/KW is higher for many batteries such as NaS, Ni-Cd than what has been quoted in literatures [114], which also note a price decline in these technologies' investment cost. Most literatures quote an efficiency of around 80-85% for Li-ion and Ni-Cd, while promise higher efficiencies of more than 90% for NaS.

Table 5.7 Short-Term Storage Payback Assessment

PAYBACK	FW 20MW			FW 50MW		Batt 50MW
	WP 22	WP 40	WP 60	WP 22	WP 60	WP 60
Regulation Offer ($/MW-hr)	2	2	2	2	2	2
Investment Cost (M$)	8.15	8.15	8.15	20.375	20.375	12.5
Rating (MW-hr)	5	5	5	12.5	12.5	12.5
Regulation served (MW-hr)	856.65	887.73	887.77	1243.21	2202.48	2260.61
AS revenue (K$)	10.768	12.512	13.567	11.737	26.338	26.684
Yearly revenue (M$)	1.96	2.275	2.47	2.135	4.795	4.86
Yearly op. cost (M$)	0.155	0.16	0.16	0.225	0.4	0.41
Yearly profit (M$)	1.805	2.115	2.31	1.91	4.395	4.45
Payback (years)	4.52	3.85	3.53	10.67	4.64	2.81
Payback w/ Mileage$ (years)	2.93	2.51	2.29	6.84	2.99	1.82

If regulation offers of each conventional generation were reduced by $12.5, leading to lesser MCPs, then the project's payback will experience a setback. For instance, in such a case the average 24 hour MCP is about $13.5, with maximum being around $17.2 and minimum at about $7.25. For the 20MW flywheel at 40% wind penetration, the 48-hour AS profit is about $9K (about $3.5K lesser than the value in Table 5.7) and the payback years

will be about 6.89 years even with mileage payment and about 10.62 years without it. As seen in section 4.4, the economic implication of lower MCPs will be heavy for bigger storage projects than smaller owing to the investment costs.

5.5.4   Impact of Cycling Cost

As observed in Figure 5.25 with flywheels, the cycling related costs are reduced by fast responding battery of 50MW too at 60% wind penetration as shown in Figure 5.26, by virtue of reducing the allocation of conventional generation capacities for regulation services. On adding cycling cost component to the regulation offers of generators as discussed in section 4.3.2, it is seen that the cycling related costs are further decreased in the system as indicated by the bar corresponding to "Batt 50 Cyc". Figure 5.27 shows the system production cost under different scenarios. Clearly the addition of battery reduces the production costs by about $74K over 40 hours by lowering the regulation MCPs and also the cycling costs involved. However it is also seen that the increase in MCPs due to additional cycling component increases the overall production cost of the system by about $69.3K, while still lower than the base case production costs including cycling costs by about $4.7K over 48 hours.
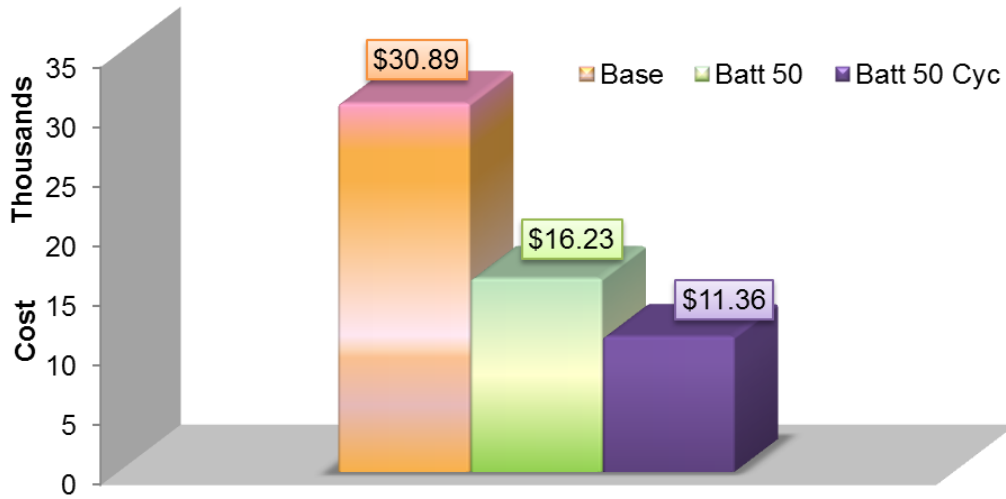
Figure 5.26 Cycling Costs with 50MW Battery at 60% Wind Penetration
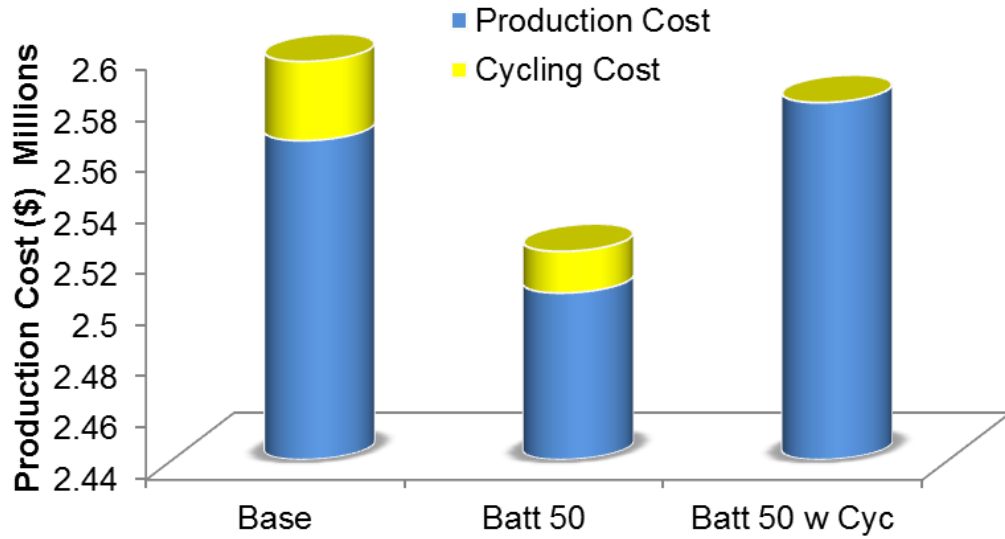
Figure 5.27 Production Cost at 60% Wind Penetration

However due to increase in MCPs of marginal units with cycling cost additions the battery earns higher revenue from AS market by about $27.8K as seen from Figure 5.28. The payback period is lesser by a year at about 1.79 years, and almost closer to the payback period with payment for its mileage performance. If the scenario is such that both the MCPs

are higher in market and mileage payment is awarded to the short-term storage, then the payback year is about 1.17 years (reduced by about 6 months).
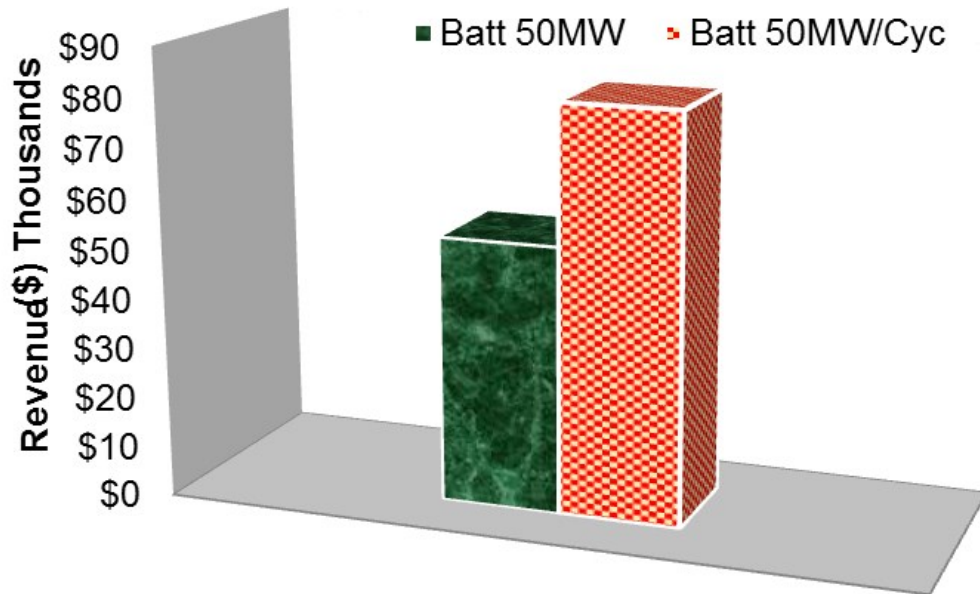
Figure 5.28 50MW Battery AS Revenue at 60% Wind Penetration

5.5.5   Regulation offers

There could be two reasons why the offers of short-term storages could be varied:

1. Short term storages are at a vantage position in the grid to get chosen in the balancing market due to its ability to ramp up faster to offset the power deviations at a lower offer. In the cost-based regulation offers, there is a component "margin adder" as explained in section 4.3 which allows the offerer to add a value (limited to a prescribed amount) to ensure the provider doesn't incur some miscellaneous losses while providing such unsteady services.

2. While short-term storages are made to cycle faster without much deterioration in operational cost and health, they could in some cases incur high maintenance

costs. Hence this is another scenario where genuinely the operational cost of a short-term storage may be higher, even if its investment cost is lower.

So in this section the analysis on storage revenues and payback is made by increasing its regulation offers, while keeping the O&M cost to original value for the first scenario above, and increasing the O&M cost too for the second case stated above. The flywheel offers were increased such that it remains the lowest bidding entity in the market, with offers of $10/MW-hr and $20/MW-hr, given that the original offer was $2/MW-hr.

Increase of offers slightly reduces regulation provision by flywheel, but however increases the revenues earned by it as shown by Figure 5.29. If the flywheel was not the marginal unit then there would not be any change in the AS revenues of the flywheel with change in the offers. But the increased revenues indicate flywheel being the marginal unit at certain hours, thereby setting a higher MCPs. This also increases the production cost as seen from Figure 5.30.
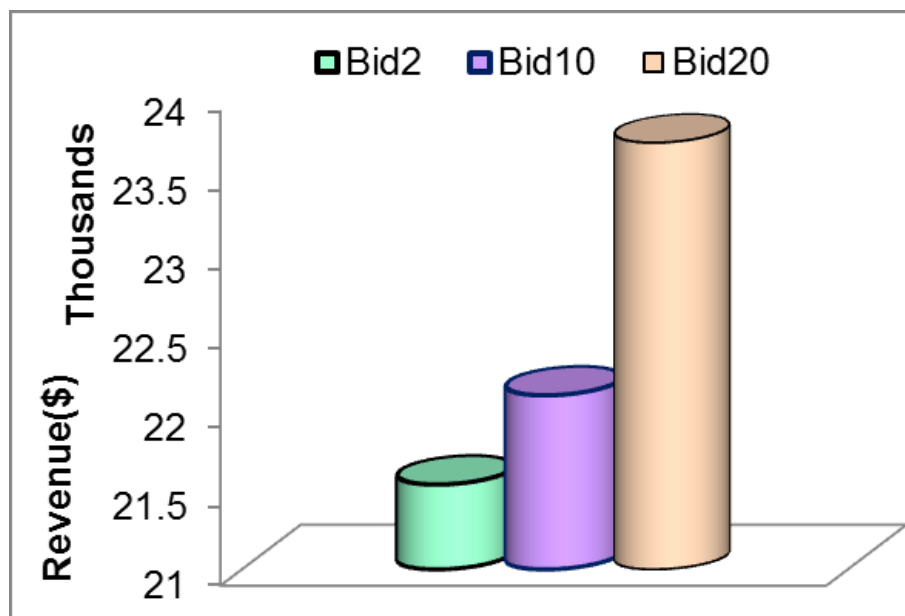
Figure 5.29 AS revenue vs. offers
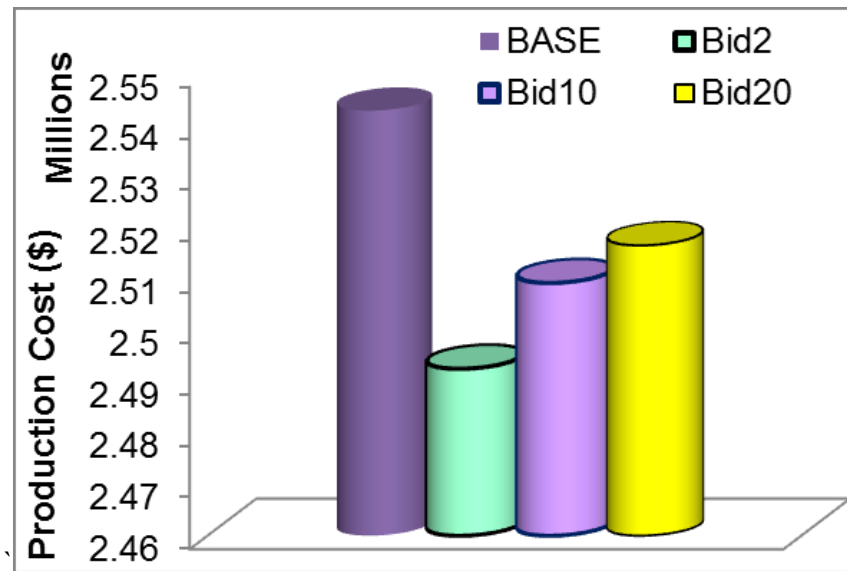
Figure 5.30 Production Cost vs. offers

Table 5.8 shows the sensitivity of payback period to storage regulation offers or in other words to different operational and maintenance costs of a same 20MW (5MWh) flywheel storage with same investment cost ($1630/KW-hr) and at same wind penetration level of 22%. If the increased offers are due to higher O&M costs incurred, then even though their higher revenues and production costs are justified, still their payback period increases due to high O&M cost. In this case, it is important for such short-term storage technologies to have a performance based payment in order to breakeven with the investment at reasonable time of about 4.5 years. By simply increasing the offer for making profit, even though the O&M costs are less, the storage will breakeven at around 4 years at the expense of system production costs.

Table 5.8 Short-Term Storage Payback sensitivity to Offers

PAYBACK	*FW 20MW @ WP 22%- Operational Cost*			*Strategic*
	Offer 2	**Offer 10**	**Offer 20**	**Offer 20**
Investment Cost (M$)	8.15	8.15	8.15	8.15
Regulation served (MW-hr)	856.65	798.84	773.07	773.07
AS Revenue (K$)	10.768	11.05	11.849	11.849
Yearly AS Revenue (M$)	1.96	2.01	2.155	2.155
Yearly operational cost (M$)	0.155	0.725	1.405	0.155
Yearly profit (M$)	1.805	1.285	0.75	2
Payback (years)	4.52	6.34	10.87	**4.075**
Payback w/ Mileage$ (years)	2.93	3.56	**4.46**	2.65

5.6 OTHER APPLICATIONS OF STATE SPACE MODELS

The state-space model of CAES presented in earlier section captured the essential dynamics of its storage reservoir related to mass flow rates in and out of the reservoir and reservoir internal pressure. These two parameters bear direct effect on the storage reservoir power intake and output. Such a state-space model is helpful in understanding the limiting factors associated with different storage technologies' reservoir capacity, in this case CAES. These smaller time-scale models help in ascribing economic value to storage's ability to flex its energy capacity by virtue of gaining control over the actual subtle limiting factors.

Since the successful demonstration of Huntorf CAES plant in 1978, there has been several dedicated efforts [115, 116, 117, 118] to design CAES model representing its detailed thermodynamic cycle. Such models enabled performing techno-economical and performance analysis, and advancing the technology. However such detailed CAES models may be too involved and prove to be a bottleneck to conduct a grid level long term simulations for planning purposes. The state space model can be simplified by assuming steady state versions of the compressor and gas turbine operations (as discussed under reservoir modeling in section 5.3.1 using equations (5.78) and (5.80)), thereby resulting in a model that simulates within reasonable time and yet enables capturing realistic reservoir operational phenomena for assessing the performance.

The developed simplified model was used as a plug-and-play module for representing storage unit within a hybrid-wind technology to devise a solution strategy to address wind farm's long-term and short-term variability (results reported in "*Hybrid Wind Systems: Design, Operation and Control*" project report submitted to DOE) [119, 120]. This section further presents another application, where performance assessment of CAES connected to a stand-alone wind-farm is performed using the developed state-space model. The sub-sections define a number of performance and economic indices that can be computed using a one year simulation of CAES plant. These can be used as criteria to evaluate the worth of different CAES configurations.

5.6.1 Performance indices

5.6.1.1 Charging time

Charging time, T_{Charge}, is defined as the time taken to charge the storage reservoir to its full capacity within the maximum pressure limit. It depends on the reservoir volume and compressor rating, and is expressed in hours

5.6.1.2 Discharging time

Discharging time, $T_{Discharge}$, is defined as the time taken to discharge the storage reservoir from its full capacity (at maximum pressure limit) to minimum pressure limit. It depends on the reservoir volume and turbine rating, and is expressed in hours.

5.6.1.3 Demand met

This is defined as the percentage of power demand requested on the CAES turbine side that is generated by CAES respecting its charge level and pressure limits.

$$P_d = \frac{\sum\limits_{t=1}^{8760} P_G{}^t}{\sum\limits_{t=1}^{8760} P_D{}^t} *100 \qquad (5.109)$$

where P_d is the CAES demand met in % and $P_D{}^t$ is the power demand requested from CAES at hour t.

5.6.1.4 Spillage

This is defined as the percentage of available wind power input into CAES compressor side spilled due to insufficient reservoir space or pressure limit hits.

$$P_{spillage} = \frac{\sum_{t=1}^{8760} \left(P_{in}^{\,t} - P_C^{\,t}\right)}{\sum_{t=1}^{8760} P_{in}^{\,t}} * 100 \tag{5.110}$$

where $P_{spillage}$ is the CAES input power spilled in %, $P_{in}^{\,t}$ is the power input command into CAES at hour t.

5.6.1.5 Carbon emissions

Traditionally reserves are fossil fuel units, and in this case we assume them as coal units. When the CAES facility is unable to meet the demand, it is supplied by such reserve units. Thus the cumulative carbon emissions from the natural gas turbine of CAES and the coal unit are calculated. This index also serves to quantify the advantages of CAES.

$$CE = \sum_{t=1}^{8760} E_{NG} \times P_G^{\,t} + E_{Coal} \times (P_D^{\,t} - P_G^{\,t}) \tag{5.111}$$

where CE is the carbon emissions from CAES and coal unit in tons/year, E_{NG} and E_{Coal} are the carbon emissions from natural gas unit and from coal unit in tons/kWh.

5.6.2 Economic indices

According to the current market policies, some of the avenues that bear significant impact on CAES economics and revenue would be energy arbitrage, charging cost, frequency regulation, spinning reserves, installed capacity, market revenues (ICAP), system upgrade cost deferral, and environmental impacts [121, 122]. For instance, revenue from energy arbitrage will be drawn by strategically charging and discharging CAES in order to take advantage of the differences in peak-load and off-peak load prices. This means that the decision on CAES configuration will also depend on the application. For higher energy

arbitrage, a CAES configuration with higher power density is suitable. In the case of revenue opportunity from frequency regulation, there is a great potential if CAES responds appropriately to ISO regulation signals. Then it stands a chance to be paid for both charging and discharging. Optimal placement of CAES in the system could possibly defer transmission and distribution upgrade costs, generating benefits of about 0.15- 1 M$/MW-year [123].

In this section, we have defined some traditional as well explorative economic indices, which can be used to evaluate the economic value of CAES. Some of the indices are defined in relation to CAES operating with a collocated wind farm.

5.6.2.1 CAES cost

Investment cost of CAES is the combination of investment costs required for turbine, compressor and reservoir. The turbine rating translates into power rating of the CAES, and reservoir rating translates into the energy rating of the CAES.

$$C_{INV} = P_{Tur} \times C_T + P_{CR} \times C_C + E_{Rated} \times S_C \qquad (5.112)$$

$$E_{Rated} = P_{Tur} \times T_{Discharge} \qquad (5.113)$$

where C_{INV} is the investment cost of CAES in \$/kW, P_{Tur} is the turbine power rating in MW, P_{CR} is the compressor power rating in MW, C_T is the turbine cost in \$/kW, C_C is the compressor cost in \$/kW, E_{Rated} is the energy rating of CAES in kWh, S_C is the CAES storage capacity cost in \$/kWh, $T_{Discharge}$ is the discharge time of reservoir in hours.

Since $T_{Discharge}$ is a function of reservoir volume, it reflects the reservoir investment. For a particular turbine rating and pressure limit, higher the reservoir capacity higher is the discharge time.

5.6.2.2 Operational cost of CAES

CAES consumes natural gas in the process of generation of electricity. The cost associated with fuel consumption and operation & maintenance over a year is calculated as operational cost per year.

$$C_{OP} = HR \times \sum_{t=1}^{8760} P_G{}^t \times C_{NG}{}^t + P_{Tur} \times C_{FOM} \tag{5.114}$$

where C_{OP} is the operational cost in $/year, P_G is the power generated by CAES in MW at hour t, HR is the CAES heat rate in MBtu/MWh, C_{NG} is the natural gas price in $/MBtu at hour t, and C_{FOM} is the annual fixed operation & maintenance cost of CAES in $/kW.

5.6.2.3 Operational revenue from CAES

The hourly electricity prices (LMPs) over a year are used to compute the operational revenue.

$$C_R = \sum_{t=1}^{8760} P_G{}^t \times E_h{}^t \tag{5.115}$$

where C_R is the operational revenue from CAES in $/year, E_h is the hourly electricity prices in $/kWh.

5.6.2.4 Production Tax Credit (PTC)

This is a business credit to the wind farm owner and is equivalent to the electricity generated from the facility. This typically applies for the first 10 years of the wind plant operation. If the CAES facility is collocated with the wind farm, then more electricity is generated by the wind facility with CAES's support. This increases the tax credits.

$$PTC_{CAES} = \sum_{t=1}^{8760} P_G{}^t \times T_{PTC} \tag{5.116}$$

where PTC$_{CAES}$ is the production tax credit through CAES in \$, T$_{PTC}$ is the tax credit in \$/kWh.

5.6.2.5 Revenue opportunity lost due to wind spillage

We propose a new index to quantify the spillage defined above as an equivalent loss in revenue opportunity, i.e., if there was an opportunity to store the spilled power and sell it at yearly average spot price. This could be used to strike a comparison between many CAES configurations.

$$S_{orl} = \eta \times EP \times \sum_{t=1}^{8760} (P_{in}^{t} - P_{c}^{t}) \tag{5.117}$$

where S$_{orl}$ is the spillage opportunity revenue loss in \$/year, η is the round trip efficiency of CAES, EP is the average electricity price \$/kWh.

5.6.2.6 Credit from reserve saved

Assuming the energy supplied by CAES to the system is typically obtained from reserves, in the presence of CAES facility the reserve required by the system is reduced, which could contribute to the yearly credits.

$$RC = \sum_{t=1}^{8760} P_{G}^{t} \times R_{p}^{t} \tag{5.118}$$

where RC is the reserve credits due to CAES in \$/year, R$_p$ is the hourly reserve price in \$/kWh.

5.6.2.7 Credits due to carbon tax reduced

In the same manner as the carbon emissions, the carbon tax is calculated. With CAES, we can expect reduction in this tax.

$$CT = \sum_{t=1}^{8760} P_G{}^t \times (T_{Coal} - T_{NG}) \qquad (5.119)$$

where CT is the carbon tax credit due to CAES in \$/year, T_{NG} is the carbon tax for natural gas unit in \$/kWh, T_{Coal} is the carbon tax for coal unit in \$/kWh.

5.6.2.8 Payback Period for CAES

It is defined as the number of years required to recover the invested amount on CAES facility through revenues. It can be computed by solving the below cost balance equation,

$$C_{INV} + C_{OP}.\sum_{n=0}^{N} \frac{1}{(1+r)^n} = NR.\sum_{n=0}^{N} \frac{1}{(1+r)^n} + 10 \times PTC_{CAES} \qquad (5.120)$$

$$\sum_{n=0}^{N} \frac{1}{(1+r)^n} = \left(C_{INV} - 10 \times PTC_{CAES}\right) \Big/ \left(NR - C_{OP}\right) \qquad (5.121)$$

where n is the payback period, r is the rate of interest, and NR is the net revenue per year given by $C_R + RC + CT$.

If the CAES is not collocated with wind farm during the first 10 years of wind farm operation, then the above equations will not include the PTC_{CAES} term. So it is treated separately from the net revenue per year term in the above equation.

5.6.3 Numerical Results

5.6.3.1 Study Description

This model can be run to simulate and analyze a stand-alone CAES or CAES collocated with wind-farm scenario. To illustrate the functionality and features of this model we have designed the CAES facility to be co-located in a wind farm. This study would

demonstrate how CAES mitigates the wind variability, increases the capacity factor, benefits environment and also generates excess revenue opportunities for the wind farm owners. It can also act as a spinning reserve to the grid.

The wind data was taken from the EWITS 2006 database for site# 2302. Figure 5.31 shows the mismatch between the forecasted and observed wind power data for this site.
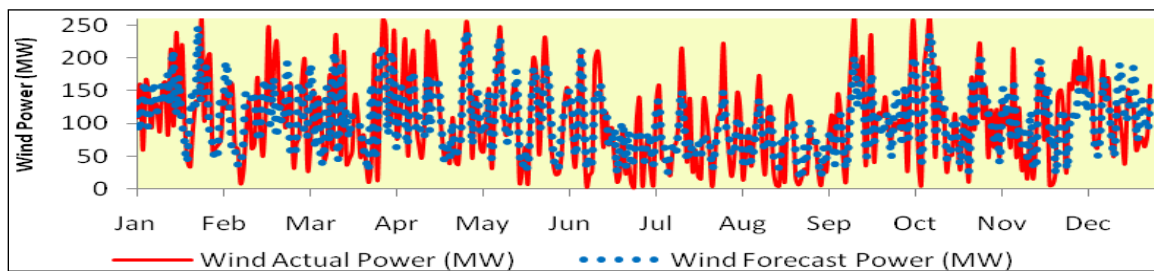
Figure 5.31 Wind mismatch

The CAES was operated in load leveling mode, i.e., it functions to smooth the wind farm output. The wind forecast power was assumed to be the scheduled wind power W_{sch}, and the difference between wind forecast and actual wind power (W_a) was sent to the CAES model. Since, the CAES was operated in wind-farm output smoothing mode, if $W_a > W_{sch}$, the excess wind output was sent to compressor (P_{in}) to store equivalent mass of air in the CAES storage reservoir. Similarly, if $W_a < W_{sch}$, then CAES was requested to generate (P_D) the required deficit. Therefore,

If $W_a > W_{sch}$, Then $P_{in} = W_a - W_{sch}$ 　　　　　　　　　　　　　(5.122)

If $W_a < W_{sch}$, Then $P_D = W_{sch} - W_a$ 　　　　　　　　　　　　　(5.123)

The CAES model was simulated in Matlab Simulink for a total of 8760 hours (1 year) using the variable time step solver ode23s. One year simulation, took about 10 minutes to complete in the load-leveling mode.

5.6.3.2 Simulation Results for 220 MW CAES

The peak input and demand to the CAES from the wind farm over a year was found to be about 200 MW and 220 MW respectively. So CAES configuration chosen for this study consists of 220MW turbine, 200MW compressor and 150,000m³ storage reservoir volume. Table 5.9 [39, 108, 124, 125] presents the constants and assumptions used for CAES simulation and evaluation. References [124, 126] provide hourly electricity and gas prices.

Table 5.9 Constants and Assumptions

Constants	Values	Constants	Values
c_{P1}	1.055 kJ/kg K	C_T	200 \$/kW
P_2/P_1	69	C_C	150 \$/kW
T_{in}	298.15 K	C_{FOM}	32.6 \$/kW
γ	1.3	S_C	40 \$/kW
c_{P2}	1.009 kJ/kg K	HR	3.8 MBtu/MWh
$\dot{m}_{CT}/\dot{m}_{fuel}$	0.25	T_{PTC}	0.021 \$/kWh
		R	287.058 Jkg^{-1} K^{-1}
T_1	823.15 K	H	70 %
T_2	1098.15 K	EP	46.14 \$/kWh
P_1	42 bar	E_{NG}	0.181 kg/kWh
P_2	11 bar	E_{Coal}	0.333 kg/kWh
P_b	1 bar	T_{NG}	0.0066 \$/kWh
η_M	48 %	T_{Coal}	0.0121 \$/kWh
η_G	99 %	R	1%

The CAES facility was fully charged in 8.629 hours and discharged in 4.154 hours. Thus the charge ratio is about 1:2. Figure 5.32 (a) shows the wind power spillage off the wind farm that was input into the CAES compressor side for storage. During this week of Jan 8-15, CAES had enough storage volume and never hit its maximum pressure limit of 70 bar as shown in Figure 5.32 (c), and hence all the wind spilled has been effectively compressed and saved. But during other periods of the simulation due to upper pressure limit hits, CAES had failed to fully compress the available wind power at the input and thus spilled the wind power. For a given pressure limits, compressor size, the rate of charging and the reservoir volume plays critical role in deciding CAES's storage ability.

Figure 5.32 (b) shows the power generated by CAES according to the power requested from CAES during the same week, in order to meet the wind farm scheduled power. It can be noticed that CAES does not supply the requested power demand all the time. There have been many occasions when the lower operational pressure limit of 13 bar was hit and there was no CAES generation at those times. In Figure 5.32 (b), we observe that there are failures to meet the demand on Jan 8th, 11th and 13th due to pressure constraints; even though some stored mass is observed in the reservoir at those times as shown in Figure 5.32(d). The simulation model takes into account these operational phenomena, and hence provides realistic opportunity to evaluate the dispatch strategy, operational performance, economic benefits associated with CAES.
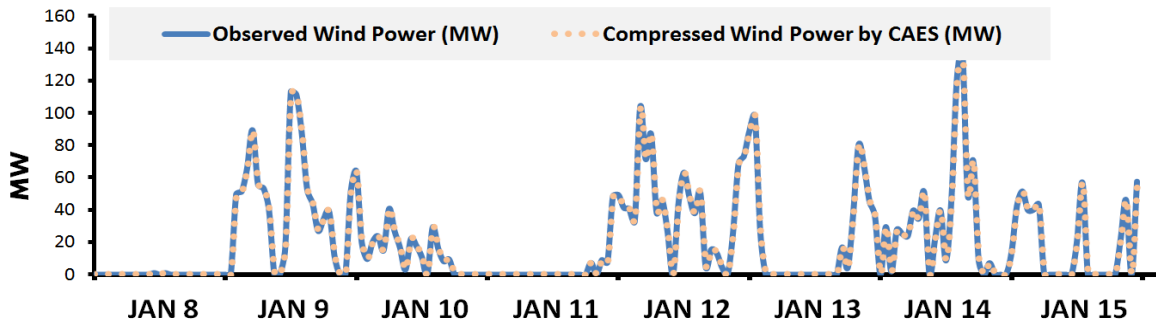
(a) CAES power input and wind spillage saved
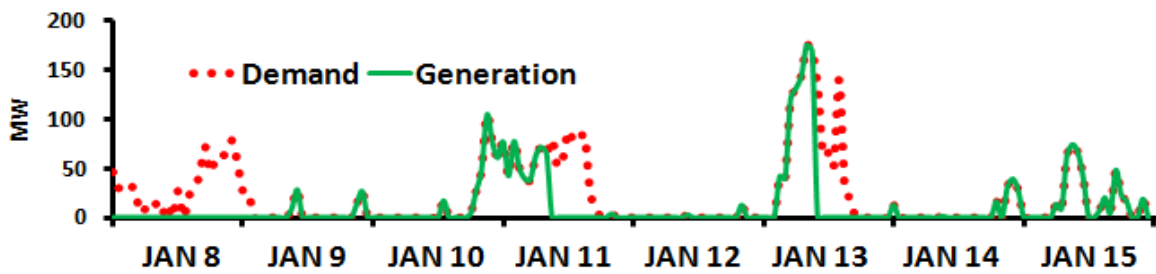
(b) CAES power generation and power requested
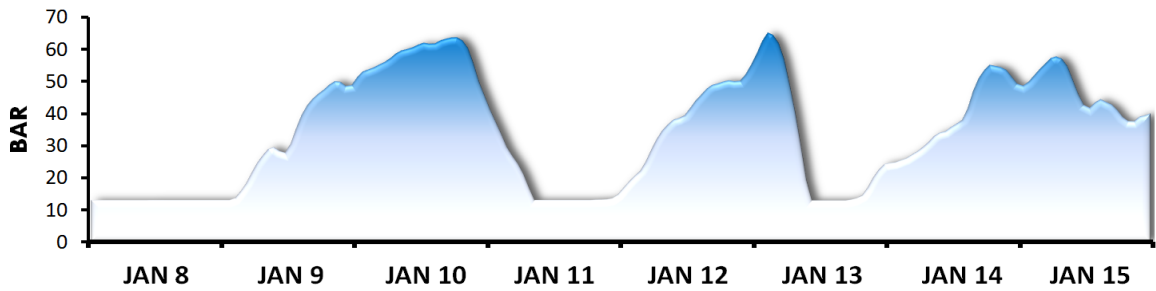
(c) Pressure of the CAES Reservoir
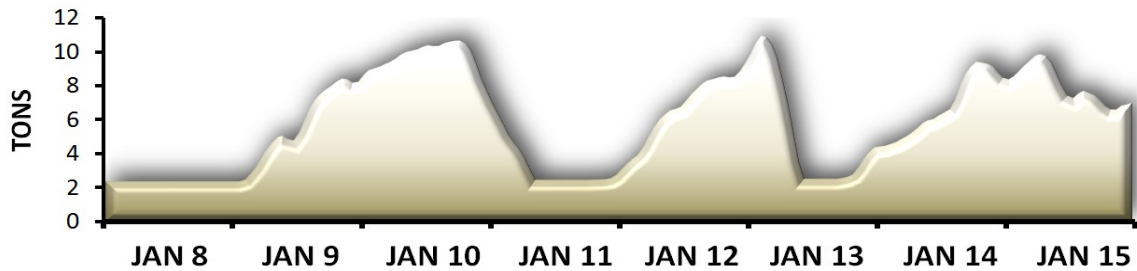
(d) Stored mass of the CAES Reservoir

Figure 5.32 Simulation results for the CAES Model: week of Jan 8-15

Table 5.10 summarizes some of the operational benefits of using a CAES facility with wind farm. The wind farm spills about 188.12 GW of power over a year's operation, and requires about 186.97GW of power from reserves to meet its scheduled power. With the introduction of CAES, only 27.23% of 188.12GW power is spilled and the rest is compressed by CAES. CAES supplies 48.33% of 186.97GW power required by wind farm, operating within its allowable pressure range throughout the year. The remaining 51.17% (96.6GW) is supplied from reserves, as shown in Table 5.10. Considering spinning reserve prices for an year, the 90GW of reserves saved will amount to a savings of 0.585M$ per year.

Since CAES reduces the reserves required from conventional generators, we can observe that the carbon emissions and carbon tax with CAES are reduced by 22%. With CAES, the capacity factor of the wind farm is increased to 0.4003 from 0.3644, as shown in Table 5.10. Thus this CAES facility provides a viable solution to the wind variability.

Table 5.10 Operational Benefits of CAES

Operational factors	Without CAES	With CAES
Demand supplied by reserve (GW)	186.97	96.6
Carbon emissions (tons/year)	62262	48527
Carbon tax (M$/year)	2.262	1.765
Capacity factor	0.3644	0.4003

Table 5.11 summarizes the economics involved with this CAES facility. Under the assumptions of cost and interest rate as shown in Table 5.9, the credits from reduced carbon

tax and reserves due to CAES facility amount to a total of 1.088M$ per year. Accounting for all the revenues as per their net present value, the payback period comes to about 84 years.

Table 5.11 Economic Evaluation of CAES

Item	Value (M$)
Investment cost	115.09
Operational cost per year	3.44
Operational revenue per year	4.03
Carbon tax credit per year	0.502
Reserve credit per year	0.586
Production tax credit per year	1.89
Payback period (years)	84

5.6.3.3 Effect of CAES sizing on economics and performance

The results of another simulation study to ascertain the impact of CAES sizing on its overall performance and cost are shown in Table 5.12. The turbine power rating is sized to 50 MW, which is a reasonable design modification considering average power demanded from the CAES throughout the year to be less than 50 MW. From this simulation, we can infer that changing even one parameter of CAES design leads to significant influence in the performance and cost of the CAES.

Table 5.12 CAES Configuration Comparison

CAES Turbine Rating	220 MW	50 MW
Charging time (hours)	8.629	8.629
Discharging time (hours)	4.154	18.371
Wind spillage (%)	27.23	28.57
Demand met by CAES (%)	48.33	47.25
Demand supplied by reserve (GW)	96.6	98.6
Carbon emissions (tons)	48527	48834
Carbon tax (M$/year)	1.765	1.77
Capacity factor	0.4003	0.399
Investment cost (M$)	115.09	77.50
Operational cost per year	3.44	2.07
Operational revenue per year	4.03	4.0
Carbon tax credit per year	0.502	0.492
Reserve credit per year	0.586	0.571
Production tax credit per year	1.89	1.85
Payback period (years)	84	22

Table 5.13 provides a spreadsheet analysis of various CAES configurations showing their impact on operational and economical indices obtained from simulation. The CAES model developed is able to capture the influence of storage reservoir dynamics on performance measures such as demand met and input spillage percentage.
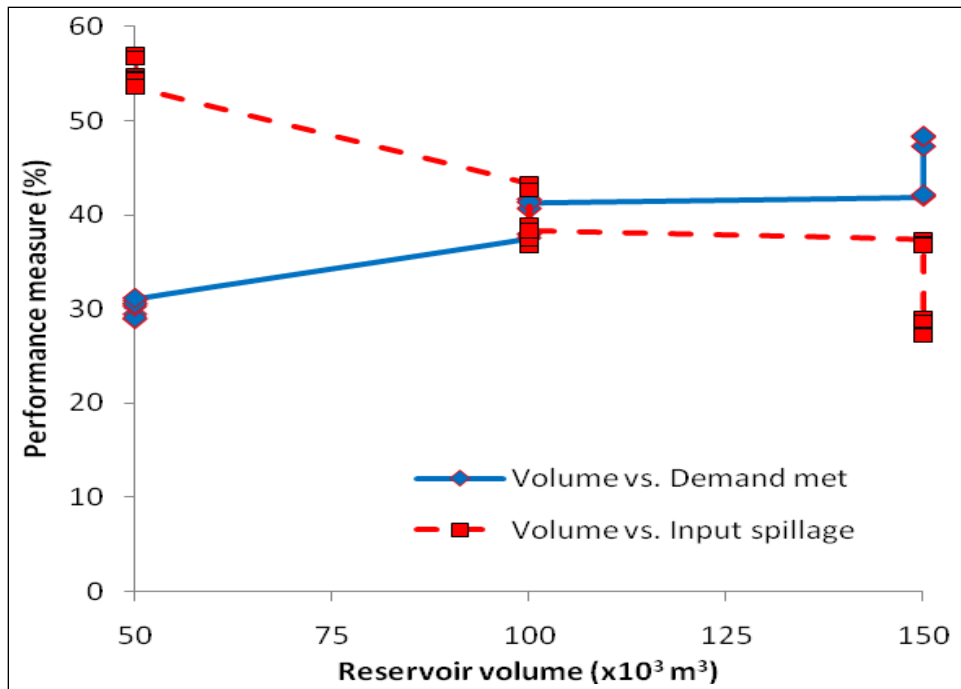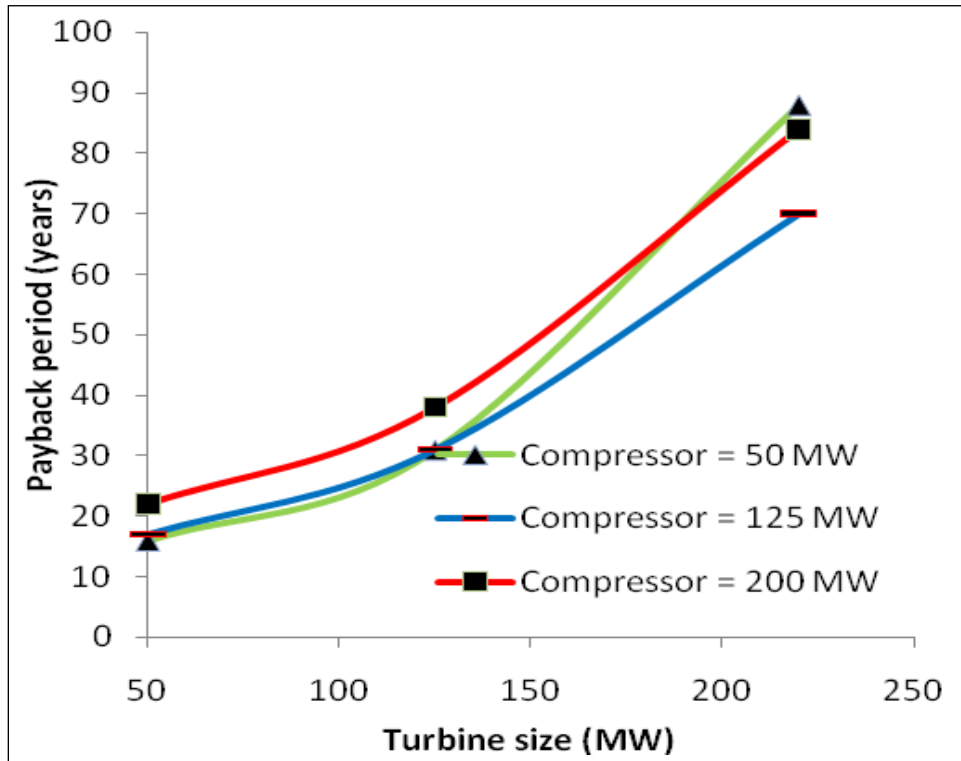
Figure 5.33 CAES reservoir volume vs. Performance

Figure 5.34 Payback period vs. Compressor/turbine sizing, Volume = 150000 m^3

www.manaraa.com

From Figure 5.33, it is seen that irrespective of turbine and compressor sizing, a good enough reservoir volume is required to ensure effective addressing of wind variability issues by CAES for this particular wind farm. However from Figure 5.34, we can infer that for a particular reservoir volume, significant operational and economic benefit is achieved by suitably sizing turbine and compressor.

Considering only economics, configuration#1 in Table 5.13 could be favored. Considering performance measures such as discharge capacity along with economics, configuration#22 with increased investment in compressor and storage reservoir could be favored.

Table 5.13 CAES Performance with different Compressor, Turbine and Reservoir Ratings

Case #	Compressor	Turbine	Volume	Charging time	Discharging time	CAES Cost	NR per year	Payback period	Demand met	Input Spillage	CO_2 emission	Capacity factor
	MW	MW	X 10^3 m^3	hours	hours	M$	M$	years	%	%	tons/yr	
1	50	50	50	11.028	6.722	30.944	1.711	12	28.88	57.05	54056	0.385
2	50	125	50	11.028	3.111	48.055	1.176	>25	29.41	56.64	53905	0.386
3	50	220	50	11.028	2.007	69.1616	0.393	>25	29.03	56.68	54013	0.386
4	125	50	50	4.411	6.833	42.4166	1.81	19	30.24	54.76	53670	0.387
5	125	125	50	4.411	3.111	59.305	1.273	>25	30.48	54.45	53601	0.387
6	125	220	50	4.411	2.007	80.4116	0.572	>25	31.1	53.55	53425	0.387
7	200	50	50	2.757	6.822	53.644	1.858	25	30.82	54.02	53503	0.387
8	200	125	50	2.757	3.111	70.555	1.281	>25	30.55	54.41	53582	0.387
9	200	220	50	2.757	2.007	91.6616	0.566	>25	31.11	53.6	53423	0.387
10	50	50	100	22.056	12.706	42.9112	2.307	13	37.53	43.32	51597	0.392
11	50	125	100	22.056	5.436	59.6805	1.794	>25	37.94	42.65	51480	0.392
12	50	220	100	22.056	3.306	80.58928	1.053	>25	37.9	42.63	51493	0.392
13	125	50	100	8.827	12.861	54.4722	2.503	17	40.6	36.66	50721	0.394
14	125	125	100	8.827	5.528	71.389	1.996	>25	41.57	37.53	50448	0.395
15	125	220	100	8.827	3.376	92.46232	1.264	>25	41.64	37.47	50430	0.395
16	200	50	100	5.513	12.401	64.8028	2.511	22	40.69	38.93	50697	0.394
17	200	125	100	5.513	5.057	80.2845	1.971	>25	41.32	38.42	50521	0.395
18	200	220	100	5.513	2.918	99.6784	1.261	>25	41.32	38.33	50521	0.395
19	50	50	150	33.083	18.753	55.0056	2.599	16	41.9	37.38	50355	0.395
20	50	125	150	33.083	7.833	71.6665	2.051	>25	42.08	36.9	50303	0.395
21	50	220	150	33.083	4.669	92.59072	1.309	>25	42.12	36.75	50292	0.395
22	125	50	150	14.555	19.028	66.2556	2.993	17	47.26	29.01	48831	0.399
23	125	125	150	14.555	8.167	82.9165	2.414	>25	48.26	27.68	48547	0.4
24	125	220	150	14.555	5.056	103.84072	1.681	>25	48.36	27.76	48518	0.4
25	200	50	150	8.629	18.371	77.5056	2.992	22	47.25	28.57	48834	0.399
26	200	125	150	8.629	7.379	94.1665	2.404	>25	48.23	27.31	48557	0.4
27	200	220	150	8.629	4.154	115.09072	1.682	>25	48.33	27.23	48527	0.4

5.6.3.4 Effect of pressure limits on economics and performance

Figure 5.35 shows the effect of maximum pressure limit on revenue and performance for the configuration#22. We can notice that as the maximum pressure limit increases, the revenue per year and the operational performance measures too increase. So it corroborates the model's ability to account for internal storage dynamics and their direct influence on CAES operational and economic outcome.

Relaxing CAES unit's energy capacities within dispatch studies based on its internal reservoir status updated every 5-mins. can enable investigating the economic incentives in making short and timely excursions over its pressure limits, rather than just keeping the limits constant in the dispatch studies.
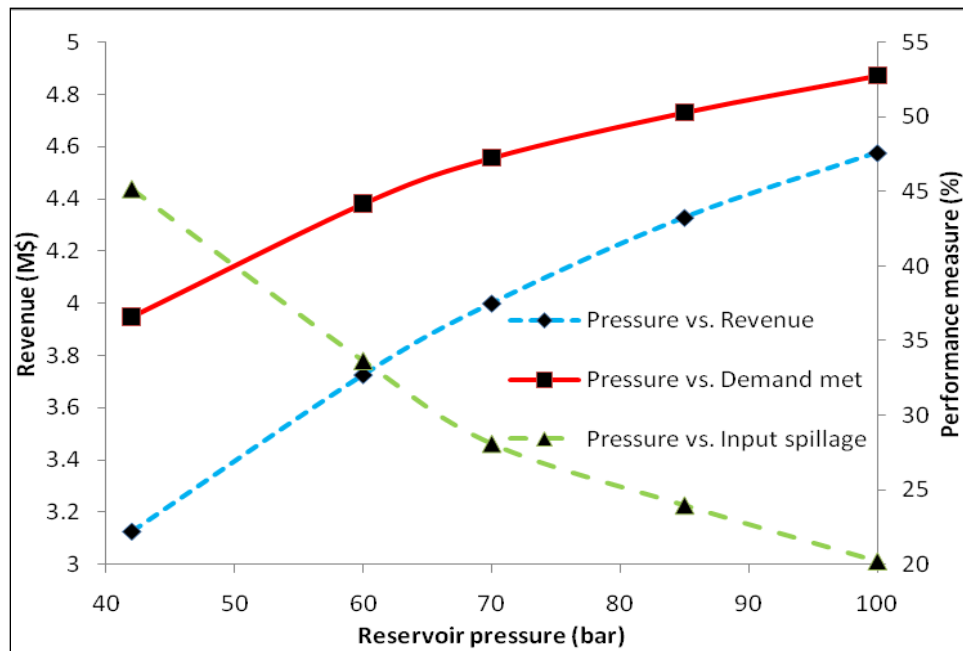
Figure 5.35 Effect of maximum pressure limit on revenue and performance

5.7 CONCLUSION

An assessment framework to evaluate the benefits and economics of short-term storage devices is presented in this chapter. The chapter discusses the state space representation of slow dynamics model of IEEE 24 bus system, and storage technologies. The short-term storages are dispatched using the real-time 5-min SCED program and subsequently the AGC simulation is run.

The impact of short-term fast responding storage on frequency response of the system is assessed using AGC simulation. AGC model of single area IEEE 24 bus RTS system is used, and battery storage is integrated. The impact of increasing wind penetrations in AGC study is modeled in terms of increasing net-load variations and consequently the increased regulation requirements, and the decrease in the system inertia as a function of hourly dispatch decisions.

The integration of short-term storage in production costing tool enables assessing the impact of such devise's capacity commitments on dispatch decisions, MCPs, and production costs. Modeling short-term storage within such resource allocation tools will also enable accommodating such devices within the future generation portfolio. However the chapter recommends importing valuable information about the short-term storage's services from small-time scale studies such as AGC into such planning tools in order to make the assessment and conclusions credible. The chapter demonstrates assessment of such storage devices of various capacities under different scenarios using PC tool, and estimates payback periods of such projects.

The chapter also presented other applications of the developed state space model of CAES. The model facilitates capturing storage dynamics' influence on CAES's operational performance and economic indices. For a co-located wind farm scenario, the model helps to assess standard CAES configurations consisting of variations in turbine, compressor and reservoir ratings using a wide range of performance indices to quantify the worth of each configuration for that particular geography.

Some significant conclusions drawn are:

1. AGC simulation results indicate the ability of the battery storage to improve frequency response in the face of increasing wind penetration and effectively aid wind integration. The benefits will be more if there is scope to relax frequency bounds.

2. The results quantified fast responding storage's benefits at the system level and machine level in terms of instantaneous ACE corrections and lowering net regulation deployments, and reducing cycling (MW swings) of conventional generation.

3. Attributing the system benefits to such device's fast response, a payment for its regulation service (MW swings) or performance as initiated by FERC and implemented in pilot projects by NE-ISO is supported. Based on the proportion of MW-miles served by short-term storage, a suggestion is made to pay the storage that proportion of total monetary savings made in the grid. Such an economic incentive improves the project's payback period significantly (by about 50%).

4. The production costing studies indicated short-term storage devices to reduce system production cost, conventional unit capacities allocated to regulation and hence their cycling. These benefits are higher with increasing capacity of short-term storages under high wind penetration levels.

5. These short-term storages also benefit the grid by reducing the requirement for regulation capacity procurements by the AS market, and consequently the production costs. This requires regular feedback of CPS scores from AGC module to the economic dispatch programs, which can accordingly procure lesser capacities for regulation.

6. The revenues earned by such devices are a function of MCPs in the system. When the regulation offers of the conventional units increase under high wind penetration due to cycling components, they increase the MCPs and thus benefit short-term storage technologies immensely. When the regulation offers are lower resulting in lower MCPs, it adversely affects the economics of such storage ventures. In such scenarios (lower wind penetration, lower historical system MCPs, presence of competitive schemes such as demand response), smaller projects pose lesser risk. However for short-term storage that have the characteristics of a battery, there are cross arbitrage opportunities as investigated in chapter 4.

CHAPTER 6   CONCLUSIONS AND FUTURE WORK

6.1 CONCLUSIONS

This dissertation developed modeling and evaluation approaches to assess the role and value of energy storage technologies in electric power grids. Among the various solution strategies for enabling higher renewable interconnection to the grid in a reliable and economical manner, storage technologies are seen as one of the very promising ones. Among the many challenges that face storage technologies' adoption and proliferation in the grid, ranging from technology maturity to operational expertise, this work focused on evaluating the economic implications of venturing into a storage project in the present and future power markets.

This work developed a high-fidelity storage dispatch model for production costing studies performed within energy and AS co-optimized market structure. The models enabled to dispatch and evaluate storage economics considering energy storage as an active participant in market affairs, rather than the traditional price taker paradigm of storage participation in grid. The model incorporated two significant features: energy limited devices' ability to provide multiple services and being able to adapt to two different broad classes of storage technologies, namely bulk energy and short-term storage devices. The dissertation also created different taxonomies for energy storage which categorized the various technologies based on their characteristics, applications and specific functionalities. These characterizations helped in capturing the technology specific features of each class of storage's operations within the dispatch model. The dissertation also developed a state space model of CAES that can monitor the reservoir's mass and pressure status dynamically.

Based on the developed dispatch model several studies were constructed to evaluate both bulk energy and short-term storage technology's contribution to the grid and profitability under various wind penetration scenarios in IEEE 24 bus RTS system. CAES is used as a representative for bulk energy storage with an investment cost of $500/KW and 80% efficiency. Flywheel and battery are used to represent short-term storage technologies with investment cost of $1630/KWh and $1000/KWh respectively, and 85% and 90% efficiencies respectively. The work implemented an integrated approach based on production costing and automatic generation control (AGC) simulation tools to evaluate short-term technologies. The dissertation also developed a systematic methodology to estimate cycling related cost impacts from generation dispatch decisions under various wind penetration, and quantifies storage's ability to reduce them.

Bulk storage is shown to provide several benefits to the grid such as relieving transmission congestion, transmission deferral, lowering the LMPs and MCPs, and reducing cycling of conventional units. Incentives for relieving cycling and increasing wind energy penetration helped in improving bulk energy storage projects' economics. Short-term storage is shown to provide several benefits such as reducing conventional unit cycling, reducing regulation energy deployment by AGC and regulation capacity procurements by dispatch tool, and reducing system MCPs and production cost. Attributing all these to the instantaneous response of these short-term devices, incentivizing its MW-mileage performance helped in improving the expected payback from such ventures.

6.1.1   Opportunities in Market

The dissertation designed an optimal storage allocation study, using which indicators were developed to identify possible candidate locations for storage investments in a market. The study indicated that placement of bulk or short-term storage always benefits the grid, but the nature of grid services provided by the storage and the extent of revenues it draws could be highly influenced by the location where it is sited, especially for bulk energy storage. By virtue of variegated opportunities the grid presents in different parts of the system, the study also indicated a distributed and mixed storage portfolio to benefit the grid operations and enable different storage projects co-exist and make reasonable profits.

The indicators for identifying candidate locations are based on the market price data, and the risks to investments can also be qualitatively judged based on comparing the market clearing prices with that of what we saw in this dissertation.

MISO and PJM real-time LMP data for two consecutive days (19th and 20th) in the months of March, June, September and December were taken, and arbitrage values were computed as per equation (4.5). The highest arbitrage value over the 48 hours in each location were plotted in descending order to see the opportunities for siting bulk storage in these markets. Figures 6.1 and 6.2 show the arbitrage plots for MISO and PJM respectively. We can see that there are many locations where the highest arbitrage from a 1MWh energy transaction is higher than the typical CAES energy discharge offer. Even considering the extremely high arbitrage values to be some special cases, still there are many buses with values around $50-$200, which is closer to the working values in this dissertation, as shown in Figure 4.27.
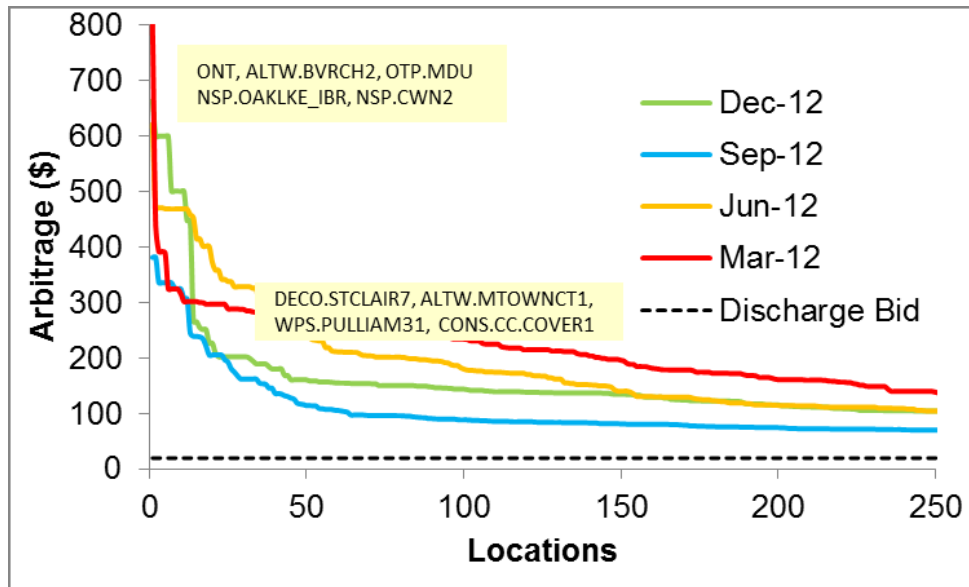
Figure 6.1 Arbitrage values in MISO buses
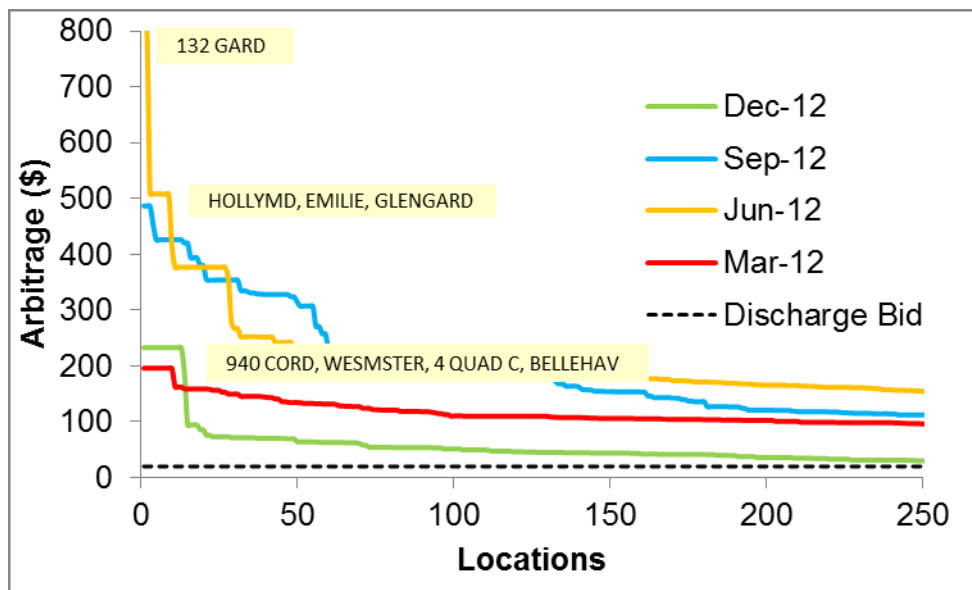
Figure 6.2 Arbitrage values in PJM buses

Figure 6.3 shows the regulation MCPs on a two randomly selected days in PJM and MISO markets in comparison to MCPs from IEEE 24 bus system, based on which all conclusions on this dissertation are drawn. The IEEE system MCPs shown are from two

types of simulation studies: base cases and lower MCP (LB: when regulation offer reduced by $12.5) simulations. Figure 6.4 shows the MCPs in the month of December 2012 in PJM market. We can notice that the MISO regulation MCPs are generally at lower side than the range of values we have been seeing in our studies. Storage (having lower AS offers) will still make revenues in MISO AS market, however lesser than the figures seen in this dissertation. However with the high energy arbitrage opportunities as seen in Figure 6.1, bulk storage technologies participating to provide multiple services in co-optimized market will find good cross arbitrage opportunities and promising revenues. With monetization schemes, the value for both energy arbitrage and AS for storage will increase. In PJM, storage technologies look attractive in co-optimization market as well as for AS alone due to the higher MCPs seen in both Figures 6.3 and 6.4.
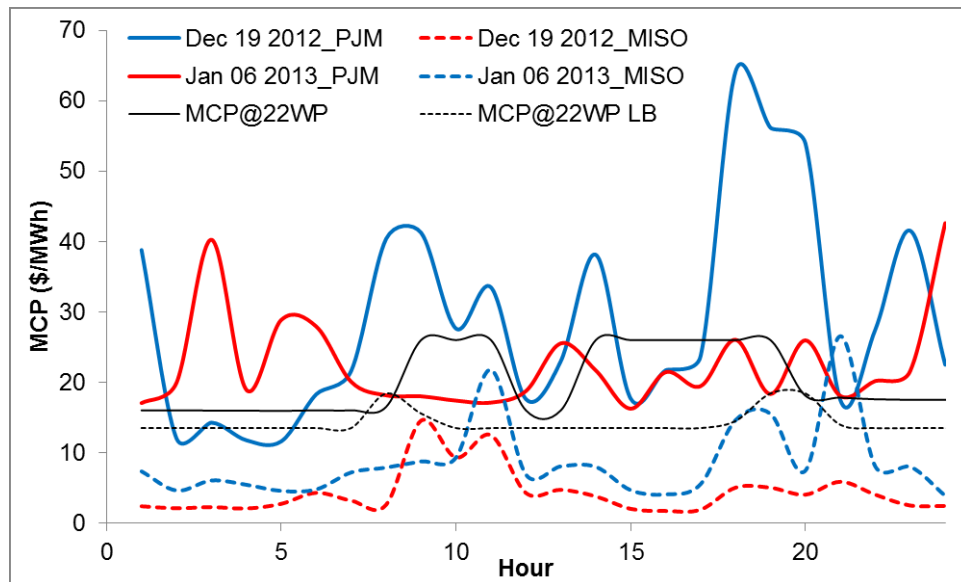
Figure 6.3 Typical regulation MCPs in MISO, PJM and IEEE 24 bus system
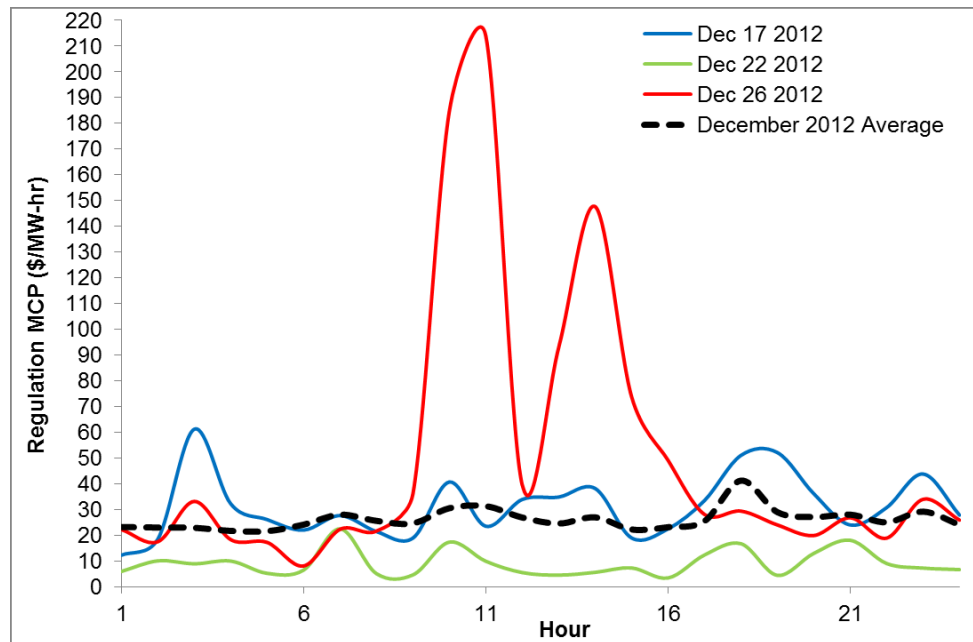
Figure 6.4 Regulation MCPs in PJM- December 2012

Similarly the opportunities in other markets can be assessed qualitatively, and by conducting production costing studies embedded with the developed high-fidelity storage model in their respective system qualitative results can be estimated.

6.1.2   Recommendations

Some selected and new recommendations unprecedented in the current markets, based on the studies conducted in this dissertation are:

1. Investigate ways to monetize storage (especially, non-CO_2 emitting) for aiding in increasing wind energy penetration – Sharing production tax credit for the energy saved from spillage can be a viable approach.

2. When fast-responding storage is present among the fleet of regulation providers, compute CPS measures at faster intervals and feed it back to the market clearing

tools, such that the hourly regulation capacity procurement can be dynamically adjusted to make grid operation economical.

3. The opportunities in a co-optimized market do not just depend on energy arbitrage values, but also the opportunities for cross-arbitrage. The lower side of LMPs together with arbitrage values helps in finding candidate locations for new ventures.

6.2 SIGNIFICANT CONTRIBUTION

The significant contributions of this research are:

1. **Modeling aspects of storage integration into grid**

   a. *High-fidelity technology adaptive storage dispatch model* for markets, which can ascertain cross arbitrage opportunities while dispatching storage for multiple services. The model can also be integrated into long term resource planning software, e.g., Iowa State University's NETPLAN.

   b. *State space modeling of CAES* to enhance price taker economic assessment that adds economic value to a storage's ability to flex its energy capacity

2. **Evaluation methodologies**

   a. Incorporate cycling related cost components into AS offers

   b. Integrated approach based on production costing and AGC simulations to assess short-term storage services, benefits and revenues

c. Monetization based on cycling cost components, wind spillage savings and MW mileage

d. AGC CPS feedback to SCED for reducing regulation capacity procurements

e. Optimal allocation of storage to find the best location, mix, and amount of storage

3. **General conclusions or useful insights**

a. Storage taxonomy based on regulation provision- helpful in modeling and categorizing storage into different classes

b. Bulk energy and short-term storage technology assessment under various wind penetration- quantifies benefits and compares technologies

c. Easy indicators for identifying opportunities for storage ventures in a co-optimized market

d. Comparisons between storage and conventional units and transmission– Storage has a role to play together with other strategies under high wind penetration.

6.3 PUBLICATIONS

1. **Trishna Das**, V. Krishnan, and James McCalley, "High-Fidelity Dispatch Model of Storage for Production Costing Studies," to be submitted to *IEEE Trans. Power Syst.*

2. V. Krishnan, **Trishna Das**, E. Ibanez, C. Lopez, and J. McCalley, "Modeling Operational Effects of Wind Generation within National Long-term Infrastructure Planning Software," *IEEE Trans. of Power Systems*, Oct 2012

3. **Trishna Das**, V. Krishnan, Y. Gu, and J. McCalley, "Compressed Air Energy Storage: State Space Modeling and Performance Analysis," in Proc. *IEEE PES General Meeting*, July 2011, **Citations: 1**

4. **Trishna Das,** and J. McCalley, "*Compressed Air Energy Storage*," Educational Chapter, 2012, **Citations: 1**

5. R. Dai, J. McCalley, D. Aliprantis, V. Ajjarapu, **Trishna Das**, D. Wu, M. Riaz,and R. Umer, "Hierarchical control for hybrid wind systems," *North American Power Symposium*, 2009

6. R. Dai, **Trishna Das**, M. Riaz, D. Aliprantis, J. McCalley, and V. Ajjarapu, "Hybrid Wind Systems: Design, Operation and Control," Final Report, *US Department of Energy*, April 2010

7. D. Wu, H. Chen, **Trishna Das**, and D. C. Aliprantis, "Bidirectional power transfer between HEVs and grid without external power converters."*Proc. IEEE Energy 2030 Conf.*, Atlanta, GA, Nov. 17-18, 2008, **Citations: 1**

8. **Trishna Das** and D.C. Aliprantis, "Small-Signal Stability Analysis of Power System Integrated with PHEVs," Proc. *IEEE Energy 2030 Conf.*, Atlanta, GA, Nov. 17-18, 2008, **Citations: 7**

6.4 DIRECTIONS FOR FUTURE WORK

1. **Market Assessment**- Economic evaluation of storage in real power network can be performed. MISO has been undertaking such efforts using PLEXOS and EGEAS software.

2. **Demand Response**

a. **Storage vs. demand response-** It will be interesting to evaluate opportunities for storage in a grid integrated with demand response programs. In some ways based on the dissertation's work, from storage point of view the resultant effect could be seen as decrease in regulation requirements or energy arbitrage opportunities seen by storage.

b. **Storage within demand response-** Another interesting perspective will be to assess storage's participation in demand response programs; though type-1 storages would be more likely to participate. In many ways, the modeling of charging operation of type-3 storages can be considered equivalent to type-1 storage modeling, which would impose electric load on the grid by charging energy that would be used later to reduce the system load during peak times. So in conjunction with a load model and type-3 storage's charging component, type-1 storage could be modeled and its participation can be evaluated in a grid integrated with demand response programs.

3. **Storage with stochastic generation dispatch-** High-fidelity storage dispatch model can be integrated within stochastic UC and ED programs to render with more flexibility to meet the uncertainties in an economic manner

APPENDIX

Table A1 System Generation Parameters and Energy Offers

Gen (Bus)	Min-Max (MW)	Offer 1(MW)/Price ($/MWh)	Offer 2(MW)/Price ($/MWh)	Offer 3(MW)/Price ($/MWh)
Oil (1)	0-40	0-20/93.7	21-40/98.8	-
Coal (1)	50-152	50/26.9	51-100/32.4	101-152/41.9
Oil (2)	0-40	0-20/93.7	21-40/98.8	-
Coal (2)	50-152	50/26.9	51-100/32.4	101-152/41.9
NG (7)	100-300	100/51.8	101-200/60.8	201-300/73.8
NG (13)	200-591	200/48.6	201-400/57.6	401-591/70.6
NG (15)	0-60	0-20/48.6	21-40/54.7	41-60/66.4
Coal (15)	50-155	50/24.5	51-100/28.5	101-155/36.5
Coal (16)	50-155	50/24.5	51-100/28.7	101-155/37.1
Nuc (18)	300-400	300/10.5	301-400/17.5	-
Nuc (21)	300-400	300/10.5	301-400/17.5	-
Coal (22)	150-300	150/24.6	151-250/32.2	251-300/44.3
Coal (23)	150-310	150/20.5	151-250/28.5	251-310/41.3
Coal (23)	150-350	150/20.6	151-250/27.8	251-350/39.3
Wind (17)	0-300	0-300/15	-	-
Wind (21)	0-400	0-400/15	-	-
Wind (22)	0-300	0-300/15	-	-

Table A2 Generation Cost-Based AS Offers

Gen	Ramp Rate (%)	SR ($/MW-hr)	NSR ($/MW-hr)	RU/RD ($/MW-hr)
Oil	6.25	7.8	-	62
Coal	3.25	8	-	26
NG	10	7.9	4.1	27

Table A3 AS Offers of Different Storage Class

Storage	Energy ($/MWh)	SR ($/MW-hr)	NSR ($/MW-hr)	RU/RD ($/MW-hr)
CAES	20.15	7.5	4	17.9/12.5
Flywheel	-	-	-	2/2
Battery	2	5	-	2/2

Table A4 Cycling Cost data for Offers from APTECH [85]

From Aptech Report - Table 2-4d – Cost elements for Most Significant Load Follow Cycles (SLFs) at Harrington Unit 3(based on CY 2008 cycles and in 2008 dollars)	Baseline Data ($/MW-hr)	
	LOW	HIGH
E1: Cost of operation – Includes operator non-fixed labor, general engineering and management cost (including planning and dispatch); excludes fixed labor	$0.0010	$0.0127
E2: Cost of maintenance – Includes maintenance and overhaul maintenance expenditures for boiler, turbine, generator, air quality control systems and balance of plant key components	$0.0047	$0.0346
E3: Cost of capital maintenance – Includes overhaul capital maintenance expenditures for boiler, turbine, generator, air quality control systems and balance of plant key components	$0.0028	$0.0256

Table A5-Typical bounds for Cycling Cost and other data for various generation types [84]

Unit Types	Coal - Small Sub Critical	Gas - Steam
Typical Load Follows Data-C&M cost ($/MW cap.)-		
Typical Ramp Rate		
25th_centile	1.91	1.17
75th_centile	3.84	2.32
Multiplying Factor - Faster Ramp Rate (1.1 to 2x)		
*Range	2 to 8	1.2 to 6

Table A6 – CO_2 Emission rates for different generation types.

Generation Type	CO_2 emissions per 1 MWh (metric tonnes)
Coal	0.834
Natural Gas	0.374
Oil	0.743
CAES	0.125
Combustion Turbine	0.511
Nuclear	0.0078

REFERENCES

[1] M. Reale, GE Energy, "New High Efficieny Simple Cycle Gas Turbine – GE's LMS100," Document GER-4222A, 2004, http://www.slideshare.net/alex_abakumov/ge-lms100

[2] D. Todd, M. Caufield, B. Helms, M. Starke, B. Kirby, and J. Kueck, "Providing Reliability Services through Demand Response: A Preliminary Evaluation of the Demand Response Capabilities of Alcoa Inc.," 2009, available at http://certs.lbl.gov/pdf/dr-alcoa.pdf.

[3] Bottling Electricity: Storage as a Strategic Tool for Managing Variability and Capacity Concerns in the Modern Grid, The Electricity Advisory Committee, Dec 2008 - http://www.oe.energy.gov/eac.html

[4] Analytic Challenges to Valuing Energy Storage, WORKSHOP REPORT, by Office of Energy Efficiency and Renewable Energy and Office of Electricity Delivery and Energy Reliability, Department of Energy, November 2011

[5] Barin, A, et.al. "Storage energy management with power quality concerns the analytic hierarchy process and the fuzzy logic", Sept. 27 2009-Oct. 1 2009 Page(s):225 - 231

[6] Ibrahim H, Ilinca A, Peroon J., "Energy storage systems—Characteristics and comparisons" Science Direct, Jan 2007

[7] E. Spahi, G. Balzer, B. Hellmich and W. Münch , "Wind Energy Storages - Possibilities", PowerTech 2007

http://ieeexplore.ieee.org/stamp/stamp.jsp?tp=&arnumber=4538387&isnumber=4538278

[8] "*Energy bags and super batteries,*" Nottingham University, June 18, 2008, http://www.nottingham.ac.uk/news/pressreleases/2008/june/energybagsandsuperbatteries.as

px

[9] "*How Hydrostor Aims To Change The Power Game By Storing Energy Under Water*," TechCrunch, July 9, 2011, http://techcrunch.com/2011/07/09/hydrostor-power-storage-under-water

[10] A. T. Gazarian, "Energy Storage for Power Systems", Peter Peregrines Ltd. 1994

[11] Ellis, M.W.; Von Spakovsky, M.R.; Nelson, D.J." Fuel cell systems: efficient, flexible energy conversion for the 21st century", Volume 89, Issue 12, Dec. 2001 Page(s):1808 – 1818 http://ieeexplore.ieee.org/stamp/stamp.jsp?tp=&arnumber=975914&isnumber=21066

[12] Oudalov, A et. al., "Optimizing a Battery Energy Storage System for Primary Frequency Control," IEEE trans. Power sys., Vol. 22, Issue 3, Aug. 2007, pp. 1259 - 1266

[13] Mercier, P. et. al., "Optimizing a Battery Energy Storage System for Frequency Control Application in an Isolated Power System," IEEE trans. Power sys., Vol. 24, Issue 3, Aug. 2009, pp. 1469 - 1477

[14] Roberts, B, Capturing grid power, pp. 32-41

[15] "Stationary Sodium-Sulfur (NAS) Battery", EPRI Report May 2006. Available Online: http://mydocs.epri.com/docs/public/000000000001011966.pdf

[16] Kodama, E.; Kurashima, Y.; "Development of a compact sodium sulphur battery", Power Engineering Journal, Volume 13, Issue 3, June 1999 Page(s):136 – 141

[17] Price, A.;" Technologies for energy storage-Present and future: flow batteries", Volume 3, 16-20 July 2000 Page(s):1541 - 1545 vol. 3 Available Online: http://ieeexplore.ieee.org/stamp/stamp.jsp?tp=&arnumber=868758&isnumber=18790

[18] Norris. B.L, Parry. R.J and Hudson. R.M, "An Evaluation Of Windfarm Stabilization And Load Shifting Using The Zinc-Bromine Battery (ZBB)", Available Online: http://www.zbbenergy.com/pdf/technicalpaper_evaluation.pdf

[19] M.F. Cowiishaw, "The Characteristics And Use Of Lead-Acid Cap Lamps", Trans. British Cave Research Association. Vol. 1. No. 4. pp.199-214. December, 1974 Available Online: http://speleotrove.com/caving/cowlishaw1974-lead-acid-cap-lamps.pdf

[20] Akhil, A.;" Trends and status of battery energy storage for utility applications", Battery Conference on Applications and Advances, 1995., Proceedings of the Tenth Annual http://ieeexplore.ieee.org/stamp/stamp.jsp?tp=&arnumber=398527&isnumber=9002

[21] Buchmann, I. "Understanding your batteries in a portable world- Article on battery choice and how to maximize service life", Battery Conference on Applications and Advances, 1999, The Fourteenth Annual 12-15 Jan. 1999 Page(s): 369 – 373

[22] John J.C. Kopera, "Inside the Nickel Metal Hydride Battery" http://www.cobasys.com/pdf/tutorial/inside_nimh_battery_technology.pdf

[23] Farahani, M.E.S.; Saeidi, N.; "Case Study of Design and Implementation of a Thermal Energy Storage System", 28-29 Nov. 2006 Page(s):6 – 11. Available Online: http://ieeexplore.ieee.org/stamp/stamp.jsp?tp=&arnumber=4154453&isnumber=4126238

[24] Huang Wei; Wang Xin, et.al. "Discussion on application of super capacitor energy storage system in microgrid", Sustainable Power Generation and Supply, SUPERGEN '09, International Conference on6-7 April 2009 Page(s):1 - 4

[25] Ruddell. A, "Investigation on Storage Technologies for Intermittent Renewable Energies: Evaluation and recommended R&D strategy ST6: FLYWHEEL" Thematic Network report 2003

[26] Flywheel Energy Storage: An alternative to batteries for uninterruptible power supply systems - www.eere.energy.gov/femp/DOE/EE-0286

[27] Beacon Power Corporation news release: "Beacon Power Announces Testing of First Megawatt of Flywheel Energy Storage"

[28] Hassenzahl, W, "Superconducting magnetic energy storage," IEEE trans. Magnetics, Vol. 25, Issue 2, Mar 1989 pp. 750 - 758

[29] Chen, L et. al., "Detailed modeling of superconducting magnetic energy storage (SMES) system," IEEE trans. Power Delivery, Vol. 21, Issue 2, April 2006 pp. 699 - 710

[30] J.R. Sears, "Thermal and Compressed Air Energy Storage (TACAS)", 2005

[31] Y.V. Makarov, et.al. "Wide-Area Energy Storage and Management System to Balance Intermittent Resources in the Booneville Power Administration and California ISO Control Areas" PNNL Report, 2008

[32] Schoenung. S.M, "Characteristics and Technologies for Long-vs. Short-Term Energy Storage", A Study by the DOE Energy Storage Systems Program, SAND2001-0765 2001

[33] Pier Final Project Report, "An Assessment Of Battery And Hydrogen Energy Storage Systems Integrated With Wind Energy Resources In California", University of California, Berkeley, September 2005

[34] Market.T, et.al, " Energy Storage System Requirements for Hybrid Fuel Cell Vehicles", NREL Report, June 2003

[35] Bents.D.J and Scullin.V.J, "Hydrogen-Oxygen PEM Regenerative Fuel Cell Energy Storage System" Glenn Research Center, Jan 2005 Available Online: http://gltrs.grc.nasa.gov

[36] Energy Efficiency Factsheet – Washington State University, 2003 Online: http://www.energy.wsu.edu/documents/engineering/Thermal.pdf

[37] Tabors Caramanis & Associates, "Source Energy And Environmental Impacts Of Thermal Energy Storage", California Energy Commission, 1996

[38] Ise, T.; Kita, M.; Taguchi, A.;" A hybrid energy storage with a SMES and secondary battery", Applied Superconductivity, IEEE Transactions on Volume 15, Issue 2, Part 2, June 2005 pp:1915 - 1918

[39] EPRI-DOE Handbook of Energy Storage for Transmission and Distribution Applications, 2003

[40] IET Journal " Full Charge Ahead"

[41] Jones, I.W, "The Sodium Sulfur Battery", Phil. Trans. R. Soc. Lond, A 1981 302, 339-350

[42] Wen.Z, "Study on Energy Storage Technology of Sodium Sulfur Battery and it's Application in Power System", PowerCon International Conference on Power System Technology, 22-26 Oct. 2006, pp:1 - 4

[43] R. Walawalkar, and J. Apt, Market analysis of emerging electric energy storage systems, A report developed for Department of Energy (DOE) and National Energy Technology Labs (NETL), DOE/NETL-2008/1330.

[44] A Report from the APS Panel on Public Affairs Committee on Energy and Environment – "Challenges of Electricity Storage Technologies" May 2007 http://www.aps.org/policy/reports/popa-reports/upload/Energy-2007-Report-ElectricityStorageReport.pdf

[45] CAES Dispatch Modeling, Available online: http://www.smartgrid.gov/sites/default/files/doc/files/Exh%2013.13%20Energy%20Market%20Report%20CES%20Part%203.pdf

[46] E. Drury, P. Delholm, and R. Sioshansi, "The value of compressed air energy storage in energy and reserve markets," *Energy*, vol. 36, pp. 4959–4973, Aug. 2011

[47] R. Deb, "Operation hydroelectric plants and pumped storage units in a competitive environment," The Electricity Journal, 13 (2000), pp. 24–32

[48] P. Kanakasabapathy, and K. Swarup, "Evolutionary Tristate PSO for Strategic Bidding of Pumped-Storage Hydroelectric Plant," *IEEE Trans. Syst., Man, and Cybernetics, Part C: Applications and Reviews*, 2010

[49] Iowa Stored Energy Park Project, "Economics Study Summary," 2001 www.carebs.org/webroot/ISEP%20Economics%20Study%20Summary.pdf

[50] Dan Rastler et. al., "MISO Energy Storage Study Phase 1 Report," A report by Electric Power Research Institute (EPRI) and MSIO, Nov. 2011

[51] Goran Strbac et. al., "Strategic Assessment of the Role and Value of Energy Storage Systems in the UK Low Carbon Energy Future," Report for Carbon Trust, prepared by *Energy Futures Lab, Imperial College London, June 2012*

[52] Energy Storage Gets A Charge From FERC – PRNewswire http://www.prnewswire.com/news-releases/energy-storage-gets-a-charge-from-ferc-132244853.html

[53] J. García-González et. al., "Stochastic joint optimization of wind generation and pumped-storage units in an electricity market," *IEEE Trans. Power Syst.*, vol. 23, no. 2, pp. 460–468, May 2008

[54] S. J. Kazempour et. al. "Self-scheduling of a joint hydro and pumped-storage plants in energy, spinning reserve and regulation markets," in *Proc. IEEE PES General Meeting*, pp. 1–8, Jul. 2009

[55] S. You, C. Traeholt, and B. Poulsen, "Economic dispatch of electric energy storage with multi-service provision," *Proc. IPEC Conference*, pp. 525-531, Oct. 2010

[56]P N. Lu, J. Chow, and A. Desrochers, "Pumped-storage hydro-turbine

bidding strategies in a competitive electricity market," *IEEE Trans. Power Syst.*, vol. 19, no. 2, pp. 834–841, May 2004

[57] H. Daneshi, and A.K. Srivastava," Impact of Battery Energy Storage on Power System with High Wind Penetration," *IEEE T&D Conf, May* 2012

[58] X. Xi, R. Sioshansi, and V. Marano, "A Stochastic Dynamic Programming Model for Co-optimization of Distributed Energy Storage," submitted to *Energy Economics Journal*, Sept 2012

[59] A. A. Thatte and L. Xie, "Towards a Unified Operational Value Index of Energy Storage in Smart Grid Environment," *IEEE Trans. Smart Grid*, Vol. 3, No. 3, pp. 1418-1426, Sept. 2012

[60] E. Drury, P. Denholm and R. Sioshansi, "The value of compressed air energy storage in energy and reserve markets," NREL 2011, Available online: http://www.nrel.gov/analysis/pdfs/drury_coopt_caes_050411.pdf

[61] D. D. Ladurantaye et. al., "Strategic Bidding for Price-Taker Hydroelectricity Producers," *IEEE Trans. Power Syst.*, vol. 22, No. 4, 2007

[62] M. Ghofrani et. al., "A Framework for Optimal Placement of Energy Storage Units Within a Power System With High Wind Penetration," to appear in *IEEE Trans. Sustainable Energy*, 2013

[63] T. Senjyu et. al.,"A technique for unit commitment with energy storage system," *International Journal of Electric Power and Energy Systems*, 2007

[64] H. Daneshi, and A. Srivastava, "Security-constrained Unit Commitment with Wind Generation and Compressed Air Energy Storage," *IET Generation, Transmission & Distribution*, vol. 6 (2), pp. 165-175, Feb. 2012

[65] Gu, Yang, "Long-term power system capacity expansion planning considering reliability and economic criteria" *Graduate, Theses and Dissertations,* 2011, http://lib.dr.iastate.edu/etd/10163

[66] R. Jiang, J. Wang, and Y. Guan, "Robust Unit Commitment With Wind Power and Pumped Storage Hydro," IEEE Trans. Power Syst., May 2012

[67] Y. Zhu and Y. Chen, "Modeling short-term Stored Energy Resources under real time look-ahead dispatch on energy and ancillary service market," IEEE Energytech, 2012

[68] Y. Chen et. al., "Incorporating short-term stored energy resource into Midwest ISO energy and ancillary service market," IEEE Trans. Power Syst., vol. 26, no. 2, pp. 829–838,

May 2011

[69] T Li, M Shahidehpour and Z Li, "Risk-constrained bidding strategy with stochastic unit commitment," IEEE Trans. Power syst., 2007

[70] T. Wu, M. Rothleder, Z. Alaywan, and A. D. Papalexopoulos, "Pricing energy and ancillary services in integrated market systems by an optimal power flow", *IEEE Trans. Power Syst.*, vol. 19, no. 1, pp.339 -347 2004

[71] T. Li and M. Shahidehpour, "Price-based unit commitment: A case of Lagrangian relaxation versus mixed integer programming," *IEEE Trans. Power Syst.*, vol. 20, no. 4, pp. 2015–2025, Nov. 2005.

[72] V. Krishnan et. al., *"*Modeling Operational Effects of Wind Generation within National Long-term Infrastructure Planning Software*,"* to appear in *IEEE Trans. Power Syst.,* 2013

[73] J. M. Arroyo and A. J. Conejo, "Optimal response of a thermal unit to an electricity spot market," *IEEE Trans. Power Syst.*, vol.15, 2000

[74] B.Parsons, M.Milligan, B.Zavadi, D.Brooks, B.Kirby, K.Dragoon and J.Caldwell, "Grid Impacts of Wind Power: A Summary of Recent Studies in the United States" NREL Report 2003

[75] ERCOT methodologies for determining ancillary service requirements

[76] California-ISO Technical Bulletin, AS-Procurement Regulation, 2001

[77] R. Zavadil et. al., *Xcel Energy and the Minnesota Department of Commerce, Wind Integration Study -Final Report*, EnerNex Corporation and Wind Logics, Inc., Sept.28 2004

[78] E. Ela, et. al, "Evolution of operating reserve determination in wind power integration studies," *IEEE PES General Meeting*, 2010

[79] CAISO 1-min. data- http://www.caiso.com/2b3e/2b3ed83725ee0ex.html

[80] T. Das, V. Krishnan, Y. Gu, and J. McCalley, "Compressed Air Energy Storage: State Space Modeling and Performance Analysis," *IEEE Power Engineering Society General Meeting*, 2011

[81] Energy Storage Council - "About Energy Storage" 2007 -

http://www.energystoragecouncil.org/aboutenergystorage.htm

[82] J.Makansi - CAREBS, "Monetizing the Balancing Function for Electricity Grid

Operations -A Policy Brief & Proposal", 2012,

http://www.carebs.org/CAREBS%20Policy%20Paper%20-%202012%20-%20Balancing%20Function%20Policy%20Framework.pdf

[83] S.A.Lefton; P. Besuner, "The Cost of Cycling Coal Fired Power Plants," Coal

Power Magazine, Winter 2006.

[84] N. Kumar et. al., "Power Plant Cycling Costs," NREL Report, 2012

http://wind.nrel.gov/public/WWIS/APTECHfinalv2.pdf

[85] Aptech report for Public Review, "Integrating Wind- Cost of Cycling Analysis for Xcel

Energy's Harrington Station Unit 3, Phase 1: Top-Down Analysis," March. 2009

http://blankslatecommunications.com/Images/Aptech-HarringtonStation.pdf

[86] D. D. Agan et. al., "Cost of Cycling Analysis for Pawnee Station Unit 1 Phase 1: Top-

Down Analysis," Prepared by APTECH Engineering Services, INC. for XCEL Energy, Nov.

2008

[87] PJM Manual 15, "Cost Development Guidelines," Feb 2012

[88] D. Lew et. al., "How Does Wind Affect Coal? Cycling, Emissions, and Costs," NREL/PR-5500-51579, Wind Power 2011, CA, http://www.nrel.gov/docs/fy11osti/51579.pdf

[89] V.Vittal, et.al., "Tools and Techniques for Considering Transmission Corridor Options to Accommodate Large Scale Renewable Energy Resources", PSERC Publication 12-23, Aug 2012

[90] J. A. Fleeman, R. Gutman, M. Heyeck (American Electric Power), M. Bahrman, B. Normark (ABB), "EHV AC and HVDC Transmission Working Together to Integrate Renewable Power," CIGRE Paper 978-2-85873-080-3, 2009

[91] N. W. Miller, M. Shao, and S. Venkataraman, "*California ISO – Frequency Response Study*," GE Energy Report, Nov. 2011

[92] J. Dumas, "*Impact of Wind Generation on ERCOT Operations*," UWIG, 2008, http://www.uwig.org/FortWorth/workshop/Dumas.pdf

[93] PJM Regulation Performance Senior Task Force, "PJM Rules and the External Experience: A Case Study of Beacon Power's Pay-For-Performance Experience in ISO-NE", May 2011

[94] N. Troy, E. Denny, and M. O'Malley, "Base-Load Cycling on a System With Significant Wind Penetration," *IEEE Trans. Power Syst.*, 2010

[95] Y.Makarov et.al, "Assessing the Value of Regulation Resources Based on Their Time Response Characteristics" PNNL Report June 2008

[96] M. Terbrueggen, "Control Performance Standards," North American Electrcic Reliability Council, http://www.nerc.com/docs/oc/ps/tutorcps.pdf

[97] *Standard BAL-001-1-Real Power Balancing Control Performance*, 2012

[98] K. Ramakrishna et. al., "*Automatic generation control of interconnected power system with diverse sources of power generation*" IJEST 2010.

[99] W. I. Rowen, Simplified Mathematical Representation of Heavy Duty Gas Turbines, ASME Journal of Engineering for Power, vol. 105, 1983, pp. 865-869

[100] S. C. Tripathy and K. P. Juengst, "Sampled data automatic generation control with superconducting magnetic energy storage in power systems," IEEE Trans. Energy Convers., vol. 12, no. 2, pp. 187–192, Jun.1997

[101] M. Robinson, "*Midwest ISO Market Design: Wind in Energy, Capacity and Ancillary Services Markets*," UWIG Workshop, 2004

[102] PSERC Report, "Impact of Increased DFIG Wind Penetration on Power Systems and Markets," 2009

[103] S. Samineni, "Modeling and Analysis of a Flywheel Energy Storage System for Voltage Sag Correction," M.S. Thesis, University of Idaho, 2003

[104] P. G. Lyons, "*Energy Storage for Power Systems with Rapidly Changing Loads*" , Thesis Dec 1992, Purdue University

[105] T.B. Ferguson, "The Centrifugal Compressor Stage", London Butterworth 1963

[106] Succar, S. and R. Williams, "Compressed Air Energy Storage: Theory, Operation, and Applications," March 2008

[107] M.Korpaas, A.T. Holen and R.Hildrum, "Operation and sizing of energy storage for wind power plants in a market system" Electrical Power and Energy Systems, 25, 599-606, 2003

[108] Moran, Shapiro, Munson and Dewitt, "Introduction to Thermal Systems Engineering" John Wiley & Sons, Inc

[109] F. Crotogino, K. U. Mohmeyer and R. Scharf, "Huntorf CAES: More than 20 years of successful operation," Spring 2001 Meeting, USA

[110] Mathworks – Documentation center, "Battery"

http://www.mathworks.com/help/physmod/powersys/ref/battery.html

[111] Tremblay O., and Dessaint L.A., "Experimental Validation of a Battery Dynamic Model for EV Applications," World Electric Vehicle Journal, Vol. 3 - ISSN 2032-6653 - © 2009 AVERE, EVS24 Stavanger, Norway, May 13 - 16, 2009

[112] N. Lu et. al., "The wide-area energy storage and management system phase II Final Report - Flywheel Field Tests," PNNL, 2010

[113] G. Thijssen and J. Enslin, "Cost Comparison for a 20 MW Flywheel-based Frequency Regulation Power Plant," KEMA-Inc. Project: BPCC.0003.001 Beacon Flywheel Project, Sept 2007

[114] M. E. Kintner-Meyer et. al., "Energy Storage for Power Systems Applications: A Regional Assesement for the Northwest Power Pools; PNNL-2307; Pacific Northwest National Lab: Palo Alto, CA, 2010

[115] E. Macchi and G. Lozza, "Study Of Thermodynamic Performance Of Caes Plants, Including Unsteady Effects," Gas Turbine Conference and Exhibition, Anaheim, CA, USA, 1987, p. 10.

[116] P. Vadasz, and D. Weiner, "Correlating Compressor and Turbine Costs to Thermodynamic Properties for CAES Plants," Cost Engineering, Vol. 29, No. 11, pp. 10-15, November 1987

[117] Nakhamkin, M., Swensen, E.C., Abitante, P.A.,Whims, M., Weiner, D., Vadasz, P., Brokman,S., "Conceptual Engineering of a 300 MW CAES Plant, Part 1: Cost Effectiveness Analysis," *36th ASME International Gas Turbine and Aeroengine Congress and Exposition*, Fl., June 1991

[118] Vadasz, P, "Compressed Air Energy Storage:Optimal Performance and Techno-Economical Indices", Int.J. Applied Thermodynamics, Vol.2, 1999

[119] R. Dai, T. Das, M. Riaz, D. Aliprantis, J. McCalley, and V. Ajjarapu, "Hybrid Wind Systems: Design, Operation and Control," Final Report, US Department of Energy, April 2010

[120] R. Dai, J. McCalley, D. Aliprantis, V. Ajjarapu, T. Das, D. Wu, M. Riaz,and R. Umer, "Hierarchical control for hybrid wind systems," *North American Power Symposium*, 2009

[121] R.Walawalkar, J.Apt and R.Mancini, "Economics of electric energy storage for energy arbitrage and regulation in New York" Energy Policy Volume 35, Issue 4, 2007

[122] Butler, P., Iannucci, J., Eyer, J., 2003, Innovative business cases for energy storage in a restructured electricity marketplace, Sandia National Laboratories report SAND2003-0362

[123] Eyer, J., Iannucci, J., Corey, G., 2004, Energy storage benefits and market analysis handbook: a study for the DOE energy storage systems program; Sandia National Laboratories SAND2004-6177

[124] Voluntary Reporting of Greenhouse Gases Program, http://www.eia.doe.gov/oiaf/1605/coefficients.html

[125] Gas Turbine prices - http://www.gas-turbines.com/trader/kwprice.htm

[126] LCG Consulting-Energy Online, MISO Actual Energy prices 2006, http://www.energyonline.com/